UNIVERSITY OF SOUTHAMPTON

Functionalised *N*-Heterocyclic Carbenes and Amido/Imino Mixed Donors as Supporting Ligands in Organometallic Catalysis.

Scott Winston

Doctor of Philosophy

Department of Chemistry

February 2003

UNIVERSITY OF SOUTHAMPTON

ABSTRACT

FACULTY OF SCIENCE

CHEMISTRY

Doctor of Philosophy

Functionalised *N*-Heterocyclic Carbenes and Amido/Imino Mixed Donors as Supporting Ligands in Organometallic Catalysis.

By Scott Winston

The following novel nitrogen donor functionalised imidazolium salts have been synthesised: (3-Ar^3-1-py-imid)Br; (3-Ar^1-1-py^2-imid)Br; (3-Ar^2-1-py^2-imid)Br; (3-Ar^2-1-py^3-imid)Br; (3-Ar^2-1-py^4-imid)Br; [3-Ar^1-1-(CH_2CONEt_2)-imid]Br; [3-^{t}Bu-1-(CH_2CONEt_2)-imid]Br; (3-Ar^3-1-pi-imid)Br; [α,α'-(3-^{t}Bu-imid-methyl)$_2$-*o*-xylene]Br; [α,α'-(3-Ar^1-imid-methyl)$_2$-*o*-xylene]Br; [α,α'-(3-Ar^2-imid-methyl)$_2$-*o*-xylene]Br; [2,6-(3-^{t}Bu-imid)$_2$lutidine]Br_2; [2,6-(3-^{t}Bu-imid)$_2$-pyridine]Br_2; [2,6-(3-Ar^1-imid)$_2$-pyridine]Br_2; [2,6-(3-Ar^2-imid)$_2$-pyridine]Br_2; [2,6-(3-Ar^2-imid-methyl)$_2$bromobenzene]Br_2; [2,6-(3-Ar^2-imid-methyl)$_2$-3,5-dimethylphenyl] Br_2; [2,6-(3-Ar^1-imid-methyl)$_2$-3,5-dimethylphenyl]Br_2; where Ar^1 = mesityl, Ar^2 = 2,6-di-*iso*-propylphenyl, Ar^3 = 3,5-dimethyl-4-(*tert*-butyl)phenyl, *t*Bu = *tert*-butyl, pi = picolyl, py^1 = 2-pyridyl, py^2 = 2-(6-trimethylsilyl-2-pyridyl), py^3 = 2-(5-trimethylsilyl-2-pyridyl), py^4 = 2-(5-trifluoromethyl-2-pyridyl), imid = imidazolium.

The following novel nitrogen and oxygen donor functionalised imidazol-2-ylidenes and imidazol-2-thiones have been synthesised: 3-Ar^2-1-py-ylid; 3-Ar^1-1-py^2-ylid; 3-Ar^2-1-py^2-ylid; 3-Ar^2-1-py^3-ylid; 3-Ar^2-1-py^4-ylid; 3-Ar^2-1-pi-ylid; 3-Ar^2-1-methoxymethyl-ylid; 2,6-(3-Ar^1-ylid)$_2$-pyridine; 2,6-(3-Ar^3-ylid)$_2$-pyridine; 2,6-(3-Ar^2-ylid-methyl)$_2$bromobenzene; 2,6-(3-Ar^2-ylid-methyl)$_2$-3,5-dimethylphenyl; 3-Ar^2-1-methoxymethyl-thione; 3-Ar^2-1-py^2-thione; 2,6-(3-Ar^1-thione)$_2$-pyridine; 2,6-(3-Ar^2-thione-methyl)$_2$bromobenzene; where ylid = imidazol-2-ylidene, thione = imidazol-2-thione.

The following novel silver (I) nitrogen donor functionalised *N*-heterocyclic carbene complexes have been synthesised: (3-Ar^3-1-py-ylid)AgBr; (3-Ar^2-1-py^2-ylid)AgBr; (3-Ar^2-1-py^3-ylid)AgBr; (3-Ar^2-1-py^4-ylid)AgBr; (3-Ar^1-1-CH_2CONEt_2-ylid)AgBr; (3-^{t}Bu-1-CH_2CONEt_2-ylid)AgBr; (3-Ar^3-1-pi-ylid)AgBr; [α,α'-(3-^{t}Bu-ylid-methyl)$_2$-*o*-xylene]Ag_2Br_2; [α,α'-(3-Ar^1-ylid-methyl)$_2$-*o*-xylene]Ag_2Br_2; [α,α'-(3-Ar^2-ylid-methyl)$_2$-*o*-xylene] Ag_2Br_2; [2,6-(3-^{t}Bu-ylid)$_2$-pyridine]Ag_2Br_2; [2,6-(3-Ar^1-ylid)$_2$-pyridine]Ag_2Br_2; [2,6-(3-Ar^2-ylid)$_2$-pyridine]Ag_2Br_2; [2,6-(3-^{t}Bu-ylid)$_2$-lutidine]Ag_2Br_2; [2,6-(3-Ar^1-ylid)$_2$-lutidine]Ag_2Br_2.

The following novel palladium (II) and nickel (II) nitrogen donor functionalised *N*-heterocyclic carbene complexes have been synthesised: (3-Ar^2-1-py^2-ylid)PdMeBr; (3-Ar^2-1-py^3-ylid)PdMeBr; (3-Ar^2-1-py^4-ylid)PdMeBr; (3-Ar^2-1-py-ylid)$PdMe_2$; (3-Ar^2-1-pi-imid)$PdBr_3$; (3-Ar^1-1-CH_2CONEt_2-ylid)$_2PdCl_2$; (3-Ar^1-1-py^2-ylid)$_2PdMe_2$; (3-Ar^2-1-py^2-ylid)$_2PdMe_2$; (3-Ar^2-1-py^4-ylid)$_2PdMe_2$; [2,6-(3-Ar^2-ylid-methyl)$_2$phenyl]PdBr; [2,6-(3-Ar^1-ylid-methyl)$_2$-3,5-dimethylphenyl]PdBr; [2,6-(3-Ar^1-ylid-methyl)$_2$-3,5-dimethylphenyl]PdBr; (3-^{t}Bu-1-pi-ylid)$NiBr_2$; (3-Ar^2-1-pi-ylid)$NiBr_2$; (3-Ar^3-1-pi-ylid)$NiBr_2$; (3-Ar^2-1-pi-ylid)Ni(S_2CNEt_2)Br; (3-Ar^2-1-methoxymethyl-ylid)$_2NiCl_2$; (3-Ar^2-1-py-ylid)$_2Ni_2Br_4$.

Comparison of Heck C-C coupling activity of several of the palladium (II) complexes showed that substitution on the nitrogen donor effected coupling activity of aryl bromides: for bidentate ligands, an electron withdrawing group increased activity more than increasing chelate ring size; for tridentate ligands the exchange of nitrogen to carbon donor did not effect catalytic activity.

The following novel mixed nitrogen based compounds have been prepared: *o*-(cy-imm)-ani; *o*-(^{t}Bu-imm)-*N*-TMS-ani; *o*-(cy-imm)-*N*-(TMS)ani; Li *o*-(^{t}Bu-imm)-*N*-(TMS)anilide; *o*-(^{t}Bu-imm)-*N*-(3,5-dimethylphenyl)ani; N,N'-Bis-(2-amino-benzylidene)-cy-1,2-diamine; where ani = aniline imm = iminomethyl, cy = cyclohexyl, TMS = trimethylsilyl. Transaminations of *o*-(^{t}Bu-imm)-*N*-TMS-ani with $Zr(NMe_2)_2Cl_2THF_2$ gave a functionalised amidinato complex and *o*-(^{t}Bu-imm)-*N*-ani with $Ti(NMe_2)_2Cl_2$ gave a Ti macrocyclic complex.

Table of Contents

Chapter 1 – Introduction to *N*-Heterocyclic Carbenes.

Chapter 2 - Imidazolium Salts and Imidazol-2-ylidenes.

Chapter 3 - *N*-Heterocyclic Carbene Complexes of Silver.

Chapter 4 - *N*-Heterocyclic Carbene Complexes of Palladium.

Chapter 5 - The Heck Reaction.

Chapter 6 - *N*-Heterocyclic Carbene Complexes of Nickel.

Chapter 7 - Amido / Imino Mixed Donor Ligand Systems and their Titanium and Zirconium Complexes

Chapter 8 - Conclusions

List of Figures

Chapter 1 – Introduction to *N*-Heterocyclic Carbenes.

Chapter 2 - Imidazolium Salts and Imidazol-2-ylidenes.

Chapter 3 - *N*-Heterocyclic Carbene Complexes of Silver.

Chapter 4 - *N*-Heterocyclic Carbene Complexes of Palladium.

Chapter 5 - The Heck Reaction.

Chapter 6 - *N*-Heterocyclic Carbene Complexes of Nickel.

Chapter 7 - Amido / Imino Mixed Donor Ligand Systems and their Titanium and Zirconium Complexes

Chapter 8 - Conclusions

Acknowledgements

Thanks go to Dr Andreas Danopoulos for guiding me through the past three years, to Dr Arran Tulloch for his good advice and help, Dr Sven Kleinhenz for his interesting outlook on safety in the laboratory, and his late night crystallographic work and Dr Steven Fiddy for all of his helpful discussions.

The inhabitants of Lab 2007 and the second floor of building 30 without doubt deserve a special mention, especially Mahoney, Tackleberry and even the singing High Tower for keeping spirits high and being good friends. Also thanks are more than due to Matt Cheetham for providing endless drinking fun, inventions and being a great Housemate.

The mountain folk of Camp X-ray must also be thanked, especially Dr Mark Light and Dr Simon Coles for teaching me crystallography (bet they regretted that) and the others downstairs who provided an out of lab asylum over the past few years.

An extra large thanks goes to Lucy, who has supported me through the final stages of completing this work which otherwise may well have seen it 'do-a-Shawn' and to my parents for giving me the support I needed to get to and go through my degree and PhD.

Thanks also go to the University of Southampton for supporting this work.

Glossary of Abbreviations

Me	methyl
Et	ethyl
^{i}Pr	*iso*-propyl
^{t}Bu	*tert*-butyl
Cp	cyclopentadiene
Cp^{-}	cyclopentadienyl
Ph	phenyl
R	general alkyl/aryl group
THF	tetrahydrofuran
THT	tetrahydrothiophene
MAO	methylalumoxane
COD	1,5-cyclooctadiene
BIPY	2,2'-bipyridine
Cy	cymene, 4-*iso*-propyltoluene
DME	dimethoxyethane
TMEDA	N,N,N',N'-tetramethyl-ethane-1,2-diamine
BARF	$B(C_6F_5)_3$
TMIY	1,3,4,5-tetramethylimidazol-2-ylidene
Brookhart's Acid	$[H(OEt_2)_2][B\{3,5\text{-}(CF_3)_2C_6H_3\}_4]$
DBA	dibenzylideneacetone
BINAP	[1,1'-binaphthalene]-2,2'-diylbis(diphenylphosphine)
DMSO	dimethoxysulfoxide
X	halide
o-	*ortho-*
m-	*meta-*
p-	*para-*
NMR	Nuclear Magnetic Resonance
$\delta_{H/C}$	chemical shift (^{1}H / ^{13}C)
ppm	parts per million
s	singlet
d	doublet
t	triplet
m	multiplet
br	broad
v.br	very broad
Hz	hertz
m/z	mass to charge ratio

Literature Publications Associated with this Thesis

'Chelating and 'pincer' dicarbene complexes of palladium; synthesis and structural studies' S. Winston, A. A. Danopoulos, A. A. D. Tulloch, G. Eastham and M. B. Hursthouse. *J. Chem. Soc., Dalton Trans*, **2003**, 1009.

'Functionalised and chelate heterocyclic carbene complexes of palladium; synthesis and, structural studies', A. A. Tulloch, S. Winston, A. A. Danopoulos, M. B. Hursthouse and R. P. Tooze. *J. Chem. Soc., Dalton Trans*, **2003**, 699.

'(Alkyliminomethyl)phenylamido complexes of zirconium and titanium', R. Porter, S. Winston, A. A. Danopoulos, M. B. Hursthouse, *J. Chem. Soc., Dalton Trans*, **2002**, 3290.

'C-H activation with *N*-heterocyclic carbene complexes of iridium and rhodium', A. A. Danopoulos and S. Winston, *J. Chem. Soc., Dalton Trans*, **2002,** 3090.

'Stable N-functionalised 'pincer' bis carbene ligands and their ruthenium complexes; synthesis and catalytic properties', A.A. Danopoulos, S. Winston, W. Motherwell, *Chem. Commun,* **2002**, 1376.

'Synthesis and structural characterisation of stable pyridine- and phosphine-functionalised *N*-heterocyclic carbenes', A. A. Danopoulos, S. Winston, T. Gelbrich, M. B. Hursthouse and R. P. Tooze, *Chem ,Commun.,* **2002**, *5*, 482.

'*N*-Functionalised heterocyclic carbene complexes of silver', A. A. D. Tulloch, A. A. Danopoulos, S. Winston, S. Kleinhenz, G. Eastham, *J. Chem. Soc., Dalton Trans.,* **2000**, 4499.

Chapter 1

Introduction to

N-Heterocyclic Carbenes

Chapter 1

Introduction to *N*-Heterocyclic Carbenes

1.1 Introduction.

Eleven years ago Arduengo and co-workers described a novel synthetic route to isolatable, stable, *N*-heterocyclic carbenes (NHCs) by deprotonation of the sterically bulky 1,3-di-adamantyl-imidazolium salt precursor using sodium hydride with catalytic amounts of DMSO anion in THF. They obtained structural characterisation of the imidazol-2-ylidene by single crystal X-ray crystallography (Fig 1.1).[1]

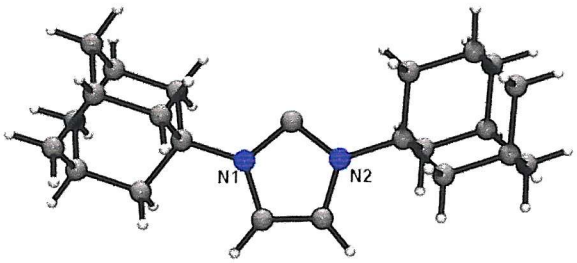

Fig 1.1 Crystal structure of 1,3-di-adamantylimidazol-2-ylidene.

This achievement refuelled an interest in an area of chemistry that originated in two laboratories in Germany in the 1960's, when research groups led by Öfele[2] in München and Wanzlick[3] in Berlin reported the first metal complexes of NHCs. They had reacted imidazolium salts with metallic precursors containing ligands of sufficient basicity (i.e. metal acetates or oxides) to deprotonate the imidazolium salt and *in situ* form imidazol-2-ylidene complexes of mercury and chromium. Wanzlick reported the isolation of a 'monomeric carbene' species as he believed he had characterised the 1,3-bis(phenyl)imidazolin-2-ylidene but had actually isolated the dimerised compound (Fig 1.2).[4]

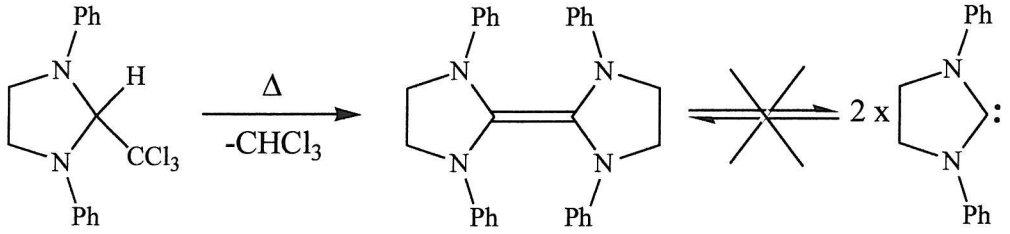

Fig 1.2 Wanzlick's dimer

More recently studies have shown that although Wanzlick only characterised a dimeric species, in solution with less sterically bulky substituents on the carbene there is an equilibrium between the dimer olefin and monomeric carbene.[5] Lappert and co-workers continued this work and developed synthetic routes to transition metal mono-NHC complexes from these dimers.[6] Metal complexes of NHCs have raised a large interest in academia over the last twelve years as it has been reported that specific metal NHC complexes show comparable high catalytic activities to the analogous trialkylphosphine complexes, but are more thermally stable and more tolerant to oxygen and water. With the constant refinement and functionalisation of NHC complexes, NHCs are becoming very popular which is shown by the many recent reviews.[7-11]

1.2 Classification of carbenes and their metal complexes.

Carbenes have played an important role in organic chemistry since their discovery in the 1950's by Skell.[12] They are two coordinate carbon species that carry no formal charge and contain two non-bonding electrons; the carbon can be considered to be in an oxidation state (II). Carbenes are highly reactive and a transient species, which cannot be easily isolated unless stabilised. There are two electronic states a carbene can take, singlet or triplet, depending on its spin-multiplicity in the ground state. A singlet state is achieved when the two non-bonding electrons of the carbene carbon are paired; the carbene is characteristically bent having adopted sp^2 hybridisation. The triplet state is achieved when the two non-bonding electrons are unpaired; typically the carbene carbon is near linear adopting *sp* hybridisation (Fig 1.3).

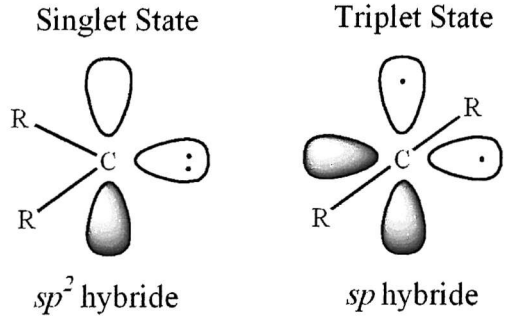

Fig 1.3 Ground state configurations of carbenes. R = substituents.

The singlet and triplet carbenes have very different electronic characteristics. The singlet carbene possesses a filled orbital in the carbon plane and a vacant orbital perpendicular to it,

therefore behaves as a Lewis base (electron donating through the lone pair) and a Lewis acid (electron accepting due to the empty *p*-orbital). The triplet carbene having two unpaired electrons instead behaves more as a diradical. The ground state of the carbene is dependent on its substituents, usually non-substituted or alkyl-substituted carbenes exist in the triplet ground state whereas heteroatom (O, N, S, Cl) substituents result in the stabilisation of the singlet state, through inductive and mesomeric effects.[7]

Research led by Fischer[13] and Schrock[14] resulted in a second formal categorisation of carbenes when coordinated to a metal fragment. In Fischer type carbene complexes the carbene carbon has heteroatom substituents and shows behaviour typical of electrophiles whilst in Schrock type carbene complexes the divalent carbon is substituted by alkyl or hydrogen groups and shows behaviour typical of nucleophiles. Fischer type carbene complexes show considerably less π-bonding between the metal and the carbon atom than that of the Schrock type carbenes (alkylidenes). Fischer carbene complexes have their HOMO centred on the metal and their LUMO centred on the carbon and the reverse of this is true of the Schrock case.

1.3 Stable Carbenes

The number of known stable carbenes is increasing rapidly.[7] However, there has been only limited research into triplet carbenes due to their highly unstable nature. The most stable triplet carbene (fig 1.3) has a half-life of only 16 seconds at room temperature in solution, although it is indefinitely stable in a crystalline form, or under cryogenic conditions.[15]

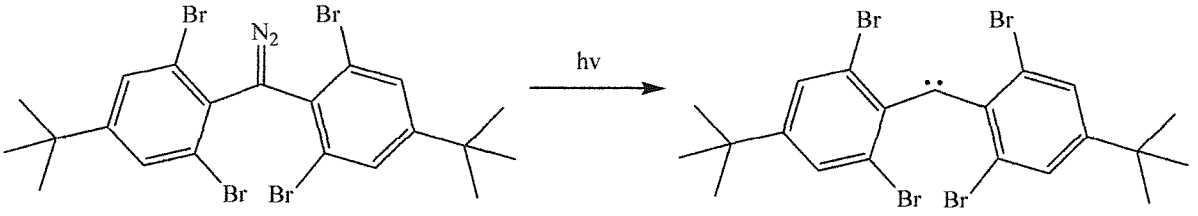

Fig 1.4 Stable triplet carbene.

Known triplet carbenes with bulky aryl substituents have only half-lives of fractions of milliseconds, which makes their study problematic.[15] Furthermore all triplet carbenes form

self-coupled by-products *via* decomposition. It is the large steric bulk of their substituents that retards the dimerisation, stabilising them for their somewhat brief existence.

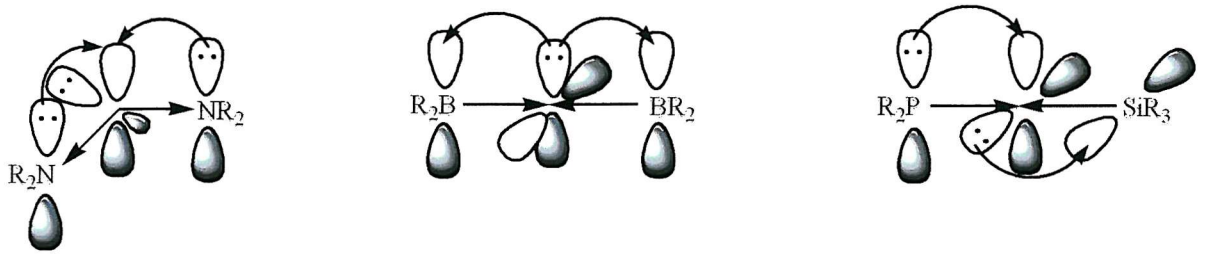

Diaminocarbene Diborylcarbene Phosphinosilylcarbene

Fig 1.5 σ and π-electronic stabilising effects in singlet carbenes.

Singlet carbenes are stabilised by appropriate choice of their substituents. In fact several are now indefinitely stable as solids and have defined melting points without decomposition.[1] The stabilisation can either be due to steric and/or electronic factors. Substituents can influence stability on the grounds of inductive effects depending on their relative electronegativity and mesomeric effects depending on overlap of any lone pairs of electrons with empty orbitals; these effects are exemplified in Fig 1.5 for three different species. In the bent diaminocarbene, the nitrogens are σ-attracting, but the lone pairs contribute to π-back donation to the empty out-of-plane carbon *p*-orbital resulting in a four-electron three-centre π–system and can be described as a push – push mesomeric, pull – pull inductive effect. Interestingly, the diboryl carbene is linear, yet a singlet carbene, and the boron is a σ-donating, π-accepting group described as a push – push inductive, pull – pull mesomeric effect. This species has a two-electron three-centre π–system. No diboryl carbenes have been isolated, but several 'masked' borylmethyleneboranes have been characterised and are considered as the masked analogues of diboryl carbenes.[16-18] The phosphinosilyl carbene shows a π-donor and π-acceptor situation that has a push – pull mesomeric effect and the inductive effect is not the primary stabilising effect.

The decomposition of singlet carbenes differs from the triplet species due to the ambiphilic nature of the former. Decomposition can occur *via* a unimolecular intramolecular 1,2-migration (Fig 1.6) from substituent to the carbene carbon.[19, 20] These concerted in-plane migrations have been shown to be impossible for aromatic carbenes such as imidazol-2-

ylidenes due to the overlap of molecular orbitals and it has more recently shown that it is an intermolecular 1,2-shift not intramolecular shift for these compounds.

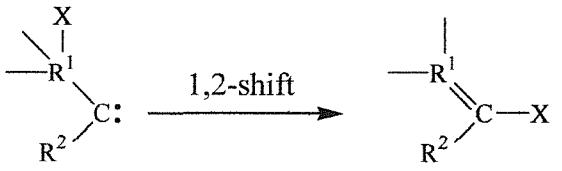

Fig 1.6 Intramolecular decomposition of singlet carbenes, R^n = substituent heteroatom.

As with triplet carbenes dimerisation of two carbene centres to form the double bonded product is also observed, although the mechanism of dimerisation differs from that of triplet carbenes (Fig 1.7).

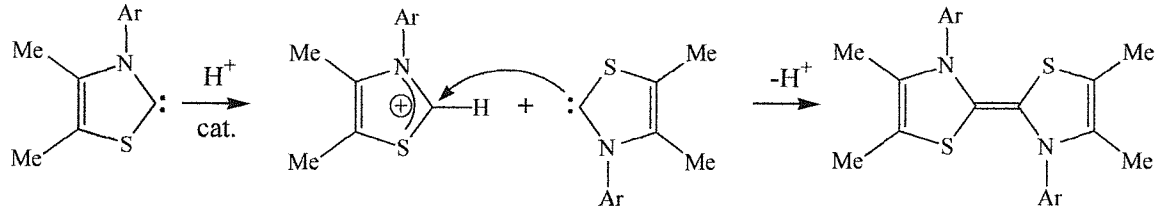

Fig 1.7 Observed dimerisation of singlet NHC's.

Decomposition *via* dimerisation does not occur without some form of catalytic acidification and so is more appropriate to consider any dimerisation of these species as the nucleophilic attack of a carbene on its conjugate acid, followed by proton elimination.[21-25]

1.4 *N*-Heterocyclic Carbenes

N-Heterocyclic carbenes are part of a larger family of singlet aminocarbenes as shown in fig 1.8. They are stabilised both sterically by bulky substituents and electronically by the lone pairs on adjacent heteroatoms (Fig 1.5).

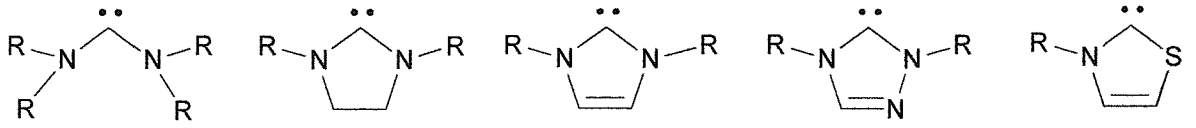

Fig 1.8 Aminocarbenes, R = substituent.

The NHCs are best described as the superposition of two zwitterionic species, as can be seen from the resonance forms shown in Fig 1.9. The unsaturated backbone in the imidazol-2-ylidenes introduces aromaticity as an additional stabilising factor. Theoretical studies into the aromaticity of saturated imidazolin-2-ylidenes versus unsaturated imidazol-2-ylidenes have shown the unsaturated imidazol-2-ylidene is approximately 20 kcal mol^{-1} more stable than the saturated species, however the major stabilising force is the nitrogen π-donation contributing 70 kcal mol^{-1} to the system.[26, 27] A recent study has drawn similar conclusions although marks the differences between carbene substituents, but still finds significant delocalisation of the π-system of imidazol-2-ylidenes.[28]

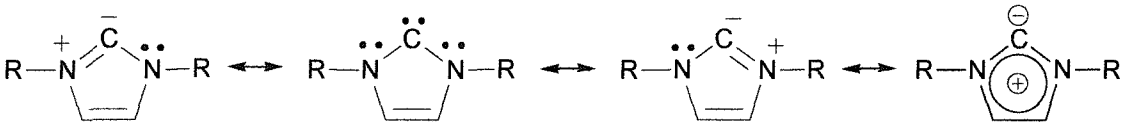

Fig 1.9 Resonance of the π-orbitals in an *N*-heterocyclic carbene R=alkyl, aryl.

Since the pioneering work of Ofele[2] and Wanzlick[3] different methods have been established for the preparation of NHCs by deprotonation of the imidazolium salt precursors. Arduengo reported deprotonation using sodium hydride or potassium hydride with catalytic amounts of DMSO anion or potassium *tert*-butoxide.[1] Herrmann and co-workers reported an improvement to Arduengo's method by carrying out the deprotonation in liquid ammonia, which dramatically reduced reaction times.[29] Kuhn described the reduction of the imidazol-2-thione precursor using potassium in boiling THF[30] and Enders and co-workers accomplished the synthesis of phenyl substituted 1,2,4-triazol-5-ylidenes by the thermal elimination of methanol, an adaptation of Wanzlick's route which this time successfully gave carbenes.[31] Enders triazole carbene became the first commercially available 'free' carbene species from Acros Organics.

The stability of these species has led to the introduction of a vast array of substituents on the nitrogen groups of the imidazol-2-ylidenes ranging from simple alkyl chains to chiral groups,[32] ringed species such as cyclophanes,[33] ferrocenyl[34] and NHCs immobilised onto polymer supports.[35] There has also been various compounds synthesised with linkages between units of imidazol-2-ylidenes to give multidentate bis- and tri-carbene species.[29, 36]

1.5 Metal Complexes of *N*-Heterocyclic Carbenes

There is growing interest in the use of NHCs as ligands on transition metals.[7, 9, 37] NHCs behave as two electron, σ-donor ligands, and in this respect they are related to ethers, amines and trialkylphosphines with regards to their coordination chemistry. They bind strongly to transition metals through metal-carbon σ-bonds and are considered to be stronger σ-donors than amines.[38,39] In fact it has been proposed that they have pronounced σ-donor properties similar to electron-rich trialkylphosphines[40] and that π-backbonding from the metal is insignificant.[41] Nolan and co-workers concluded from studies that NHCs behave as better donors than the phosphines after measuring 'titrations' of $TiCl_4.2PR_3$ with two equivalents of NHC to give the $TiCl_4.2NHC$ and similar behaviour was noted with vanadium.[42, 43] Cloke and co-workers have also reported ligand exchanges between $Pd(PR_3)_2$ and $Pd(NHC)_2$ in solution showing that the NHC is a labile species even though strongly bound.[44]

There are three commonly used procedures for the synthesis of NHC transition metal complexes (Fig 1.10).

A. *In situ* deprotonation of imidazolium salts in the presence of a metal precursor,[45]

B. Reaction of an isolated 'free' NHC with an appropriate metal precursor,[46]

C. Transmetallation of the NHC from a suitable metal precursor.[47]

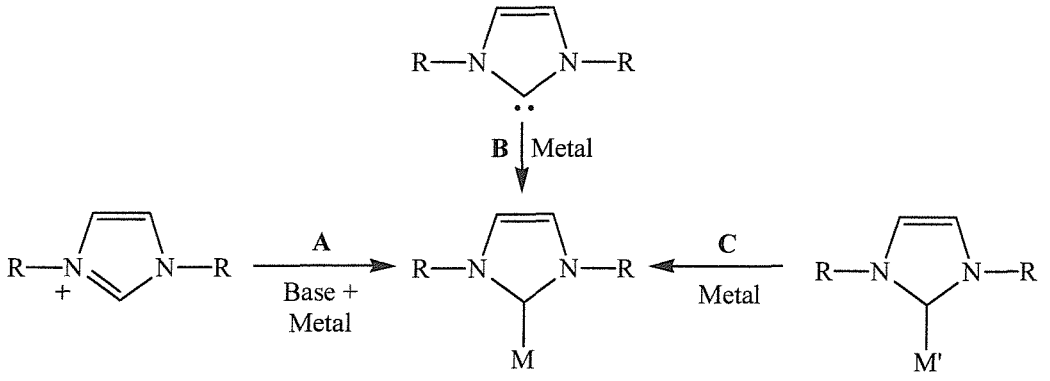

Fig 1.10 Methods of synthesising NHC metal complexes, M, M' = metal, R = substituents.

Route **A** (Fig 1.10) shows the *in situ* formation of the imidazol-2-ylidene from the precursor imidazolium salt, which is then trapped onto a metal by displacing another ligand. This method can also be applied by using metal precursors with ligands of sufficient basicity to complete the deprotonation, such as metal acetates or oxides.

Route **B** demonstrates a similar method, but instead the carbene has been pre-formed and isolated, giving enhanced control of the reaction by eliminating the possibility of base induced side reactions with other components and as a route has improved atom economy.

Route **C** shows transmetallation involving the use of a precursor metal complex where the metal-carbene bond is weaker than that of the product metal-carbene bond. Silver complexes have shown to be excellent in performing clean and high yielding transmetallations.[47-49]

Many NHC complexes have been characterised, with several examples having been reported by the founders of this chemistry[2, 3] and others with various mono- and bis-carbene complexes,[50] bimetallic species[51] and mixed donor chelating complexes[9, 49, 52-54] having been isolated. Such is the interest in the field of NHCs and their varied uses that out of the transition elements it is only technetium that has no known NHC complexes, due presumably only to its limited lifetime. NHC complexes of the lanthanides and actinides are known with complexes of lanthanum, samarium, europium, ytterbium and uranium having been characterised.[55-59] There are many reviews covering the area.[9, 37, 60] There are over 100 metal complexes of NHCs reported on the Cambridge Structural Database and this figure is constantly growing.

1.6 Ligand Architecture and Catalysis

The thermal stability and chemical inertness of the metal-carbene bond makes these ligands ideal as ancillary anchors in organometallic catalysis. High thermal robustness and stability is not the only advantage,[53] as NHCs have significant scope for electronic and steric tuning as is shown in Fig 1.11.

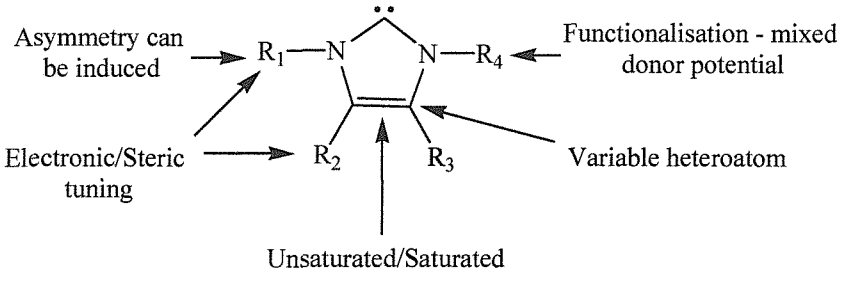

Fig 1.11 Tuning opportunities in NHCs.

The ability to functionalise the imidazol-2-ylidene with other donor atoms opens many options for designing ligands with high potential in catalysis. For example, it is possible to design a ligand that contains donor groups that are 'dangling' in a precatalyst, but could provide electronic stabilisation for a catalyst during dormant periods after activation minimising decomposition.[61] Bridging or chelating systems can be designed and chirality can be induced on a metal centre through incorporation of chiral substituents on the ligand backbone[62] or through chirality in the functional group as shown in the rhodium complexes in Fig 1.12.[63, 64]

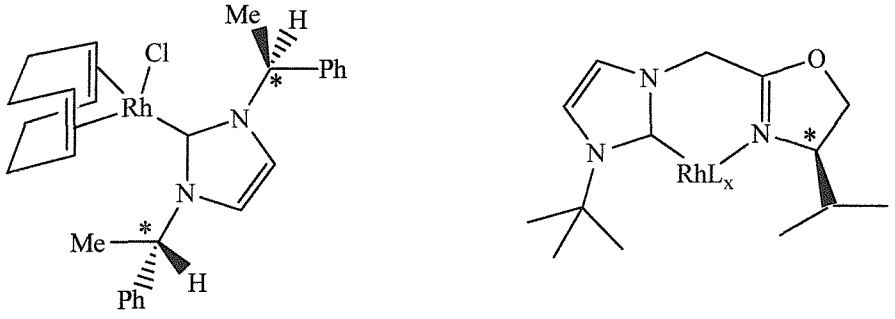

Fig 1.12 Chiral NHC precatalysts used for Hydrosilylation.

Functionalisation of the heterocyclic ring and its substituents give rise to a plethora of potential ligand designs that only is limited by synthetic viability.

It has been shown that late transition metal carbene complexes are often remarkably stable towards oxygen denature and have high thermal stability. As NHCs have similar metal bonding properties to the well-utilised trialkylphosphines, it is no surprise that their use as catalyst spectator ligands is being continuously investigated.[8] Traditionally, group 10 metal-trialkylphosphine complexes have proven to be the most active precatalysts for a variety of C-C coupling reactions with the earliest commonly used precatalysts being $Pd(PPh_3)_4$ or $Pd(PPh_3)_2Cl_2$. Since these precatalysts a wide range of supporting ligands have been reported for individual coupling processes, far too many to describe here.[65] However, these simple trialkylphosphine complexes are still the benchmark for many activity comparisons. Recently they have been used to activate the cheaper aryl chloride substrates, sparking industrial interest.[66, 67] With the advent of 'free' imidazol-2-ylidenes[1] it was no surprise that research efforts focused on the use of the new ligands as catalyst spectators.[8]

Heck catalysis involving metal NHC precatalysts will be described in this thesis but reports describing improving catalytic activity in other C-C coupling reactions such as Suzuki couplings,[68] Stille coupling (tin reagents/aryl halide),[65] Sonogashira coupling (alkyne/aryl halide),[8] Kumada coupling (Grignard/aryl halide),[69] CO-ethylene co-polymerisations,[70] aryl amination[71, 72] and hydrosilylation[63] are constantly appearing in the literature through the ability to design ligands for specific reactions.

1.7 The Heck Reaction

The arylation and vinylation of alkenes with aryl or vinyl halides was first achieved over 30 years ago independently by Mizoroki[73] and Heck,[74] although now the process is known universally as the Heck reaction (Fig 1.13).[75-77] Until 1988 papers reporting the Heck reaction were few and far between, but by the late 1990's this had rapidly changed with continuous reports on the process.[78, 79]

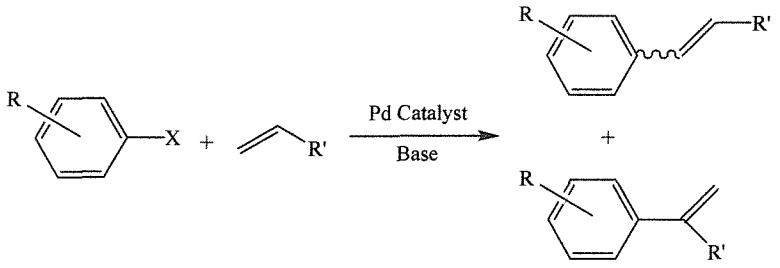

Fig 1.13 The Heck reaction.

The Heck reaction is of industrial importance, one reported use being in the production of Prosulfuron®, a brand name herbicide manufactured by Novartis.[80] The Heck coupled product is shown in Fig 1.14 along with the final product.

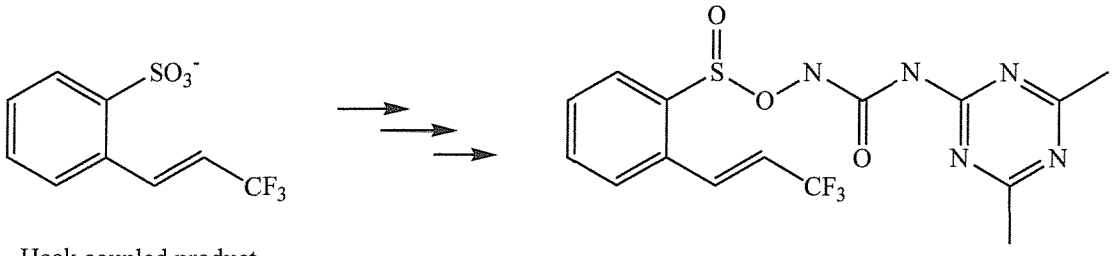

Heck coupled product

Prosulfuron

Fig 1.14 Intermediate produced from Heck catalysis (left) and Prosulfuron (right).

Heck catalysis can be carried out utilizing any source of palladium that allows the palladium to reach an oxidation state of zero, which is believed to be necessary for the oxidative

addition of the aryl-halide bond. $Pd(OAc)_2$ and Pd/C are known active catalysts in the Heck reaction for the coupling using aryl iodides and bromides.[75] Initial publications in this field reported that these systems rapidly dropped palladium black, which limited their use until it was realised that the addition of phosphines to the reaction mixture stabilised the active palladium species, increasing lifetime and yields.[81] Fu and co-workers reported that the use of $Pd_2(DBA)_3$ with $P(^tBu)_3$ was successful in activating aryl chlorides,[82] but the need of an inert atmosphere with the easily oxidiseable $P(^tBu)_3$ limits industrial interest. Jensen and co-workers recently reported a tridentate phosphinito system which also gave extremely high yields for the coupling of aryl chlorides with styrene.[83] The use of trialkylphosphines inevitably led on to the use of NHC precatalysts as mimics of these systems[84] and to date there are NHC precatalysts that match the activity of the phosphine systems at coupling activated aryl chlorides (Fig 1.15).[48, 84]

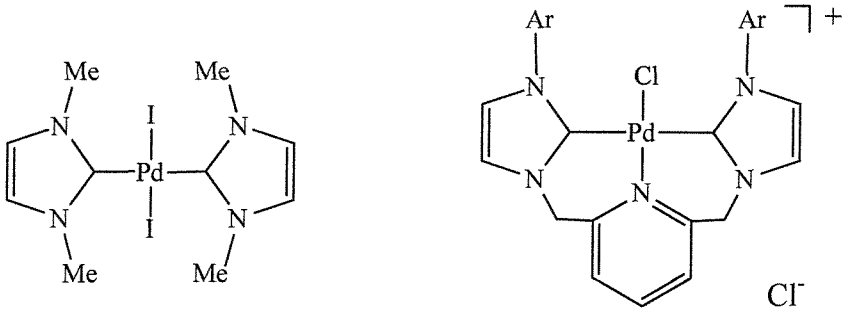

Fig 1.15 NHC precatalysts active for coupling activated aryl chlorides. Ar = mesityl, 2,6-di-*iso*-propylphenyl.

Current research is aimed at obtaining an NHC catalyst that is active for the cheaper aryl chlorides, as then the use of expensive unrecoverable palladium catalysts could be industrially justified. The first example of a chiral bidentate bis-carbene palladium and nickel complex was reported recently that was active for Heck coupling but no enantiomeric results have been disclosed.[85] Further discussion of the mechanism and the Heck reaction can be found in Chapter 5.

1.8 Background to this Project

This project continues work initiated by the Danopoulos Group into palladium-based pyridine functionalised imidazol-2-ylidene complexes for use as precatalysts for C-C coupling reactions.[48]

Initial reports described the production of a range of novel pyridine, methoxy and phosphine functionalised imidazolium salts of the form shown in Fig 1.16. Good synthetic routes were established for the synthesis of the pyridine functionalised imidazolium salts and from these ranges of silver, copper and palladium complexes were prepared. Examples of nickel, rhodium and ruthenium NHC complexes were also characterised.[48]

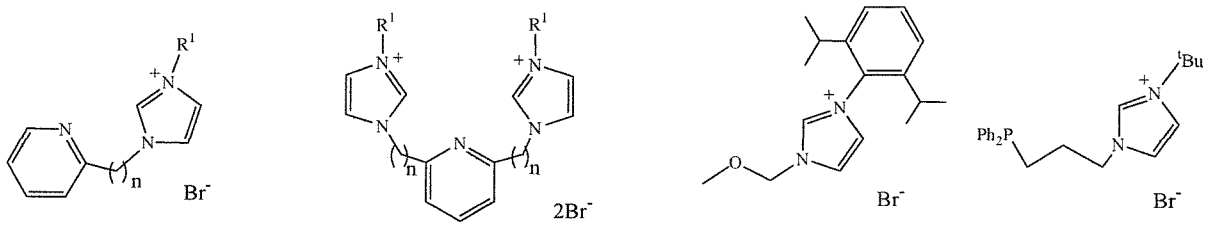

Fig 1.16 Previously synthesised functionalised imidazolium salts, n = 0, 1, R = *tert*-butyl, mesityl, 2,6-di-*iso*-propylphenyl.

Synthetic routes to palladium(II) imidazol-2-ylidene complexes were reported based on two of the three known methods of making NHC complexes, *in situ* deprotonation of imidazolium salts and transmetallation from silver (I) precursors.

It was reported that palladium(II) mono-imidazol-2-ylidene complexes could successfully be prepared using *in situ* deprotonation of the pyridine functionalised imidazolium salt precursors and trapping the imidazol-2-ylidene with Pd(COD)MeBr to give complexes of the form Pd(Ligand)MeBr.[86] Attempts were made to isolate the 'free' functionalised carbene, 1-picolyl-3-(*tert*-butyl)-imidazol-2-ylidene, which met with limited success. Deprotonation using lithium di-*iso*-propylamide led to a red solid that could not be identified. Observation of the stable carbene *in situ* was possible by proton NMR spectroscopy, but upon attempted isolation the imidazol-2-ylidene rapidly decomposed to an intractable mixture. It was believed that the methylene bridge or *tert*-butyl functionality were susceptible to attack by another imidazol-2-ylidene causing decomposition.[48]

The use of transmetallation reagents to exchange an NHC between silver(I) and late transition metals was reported by Lin and co-workers who used silver NHC complexes as precursors to palladium NHC complexes.[87] This methodology was adapted to suit these novel pyridine functionalised imidazolium salts and the use of silver(I) oxide afforded the desired

silver NHC halide complexes. Structural study of these complexes showed a variety of NHC ligand environments coordinated to the silver centre, mono- and bis-NHC silver complexes were characterised. There was no determinable reason as to why some silver complexes existed as Ag(ligand)X and others as $[Ag(ligand)_2]^+[AgX_2]^-$ where X = halide.[88] Copper analogues of these complexes were also prepared using similar methodology and again a variety of structural motifs were identified from the products.[89]

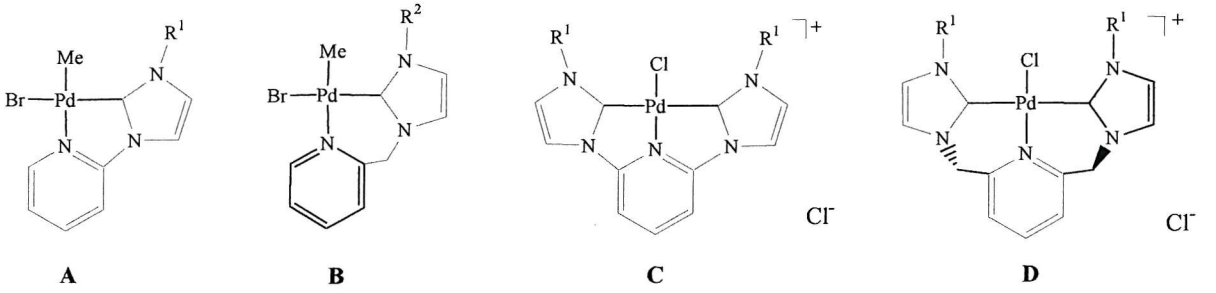

Fig 1.17 Palladium (II) NHC complexes previously characterised, R^1 = mesityl, 2,6-di-*iso*-propylphenyl, R^2 = *tert*-butyl, mesityl, 2,6-di-*iso*-propylphenyl

From the silver NHC transmetallation reagents a variety of palladium(II) NHC complexes were prepared (Fig 1.17) by reaction with Pd(COD)MeBr or $Pd(COD)Cl_2$. These complexes contained bidentate mono-carbene chelates or tridentate bis-carbene chelating ligand systems. An interesting and important feature of the bis-carbene chelates is the effect of increasing the chelate ring size by the incorporation of a methylene bridge (complex **C** and **D**, fig 1.15).

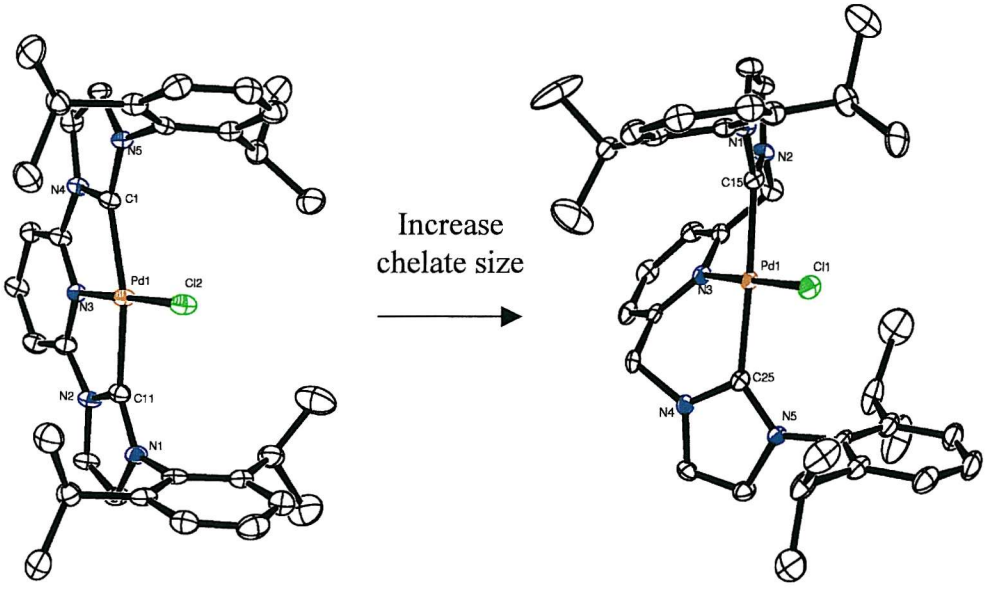

Fig 1.18 Crystal structures of **C** (left) and **D** (right), anions and hydrogens removed for clarity.

The increase in chelate size to six members has a dramatic effect on the shape of the complex. The five-membered chelate complex is planar, but the six-membered chelate complex contains a C_2 symmetrical twist through the complex (Fig 1.18).[62] This twist is not just a solid state effect, by addition of the chiral discriminating agent Pirkle's Acid [*S*-(+)-2,2,2-trifluoro-1-(9-anthryl)ethanol] to a solution of complex **D**, binding of the agent to one of the enantiomers is observed in the proton NMR. The most notable change in the spectrum was the peaks from the *iso*-propyl groups changing from four to eight doublets (Fig 1.19). The eight peaks are observed up to 80°C showing the rigidity of the ligand and that a high energy barrier exists for enantiomer interconversion.[62] Similar C_2 twists were observed for the mesityl analogue and others have reported similar observations when simple alkyl substituents replace the aryl groups showing that these have little effect on this twist and it is purely the chelate ring sizes.[90]

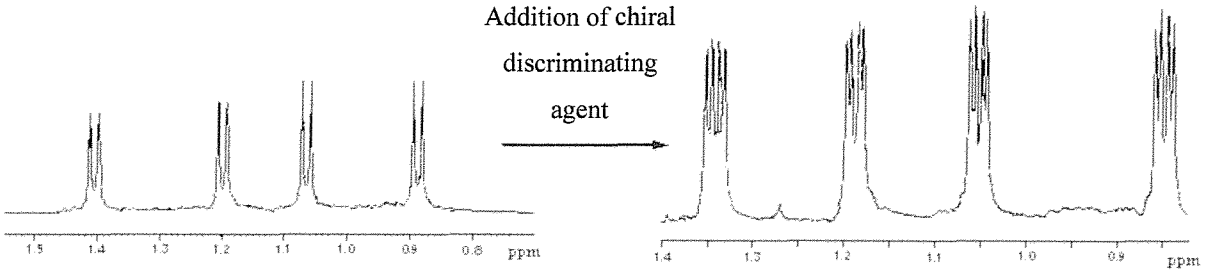

Fig 1.19 NMR changes of *iso*-propyl protons on addition of Pirkle's Acid to complex **D**.

Complexes of type **A** - **D** were extensively tested as precatalysts for the Heck reaction[75, 91] and initial tests for amination activity were performed. From the resulting activity of the precatalysts shown in Fig 1.17 the following conclusions were drawn about comparative Heck C-C coupling ability:[48, 86]

1. All precatalysts were excellent at coupling aryl iodides, comparable to the best known systems,[92]
2. Tridentate ligand complexes showed greater activity than bidentate ligand complexes for coupling aryl bromides, both showed low activity towards aryl chlorides,
3. The larger the chelating ring size the higher the activity for bidentate ligands,
4. Chelating ring size has no effect for tridentate ligands.

Synthesis involving other transition metals resulted in the isolation and characterisation of the following M(II) complexes (Fig 1.20).

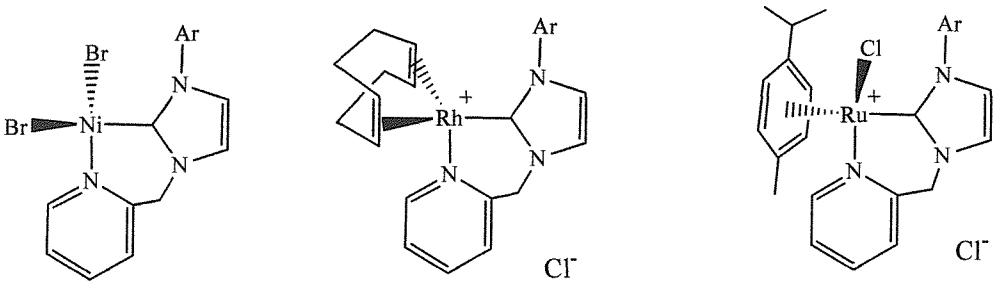

Fig 1.20 Nickel, rhodium and ruthenium imidazol-2-ylidene complexes characterised, Ar = mesityl.

The nickel complex was the first example of a mixed donor *N*-heterocyclic carbene complex of nickel; structural data was obtained for the nickel and rhodium complexes. Since these initial complexes[48] were reported we have described preliminary results on the C-H activation in iridium (**E**, Fig 1.21) and rhodium (**F** and **G**, Fig 1.22) complexes as depicted in.[61] Two interesting features are noted in this system. The first is that when iridium is used there is a preference for C-H activation to occur in favour of pyridine binding to the metal centre. C-H activation in iridium complexes is not unusual and, as will be described in the next section, can occur at unexpected places.[93]

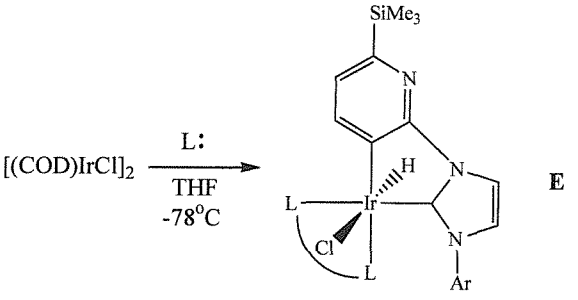

Fig 1.21 C-H activation in iridium NHC complexes. L: = 'free' carbene, L-L = COD.

The second feature is the nature of the complex of rhodium (Fig 1.22). Initially the square planar metal (**F**) centre comprises the carbene carbon, cyclooctadiene and a chloride; the pyridine nitrogen remains uncoordinated, pointing away from the metal centre. There is a close contact between the rhodium and the H on the pyridine ring, Rh – H = 2.532 Å showing the tendency, as in the iridium complex, towards activating the C-H bond.

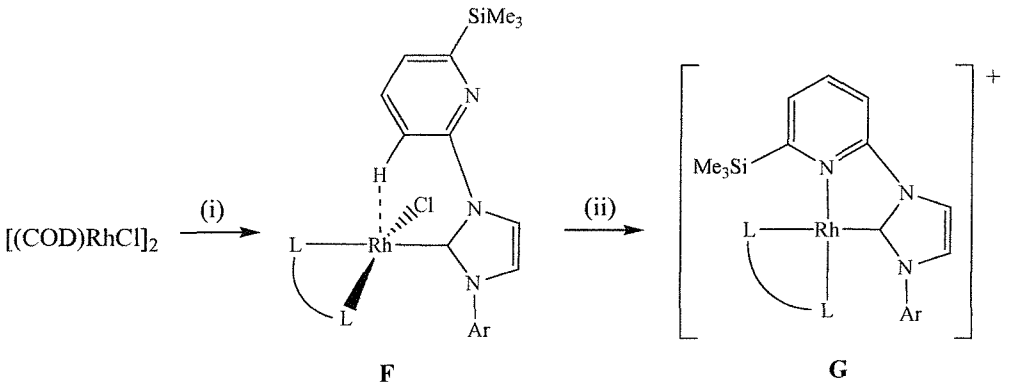

Fig 1.22 Variable ligand coordination in a rhodium NHC complex. (i) 1eq 'free' carbene in thf, -78°C to room temperature, (ii) $Na\{B[3,5\text{-}C_6H_3(CF_3)_2]_4\}$ in diethylether. L-L = COD

In order to test whether the C-H bond would activate, the chloride was exchanged for a bulky non-coordinating anion by exchange with tetrakis[3,5-bis(trifluoromethyl)phenyl]borate (Brookhart's anion). The complex did not C-H activate but instead instantaneously formed the air stable salt **G** in quantitative yield, in which the pyridyl functional group swings in to coordinated to the metal. It is plausible to assume that pre-dissociation of the chloride is necessary before the coordination of pyridine occurs.[61] The hemilability of the pyridine demonstrates how this ligand architecture is flexible and the possibilities of alternating binding modes when supporting an activated species.

1.9 Some Unusual Structural Properties of NHC Complexes

With the increased activity in the research of NHC complexes unexpected properties have begun to become apparent. Crabtree and co-workers have fully characterised iridium complexes of type **H** containing an alternative C-H activated heterocyclic ring leading to 'abnormal' binding of the NHC as shown in Fig 1.23.[94, 95]

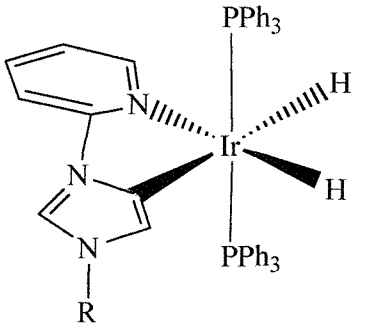

H

Fig 1.23 Reverse binding of NHC, R = Me, n-Bu, ^{i}Pr, mesityl.

By using the mesityl substituted ligand it was possible to isolate an important intermediate of this transformation and characterise it by X-ray crystallography.

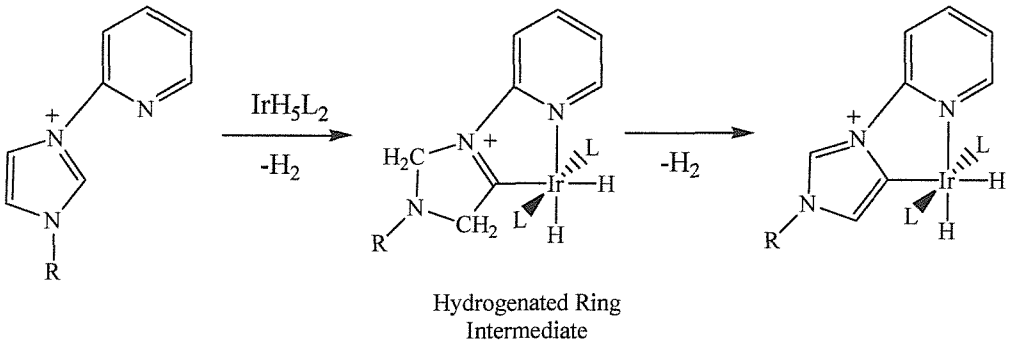

Fig 1.24 Intermediate during abnormal binding of NHC. L = PPh_3, R = mesityl.

In the structure of the intermediate it is clear that the nitrogen bearing the mesityl group has regained sp^3 hybridisation as tetrahedral geometry is observed about the nitrogen. The factor considered responsible for the formation of these 'abnormal' carbene complexes is related to the nature of the anion of the imidazolium salt. Replacement of the Br^- by SbF_6^- leads to the observation of the abnormal binding. In the ^1H NMR it was interesting to note that the peak corresponding to the imidazolium proton was shifted from 10.5 ppm to 8.5 ppm (in the imidazolium salt) just by the change of the counter-ion, denoting hydrogen bonding effects between the imidazolium and the anion. By further reacting the BF_4^- and PF_6^- salts with $IrH_5(PPh_3)_2$ 1:1 mixtures of the expected C2 and abnormal C5 bound complexes were isolated. From deuterated NMR experiments with IrD_5L_2 it was observed that the imidazol-2-ium proton in the product is not the original imidazolium proton from the salt, but becomes deuterated at some point along the product formation. Currently the exact mechanistic process is still unconfirmed, but by changing the imidazolium counter ion, the imidazolium binding point can be controlled.[95-97]

Cavell and co-workers have shown another behavioural feature of Pd(II) methyl complexes incorporating simple alkyl substituted NHCs.[98] They have observed that these complexes can undergo a concerted reductive elimination (Fig 1.25) of the methylimidazolium cation to give Pd(0). This could have adverse implications on the use of NHC complexes in catalytic systems if this elimination is proven to be ubiquitous, as it would indicate a potential deactivation route of the catalysts.

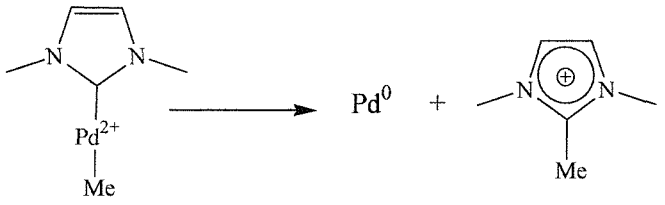

Fig 1.25 Possible reductive elimination of NHC complexes.

Further work into this pathway has shown that this elimination is completely retarded in chelate NHC complexes[99] or under catalytic conditions where kinetically any coupling reaction is found to be favoured relative to reductive elimination.[100] This decomposition pathway may pose problematic for the design of a mono-carbene catalyst that could show living behaviour if at the end of catalytic cycles palladium is ejected from the reaction.

1.10 Aims.

The aims of this research were to further develop the promising Heck catalyst systems previously reported by the Danopoulos Group by:

1. Improving synthetic routes to the Pd(II) precatalysts previously developed by seeking alternatives to the use of silver transmetallation reagents,[88] including the use of the functionalised 'free' imidazol-2-ylidenes.

2. Tuning of the current Pd(II) pyridine functionalised imidazol-2-ylidene complexes by functionalisation of the ligand backbone to study differences in the Heck coupling activity.[48]

3. Exploring synthetic routes to novel nickel(II) pyridine functionalised imidazol-2-ylidene complexes and investigate catalytic activity of the complexes isolated.

4. Further explore amido/imino mixed donor ligand complexes of zirconium and titanium in continuation of previous work.[101]

Summary of the preceding work to this thesis places in context the results described in the following chapters, which extend findings made in the previous few years into the varied chemistry of pyridine functionalised imidazol-2-ylidenes. The investigations into these ligands and their complexes have been reported in a number of publications by us and others who are involved in competing research.[48, 53, 54, 88, 90, 99, 102-105]

1.11 References

[1] A. J. Arduengo, R. L. Harlow, M. Kline, *J. Am. Chem. Soc.*, **1991**, *113*, 361.
[2] K. Öfele, *J. Organomet. Chem.*, **1968**, *12*, 42.
[3] H. W. Wanzlick, H. J. Schöenherr, *Angew. Chem. Int. Ed. Engl.*, **1968**, *7*, 141.
[4] H. W. Wanzlick, E. Schikora, *Angew. Chem.*, **1960**, *72*, 494.
[5] V. P. W. Bohm, W. A. Herrmann, *Angew. Chem. Int. Ed. Engl.*, **2000**, *39*, 4036.
[6] D. J. Cardin, B. Cetinkaya, M. F. Lappert, *Chem. Rev.*, **1972**, *72*, 545
[7] D. Bourissou, O. Guerret, F. P. Gabbai, G. Bertrand, *Chem. Rev.*, **2000**, *100*, 39.
[8] A. C. Hillier, G. A. Grasa, M. S. Viciu, H. M. Lee, C. L. Yang, S. P. Nolan, *J. Organomet. Chem.*, **2002**, *653*, 69.
[9] W. A. Herrmann, *Angew. Chem. Int. Ed. Engl.*, **2002**, *41*, 1290
[10] A. J. Arduengo, *Acc. Chem. Res.*, **1999**, *32*, 913.
[11] T. Weskamp, V. P. W. Bohm, W. A. Herrmann, *J. Organomet. Chem.*, **2000**, *600*, 12.
[12] P. S. Skell, R. S. Sandler, *J. Am. Chem. Soc.*, **1958**, *80*, 2024.
[13] E. O. Fischer, A. Maasböl, *Angew. Chem. Int. Ed. Engl.*, **1964**, *3*, 580.
[14] R. R. Schrock, *J. Am. Chem. Soc.*, **1974**, *96*, 6796.
[15] H. Tomioka, M. Hattori, K. Hirai, S. Murata, *J. Am. Chem. Soc.*, **1996**, *118*, 8723.
[16] A. Berndt, *Angew. Chem. Int. Ed. Engl.*, **1993**, *32*, 985.
[17] A. Berndt, D. Steiner, D. Schweikart, C. Balzeriet, M. Menzel, H. J. Winkler, S. Mehle, M. Unerzagt, T. Happel, P. v. R. Schleyer, G. Subramanian, M. Hofmann, *Advances in Boron Chemistry*, Cambridge, **1997**.
[18] H. Klusik, A. Berndt, *Angew. Chem. Int. Ed. Engl.*, **1983**, *22*, 877.
[19] F. Ford, T. Yuzawa, M. S. Platz, S. Matzinger, M. Fulscher, *J. Am. Chem. Soc.*, **1998**, *120*, 4430.
[20] A. Nickon, *Acc. Chem. Res.*, **1993**, *26*, 84.
[21] L. Nyulaszi, T. Veszpremi, A. Forro, *Phys. Chem. Chem. Phys*, **2000**, *2*, 3127.
[22] S. Sole, H. Gornitzka, O. Guerret, G. Bertrand, *J. Am. Chem. Soc.*, **1998**, *120*, 9100.
[23] A. J. Arduengo, J. R. Goerlich, W. J. Marshall, *Liebigs Ann.-Recl.*, **1997**, 365.
[24] R. W. Alder, M. E. Blake, *Chem. Commun.*, **1997**, 1513.
[25] Y.-T. Chen, F. Jordan, *J. Org. Chem.*, **1991**, *56*, 5029.
[26] C. Boehme, G. Frenking, *J. Am. Chem. Soc.*, **1996**, *118*, 2039.
[27] C. Heinemann, T. Muller, Y. Apeloig, H. Schwarz, *J. Am. Chem. Soc.*, **1996**, *118*, 2023.
[28] M. Tafipolsky, W. Scherer, K. Ofele, G. R. J. Artus, B. Pederson, W. A. Herrmann, G. S. McGrady, *J. Am. Chem. Soc.*, **2002**, *124*, 5865.
[29] W. A. Herrmann, M. Elison, J. Fischer, C. Köcher, G. R. J. Artus, *Chem. Eur. J.*, **1996**, *2*, 772.
[30] N. Kuhn, T. Kratz, *Synthesis*, **1993**, 561.
[31] D. Enders, K. Breuer, G. Raabe, J. Runsink, J. H. Teles, J. P. Melder, K. Ebel, S. Brode, *Angew. Chem. Int. Ed. Engl.*, **1995**, *34*, 1021.
[32] W. A. Herrmann, L. J. Goossen, G. R. J. Artus, C. Köcher, *Organometallics*, **1997**, *16*, 2472.
[33] M. E. Haeg, B. J. Whitlock, H. W. W. Jr, *J. Am. Chem. Soc.*, **1989**, *111*, 692.
[34] B. Bildstein, *J. Organomet. Chem.*, **2001**, *617*, 28.
[35] J. Schwarz, V. P. W. Bohm, M. G. Gardiner, M. Grosche, W. A. Herrmann, W. Hieringer, G. Raudaschl-Sieber, *Chem. Eur. J.*, **2000**, *6*, 1773.
[36] H. V. R. Dias, W. Jin, *Tetrahedron Lett.*, **1994**, *35*, 1365.
[37] W. A. Herrmann, C. Köcher, *Angew. Chem. Int. Ed. Engl.*, **1997**, *36*, 2163.
[38] E. A. Carter, W. A. Goddard, *J. Phys. Chem.*, **1986**, *90*, 998.

[39] S. S. Krishnamurthy, *Curr. Sci.*, **1991**, *60*, 619.
[40] M. F. Lappert, *J. Organomet. Chem.*, **1988**, *32*, 6.
[41] J. C. Green, R. G. Scurr, P. L. Arnold, F. G. N. Cloke, *Chem. Commun.*, **1997**, 1963.
[42] J. Huang, H. J. Schanz, E. D. Stevens, S. P. Nolan, *Organometallics*, **1999**, *18*, 2370.
[43] W. A. Herrmann, K. Ofele, M. Elison, F. E. Kuhn, P. W. Roesky, *J. Organomet. Chem.*, **1994**, C7
[44] L. R. Titcomb, S. Caddick, F. G. N. Cloke, D. J. Wilson, D. McKerrecher, *Chem. Commun.*, **2001**, 1388
[45] D. Enders, H. Gielen, G. Raabe, J. Runsink, J. H. Teles, *Chem. Ber.*, **1996**, *129*, 1483.
[46] A. A. Danopoulos, S. Winston, W. B. Motherwell, *Chem. Commun.*, **2002**, 1376.
[47] H. M. Wang, I. J. B. Lin, *Organometallics*, **1998**, *17*, 972.
[48] A. A. D. Tulloch, PhD thesis, University of Southampton (Southampton), **2001**.
[49] P. L. Arnold, *Heteroatom Chem.*, **2002**, *13*, 534.
[50] M. Albrecht, R. H. Crabtree, J. Mata, E. Peris, *Chem. Commun.*, **2002**, 32.
[51] W. A. Herrmann, P. W. Roesky, M. Elison, G. R. J. Artus, K. Öfele, *Organometallics*, **1995**, *14*, 1085.
[52] P. L. Arnold, A. C. Scarisbrick, A. J. Blake, C. Wilson, *Chem. Commun.*, **2001**, 2340.
[53] E. Peris, J. A. Loch, J. Mata, R. H. Crabtree, *Chem. Commun.*, **2001**, 201.
[54] S. Grundemann, M. Albrecht, A. Kovacevic, J. W. Faller, R. H. Crabtree, *J. Chem. Soc.-Dalton Trans.*, **2002**, 2163.
[55] A. J. Arduengo, M. Tamm, S. J. McLain, C. J. Calabrese, F. Davidson, W. J. Marshall, *J. Am. Chem. Soc.*, **1994**, *116*, 7927.
[56] H. Schumann, M. Glanz, J. Winterfield, H. Hemling, N. Kuhn, T. Kratz, *Angew. Chem. Int. Ed. Engl.*, **1994**, *33*, 1733.
[57] H. Schumann, M. Glanz, J. Winterfield, H. Hemling, N. Kuhn, T. Kratz, *Chem. Ber.*, **1994**, *127*, 2369.
[58] F. Munck, Dissertation thesis, Technische Universitat Munchen (Munchen), **1996**.
[59] G. R. J. Artus, Dissertation thesis, Technische Universitat Munchen (Munchen), **1996**.
[60] M. Regitz, *Angew. Chem. Int. Ed. Engl.*, **1996**, *35*, 725.
[61] A. A. Danopoulos, S. Winston, M. B. Hursthouse, *J. Chem. Soc. Dalton. Trans.*, **2002**, 3090.
[62] A. A. D. Tulloch, A. A. Danopoulos, G. J. Tizzard, S. J. Coles, M. B. Hursthouse, R. S. Hay-Motherwell, W. B. Motherwell, *Chem. Commun.*, **2001**, 1270.
[63] W. A. Herrmann, L. J. Goossen, M. Spiegler, *Organometallics*, **1998**, *17*, 2162.
[64] W. A. Herrmann, L. J. Goossen, C. Köcher, G. R. J. Artus, *Angew. Chem. Int. Ed. Engl.*, **1996**, *35*, 2805.
[65] A. F. Littke, G. C. Fu, *Angew. Chem. Int. Ed. Engl.*, **2002**, *41*, 4176.
[66] *C & EN*, **1998**, *July 13*, 71.
[67] *C & EN*, **1998**, *June 1*, 24.
[68] C. M. Zhang, J. Huang, M. L. Trudell, S. P. Nolan, *J. Org. Chem.*, **1999**, *64*, 3804.
[69] M. Yamamura, I. Moritani, S.-i. Murahashi, *J. Organomet Chem.*, **1975**, *91*, C39
[70] M. G. Gardiner, W. A. Herrmann, C. P. Reisinger, J. Schwarz, M. Spiegler, *J. Organomet. Chem.*, **1999**, *572*, 239.
[71] J. F. Hartwig, *Science*, **2002**, *297*, 1653.
[72] M. S. Viciu, R. M. Kissling, E. D. Stevens, S. P. Nolan, *Org. Lett.*, **2002**, *4*, 2229.
[73] T. Mizoroki, K. Mori, A. Ozaki, *Bull. Chem. Soc. Jpn.*, **1971**, *44*, 581.
[74] R. F. Heck, *Acc. Chem. Res.*, **1979**, *12*, 146.
[75] A. Biffis, M. Zecca, M. Basato, *J. Mol. Catal. A - Chem.*, **2001**, *173*, 249.
[76] I. P. Beletskaya, A. V. Cheprakov, *Chem. Rev.*, **2000**, *100*, 3009.

[77] W. A. Herrmann, *Applied Homogeneous Catalysis with Organometallic Compounds*, Wiley-VCH, Weinheim, **2000**.
[78] W. Cabri, I. Candiani, *Acc. Chem. Res.*, **1995**, *28*, 2.
[79] A. d. Meijere, F. E. Meyer, *Angew. Chem. Int. Ed. Engl.*, **1994**, *33*, 2379.
[80] P. Baumeister, W. Meyer, K. Ortle, G. Seifurt, U. Seigrist, H. Steiner, *Chimia*, **1997**, *51*, 144.
[81] H. A. Dieck, R. F. Heck, *J. Am. Chem. Soc.*, **1974**, *96*, 1133.
[82] A. F. Littke, G. C. Fu, *J. Org. Chem.*, **1999**, *64*, 10.
[83] D. Morales-Morales, R. Redon, C. Yung, C. M. Jensen, *Chem. Commun.*, **2000**, 1619.
[84] W. A. Herrmann, M. Elison, J. Fischer, C. Köcher, G. R. J. Artus, *Angew. Chem. Int. Ed. Engl.*, **1995**, *34*, 2371.
[85] D. S. Clyne, J. Jin, E. Genest, J. C. Gallucci, T. V. RajanBabu, *Org. Lett.*, **2000**, *2*, 1125.
[86] A. A. D. Tulloch, A. A. Danopoulos, R. P. Tooze, S. M. Cafferkey, S. Kleinhenz, M. B. Hursthouse, *Chem. Commun.*, **2000**, 1247.
[87] K. M. Lee, C. K. Lee, I. J. B. Lin, *Angew. Chem. Int. Ed. Engl.*, **1997**, *17*, 1850.
[88] A. A. D. Tulloch, A. A. Danopoulos, S. Winston, S. Kleinhenz, G. Eastham, *J. Chem. Soc. Dalton. Trans.*, **2000**, 4499.
[89] A. D. Tulloch, A. A. Danopoulos, S. Kleinhenz, M. E. Light, M. B. Hursthouse, G. Eastham, *Organometallics*, **2001**, *20*, 2027.
[90] D. J. Nielsen, K. J. Cavell, B. W. Skelton, A. H. White, *Inorg. Chim. Acta.*, **2002**, *327*, 116.
[91] R. F. Heck, J. P. Nolley, *J. Org. Chem.*, **1972**, *37*, 2320.
[92] M. Ohff, A. Ohff, D. Milstein, *Chem. Commun.*, **1999**, 357.
[93] R. H. Crabtree, *J. Chem. Soc. Dalton. Trans.*, **2001**, 2951.
[94] S. Grundemann, A. Kovacevic, M. Albrecht, J. W. Faller, R. H. Crabtree, *Chem. Commun.*, **2001**, 2274.
[95] S. Grundemann, A. Kovacevic, M. Albrecht, J. W. Faller, R. H. Crabtree, *J. Am. Chem. Soc.*, **2002**, *124*, 10473.
[96] R. H. Crabtree, in *XXth International Conference on Organometallic Chemistry*, Dassia, Corfu, **2002**.
[97] A. Kovacevic, S. Grundemann, J. R. Miecznikowski, E. Clot, O. Eisenstein, T. H. Crabtree, *Chem. Commun.*, **2002**, 2580.
[98] D. S. McGuinness, K. J. Cavell, *Organometallics*, **2000**, *19*, 4918.
[99] D. J. Nielsen, A. M. Magill, B. F. Yates, K. J. Cavell, B. W. Skelton, A. H. White, *Chem. Commun.*, **2002**, 2500.
[100] D. S. McGuinness, N. Saendig, B. F. Yates, K. J. Cavell, *J. Am. Chem. Soc.*, **2001**, *123*, 4029.
[101] C. Weymann, A. A. Danopoulos, G. Wilkinson, T. K. N. Sweet, M. B. Hursthouse, *Polyhedron*, **1996**, *15*, 3605.
[102] A. A. Danopoulos, S. Winston, T. Gelbrich, M. B. Hursthouse, R. P. Tooze, *Chem. Commun.*, **2002**, 482.
[103] J. A. Loch, M. Albrecht, E. Peris, J. Mata, J. W. Faller, R. H. Crabtree, *Organometallics*, **2002**, *21*, 700.
[104] S. Winston, A. A. Danopoulos, A. A. D. Tulloch, G. Eastham, M. B. Hursthouse, *J. Chem. Soc. Dalton. Trans.*, **2003**, 1009.
[105] A. A. D. Tulloch, S. Winston, A. A. Danopoulos, G. Eastham, M. B. Hursthouse, *J. Chem. Soc. Dalton. Trans.*, **2003**, 699.

Chapter 2

Imidazolium Salts

and

Imidazol-2-ylidenes.

Chapter 2

Imidazolium Salts and Imidazol-2-ylidenes.

2.1 Introduction.

The common starting point for the introduction of a *N*-heterocyclic carbene to a metal centre is *via* the precursor imidazolium salt. Isolated carbene species can also be employed but these in turn are also synthesised from the precursor imidazolium salt. There are several reported synthetic methods to form imidazolium salts, each using different routes depending on the required nitrogen substituents. The most common are used to produce the widely studied imidazol-2-ylidenes.

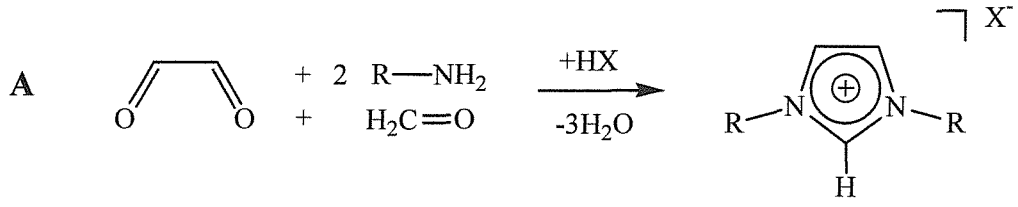

Fig 2.1 Synthesis of symmetrical imidazolium salts.

Method **A** (Fig 2.1) shows the synthesis of a symmetrical imidazolium salt. This simple one-pot synthesis[1] using glyoxal, a primary amine and formaldehyde is very straightforward and the analogous synthesis for the asymmetric imidazolium salts using this methodology has been reported.[2, 3] Several other routes, as can be seen in Fig 2.2, have been employed in the formation of asymmetric imidazolium salts. Method **B** shows the synthesis of an asymmetric biaryl imidazolinium salt (saturated backbone) generated from the 1,2-diamine precursor using orthoformate to ring close the heterocycle.[4] Method **C** shows the use of thiophosgene to again ring close a diamine precursor to form the imidazol-2-thione[5] which can then be cleaved to give the isolatable carbene, not the imidazolium ligand precursor. Method **D** shows the formation of the imidazolide anion before the addition of two aryl- or alkyl-halides (or triflates) to give the desired substitution on the imidazolium salt.

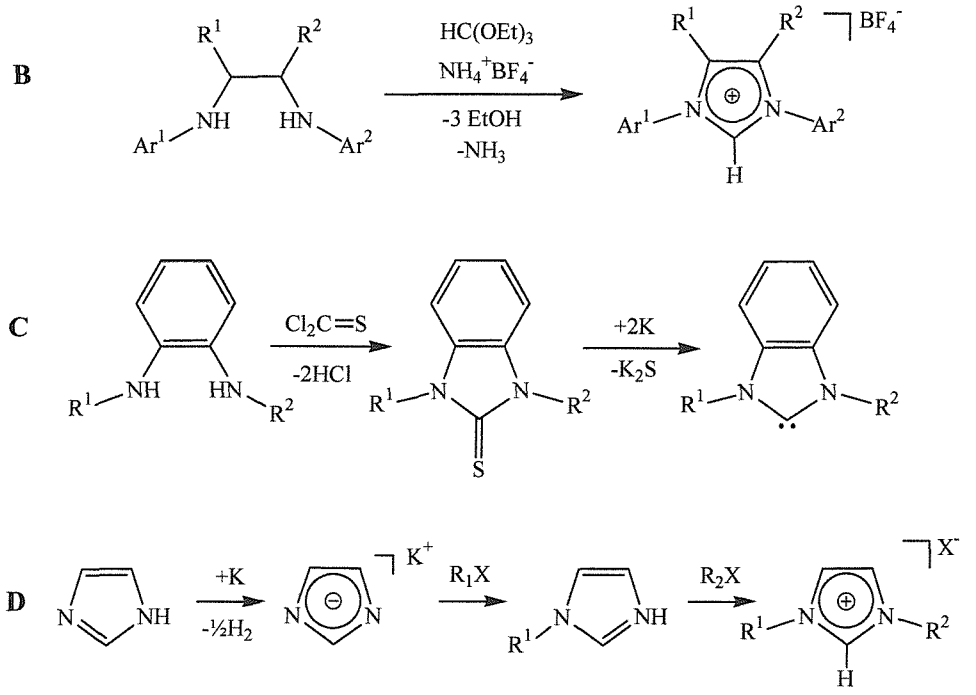

Fig 2.2 Synthesis of asymmetric imidazolium salts, Ar = aryl, R = functional group, X = halide, triflate.

Method **E** (Fig 2.3), the choice for this work, shows the synthesis of mono-substituted aryl imidazoles. Starting from the aryl amine, conversion to the isothiocyanate before transformation to the acetalylthiourea, ring closing this to a mercapto-imidazole and desulfurisation using nitric acid yields the 3-(aryl)-imidazole.[6]

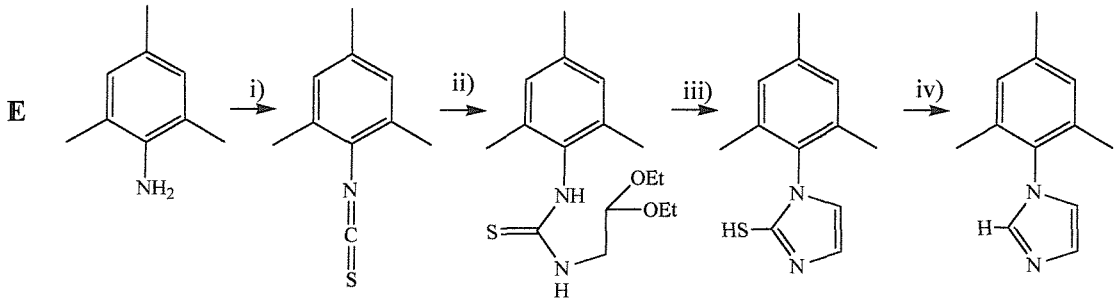

Fig 2.3 Synthesis of aryl substituted imidazole; i) $SCCl_2$, H_2O; ii) $H_2NCH_2CH(OEt)_2$, EtOH, reflux; iii) 10% HCl, reflux; iv) 4 eq 20% aqueous HNO_3.

This method can be easily scaled up so that large quantities (70 - 100 g) of aryl-imidazole can be synthesised in high yields (>80%) in less than 72 hours. The aryl-imidazole is then used to produce the imidazolium salts as will be described in this chapter. The *tert*-butyl imidazole used in this project to form the imidazolium salts was synthesised using a route based on Method **A** not Method **E** and is then used in a similar fashion to the aryl-imidazoles.[7]

2.2 Results and Discussion – Imidazolium Salts.

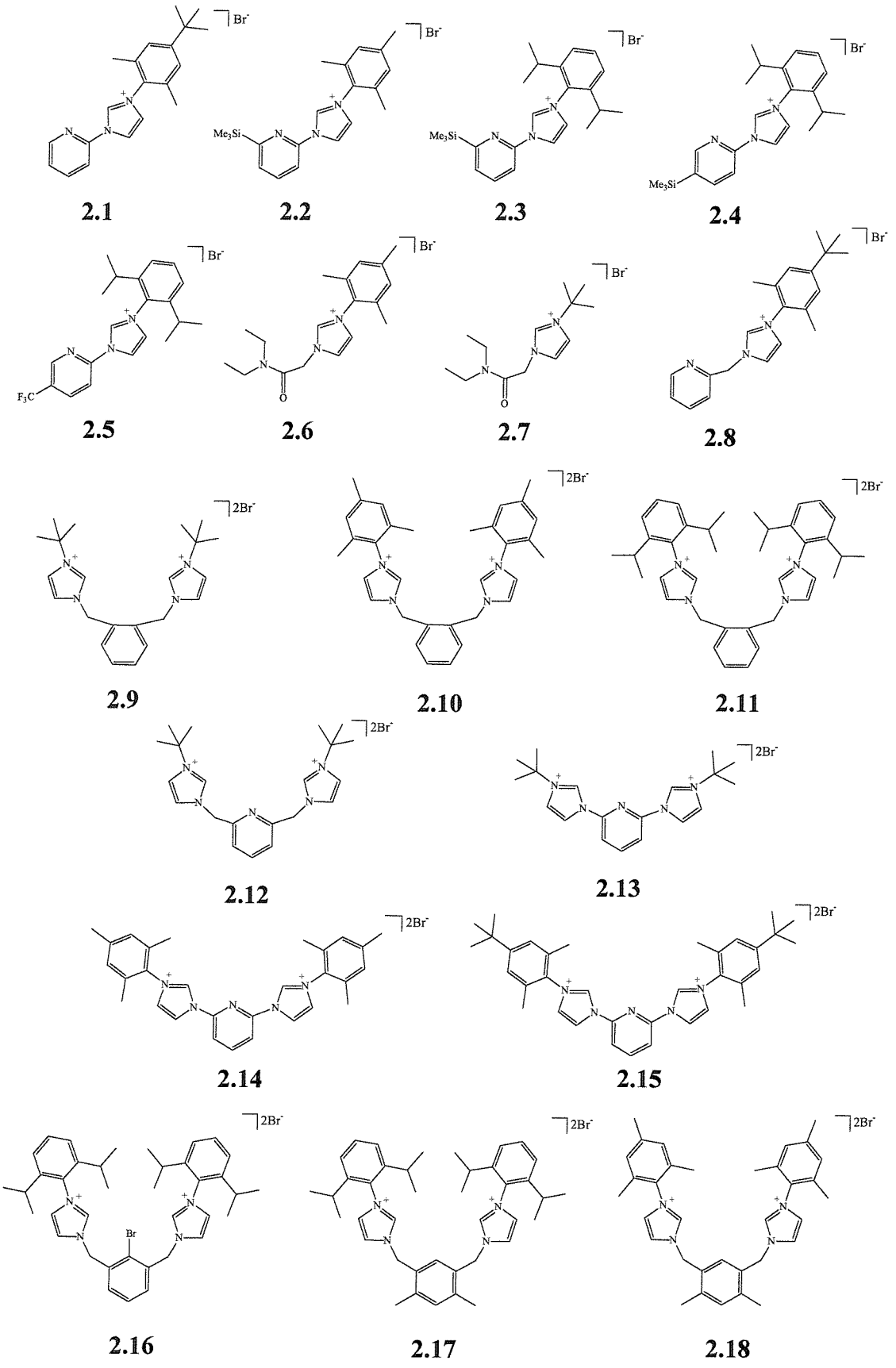

Fig 2.4 New imidazol-2-ium salts synthesised.

2.2.1 Ligand Design.

As has been described, *N*-heterocyclic carbenes have donor characteristics to metals similar to trialkylphosphines that are commonly used in catalytic processes as ligands. Disadvantages of using phosphines in catalysis include low thermal stabilities and tolerance to oxygen of the resulting complexes. The compounds shown in Fig 2.4 were all designed as phosphine analogues acting as chelating or hemilabile ligands of varying bite angles and rigidity when coordinated to a metal centre. The variances should have implications on catalytic properties. Compounds **2.1** – **2.5** are mixed donor bidentate chelates and provide slight differences in aryl group (**2.1** – **2.3**) and substitution on the pyridine ring allows fine steric (**2.2** – **2.4**) and electronic tuning (**2.5**) of a potential catalyst system. These targeted ligand environments emulate known phosphine-pyridine systems.[8] Compounds **2.6** and **2.7** were designed in order to compare the effect of the pyridine ring to an acetamide system. Compound **2.8** was synthesised in order to study the effect of chelate ring size on specific catalytic systems when increased from 5 to 6 membered rings. Compound **2.9** – **2.18** are bis-carbene species with different functional spacers linking the imidazolium groups. Compounds **2.9** – **2.11** are bidentate ligand precursors incorporating *o*-xylene linkers, compounds **2.12** – **2.18** are designed as tridentate chelating precursors to emulate known 'pincer' phosphine systems.[9] These new imidazolium salts were designed as an advancement of work initiated by us[7, 10, 11] and others[12-14] which has successfully shown that pyridine functionalised imidazol-2-ylidene palladium complexes behave as excellent precatalysts for the Heck reaction.

2.2.2 Synthesis of Imidazolium Salts.

The functionalisation of the unsubstituted nitrogen of the aryl-imidazole is performed *via* three different quaternisation methods (**A** - **C** shown in fig 2.5 – 2.7). The synthesis of the imidazolium salts depends on the chemical nature of the linkage between the aryl-imidazole and the substituent group being added.

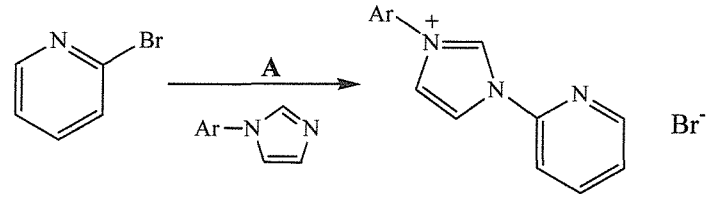

Fig 2.5 Synthesis of directly linked bridged pyridine functionalised imidazolium salts.

Method **A** shows a direct linkage between the imidazole and pyridine ring, as in compounds **2.1** - **2.5** and **2.13** - **2.15**. 3-Mesityl-, 3-(2,6-di-*iso*-propylphenyl)- or 3-(2,6-dimethyl-4-*tert*-butylphenyl)-imidazole is taken in excess with 2-bromopyridine or substituted 2-bromopyridine for **2.1** - **2.5** or 2,6-dibromopyridine for **2.13** - **2.15** and sealed under vacuum inside a small ampoule. The ampoule is then submerged in to an oil bath at 150 – 160 °C to form a melt and left strirring for 5 – 7 days. The ampoule is cooled and opened to yield quantitative product after washing with diethylether to remove the excess aryl-imidazole.

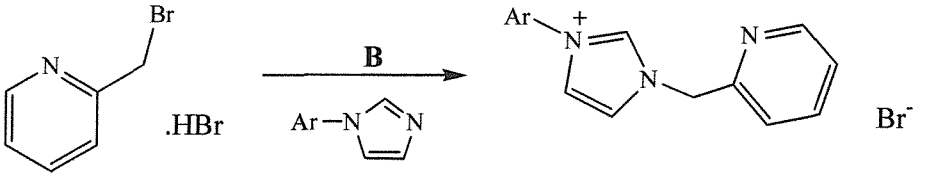

Fig 2.6 Synthesis of methylene bridged pyridine functionalised imidazolium salts.

Method **B** shows the addition of a methylene bridge between aryl-imidazole and pyridine for compounds **2.8** and **2.12**. The quaternisation is completed at room temperature in methanol but the synthesis involves the use of the 2-bromomethylpyridine hydrobromide (for **2.8**) or 2,6-dibromomethylpyridine hydrobromide (for **2.12**). The first step of the synthesis involves careful neutralisation of the appropriate hydrobromide salt with a weak base. Extreme care must be taken when neutralising the salts, as the neutralised species are extremely potent lachrymators. Preparing a concentrated aqueous solution of the hydrobromide, layering this with diethylether, cooling over ice and neutralising the acid with a saturated sodium carbonate solution accomplishes this. The diethylether layer is then separated, dried with anhydrous magnesium sulfate and added directly to a methanolic solution of the appropriate imidazole. Under gentle vacuum the diethylether is then removed to leave a methanolic solution that is either stirred at room temperature for 12 hours or refluxed for 3 hours. The product can then be precipitated from the solution by reducing the solvent to *ca.* 7 - 8 cm^3 and adding acetone.

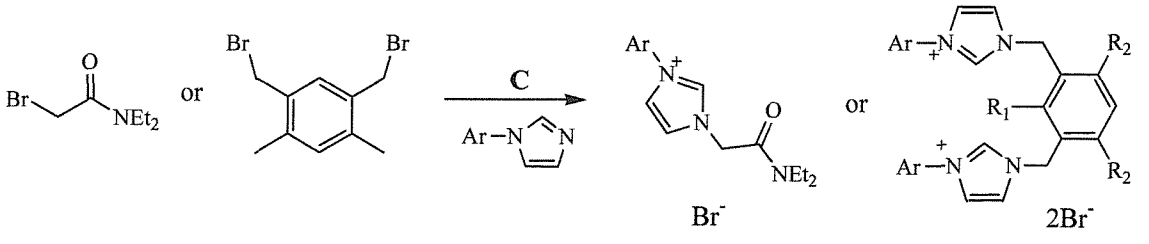

Fig 2.7 Synthesis of non-pyridine functionalised imidazolium salts.

Method **C** shows the quaternisation of the non-pyridine functional compounds, the same general procedure was universally applied; a suitable bromide precursor was taken with 3-(aryl)-imidazole and refluxed in 1,4-dioxane for 12 hours, the product usually precipitated from solution on cooling. For **2.6** and **2.7**, 2-bromo-*N,N*-diethylacetamide was used, although for **2.7** an oil was isolated that could be solidified by triturating with diethylether. Compounds **2.9** – **2.11** were based on the α,α'-dibromo-*o*-xylene and again these were refluxed with an excess of appropriate imidazole to give the bis-imidazolium salts in good yields (>78%). Compound **2.16** was prepared from reaction of 3-(2,6-di-*iso*-propylphenyl)imidazole with 2-bromo-1,3-bis(bromomethyl)benzene and **2.17** and **2.18** could be prepared from 3-(aryl)-imidazole with 1,3-bis(bromomethyl)-4,6-dimethylbenzene in good yields (>80%).

2.2.3 Imidazolium Salt Characterisation.

2.2.3.1 NMR Spectroscopy.

The most powerful tool for characterisation of the imidazolium salts was proton (^{1}H) and carbon ($^{13}C\{^{1}H\}$) NMR spectroscopy. It was possible to obtain very clean and easily assignable NMR spectra of the compounds from crude products, as the syntheses were very clean. The most characteristic peaks for these compounds was a singlet between 10 – 12 ppm in the proton NMR and a peak between 150 – 173 ppm in the carbon NMR for the 2-imidazolium carbon of the heterocycle. Other characteristic peaks are described for all compounds.

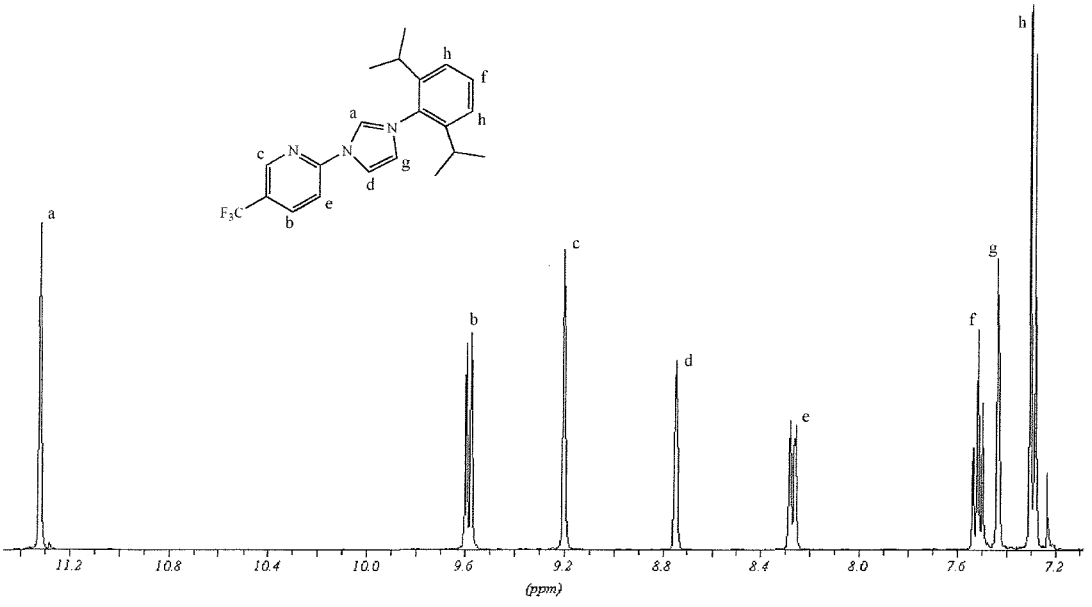

Fig 2.8 NMR spectrum (above and next page) of compound **2.5**.

Compounds **2.1** – **2.5**, **2.8** and **2.12** – **2.15** had similar NMR spectra due to their structural resemblance, with only slight variances in the aromatic region depending on whether the pyridine was functionalised, at which position and if there was a methylene linkage between the heterocycle and pyridine ring. The 'pincer' bis-imidazolium salts had simplified spectra due to the presence of a mirror plane of symmetry through the molecules. Fig 2.8 shows the NMR of **2.5**, the peak splittings and chemical shifts allow assignment as shown. The low field region shows all aromatic signals as well as the imidazolium peak. The asymmetry of the imidazolium salt leads to very different shifts of the backbone protons (peaks d and g) with a difference of *ca.* 1.5 ppm. The extreme low-field shift of the imidazolium proton at *ca.* 11.0 ppm is typical for these salts; others have noted the chemical shift of this proton depends on the hydrogen bonding abilities of the anion.[15] For the pyridine and pyridyl functionalised imidazolium salts the following characteristic peaks were observed in $CDCl_3$ for these related compounds:

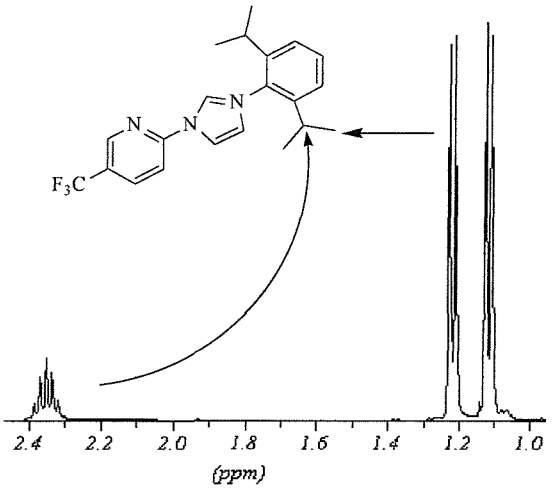

Fig 2.8 Continued from previous page.

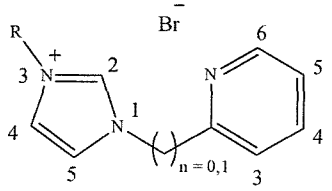

Fig 2.9 Numbering scheme for 2.1 – 2.5, 2.8 and 2.12 – 2.15. R = tert-butyl, mesityl, 2,6-di-iso-propylphenyl or 2,6-dimethyl-4-(tert-butyl)-phenyl.

- If R = mesityl singlets at 2.1, 2.3 and 7.0 ppm.
- If R = 2,6-di-*iso*-propylphenyl doublets at 1.1 and 1.3 ppm, a septet at 2.4 ppm and a doublet and triplet or broad singlets between 7.2 and 7.6 ppm.
- If R = 2,6-dimethyl-4-(*tert*-butyl)-phenyl singlets at 1.2, 2.1 and 7.1 ppm.
- If R = *tert*-butyl a singlet at 1.3 ppm.
- For the 4- and 5-imidazolium protons two singlets between 7.2 – 7.4 and 8.5 – 8.9 ppm for n = 0 or 7.2 – 7.4 and 8.1 – 8.3 ppm for n = 1.

For the pyridine ring protons chemical shifts varied depending on the substitution pattern of the ring. If a methylene bridge was incorporated then peaks were observed between 7.7 – 8.5 ppm, without a methylene bridge peaks were observed in the range 7.4 – 9.6 ppm. Depending on whether the compound was a mono- or bis-imidazolium salt the number of peaks varied, three or four peaks were observed for a mono-imidazolium salt depending on substitution and two peaks for a bis imidazolium salt. The lowest field peak observed was in **2.5** on the 3-position of the pyridine ring where the electron withdrawing CF_3 in the 5-position shifts all peaks further downfield.

Compounds **2.6** and **2.7** have a diethylacetamide group tethered to the imidazolium ring. Characteristic peaks for these compounds were; diastereotopic signals from the ethyl groups as triplets at 1.1 and 1.3 and quartets at 3.4 and 3.6 ppm, methylene bridges at 5.7 – 6.0 ppm and the 4- and 5-imidazolium protons as two singlets at 7.2 – 7.9 ppm. The aryl/alkyl substituent showed peaks as observed for the pyridine functionalised compounds.

The non-pyridine 'pincer' chelates **2.9** – **2.11** and **2.16** - **2.18** again have simplified spectra due to the presence of a mirror plane of symmetry through the molecules. NMR peaks from the aryl/alkyl substituents on the 3-imidazolium position gave peaks as described for the pyridine functionalised compounds. The *o*-phenylene linked bis-imidazolium compounds **2.9** – **2.11** were further identified as follows. Compound **2.9** (D_2O) showed the presence of the methylene bridges as a singlet at 5.5 ppm, the imidazolium backbone protons as singlets at 7.2 and 7.6 ppm, xylyl protons as two multiplets at 7.3 and 7.5 ppm and the imidazolium proton at 8.8 ppm. Compounds **2.10** and **2.11** ($CDCl_3$) containing the aryl substituents showed characteristic peaks for the methylene bridges as a singlet between 6.1 – 6.3 ppm, the imidazolium backbone as singlets at 7.1 – 7.2 and 8.1 – 8.3 ppm and the *o*-phenylene protons as two multiplets between 7.2 – 7.8 ppm. The 2-imidazolium proton was observed at 10.1 – 10.7 ppm, much further downfield than for the alkyl substituted heterocycle **2.9**.

For compounds **2.16** - **2.18** where a substituted xylyl linker bridges the two imidazolium rings, characteristic peaks for the xylyl ring methyls were observed as singlets at 2.3 – 2.5 ppm and the two aromatic protons as singlets at 7.0 and 7.9 ppm. The methylene bridges were observed at 5.8 – 6.0 ppm and all other protons were observed in the ranges described for the pyridyl functionalised imidazolium salts.

$^{13}C\{^{1}H\}$ NMR spectroscopy of the imidazolium salts showed diagnostic peaks confirming the observations in the proton NMR spectrum. The most indicative signal was from the imidazolium carbon, observed in the range 150 – 173 ppm in $CDCl_3$. Resonances could be seen for aromatic carbons between 124 – 140 ppm, the 4- and 5-imidazolium carbons in the range 115 – 122 ppm. The methylene bridges where appropriate between 50 – 67 ppm and aryl substituent peaks from the 3-imidazolium position were observed between 15 – 40 ppm depending on the substitution, i.e. methyl, *iso*-propyl or *tert*-butyl.

2.2.3.2 Electrospray Mass Spectrometry.

Electrospray mass spectrometry was highly diagnostic as the positive ion detection mode could easily identify the precharged imidazolium moieties. The resulting peaks from electrospray mass spectrometry correspond to mass divided by the charge, hence for the mono-imidazolium compounds (**2.1** – **2.8**) the parent peak M^+ was observed and for the bis-imidazolium (**2.9** – **2.18**) compounds the parent peak $½M^{2+}$ was detected.

As a diagnostic tool this also proved useful for monitoring reaction progression in the synthesis of the imidazolium salts. The bromopyridine precursors used were easily identifiable on the electrospray systems and so reaction completion could be determined by following the presence of the precursors. Unlike with NMR samples where 5 -10 mg in 1 cm^3 of deuterated solvent is necessary for a proton NMR spectrum to follow reaction progression, much less material is needed when observing reaction progression by mass spectrometry, typically only 1 μg in 1 cm^3 of dichloromethane. In addition for the 'pincer' compounds the presence of any mono-substituted intermediate species could be monitored until the desired product was formed.

2.2.3.3 Single crystal X-ray diffraction.

Growth of X-ray quality crystals was possible by allowing slow-evaporation of dichloromethane solutions or by layering dichloromethane solutions with diethylether. The structure of the previously synthesised 3-(2,6-di-*iso*-propylphenyl)-1-(2-pyridyl)-imidazolium bromide (Fig 2.) was confirmed.[7]

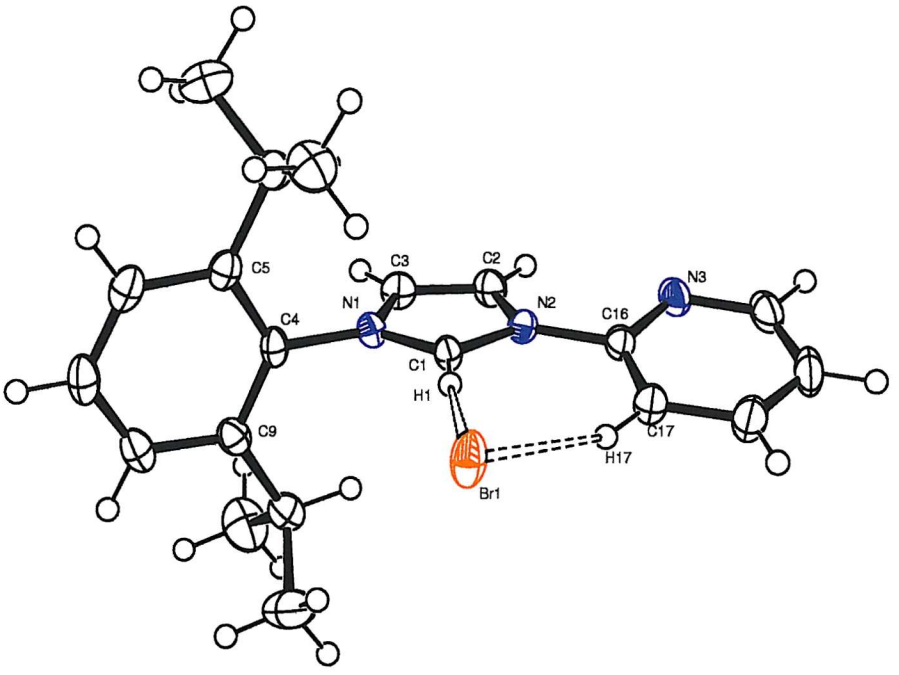

Fig 2.10 X-ray crystal structure of 3-(2,6-di-*iso*-propylphenyl)-1-(2-pyridyl)-imidazolium bromide.

Table 2.1 Selected bond lengths (Å) and angles (°) for 3-(2,6-di-*iso*-propylphenyl)-1-(2-pyridyl)-imidazolium bromide.

C1 – N1	1.330(5)	N1 – C1 – N2	107.9(3)
C1 – N2	1.343(5)	C5 – C4 – N1 – C1	93.2(3)
C2 – C3	1.346(6)	C1 – N2 – C16 – N3	170.6 (4)
Br1 – H1	2.535(5)	C1 – H1 – Br1	173.9 (3)
Br1 – H17	2.782(5)		

In this structure the imidazolium proton is *trans* to the pyridine lone pair, which is a result of packing as the bromine counter ion creates a hydrogen-bonding network in the solid state as can be seen by the bromine to hydrogen bond lengths of 2.5 – 2.7 Å which is well within the distance considered to be a hydrogen bond (less than 3.1 Å). All other bond lengths and angles in the structure are typical of known imidazolium salts that contain unsaturated backbones.[16, 17] This near linear hydrogen bonding is considered as a weak hydrogen bond consisting of mainly electrostatic charges based on the bond length. This interaction also explains the low-field shift of this hydrogen in the 3-position on the pyridine in the proton NMR if this bonding is maintained in solution.

2.3 Results and Discussion - Imidazol-2-ylidenes.

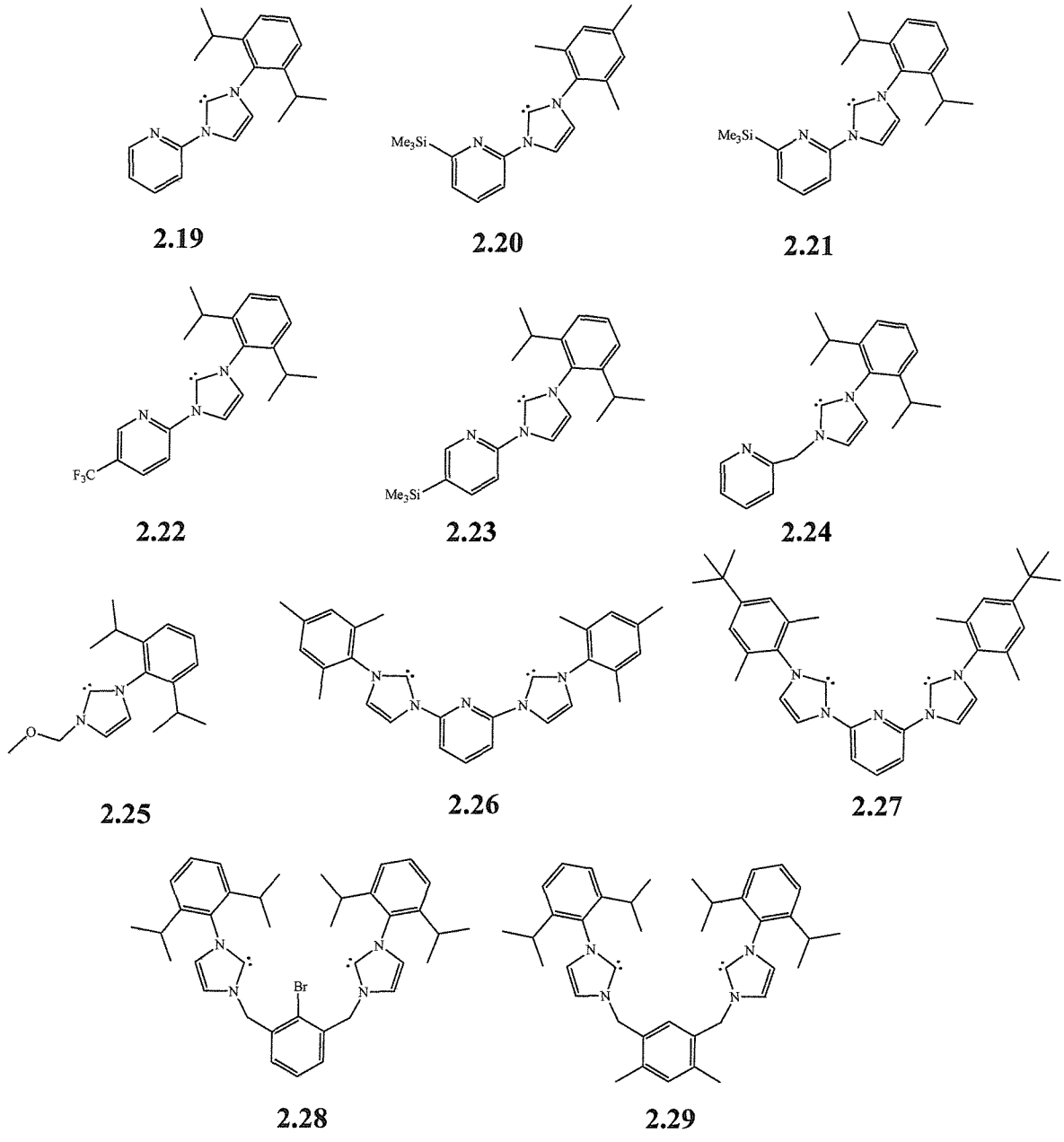

2.19 **2.20** **2.21**

2.22 **2.23** **2.24**

2.25 **2.26** **2.27**

2.28 **2.29**

Fig 2.11 New imidazol-2-ylidenes synthesised.

Arduengo's isolation of stable carbenes greatly advanced interest and revitalised research into the study of *N*-heterocyclic carbenes. The possibility of having a 'carbene-in-a-bottle' would save time and reduce synthetic steps in the formation of NHC complexes, but there was a common belief that large bulky protecting groups were needed in conjunction with the stabilising abilities of the nitrogen heteroatoms to access these isolatable stable carbenes. The isolation of 'free' imidazol-2-ylidenes opens up more options in the choice of metal precursors that can be used to form metal complexes and improves atom economy as *in situ* deprotonations are no longer required.

2.3.1 Synthesis and Isolation of 'Free Carbenes'.

An alternative synthesis to the current literature routes, as described in the introduction, of deprotonating imidazolium salts was sought to increase the selectivity of the deprotonation. Previous attempts to deprotonate imidazolium salts to yield the corresponding imidazol-2-ylidenes had not met with complete success. The use of lithium di-*iso*-propylamide gave only red solids after work-up, which were intractable mixtures by NMR, although *in situ* analysis of these reaction mixtures showed the presence of the 'free' carbene.[7] This limited success spurred on the hunt for more suitable conditions. A novel general route to the functionalised imidazol-2-ylidenes or 'free carbenes' was developed *via* the deprotonation of the imidazolium salts using potassium bis-silylamide.[18, 19]

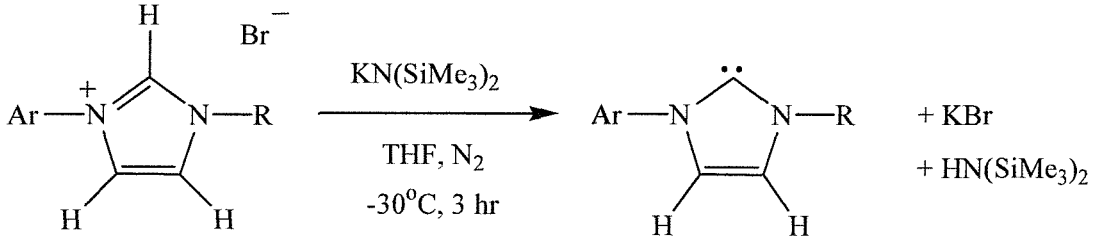

Fig 2.12 Synthesis of imidazol-2-ylidene, Ar = mesityl, 2,6-di-*iso*-propylphenyl, R = functional group.

The deprotonation was performed by mixing an equivalent amount of potassium bis-silylamide and imidazolium salt, followed by the addition of precooled (–78°C) THF to the mixture and allowing to warm to –30°C and maintaining this temperature for three hours. The mixture was then allowed to warm to room temperature, the THF removed *in vacuo* and the resulting solid washed with cold petrol. Residual solid was extracted into toluene from which product was crystallised by cooling to –30°C. Initial concerns into the possible deprotonation of the methylene linkages found in compounds **2.24**, **2.28** and **2.29** by either the base or the 'free carbene' proved to be unfounded. This method has been successfully scaled up to produce multi-gram quantities of **2.19**, **2.26** and **2.27** (3 - 4 g). Other 'free' carbenes have also been produced up to *ca.* 2 g of product per reaction. As has been observed this synthetic route is selective to deprotonation of the 2-imidazolium proton and tolerant to functional groups which gives this a wide scope for general use.

2.3.2 Characterisation of 'Free' Carbenes.

2.3.2.1 NMR Spectroscopy.

Identification of the isolated imidazol-2-ylidenes was primarily achieved using NMR spectroscopy. Due to the air sensitivity of the carbenes all NMR samples were prepared under nitrogen using dried NMR solvents, predominantly distilled d_6-benzene, and NMR tubes fitted with Suba-seal caps or Teflon taps. The most significant diagnostic feature of the NMR spectra was the shift of the precursor imidazolium carbon from 145 - 169 ppm much further downfield to 215 – 225 ppm for the imidazol-2-ylidene. In the ^{1}H NMR spectra the disappearance of the signal at 10 – 11 ppm also indicated formation of the carbene.

For the pyridine and pyridyl functionalised imidazol-2-ylidenes **2.19** – **2.24**, **2.26** and **2.27** the following characteristic peaks were observed in C_6D_6 for these related compounds:

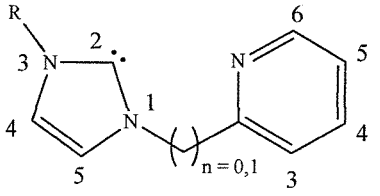

Fig 2.13 Numbering scheme for **2.19** – **2.24**, **2.26** and **2.27**. R = mesityl, 2,6-di-*iso*-propylphenyl or 2,6-dimethyl-4-(*tert*-butyl)-phenyl.

- If R = mesityl singlets at 2.0, 2.1 and 6.7 ppm.
- If R = 2,6-di-*iso*-propylphenyl doublets at 1.1 and 1.2 ppm, a septet at 3.0 ppm and a doublet and triplet or broad singlets between 7.2 and 7.3 ppm.
- If R = 2,6-dimethyl-4-(*tert*-butyl)-phenyl singlets at 1.3, 2.2 and 7.1 ppm.
- For the 4- and 5-imidazol-2-ylidene protons two singlets between 6.3 – 6.8 and 8.3 – 8.5 ppm for n = 0 or at 6.5 and 7.2 ppm for n = 1.
- If n = 1 then a singlet at 5.5 ppm from the methylene bridge.

A direct comparison of the pyridine functionalised imidazolium salt to its 'free' carbene is not possible due to the use of different NMR solvents. The imidazolium salts are insoluble in benzene, which is the NMR solvent for the 'free' carbenes as they rapidly decompose in chloroform. However some general comparative features are observed by the removal of the proton. Firstly the 4- and 5-imidazolium protons shift upfield but retain the large difference

in chemical shifts as in the pyridine functionalised imidazolium salts. For the pyridine functionalised imidazol-2-ylidenes the chemical shifts of the pyridine protons also move slightly upfield as the previous hydrogen bonding halide is removed from the system. The highest pyridine proton resonance is now at 8.7 ppm (**2.22**) whereas it had been at 9.6 ppm as the imidazolium salt (**2.5**). Upon deprotonation compounds **2.19** – **2.23** become fully conjugated aromatic systems and the relevance of this will be noted later.

The precursor imidazolium salt of **2.25** had been previously prepared[7] and deprotonation of this led to the isolated carbene. As with previous compounds the 2,6-di-*iso*-propylphenyl peaks were as the pyridine functionalised compounds, other characteristic peaks (d_8-toluene) are; a methoxy peak as a singlet at 3.2 pm; methylene bridge as a singlet at 5.3 ppm; 4- and 5-imidazol-2-ylidene peaks as two singlets at 6.5 and 6.7 ppm, much closer together than in the pyridine functionalised compounds. The change from the imidazolium to the aromatic imidazol-2-ylidene also reduces the chemical shift resonance difference between the peaks from the 4- and 5-imidazol-2-ylidene of 0.7 ppm (previously 7.2 and 8.1 ppm).

The simplification of the NMR spectra for the precursor bis-imidazolium salts carried through to the bis-carbenes **2.26** – **2.29** due to the continued presence of the mirror plane of symmetry through the molecules. For compounds **2.26** – **2.29** the same characteristic changes are noted i.e. the loss of the imidazolium proton signal in the ^{1}H NMR spectra and the down field shift of the carbene carbon signal in the $^{13}C\{^1H\}$ NMR spectra. Other peaks for **2.26** and **2.27** are as listed for the pyridine functionalised compounds above, the characteristic peaks for **2.28** and **2.29** are as follows; the 2,6-di-*iso*-propylphenyl group gives doublets at 1.1 and 1.2 ppm, a septet at 3.0 ppm and a doublet and triplet or broad singlets between 7.0 and 7.2 ppm, 4- and 5-imidazol-2-ylidene peaks 6.6 – 6.7 and 7.0 – 7.3 ppm, peaks from the aryl linker were observed as a multiplet at 7.0 – 7.1 ppm for **2.28** and as two singlets at 6.3 and 6.4 for **2.29.**

2.3.2.2 Single crystal X-ray diffraction.

X-ray quality crystals of the isolated carbenes could be grown by cooling concentrated solutions of toluene or where soluble from petroleum ether. All of the compounds were isolated as crystals but the majority formed needle type crystalline structures and so data collection was not possible due to the small crystal size. Several samples were submitted to Daresbury SRS to use the enhanced X-ray source but not all collections were fruitful.

Crystals of the mono-carbene compounds **2.20** and **2.21** were obtained from cooling petroleum ether solutions and the structure of **2.20** is shown below. The presence of the trimethylsilyl group gave improved crystallinity to the compounds and their structures were the easiest to obtain.

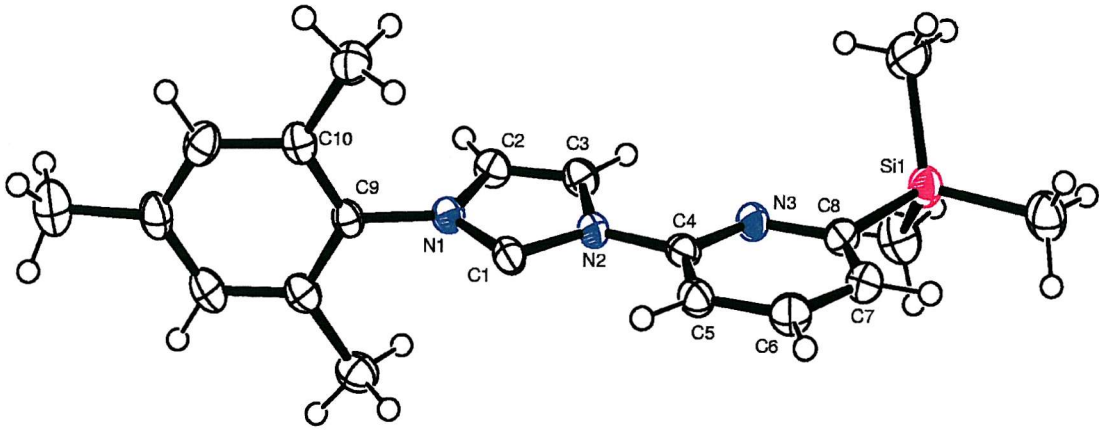

Fig 2.14 Crystal structure of **2.20**

Table 2.2 Selected bond lengths (Å) and angles (°) for **2.20**

C1 – N1	1.355 (3)	N1 – C1 – N2	101.4 (2)
C1 – N2	1.386 (3)	C1 – N2 – C3	112.4 (2)
C2 – C3	1.329 (4)	C1 – N1 – C2	113.3 (2)
C2 – N1	1.405 (3)	C1 – N2 – C4 – N3	178.5 (5)
C3 – N2	1.396 (3)	C10 – C9 – N1 – C1	91.8 (5)

It is interesting to note the minimum energy packing in this system involves maximum repulsion of the lone pair of electrons on the pyridine nitrogen to the lone pair located on the carbene. They are in a *'trans'* geometry with a twist angle of 178.5°, similar repulsions are observed in the structure of 2,2-bipyridyl where the lone pairs also are *trans* about the pyridine-pyridine bond.[20] As in the imidazolium salt the aryl group is near to 90° to the heterocyclic ring due to steric repulsion. In comparison to the imidazolium salt structure (Fig 2.), presuming that the trimethylsilyl group is having little electronic effect on the delocalized system, there is lengthening of the N-$C_{carbene}$ bonds by 0.025 – 0.035 Å beyond the bond e.s.d's and a shrinking in the angle N–C–N by *ca.* 6°. Both of these variances are known characteristics of imidazol-2-ylidenes and it is normal for the angle to close up and bond lengths to stretch upon deprotonation.[21] We also reported the isolation of a bis-imidazol-2-ylidene species (the 2,6-di-*iso*-propylphenyl analogue of imidazolium salt **2.6**), the structure of which has similar structural properties to that of the **2.20** and **2.21** with both carbenes in a *'trans'* geometry to the pyridine.[19]

2.3.3 'Free' Carbene stability and reactivity.

Once isolated from the reaction medium the imidazol-2-ylidenes **2.19** – **2.29** show no sign of decomposition when stored as solids under an inert atmosphere at room temperature. When brought into air the carbenes rapidly decompose, as they appear extremely hygroscopic. All of the compounds decompose before melting as heated but are all thermally stable to a minimum of 100°C before any decomposition is observed. It was possible to obtain elemental analysis of the compounds. In solution if not maintained under an inert atmosphere decomposition is instantaneous to intractable mixtures as determined by ^{1}H and $^{13}C\{^{1}H\}$ NMR spectroscopy. If dry and inert conditions are maintained the carbenes generally show good solubility and stability in polar solvents such as toluene and THF. Many of the compounds also have reasonable solubility in petroleum ether. Although the imidazol-2-ylidenes show good solubility in many solvents, they are not stable in all solvents. In dry acetone, chloroform and acetonitrile rapid decomposition occurred in under an hour, presumably the nucleophilic carbene attacks the solvent. In dichloromethane decomposition began instantaneously but was not as rapid (intractable mixture by NMR spectroscopy after 4 hours) inferring it could be possible to use this as a reaction solvent if stable products were being formed quickly.

2.3.4 Reactions of imidazol-2-ylidenes with sulfur.

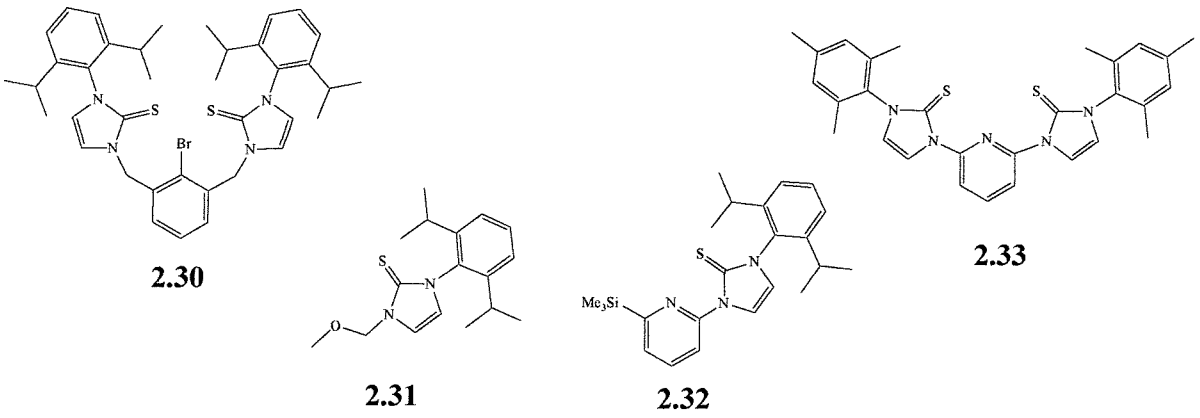

2.30 **2.31** **2.32** **2.33**

Fig 2.15 New functionalised imidazole-2-thiones synthesised.

In the late 1980's it was realised that imidazole-2-thiones seemed well suited to polymer cross-linking applications and renewed interest in these species came about.[22-24] Previous research in to imidazole-2-thiones stretches back to the 1960's and several metal complexes of these species are known.[25] A synthetic route to transform imidazolium salts to imidazol-2-

thiones involving methanolic potassium carbonate (Fig 2.) was established which at the time only presumed and did not prove that imidazol-2-ylidenes were the intermediates.[26]

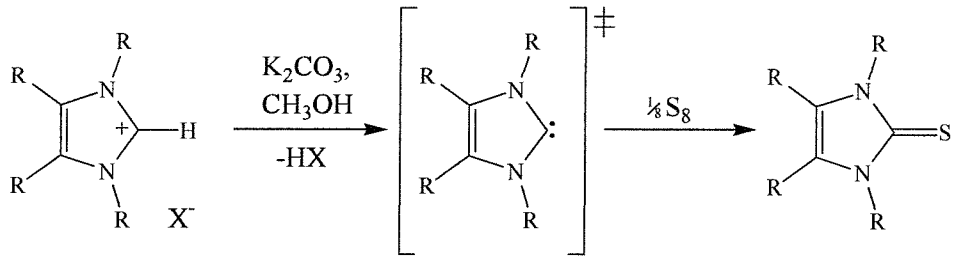

Fig 2.16 Synthesis of imidazol-2-thiones.

Imidazol-2-thiones represent another source of imidazol-2-ylidenes and it is known that reaction of these with potassium in the presence of metal precursors leads to imidazol-2-ylidene complexes. Reaction of the 'free' carbenes **2.21**, **2.25**, **2.26** and **2.28** with flowers of sulfur in toluene at room temperature gave the air stable mono- and bis-imidazol-2-thione compounds **2.30** – **2.33**.

This proved that these 'free' carbenes are quite tolerant of functional groups without decomposition *via* self-coupling reactions, as they are quite stable in solution unless a group is provided for the nucleophilic carbene to attack. The functionalised imidazole-2-thiones could be used to access new metal complexes through which the sulfur could be coordinated or the C=S bond can be cleaved with potassium to regain the imidazol-2-ylidene.

2.3.4.1 Characterisation of Imidazol-2-thiones.

The primary characterisation techniques used to identify the imidazole-2-thiones was $^{13}C\{^1H\}$ NMR spectroscopy and mass spectrometry. In the $^{13}C\{^1H\}$ NMR spectra the imidazole-2-thione carbon appeared in the region 162 – 166 ppm for compounds **2.30** – **2.33** much further upfield than in the free carbene precursor, at 215 – 225 ppm. This shift is typical of other known imidazol-2-thiones.[27] Proton NMR spectroscopy was not as indicative as only slight shifts in peak positions was observed for most signals, although shifts downfield of up to 0.5 ppm were observed for the 4- and 5-imidazol-2-thione protons from their imidazolium salt precursors. Mass spectrometry proved highly diagnostic to confirm the presence of the sulphur as parent ion peaks $(M + 1)^+$ were observed in the positive electrospray spectra of these compounds. Elemental analysis also confirmed the chemical identity of these compounds.

2.4 Conclusions

A variety of imidazolium salts have been prepared using simple synthetic techniques and are reported here. These reactions follow two generally high yielding methods which give compounds that require only trivial workups. The ease in which the second donor functionality can be added to the imidazolium group indicates this is a small selection of what could potentially be achieved with further study, as only nitrogen donors have been used for this work. Phosphine functionalised *N*-heterocyclic carbenes are known.[18, 28]

A novel selective method of isolating stable functionalised imidazol-2-ylidenes has been reported and the successful deprotonation of the synthesised imidazolium salts has been achieved with full characterisation. It has been shown that these 'free' imidazol-2-ylidenes are quite stable species in selected dry solvents but decompose rapidly in chlorinated solvents or in contact with air. In the presence of an excess of sulfur the imidazol-2-thiones are isolated in quantitative yields.

The isolation of these three families of compounds opens the doors to different methods of introducing imidazol-2-ylidenes to transition metal centres, *via* substitution reactions of 2-electron σ-donors for the imidazol-2-ylidenes or *via in situ* deprotonation of the imidazolium salts, or reduction of the imidazol-2-thiones in the presence of a metal precursor.

2.5 Experimental Section

Elemental analyses were carried out by the University College London Microanalytical Laboratory. Nuclear Magnetic Resonance (NMR) data were recorded on Bruker AM-300 or Bruker AC-300 operating at 300 MHz (^{1}H) or a Bruker Avance DPX-400 operating at 400 MHz (^{1}H). The spectra were referenced internally using the signal from the residual protio-solvent (^{1}H) or the signals of the solvent (^{13}C{^{1}H}) and chemical shifts reported in ppm. Mass Spectra (MS) were obtained from acetonitrile solutions from a Micromass Platform using electrospray ionisation. Gas Chromatography Mass Spectrometry (GC-MS) were recorded on a ThermoQuest TraceMS from dichloromethane solutions. Gas Chromatograms (GC) were carried out using a Varian 3400 fitted with Varian 1200 autosampler and Hewlett Packard Integrator. All experiments were carried out using standard Schlenk techniques under nitrogen unless stated. Air sensitive compounds were handled in a Unibraun nitrogen atmosphere glove box. All solvents were degassed and distilled before use and all glassware was thoroughly dried and kept in an oven at 120°C prior to use. All chemicals were purchased from Aldrich, Acros Organics or Avocado and used without further purification unless otherwise stated. The following were made from literature method: 2-bromo-6-trimethylsilylpyridine,[29] 2-bromo-5-trimethylsilylpyridine,[29] 4-*tert*-butyl-2,6-dimethylaniline, 1-(mesityl)imidazole,[6] 1-(2,6-di-*iso*-propylphenyl)imidazole,[6] 1-(*tert*-butyl)imidazole,[7] 1-[4-(*tert*-butyl)-2,6-dimethylphenyl]imidazole,[6] potassium bis-silylamide,[30] 2-bromomethylpyridine hydrobromide,[31, 32] 2,6-dibromomethylpyridine hydrobromide,[31, 32] 2,6-methylbromide-3,5-dimethylbenzene,[33] 1-(2-pyridyl)-3-(2,6-di-*iso*-propylphenyl)-imidazolium bromide,[7, 34] 1-(2-methoxymethyl)-3-(2,6-di-*iso*-propylphenyl)-imidazolium bromide.[7]

2.5.1 Imidazolium Salt Synthesis

Two general methods were used for the formation of compounds **2.1** – **2.18** as described below unless stated otherwise.

General Method 1

2-bromopyridine or 2,6-dibromopyridine and 3-(aryl)imidazole in a 1:1.5 ratio per bromine:imidazole were placed inside a small glass ampoule with stirrer bead and after sealing under vacuum was submerged into an oil bath at 150°C and stirred for 5-7 days. After cooling to room temperature the ampoule was opened and the dark solid extracted into

chloroform (20 cm^3) and by precipitation with petroleum ether (40/60), a cream coloured solid was isolated. The solid was washed with diethylether (3 x 30 cm^3) to remove excess 3-(aryl)imidazole to yield white product in quantitative yields. Recrystallisation afforded crystalline product by layering dichloromethane solutions with diethyl ether. The salts were then dried azeotropically in benzene using Dean-Stark apparatus and stored under an inert atmosphere.

General Method 2

Bromoalkyl compound and 3-(aryl)imidazole in 1:1.5 ratio per bromine:imidazole were refluxed in 1,4-dioxane (*ca.* 100 cm^3) for up to 12 hours. On cooling precipitation of crude product occurred which was collected by filtration, washed with diethylether (3 x 30 cm^3) to remove excess 3-(aryl)imidazole and the resulting colourless product could be purified by recrystallisation although this typically was not necessary. The salts were then dried azeotropically in benzene using Dean-Stark apparatus and stored under an inert atmosphere.

1-(2-pyridyl)-3-[4-(*tert*-butyl)-2,6-dimethyl-phenyl]imidazolium bromide 2.1

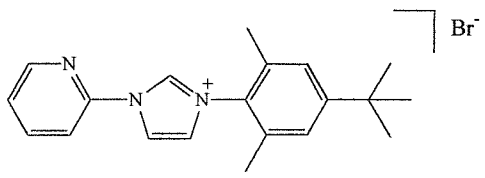

Prepared using general method 1 from 2-bromopyridine (2.07 g, 0.013 mol) and 1-[2,6-dimethyl-4-(*tert*-butyl)phenyl]imidazole (3.27 g, 0.014 mol). Yield 4.80 g, 95%. MS (ES+) *m/z* 306 (M^+). $\delta_H(CDCl_3)$ 1.3 [9H, s, $C(CH_3)_3$], 2.2 (6H, s, phenyl-CH_3), 7.2 (2H, s, phenyl H), 7.4 - 7.5 (2H, m, pyr H and 4-imidazolium), 8.1 (1H, t, pyr H), 8.6 (1H, d, pyr H), 8.9 (1H, s, 5-imidazolium), 9.2 (1H, d, pyr H), 11.0 (1H, s, 2-imidazolium). $\delta_C(CDCl_3)$ 18.7 [$C(CH_3)_3$], 31.6 [$C(CH_3)_3$], 35.2 (phenyl-CH_3), 116.9, 121.0 (4- and 5-imidazolium) 124.8, 126.0, 127.0, 131.0, 134.2, 136.0, 141.3, 146.4, 149.3, 155.0, (aromatic and 2-imidazolium). Found C, 61.78, H, 6.19, N, 10.72, $C_{20}H_{24}N_3Br$ requires C, 62.18, H, 6.26, N, 10.88%.

1-(6-trimethylsilyl-2-pyridyl)-3-(mesityl)imidazolium bromide 2.2

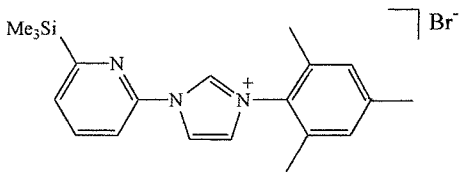

Prepared using general method 1 from 2-bromo-6-trimethylsilylpyridine (1.00 g, 4.3 mmol) and 1-(mesityl)imidazole (0.98 g, 5.2 mmol). Yield 1.89 g, 96%. MS (ES+): *m/z* 336 (M^+). NMR $\delta_H(CDCl_3)$ 0.31 [9H, s, $Si(CH_3)_3$], 2.15 (6H, s, *o*-mesityl-CH_3), 2.3 (3H, s, *p*-mesityl-CH_3), 7.0 (2H, s, *m*-mesityl *H*), 7.4 and 8.9 (2 x 1H, s, 4- and 5-imidazolium), 7.6 (1H, d, pyr H), 7.9 (1H, 7, pyr

H), 9.0 (1H, d, pyr H), 11.2 (1H, s, 2-imidazolium). $\delta_C(CDCl_3)$ –1.7 [$Si(CH_3)_3$], 18.0, 21.3 (mesityl-CH_3), 115.3, 120.1 (4- and 5-imidazolium) 124.1, 130.1, 130.5, 130.3, 130.7, 134.1, 138.8, 141.6, 145.9, (aromatic), 169.1 (2-imidazolium). Found C, 57.75, H, 6.03, N, 9.98, $C_{20}H_{25}N_3BrSi$ requires C, 57.82, H, 6.07, N, 10.11%.

1-(6-trimethylsilyl-2-pyridyl)-3-(2,6-di-*iso*-propylphenyl)imidazolium bromide 2.3

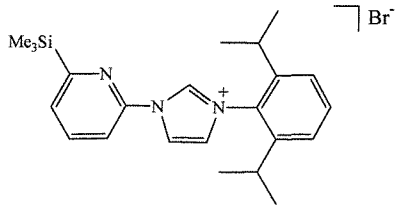

Prepared using general method 1 from 2-bromo-6-trimethylsilylpyridine (1.00 g, 4.3 mmol) and 1-(2,6-di-*iso*-propylphenyl)imidazole (1.08 g, 4.7 mmol). Yield 1.83 g, 93%. MS (ES+): *m/z* 378 (M^+). NMR $\delta_H(CDCl_3)$ 0.4 [9H, s, $Si(CH_3)_3$], 1.1, 1.3 [2 x 6H, d, diastereotopic $CH(CH_3)_2$], 2.4 [2H, septet, $CH(CH_3)_2$], 7.3 and 8.5 (2 x 1H, s, 4- and 5-imidazolium), 7.4 (2H, d, *m*-$^iPr_2C_6H_2H$), 7.6 (1H, t, *p*-$^iPr_2C_6H_2H$), 8.2 (1H, d, pyr H), 9.3 (1H, d, pyr H), 9.4 (1H, br. s, pyr H), 10.9 (1H, s, 2-imidazolium). $\delta_C(CDCl_3)$ –1.6 [$Si(CH_3)_3$], 24.2, 24.6 [$CH(CH_3)_2$], 28.8 [$CH(CH_3)_2$], 115.3, 120.8 (4- and 5-imidazolium) 124.6, 125.0, 125.9, 130.3, 131.8, 135.3, 138.9, 145.6, 146.0, (aromatic), 169.3 (2-imidazolium). Found C, 59.45, H, 7.06, N, 9.43, $C_{23}H_{32}BrN_3Si$ requires C, 60.25, H, 7.03, N, 9.16%.

1-(5-trimethylsilyl-2-pyridyl)-3-(2,6-di-*iso*-propylphenyl)imidazolium bromide 2.4

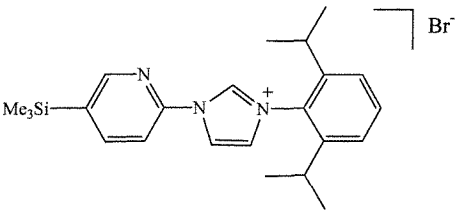

Prepared using general method 1 from 2-bromo-5-trimethylsilylpyridine (1.50 g, 6.5 mmol) and 1-(2,6-di-*iso*-propylphenyl)imidazole (1.60 g, 7.0 mmol). Yield 2.60 g, 87 %. MS (ES+): *m/z* 378 (M^+). NMR $\delta_H(CDCl_3)$ 0.4 [9H, s, $Si(CH_3)_3$], 1.1, 1.3 [2 x 6H, d, diastereotopic $CH(CH_3)_2$], 2.4 [2H, septet, $CH(CH_3)_2$], 7.1 (2H, d, *m*-$^iPr_2C_6H_2H$), 7.2 and 8.4 (2 x 1H, s, 4-and 5-imidazolium), 7.4 (1H, t, *p*-$^iPr_2C_6H_2H$), 8.0 (1H, d, pyr H), 8.9 (1H, d, pyr H), 9.1 (1H, s, pyr H), 10.6 (1H, s, 2-imidazolium). $\delta_C(CDCl_3)$ –1.2 [$Si(CH_3)_3$], 24.2, 24.4 [$CH(CH_3)_2$], 29.0 [$CH(CH_3)_2$], 115.5, 121.1 (4- and 5-imidazolium) 124.7, 125.0, 125.5, 132.4, 135.1, 138.7, 145.2, 146.3, 152.0, (aromatic), 173.3 (2-imidazolium).

1-(5-trifluoromethyl-2-pyridiyl)-3-(2,6-di-*iso*-propylphenyl) imidazolium bromide 2.5

Prepared using general method 1 from 2-bromo-5-trifluoromethylpyridine (0.50 g, 2.2 mmol) and 1-(2,6-di-*iso*-propylphenyl)imidazole (0.62 g, 2.7 mmol). Yield 0.95 g, 98%. MS (ES+): *m/z* 362 (M^+). $\delta_H(CDCl_3)$ 1.16, 1.26 [2 x 6H, d, diastereotopic $CH(CH_3)_2$], 2.4 [2H, septet,

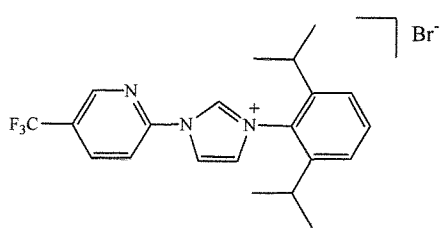

$CH(CH_3)_2]$, 7.2 (2H, d, $^iPr_2C_6H_2H$), 7.3 and 8.7 (1H, s, 4- and 5-imidazolium), 7.5 (1H, t, $^iPr_2C_6H_2H$), 8.3 (1H, d, pyr H), 9.2 (1H, s, pyr H), 9.6 (1H, d, pyr H), 11.3 (1H, s, 2-imidazolium). $\delta_C(CDCl_3)$ 24.6, 24.8 $[CH(CH_3)_2]$, 29.3 $[CH(CH_3)_2]$, 117.4, 121.2 (4- and 5-imidazolium) 125.2, 126.1, 127.1, 130.2, 132.7, 137.0, 138.8, 145.4, 146.4, (aromatic), 148.5 (2-imidazolium). Trifluoromethyl carbon not observed. Found C, 53.39, H, 5.28, N, 9.07, $C_{21}H_{23}N_3BrF_3$ requires C, 55.55, H, 5.10, N, 9.25%.

1-(*N,N*-diethylcarbamoylmethyl)-3-(mesityl)-imidazolium bromide 2.6

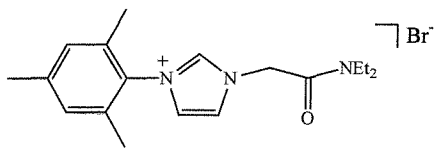

Prepared using general method 2 from 2-bromo-N,N-diethylacetamide (2.00 g, 10.0 mmol) and 1-(*tert*-butyl)imidazole (2.30 g, 12.5 mmol). Yield 3.00 g, 80%, mp. 175°C. MS (ES+): *m/z* 300 (M^+). $\delta_H(CDCl_3)$ 1.1, 1.3 (2 x 3H, t, diastereotopic CH_2CH_3), 2.1 (6H, s, *o*-mesityl CH_3), 2.3 (3H, s, *p*-mesityl CH_3), 3.4 and 3.6 (2 x 2H, q, diastereotopic CH_2CH_3), 6.0 (2H, s, CH_2)), 6.9 (2H, s, *m*-mesityl H), 7.2 and 7.9 (2 x 2H, s, 4- and 5-imidazolium H), 10.3 (2H, s, 2-imidazolium).

1-(*N,N*-diethylcarbamoylmethyl)-3-(*tert*-butyl)imidazolium bromide 2.7

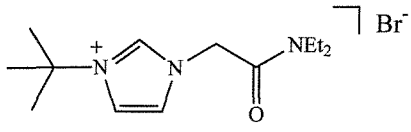

Prepared using general method 2 from 2-bromo-N,N-diethylacetamide (2.00 g, 10.0 mmol) and 1-(*tert*-butyl)imidazole (1.90 g, 15.0 mmol) After cooling to room temperature, a colourless oil separated. The supernatant was decanted and the oil triturated with ether until it solidified. Yield 2.4 g, 75%, mp. 118°C. MS (ES+): *m/z* 238 (M^+). $\delta_H(CDCl_3)$ 1.1, 1.3 (2 x 3H, t, diastereotopic CH_2CH_3), 1.7 [9H, s, $C(CH_3)_3$], 3.2 and 3.5 (2 x 2H, q, diastereotopic CH_2CH_3), 5.7 (2H, s, CH_2), 7.3 and 7.6 (2H, s, 4- and 5-imidazolium), 10.3 (1H, s, 2-imidazolium).

1-(2-picolyl)-3-[4-(*tert*-butyl)-2,6-dimethyl-phenyl]imidazolium bromide 2.8

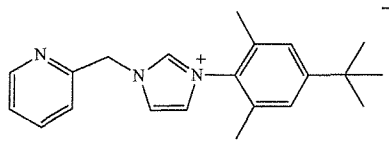

At 0°C, an aqueous solution of 2-bromomethylpyridine hydrogen bromide (10 cm^3, 2.00 g, 83.0 mmol) was layered with diethylether (10 cm^3), and whilst rapidly stirring a saturated aqueous sodium carbonate solution added dropwise. The liberated free pyridine was extracted into the diethylether. To the separated diethylether phase was added a

solution of 1-[2,6-dimethyl-4-(*tert*-butyl)phenyl]imidazole (1.92 g, 83.0 mmol) in methanol (10 cm^3) and the diethylether was gently removed under vacuum leaving the reactants in methanol. Methanol was added if the solution reduced to below 10 cm^3. The resulting solution was stirred at room temperature for 12 hours or at reflux for 3 hours. After filtering the reaction mixture the volatiles were removed under vacuum, and the resulting solid was washed with diethylether (3 x 15 cm^3) giving the product as white solid. In most cases, the product obtained at this stage were spectroscopically and analytically pure. If not, purification was carried out by recrystallisation from a saturated solution of dichloromethane layered with diethylether. Yield 1.03 g, 32%. MS (ES+) *m/z* 321 (M^+). NMR $\delta_H(CDCl_3)$ 1.3 [9H, s, $C(CH_3)_3$], 2.1 (6H, s, phenyl-CH_3), 6.2 (2H, s, CH_2), 7.1 (2H, s, phenyl H) 7.2 and 8.1 (2 x 1H, s, 4- and 5-imidazolium), 7.7 (1H, t, pyr H), 7.9 (1H, d, pyr H), 8.5 (1H, d, pyr H), 10.3 (1H, s, 2-imidazolium). $\delta_C(CDCl_3)$ 18.5 [$C(CH_3)_3$], 31.7 [$C(CH_3)_3$], 35.3 (phenyl-CH_3), 54.5 (CH_2), 115.2, 118.3 (4,5-imidazolium) 123.0, 124.3, 124.5, 124.9, 126.9, 131.7, 134.6, 138.3, 141.3, 146.4, 149.3, 150.2, (aromatic and 2-imidazolium)

3,3'-Di(*tert*-butyl)-1,1'-*o*-phenylenedimethylenebis(imidazolium) dibromide 2.9

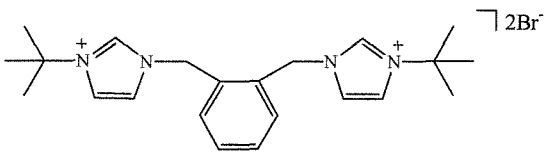

Prepared using general method 2 from α,α'-dibromo-o-xylene (1.00 g, 3.8 mmol) and 1-(*tert*-butyl)imidazole (2.00 g, 8.3 mmol). Yield 1.92 g, 92%. mp 247 °C (decomp), MS (ES+) *m/z* 176.3 $(½M)^+$. $\delta_H(D_2O)$ 1.5 [18H, s, $C(CH_3)_3$], 5.5 (4H, s, CH_2), 7.2 and 7.6 (2 x 2H, s, 4- and 5-imidazolium), 7.3 and 7.5 (2 x 2H, m, xylyl), 8.8 (2H, s, 2-imidazolium). $\delta_C(D_2O)$ 31.5 [$C(CH_3)_3$], 52.8 (CH_2), 63.0 [$C(CH_3)_3$], 123.2, 124.9, 133.3, 134.3, 136.4 (xylyl and imidazolium). Found: C, 50.85; H, 5.99; N, 10.48; $C_{22}H_{34}N_4OBr_2$ requires C, 49.82; H, 6.46; N, 10.56%.

3,3'-Dimesityl-1,1'-*o*-phenylenedimethylenebis(imidazolium) dibromide 2.10

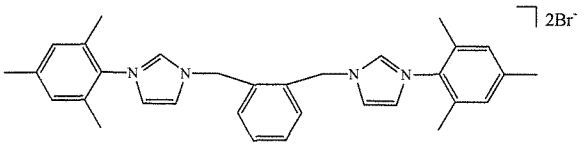

Prepared using general method 2 from α,α'-dibromo-o-xylene (1.00 g, 3.8 mmol) and 1-(mesityl)imidazole (1.55 g, 8.3 mmol). Yield 2.2 g, 92%. mp 254 °C (decomp), MS (ES+) *m/z* 238.4 $(½M)^+$. $\delta_H(D_2O)$ 2.0 (12H, s, *o*-mesityl CH_3), 2.2 (6H, s, *p*-mesityl CH_3), 6.3 (4H, s, CH_2), 6.9 (4H, s, *m*-mesityl H), 7.2 and 8.3 (2 x 2H, s, 4- and 5-imidazolium H), 7.2 and 7.3 (2 x 2H, m, xylyl), 10.1 (2H, s, 2-

imidazolium). $\delta_C(CDCl_3)$ 18.2, 21.5 (mesityl CH_3), 50.5 (CH_2), 123.8, 124.9, 129.7, 130.2, 130.4, 131.1, 133.1, 134.7, 138.0, 141.6 (xylyl, mesityl and imidazolium). Found: C, 58.16; H, 5.86; N, 7.36; $C_{32}H_{38}N_4OBr_2$ requires C, 58.73; H, 5.85; N, 8.56%.

3,3'-Di-(2,6-di-*iso*-propylphenyl)-1,1'-*o*-phenylenedimethylenebis(imidazolium) dibromide 2.11

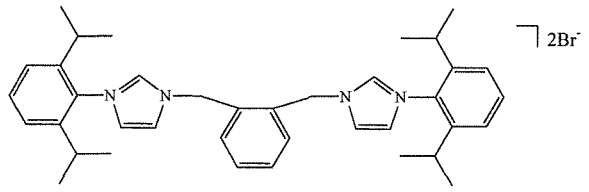

Prepared using general method 2 α,α'-dibromo-o-xylene (1.0 g, 3.8 mmol) and 1-(2,6-di-*iso*-propylphenyl)imidazole (1.90 g, 8.3 mmol). Yield 2.13 g, 78%. mp 252 °C (decomp), MS (ES+) *m/z* 280.5 ($½M^{2+}$). NMR $\delta_H(CDCl_3)$ 1.1, 1.2 [2 x 12H, d, diastereotopic $CH(CH_3)_2$], 2.2 (4H, septet, $CH(CH_3)_2$), 6.1 (4H, s, CH_2), 6.9 (4H, s, *m*-mesityl H), 7.1 and 8.7 (2 x 2H, s, 4- and 5-imidazolium), 7.2 and 7.8 (2 x 2H, m, xylyl), 7.2 (4H, d, *m*-$^iPr_2C_6H_2H$) 7.5 (2H, t, *p*-$^iPr_2C_6H_2H$), 10.7 (2H, s, 2-imidazolium). $\delta_C(CDCl_3)$ 24.2, 24.6 [$CH(CH_3)_2$], 28.8 [$CH(CH_3)_2$], 53.7 (CH_2), 124.2, 124.4, 124.8, 130.3, 132.0, 138.6, 139.1, 145.3, 153.5 (xylyl, phenyl and imidazolium C). Found: C, 59.52; H, 6.46; N, 7.60; $C_{38}H_{52}N_4OBr_2$ requires C, 60.31; H, 6.93; N, 7.40%.

1,1-bis[3-(*tert*-butyl)-imidazolium]-pyridine dibromide 2.12

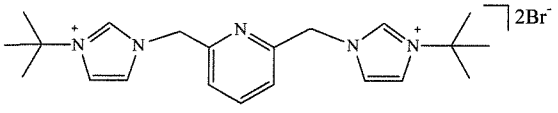

Prepared using the same method as for **2.8** using 2,6-dibromomethylpyridine hydrobromide (4.0 g, 0.011 mol) and 1-(*tert*-butyl)imidazole (2.87 g, 0.023 mol). Yield 4.43 g, 83%. MS (ES): *m/z* 434 $(M + 2MeCN)^+$, 177 $(½M)^+$. NMR $\delta_H(D_2O)$: 1.7 [18H, s, $C(CH_3)_3$], 5.3 (4H, s, CH_2), 7.3 and 7.6 (2 x 2H, s, 4- and 5-imidazolium), 7.4 (2H, d, pyr H), 7.8 (1H, t, pyr H). 2-imidazolium protons not observed due to ^2D scrambling. $\delta_C(D_2O)$: 31.4 [$C(CH_3)_3$], 55.9 (CH_2), 62.6 [$C(CH_3)_3$], 122.7, 125.5 (4- and 5-imidazolium), 125.8, 142.4, 155.9 (pyridine *C*), 174.0 (2-imidazolium).

1,1-bis[3-(*tert*-butyl)-imidazolium]-pyridine dibromide 2.13

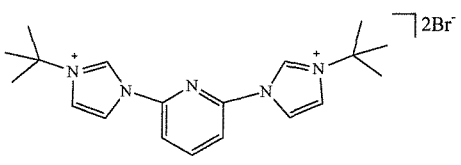

This was prepared as general method 1 from 2,6-dibromopyridine (2.0 g, 8.4 mmol) and 1-(*tert*-butyl)-imidazole (3.9 g, 21.1 mmol). Yield 97%. MS (ES): *m/z* 367 $(M + MeCN)^+$. NMR $\delta_H(D_2O)$: 1.7 [18H, s,

C(CH_3)$_3$], 7.9 and 8.3 (2 x 2H, s, 4- and 5-imidazolium), 8.0 (2H, d, pyr *H*), 8.4 (1H, t, pyr H). 2-imidazolium protons not observed due to ^{2}D scrambling. $\delta_C(D_2O)$: 31.0 [C(CH_3)$_3$], 63.5 [*C*(CH_3)$_3$], 117.3, 122.1 (4- and 5-imidazolium), 123.5, 146.8, 148.0 (pyridine *C*).

1,1-bis[3-(mesityl)-imidazolium]-pyridine dibromide 2.14

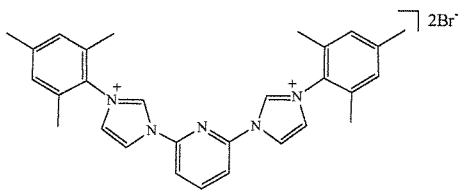

This was prepared as general method 1 from 2,6-dibromopyridine (2.0 g, 8.4 mmol) and 1-(mesityl)-imidazole (3.9 g, 21.1 mmol). Yield: 95%. Mp: > 250°C. MS (ES): *m/z* 225 (½M$^+$). NMR $\delta_H(D_2O)$: 2.08 (12H, s, *o*-CH_3), 2.36 (6H, s, *p*-CH_3), 7.15 (4H, s, $C_6H_2Me_3$), 7.8 and 8.8 (2 x 2H, s, 4- and 5-imidazolium), 8.10 and 8.50 (2H, d and 1H, t, pyridine ring protons). $\delta_H(CDCl_3)$: 18.0, 21.2 (mesityl CH_3), 116.9, 122.3 (4- and 5-imidazolium), 123.7, 130.0, 130.6, 134.1, 137.5, 141.5, 145.5 (aromatic) 2-imidazolium not observed. Found: C, 57.00; H, 5.10; N, 11.42. $C_{37}H_{47}Br_2N_5$ calculated: C, 57.16; H, 5.13; N, 11.49%.

1,1-bis{3-[2,6-dimethyl-4-(*tert*-butyl)phenyl]-imidazolium}-pyridine dibromide 2.15

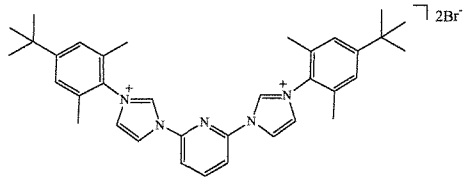

Prepared using general method 1 from 2,6-dibromopyridine (2.00 g, 8.4 mmol) and 1-[4-(*tert*-butyl)-2,6-dimethylphenyl]imidazole (4.24 g, 18.5 mmol). Yield 5.41 g, 93%. $\delta_H(CDCl_3)$ 1.2 [18H, s, C(CH_3)$_3$], 2.1 (12H, s, phenyl-CH_3), 7.1 (4H, s, phenyl H), 7.3 and 8.8 (2 x 2H, s, 4- and 5-imidazolium), 8.3 (1H, t, pyr H), 9.1 (2H, d, pyr H), 11.0 (2H, s, 2-imidazolium).

2,6-bis[3-(2,6-di-*iso*-propylphenyl)-imidazolium-1-ylmethyl]-1-bromobenzene dibromide 2.16

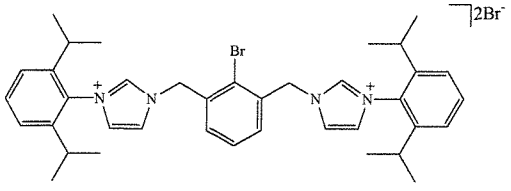

Prepared using general method 2 from 2,6-bromomethylbromobenzene (1.00 g, 2.9 mmol) and 1-(2,6-di-*iso*-propylphenyl)-imidazole (1.41 g, 7.3 mmol). Yield 1.94 g, 84%. $\delta_H(CDCl_3)$ 1.1, 1.2 [2 x 12H, d, CH(CH_3)$_2$], 2.4 [4H, septet, C*H*(CH_3)$_2$], 5.8 (4H, s, CH_2), 6.9 (2H, d, aromatic), 7.1 and 8.7 (2 x 2H, s, 4- and 5-imidazolium), 7.2 (1H, t, aromatic H), 7.3 (4H, d, Pr$^i_2$C$_6$H$_2$*H*), 7.4 (2H, t, Pr$^i_2$C$_6$H$_2$*H*), 10.3 (2H, s, 2-imidazolium). Found: C, 67.06; H, 7.07; N, 8.47. $C_{40}H_{52}Br_2N_4(3H_2O)$ calculated: C, 67.06; H, 7.11; N, 8.79%.

2,6-bis[3-(2,6-di-*iso*-propylphenyl)imidazolium]-3,5-dimethylphenyl dibromide 2.17

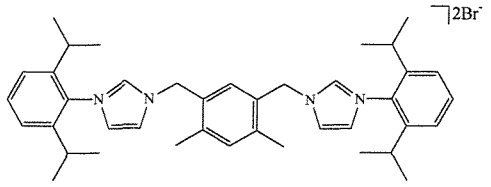

Prepared using general method 2 from 1,3-bis (bromomethyl) - 4,6 - dimethyl benzene (2.5 g, 8.65 mmol) and 1-(2,6-di-*iso*-propylphenyl)-imidazole (2.17 g, 9.5 mmol). Yield: 5.3 g, 82%. MS (ES): *m/z* 294 ½(M)$^+$. NMR $\delta_H(CDCl_3)$ 1.15, 1.20 [2 x 12H, d, CH(C*H*$_3$)$_2$], 2.3 [4H, septet, C*H*(CH$_3$)$_2$], 2.45 (6H, s, aromatic methyls), 5.95 (4H, s, CH$_2$), 6.95 and 7.95 (2 x 1H, s, aromatic), 7.12 and 8.88 (2 x 2H, s, 4- and 5-imidazolium), 7.33 (4H, d, Pr$^i_2$C$_6$*H*$_2$H), 7.50 (2H, t, Pr$^i_2$C$_6$H$_2$*H*), 10.7 (2H, s, 2-imidazolium). Found: C, 59.07; H, 7.35; N, 6.61. $C_{40}H_{52}Br_2N_4(3H_2O)$ calculated: C, 59.85; H, 7.28; N, 6.98%.

2,6-bis[3-(mesityl)-imidazolium]-3,5-dimethylphenyl dibromide 2.18

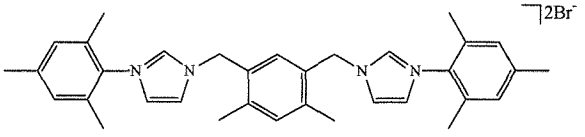

Prepared using general method 2 from 1,3-bis(bromomethyl)-4,6-dimethylbenzene (0.81 g, 2.78 mmol) and 1-(mesityl)-imidazole (1.15 g, 6.13 mmol). Yield: 1.61 g, 87 % MS (ES): *m/z* 252 ½ (M)$^+$. $\delta_H(CDCl_3)$ 2.0 (12H, s, mesityl *o*-CH$_3$), 2.3 (2 x 6H, s, mesityl *p*-CH$_3$ and phenyl *m*-CH$_3$), 5.8 (4H, s, CH$_2$), 6.9 (4H, s, mesityl H), 7.0 and 7.8 (2 x 1H, s, phenyl H), 7.1 and 8.4 (2 x 2H, s, 4- and 5-imidazolium H), 10.3 (1H, s, 2-imidazolium). $\delta_C(CDCl_3)$ 17.5, 19.1, 20.9 (aromatic CH$_3$) 66.9 (CH$_2$) 123.1, 124.6 (4- and 5-imidazolium), 129.5, 129.7, 130.6, 133.8, 134.0, 137.3, 137.4, 138.9, 141.0 (aromatic and 2-imidazolium).

2.5.2 Carbene Synthesis

General Method 3

The appropriate precursor imidazolium salt was dried azeotropically using Dean-Stark apparatus prior to use. In a glove box the precursor imidazole was placed into a Schlenk flask with 1.2 equivalents per imidazole of KN[Si(CH$_3$)$_2$] and the solids cooled to –78°C. Precooled THF (20 - 30 cm^3) was added via cannula and the mixture stirred until the bath temperature rose to –30°C, and then held at this temperature for 3 hours. The solution was then allowed to warm to room temperature, solvent removed *in vacuo,* and the pale residue was washed with petroleum ether (40/60) (2 x 15 cm^3). Product was extracted into toluene (30 cm^3) and solvent removed *in vacuo* to yield white crystalline product. Yields 70 – 85%.

X-ray quality crystals were grown by allowing slow cooling of concentrated toluene or petroleum solutions.

[1-(2-pyridyl)]-3-(2,6-di-*iso*-propylphenyl)-imidazol-2-ylidene 2.19

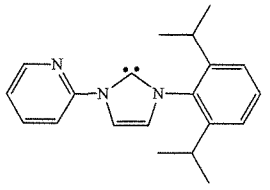

Prepared using general method 3 from [1-(2-pyridyl)]-3-(2,6-di-*iso*-propylphenyl)-imidazolium bromide (3.00 g, 7.8 mmol) and $KN(SiMe_3)_2$ (1.71 g, 8.6 mmol). Yield quantitative. Mp. 138 – 140°C (decomp). $\delta_H(C_6D_6)$ 1.1, 1.2 [2 x 6H, d, ^{i}Pr $CH(CH_3)_2$], 2.9 [2H, septet, ^{i}Pr $CH(CH_3)_2$], 6.6 (1H, t, pyridyl *H*), 6.7 and 8.4 (2 x 1H, s, 4- and 5-imidazol-2-ylidene), 7.1 (1H, t, pyridyl *H*), 7.2 (2H, d, $^i Pr_2C_6H_2H$), 7.3 (1H, t, $^i Pr_2C_6H_2H$), 8.3 (1H, d, pyr H), 8.8 (1H, d, pyr H). $\delta_C(C_6D_6)$ 22.6, 22.9 [^{i}Pr $C(CH_3)_2$], 27.1 [^{i}Pr $C(CH_3)_2$], 113.3, 115.0 (4- and 5-imidazol-2-ylidene), 119.8, 121.5, 122.3, 127.7 ($^i Pr_2C_6H_3$), 136.6, 137.3, 144.8, 146.4, 152.9 (pyridyl) 218.3 (2-imidazol-2-ylidene). Found: C, 77.62; H, 7.54; N, 13.55, $C_{20}H_{23}N_3$ requires C, 78.65; H, 7.59; N, 13.76%.

[1-(2-pyridyl-6-trimethylsilyl)]-3-(mesityl)-imidazol-2-ylidene 2.20

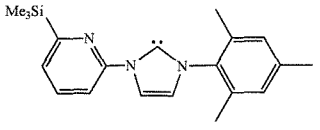

Prepared using general method 3 from **2.2** (1.00 g. 2.1 mmol) and potassium bis-silylamide (0.52 g, 2.6 mmol). Yield quantitative. $\delta_H(C_6D_6)$ 0.4 [9H, s, $Si(CH_3)_3$], 2.0 (6H, s, mesityl-CH_3), 2.1 (3H, s, mesityl-CH_3), 6.3 (1H, s, 4-imidazol-2-ylidene), 6.7 (2H, s, mesityl H), 6.9 (1H, d, pyr H), 7.1 (1H, t, pyr H), 8.3 (1H, s, 5-imidazol-2-ylidene), 8.6 (1H, d, pyr H). $\delta_C(C_6D_6)$ – 1.7 [$Si(CH_3)_3$], 17.9, 20.9 (mesityl-CH_3), 114.1, 116.5 (4- and 5-imidazol-2-ylidene), 121.3, 126.6, 129.1, 135.2, 136.4, 137.4, 138.9, 153.9, 166.0 (aromatic), 216.5 (2-imidazol-2-ylidene).

Crystal data for **2.20**: $C_{20}H_{25}N_3Si$, clear plate (0.10 x 0.05 x 0.01 mm^3), Mw 335.52, Monoclinic, $P2_1/c$ (No. 14), a = 16.3940(9) Å, b = 10.8288(5) Å, c = 10.9527(5) Å, $\alpha = \gamma$ = 90°, β = 91.642(2)°, V = 1943.61(17) $Å^3$, Z = 4, μ = 0.126 mm^{-1}, T = 150 K, Total reflections = 12760, unique reflections = 4356 (R_{int} = 0.0863), Final R indices [$I>2\sigma(I)$] R = 0.0635, R_w = 0.1358 (all data). Local Code 02sw054.

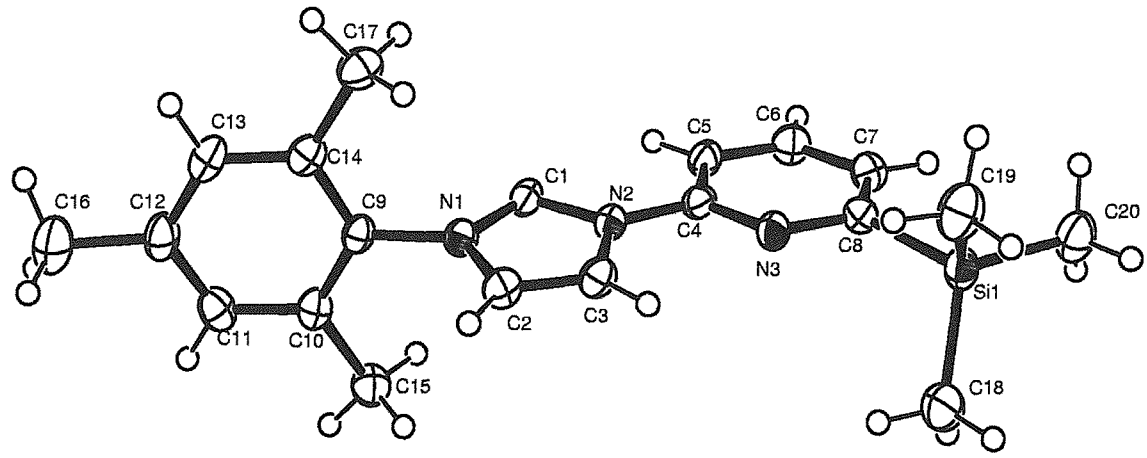

Fig 2.17 Crystal Structure of **2.20**.

Table 2.3 Bond lengths (Å) for **2.20**.

C1 – N1	1.355(3)	C4 – N2	1.415(3)	C9 – C14	1.393(3)	C13 – C14	1.383(4)
C1 – N2	1.386(3)	C5 – C6	1.380(4)	C9 – N1	1.444(3)	C14 – C17	1.505(4)
C2 – C3	1.329(4)	C6 – C7	1.392(4)	C10 – C11	1.388(4)	C18 – Si1	1.858(3)
C2 – N1	1.405(3)	C7 – C8	1.385(4)	C10 – C15	1.505(4)	C19 – Si1	1.861(3)
C3 – N2	1.396(3)	C8 – N3	1.363(3)	C11 – C12	1.390(4)	C20 – Si1	1.859(3)
C4 – N3	1.334(3)	C8 – Si1	1.888(3)	C12 – C13	1.388(4)		
C4 – C5	1.393(4)	C9 – C10	1.391(4)	C12 – C16	1.514(4)		

Table 2.4 Bond angles (°) for **2.20**.

N1 – C1 – N2	101.4(2)	C10 – C9 – N1	119.1(2)	C1 – N1 – C2	113.3(2)
C3 – C2 – N1	106.2(2)	C14 – C9 – N1	118.4(2)	C1 – N1 – C9	125.5(2)
C2 – C3 – N2	106.7(2)	C11 – C10 – C9	117.4(2)	C2 – N1 – C9	121.2(2)
N3 – C4 – C5	124.1(2)	C11 – C10 – C15	121.5(2)	C1 – N2 – C3	112.4(2)
N3 – C4 – N2	114.4(2)	C9 – C10 – C15	121.2(2)	C1 – N2 – C4	124.4(2)
C5 – C4 – N2	121.4(2)	C10 – C11 – C12	122.1(3)	C3 – N2 – C4	123.1(2)
C6 – C5 – C4	117.2(2)	C11 – C12 – C13	118.3(2)	C4 – N3 – C8	118.1(2)
C5 – C6 – C7	119.9(3)	C11 – C12 – C16	120.3(3)	C18 – Si1 – C20	111.13(14)
C8 – C7 – C6	119.4(3)	C13 – C12 – C16	121.4(3)	C18 – Si1 – C19	109.90(16)
N3 – C8 – C7	121.3(2)	C14 – C13 – C12	121.8(2)	C20 – Si1 – C19	109.86(14)
N3 – C8 – Si1	112.25(19)	C13 – C14 – C9	117.9(2)	C18 – Si1 – C8	107.43(13)
C7 – C8 – Si1	126.4(2)	C13 – C14 – C17	122.0(2)	C20 – Si1 – C8	109.07(13)
C10 – C9 – C14	122.4(2)	C9 – C14 – C17	120.1(2)	C19 – Si1 – C8	109.40(12)

[1-(2-pyridyl-6-trimethylsilyl)]-3-(2,6-di-*iso*-propylphenyl)-imidazol-2-ylidene 2.21

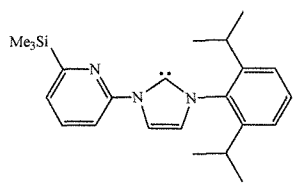

Prepared using general method 3 from **2.3** (1.50 g, 7.8 mmol) and $KN(SiMe_3)_2$ (1.71 g, 8.6 mmol). Yield quantitative. Mp. 168 – 170°C (decomp). $\delta_H(C_6D_6)$ 0.3 [9H, s, $Si(CH_3)_3$], 1.15, 1.25 [2 x 6H, d, ^iPr $CH(CH_3)_2$], 3.0 [2H, septet, ^iPr $CH(CH_3)_2$], 6.7 and 8.4 (2 x 1H, s,

4- and 5-imidazol-2-ylidene), 7.1 - 7.2 (3 x 1H, d, pyr *H*,), 7.2 (2H, d, $^{i}Pr_2C_6H_2H$), 7.3 (1H, t, $^{i}Pr_2C_6H_2H$), 8.8 (2 x 1H, s, pyr H). $\delta_C(C_6D_6)$ 0.2 [Si(CH_3)$_3$], 25.8, 26.1 [^{i}Pr C(CH_3)$_2$], 30.2 [^{i}Pr C(CH$_3$)$_2$], 115.8, 118.0 (4- and 5-imidazol-2-ylidene), 124.5, 127.3, 128.5, 130.9, 131.0, 138.2, 140.4, 147.9, 155.6 (aromatic), 219.5 (2-imidazol-2-ylidene). Found: C, 71.78; H, 8.17; N, 11.69, $C_{23}H_{31}N_3Si_1$ requires C, 73.16; H, 8.27; N, 11.13%.

Crystal data for **2.21**: $C_{46}H_{62}N_6Si_2$, clear block (0.15 x 0.15 x 0.03 mm^3), Mw 755.20, Monoclinic, $P2_1/n$ (No. 14), a = 22.1736(5) Å, b = 10.6162(2) Å, c = 22.1766(6) Å, $\alpha = \gamma$ = 90°, β = 99.1950(10)°, V = 5153.3(2) Å^3, Z = 4, μ = 0.101 mm^{-1}, T = 150 K, Total reflections = 44430, unique reflections = 9033 (R_{int} = 0.1776), Final R indices [$I>2\sigma(I)$] R = 0.1042, R_w = 0.2662 (all data). Local Code 01sw061. Unit cell contains two independent molecules.

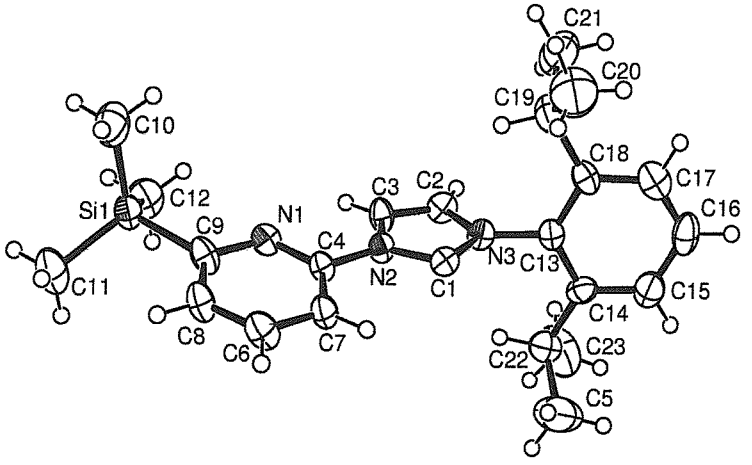

Fig 2.18 Crystal structure of **2.21**.

Table 2.5 Bond lengths (Å) for **2.21**.

C1 – N2	1.366(7)	C5 – C22	1.506(10)	C12 – Si1	1.845(7)	C17 – C18	1.392(8)
C1 – N3	1.360(7)	C6 – C7	1.369(8)	C13 – C18	1.390(8)	C18 – C19	1.508(9)
C2 – C3	1.311(7)	C6 – C8	1.370(8)	C13 – C14	1.395(8)	C19 – C20	1.489(10)
C2 – N3	1.387(7)	C8 – C9	1.396(8)	C13 – N3	1.439(7)	C19 – C21	1.553(10)
C3 – N2	1.392(7)	C9 – N1	1.377(7)	C14 – C15	1.385(8)	C22 – C23	1.542(10)
C4 – N1	1.326(7)	C9 – Si1	1.877(7)	C14 – C22	1.502(9)		
C4 – C7	1.396(8)	C10 – Si1	1.853(7)	C15 – C16	1.405(9)		
C4 – N2	1.417(7)	C11 – Si1	1.861(6)	C16 – C17	1.352(9)		

Table 2.6 Bond angles (°) for **2.21**.

N2 – C1 – N3	101.6(5)	C14 – C13 – N3	118.0(6)	C14 – C22 – C23	112.3(6)
C3 – C2 – N3	106.7(5)	C15 – C14 – C13	116.8(6)	C5 – C22 – C23	110.1(7)
C2 – C3 – N2	106.9(5)	C15 – C14 – C22	120.3(6)	C12 – Si1 – C10	109.5(4)
N1 – C4 – C7	123.8(6)	C13 – C14 – C22	122.9(6)	C12 – Si1 – C11	110.7(3)
N1 – C4 – N2	115.8(5)	C14 – C15 – C16	120.7(7)	C10 – Si1 – C11	110.0(3)
C7 – C4 – N2	120.3(6)	C17 – C16 – C15	119.8(7)	C12 – Si1 – C9	108.9(3)

C7 – C6 – C8	120.2(6)	C16 – C17 – C18	122.5(7)	C10 – Si1 – C9	109.5(3)
C6 – C7 – C4	117.8(6)	C17 – C18 – C13	116.1(6)	C4 – N1 – C9	118.0(5)
C6 – C8 – C9	119.7(6)	C17 – C18 – C19	121.7(6)	C1 – N2 – C3	112.2(5)
N1 – C9 – C8	120.6(6)	C13 – C18 – C19	122.2(6)	C1 – N2 – C4	123.8(5)
N1 – C9 – Si1	116.5(4)	C20 – C19 – C18	111.8(6)	C3 – N2 – C4	124.0(5)
C8 – C9 – Si1	122.9(5)	C20 – C19 – C21	110.5(6)	C1 – N3 – C2	112.7(5)
C18 – C13 – C14	124.0(6)	C18 – C19 – C21	109.9(6)	C1 – N3 – C13	122.1(5)
C18 – C13 – N3	118.0(6)	C14 – C22 – C5	111.5(6)	C2 – N3 – C13	125.1(5)

[1-(2-pyridyl-5-trimethylsilyl)]-3-(2,6-di-*iso*-propylphenyl)-imidazol-2-ylidene 2.22

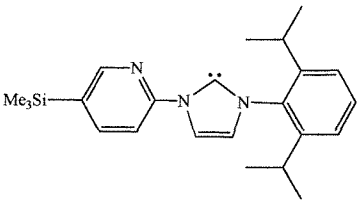

Prepared using general method 3 from **2.4** (1.00 g, 2.1 mmol) and $KN(SiMe_3)_2$ (0.48 g, 2.4 mmol). Yield quantitative. $\delta_H(C_6D_6)$ 0.3 [9H, s, $Si(CH_3)_3$] 1.1, 1.2 [2 x 6H, d, ^{i}Pr $CH(CH_3)_2$], 3.0 [2H, septet, ^{i}Pr $CH(CH_3)_2$] 6.7 and 8.5 (2 x 1H, s, 4- and 5-imidazol-2-ylidene), 7.1 (1H, d, pyr *H*), 7.2 (2H, d, $^i Pr_2C_6H_2H$), 7.3 (1H, t, $^i Pr_2C_6H_2H$), 7.4 (1H, d, pyr *H*), 8.8 (1H, s, pyr H). $\delta_C(C_6D_6)$ 0.2 [$Si(CH_3)_3$], 23.9, 24.3 [^{i}Pr $C(CH_3)_2$], 28.5 [^{i}Pr $C(CH_3)_2$], 116.3, 119.8 (4- and 5-imidazol-2-ylidene), 122.8, 123.7, 124.6, 129.1, 129.8, 138.2, 143.3, 152.4 (aromatic), 218.7 (2-imidazol-2-ylidene).

[1-(2-pyridyl-5-trifluoromethyl)]-3-(2,6-di-*iso*-propylphenyl)-imidazol-2-ylidene 2.23

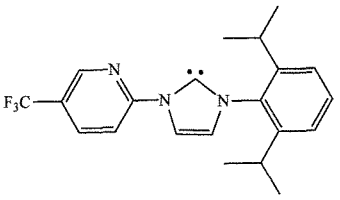

Prepared using general method 3 from **2.5** (1.00 g, 2.6 mmol) and $KN(SiMe_3)_2$ (0.60 g, 3.2 mmol). Yield quantitative. $\delta_H(C_6D_6)$ 1.2, 1.3 (2 x 6H, d, ^{i}Pr CH_3), 3.0 [2H, septet, ^{i}Pr $CH(Me)_2$], 6.8 and 8.3 (2 x 1H, s, 4- and 5-imidazol-2-ylidene), 7.2 (2H, d, $^i Pr_2C_6H_2H$), 7.4 (1H, t, $^i Pr_2C_6H_2H$), 8.6 (1H, s, pyr H), 8.7 (2 x 1H, s, pyr H). $\delta_C(C_6D_6)$ 24.3, 24.6 [^{i}Pr $C(CH_3)_2$], 28.9 [^{i}Pr $C(CH_3)_2$], 114.8, 116.8 (4- and 5-imidazol-2-ylidene), 123.7, 124.2, 124.5, 127.9 ($^i Pr_2C_6H_3$), 138.7, 145.4, 145.6, 146.4, 156.8 (pyridyl), 221.5 (2-imidazol-2-ylidene). Trifluoromethyl carbon not observed.

[1-(2-picolyl)]-3-(2,6-di-*iso*-propylphenyl)-imidazol-2-ylidene 2.24

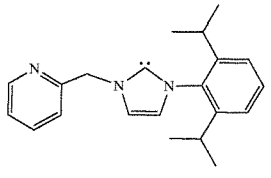

Prepared using general method 3 from [1-(2-pyridin-2-ylmethyl)]-3-(2,6-di-*iso*-propylphenyl)-imidazol-2-ium bromide (0.20 g, 0.5 mmol) and $KN(SiMe_3)_2$ (0.12 g, 0.6 mmol). Yield quantitative. $\delta_H(C_6D_6)$ 1.1, 1.3 (2 x 6H, d, ^{i}Pr CH_3), 2.9 [2H, septet, ^{i}Pr $CH(CH_3)_2$], 5.5 (2H, s, CH_2), 6.5 and 7.2 (2 x 1H, s, 4- and 5-imidazol-2-ylidene), 7.0 - 7.2 (3H, m, pyr H), 7.2 (2H, d, $^i Pr_2C_6H_2H$), 7.3 (1H, t, $^i Pr_2C_6H_2H$), 8.5 (1H, s, pyr H). $\delta_C(C_6D_6)$

23.8, 24.5 [^{i}Pr C(CH_3)$_2$], 28.5 [^{i}Pr C(CH$_3$)$_2$], 57.1 (CH_2), 119.2, 121.8, 122.2, 122.4, 123.6, 127.6, 128.3, 128.9, 136.2, 146.3, 149.4 (aromatics, 4- and 5-imidazol-2-ylidene), 190 (2-imidazol-2-ylidene).

[1-(2-methoxymethyl)]-3-(2,6-di-*iso*-propylphenyl)-imidazol-2-ylidene 2.25

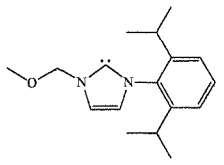

Prepared using general method 3 from [1-(2-methoxymethyl)]-3-(2,6-di-*iso*-propylphenyl)-imidazol-2-ium bromide (0.55 g, 1.55 mmol) and KN(SiMe$_3$)$_2$ (0.37 g, 1.86 mmol). Yield quantitative. Mp. 100 – 102 °C (decomp). δ_H($C_6D_5CD_3$) 1.1, 1.3 [2 x 6H, d, ^{i}Pr CH(CH_3)$_2$], 2.7 [2H, septet, ^{i}Pr CH(CH$_3$)$_2$], 3.2 (3H, s, O-CH$_3$), 5.3 (2H, s, CH$_2$ bridge), 6.5 and 6.7 (1H, s, 4- and 5-imidazol-2-ylidene), 7.2 (2H, d, ^{i}Pr$_2$C$_6$$H_2$H), 7.3 (1H, t, ^{i}Pr$_2C_6H_2$$H$). δ_C($C_6D_5CD_3$) 24.5, 24.8 [^{i}Pr C(CH_3)$_2$], 28.8 [^{i}Pr C(CH$_3$)$_2$], 55.5 (CH_2), 82.3 (O-CH_3), 118.8, 123.3, 124.2, 129.7, 137.8, 146.3 (aromatics,4- and 5-imidazole-2-ylidene), 215 (2-imidazol-2-ylidene).

1,1-bis[3-(mesityl)-imidazol-2-ylidene]-pyridine 2.26

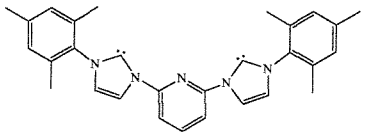

Prepared using general method 3 from **2.14** (2.00 g, 3.2 mmol) and KN(SiMe$_3$)$_2$ (1.57 g, 7.8 mmol). Yield quantitative. Mp. 215 - 217°C (decomp). δ_H(C_6D_6) 2.1 (12H, s, mesityl-CH$_3$), 2.2 (6H, s, mesityl-CH$_3$), 6.5 and 8.1 (2 x 2H, s, 4- and 5-imidazol-2-ylidene), 7.1 (4H, s, aromatic-H), 7.2 (2H, br. s, pyr H), 8.6 (1H, d, pyr H). δ_C(C_6D_6) 18.4, 21.3 (mesityl-CH$_3$), 111.8, 116.8 (4- and 5-imidazol-2-ylidene), 121.8, 126.0, 129.5, 129.6, 135.6, 137.9, 139.3, 141.0 (aromatic) 220.2 (2-imidazol-2-ylidene).

1,1-bis[3-(2,6-dimethyl-4-tert-butyl-phenyl)-imidazol-2-ylidene]-pyridine 2.27

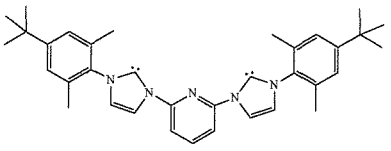

Prepared using general method 3 from **2.15** (2.00 g, 3.2 mmol) and KN(SiMe$_3$)$_2$ (1.57 g, 7.8 mmol). Yield quantitative. δ_H(C_6D_6) 1.3 [18H, s, phenyl-C(CH$_3$)$_3$], 2.2 (6H, s, phenyl-CH$_3$), 6.4 and 8.1 (2 x 2H, s, 4- and 5-imidazol-2-ylidene), 7.1 (4H, s, aromatic-H), 7.2 (2H, br. s, pyr H), 8.6 (1H, d, pyr H). δ_C(C_6D_6) 17.9, 20.9 (aromatic-CH$_3$), 31.0 [C(CH_3)$_3$], 65.7 (CH_2), 111.6, 116.6 (4- and 5-imidazol-2-ylidene), 121.5, 125.6, 135.2, 139.0, 140.8, 151.0 (aromatic), 220.1 (2-imidazol-2-ylidene).

2,6-bis[3-(2,6-di-*iso*-propylphenyl)-imidazol-2-ylidene]-1-bromobenzene 2.28

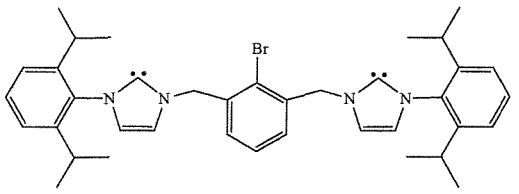

Prepared using general method 3 from **2.16** (2.00 g, 3.2 mmol) and $KN(SiMe_3)_2$ (1.57 g, 7.8 mmol). Yield quantitative. Mp. 183 – 185°C (decomp). $\delta_H(C_6D_6)$ 1.2, 1.4 [2 x 12H, d, $CH(CH_3)_2$], 3.0 [4H, septet, ^{i}Pr $CH(CH_3)_2$], 5.5 (4H, s, CH_2), 6.7 and 7.3 (2 x 2H, s, 4- and 5-imidazol-2-ylidene), 7.0 – 7.1 (6H, m, aromatic), 7.4 (3H, t, aromatic). $\delta_C(C_6D_6)$ 23.8, 24.6 [^{i}Pr $C(CH_3)_2$], 28.6 [^{i}Pr $C(CH_3)_2$], 55.2 (CH_2), 119.1, 122.5 (4- and 5-imidazol-2-ylidene), 123.8, 128.2, 128.3, 128.4, 128.9, 138.9, 139.3, 146.2 (aromatic), 219.5 (2-imidazol-2-ylidene).

2,6-bis[3-(2,6-di-*iso*-propylphenyl)-imidazol-2-ylidene]-3,5-dimethylphenyl 2.29

Prepared using general method 3 from **2.17** (2.00 g, 3.2 mmol) and $KN(SiMe_3)_2$ (1.57 g, 7.8 mmol). Yield quantitative. Mp. 120 – 122 °C (decomp).

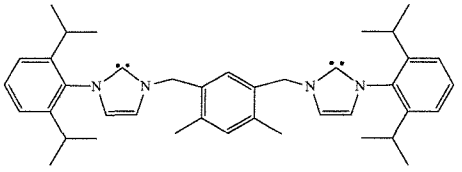

$\delta_H(C_6D_6)$ 1.0, 1.2 [2 x 12H, d, ^{i}Pr $CH(CH_3)_2$], 1.9 (6H, s, aromatic CH_3), 2.7 [4H, septet, ^{i}Pr $CH(CH_3)_2$], 5.2 (4H, s, CH_2), 6.3 and 6.4 (2 x 1H, s, aromatic), 6.6 and 7.0 (2 x 2H, s, 4- and 5-imidazol-2-ylidene), 7.1 (4H, d, ^{i}Pr$_2$C$_6$H$_2$H), 7.2 (2H, t, ^{i}Pr$_2$C$_6$H$_2$H). $\delta_C(C_6D_6)$ 20.2 (aromatic CH_3), 24.2, 25.0 [^{i}Pr $C(CH_3)_2$], 28.8 [^{i}Pr $C(CH_3)_2$], 49.4 (CH_2), 117.8, 122.2 (4- and 5-imidazol-2-ylidene), 123.9, 129.2, 130.0, 131.8, 137.8, 138.2, 139.4, 146.7 (aromatic) 218.8 (2-imidazol-2-ylidene). Found: C, 80.64; H, 8.72; N, 10.12, $C_{40}H_{52}N_4$ requires C, 81.87; H, 8.59; N, 9.55%.

2.5.3 Reactions of 'Free' Carbenes with Sulfur.

General Method 4

At room temperature, to a solution of appropriate carbene in dry toluene (*ca.* 10 cm^3) was added a suspension of sulfur flowers (3 equivs per carbene) in toluene and the mixture allowed to stir for 2 hours. The solution was filtered to remove excess sulfur and pumped to dryness to give white powders of the products.

2,6-bis[3-(2,6-di-*iso*-propylphenyl)-imidazol-2-thione-1-methyl]-1-bromobenzene 2.30

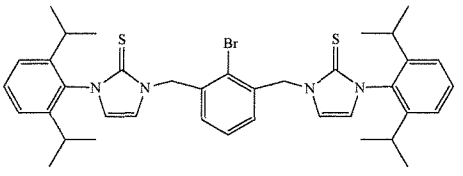

Prepared using general method 4 from **2.28** (0.12 g, 0.18 mmol) and flowers of sulphur (0.04 g, 1.1 mmol). Yield quantitative. MS (ES): *m/z* 703 $(M)^+$. $\delta_H(CDCl_3)$ 1.1, 1.3 [2 x 12H, d, ^{i}Pr $CH(CH_3)_2$], 2.6 [4H, septet, ^{i}Pr $CH(CH_3)_2$], 5.5 (4H, s, CH_2), 6.7 and 6.8 (2 x 2H, s, 4- and 5-imidazol-2-thione), 7.2 (2H, d,

aromatic), 7.3 (4H, d, aromatic), 7.4 (2H, t, aromatic). $\delta_C(CDCl_3)$ 23.8, 24.7 [^iPr C(CH_3)$_2$], 29.4 [^iPr $C(CH_3)_2$], 52.1 (CH_2), 117.4, 119.4 (4- and 5-imidazol-2-thione), 124.7, 128.6, 129.4, 130.6, 138.9, 134.0, 137.0, 146.8 (aromatic), 166.0 (2-imidazol-2-thione). Found: C, 65.01; H, 6.48; N, 8.01, $C_{38}H_{45}N_4S_2Br_1$ requires C, 65.03; H, 6.46; N, 7.98%.

[1-(2-methoxymethyl)]-3-(2,6-di-*iso*-propylphenyl)-imidazol-2-thione 2.31

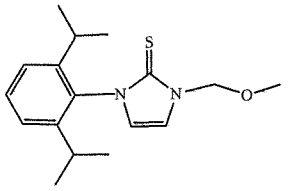

Prepared using general method 4 from **2.25** (0.10 g, 0.36 mmol) and flowers of sulphur (0.04 g, 1.1 mmol). Yield quantitative. MS (ES): *m/z* 305 $(M)^+$. $\delta_H(CDCl_3)$ 1.1, 1.3 (2 x 6H, d, ^iPr CH_3), 2.5 [2H, septet, ^iPr CH(CH_3)$_2$], 3.5 (3H, s, O-CH_3), 5.6 (2H, s, CH_2 bridge), 6.7 and 7.1 (1H, s, 4- and 5-imidazol-2-thione), 7.3 (2H, d, $^iPr_2C_6H_2H$), 7.5 (1H, t, $^iPr_2C_6H_2H$). $\delta_C(CDCl_3)$ 22.3, 23.3 [^iPr C(CH_3)$_2$], 27.6 [^iPr $C(CH_3)_2$], 55.9 (CH_2), 77.0 (O-CH_3), 115.4, 118.2 (4- and 5-imidazole-2-thione), 123.8, 129.1, 132.2, 145.5 (aromatics), 165.3 (2-imidazol-2-thione). Found: C, 67.06; H, 7.98; N, 9.13, $C_{17}H_{24}N_2S_1O_1$ requires C, 67.07; H, 7.95; N, 9.20%.

[1-(2-pyridyl-6-trimethylsilyl)]-3-(2,6-di-*iso*-propylphenyl)-imidazol-2-thione 2.32

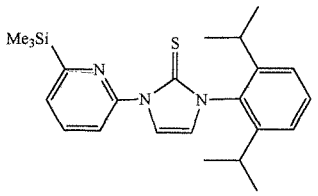

Prepared using general method 4 from **2.21** (0.1 g, 0.26 mmol) and flowers of sulphur (0.03 g, 0.79 mmol). Yield quantitative. MS (ES): *m/z* 410 $(M)^+$. $\delta_H(CDCl_3)$ 0.3 [9H, s, Si(CH_3)$_3$], 1.1, 1.3 [2 x 6H, d, ^iPr CH(CH_3)$_2$], 2.7 [2H, septet, ^iPr CH(CH_3)$_2$], 6.7 and 8.0 (2 x 1H, s, 4- and 5-imidazol-2-thione), 7.3 (2H, d, $^iPr_2C_6H_2H$), 7.5 (2 x 1H, d, pyridyl H), 7.8 (1H, t, $^iPr_2C_6H_2H$), 9.3 (1H, d, pyridyl H). $\delta_C(CDCl_3)$ 0.3 ($SiMe_3$), 22.4, 23.5 (^iPr CH_3), 27.6 [^iPr C(CH_3)$_2$], 115.2, 119.6 (4- and 5-imidazol-2-thione) 124.2, 127.1, 128.0, 129.1, 132.3, 134.5, 145.6, 148.9, 162.9, (aromatic), 166.2 (2-imidazol-2-thione).

2,6-bis[3-(mesityl)-imidazol-2-thione]-pyridine 2.33

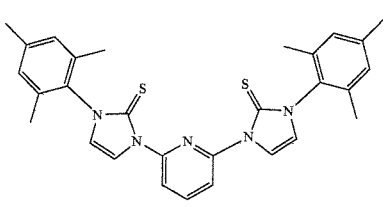

Prepared using general method 4 from **2.26** (0.12 g, 0.27 mmol) and flowers of sulphur (0.05 g, 1.6 mmol). Yield quantitative. MS (ES): *m/z* 512 $(M)^+$. $\delta_H(CDCl_3)$ 2.1 (12H, s, mesityl CH_3), 2.3 (6H, s, mesityl-CH_3), 6.7 and 7.7 (2 x 2H, s, 4- and 5-imidazol-2-thione), 6.9 (4H, s, mesityl H), 8.0 (1H, t, pyridyl H), 9.1 (2H, d, pyridyl H). $\delta_C(CDCl_3)$ 16.2, 20.1 (mesityl-CH_3), 115.4, 117.1 (4- and 5-imidazol-2-thione), 124.2, 127.1, 132.3, 134.7, 138.7, 139.0, 147.4 (aromatic) 162.1 (2-imidazol-2-thione).

2.6 References

[1] J. Wallach, *Ber. Dtsch. Chem. Ges*, **1925**, *15*, 645.
[2] A. J. Arduengo, *Vol. A2*, US Patent Office, US, **1992**, p. 5.077.414.
[3] H. V. R. Dias, W. Jin, *Tetrahedron Lett.*, **1994**, *35*, 1365.
[4] M. Scholl, S. Ding, C. W. Lee, R. H. Grubbs, *Org. Lett.*, **1999**, *1*, 953.
[5] B. Bildstein, M. Malaun, H. Kopacka, K. H. Ongania, K. Wurst, *J. Organomet. Chem.*, **1999**, *572*, 177.
[6] A. L. Johnson, *US Patent Office*, **1972**, No. 3637731.
[7] A. A. D. Tulloch, PhD thesis, University of Southampton (Southampton), **2001**.
[8] E. Drent, P. H. M. Budzelaar, *J. Organomet. Chem.*, **2000**, *593*, 211.
[9] N. Rahmouni, J. A. Osborn, A. D. Cian, J. Fischer, A. Ezzamarty, *Organometallics*, **1988**, *17*, 2470.
[10] A. A. D. Tulloch, A. A. Danopoulos, G. J. Tizzard, S. J. Coles, M. B. Hursthouse, R. S. Hay-Motherwell, W. B. Motherwell, *Chem. Commun.*, **2001**, 1270.
[11] A. A. D. Tulloch, A. A. Danopoulos, R. P. Tooze, S. M. Cafferkey, S. Kleinhenz, M. B. Hursthouse, *Chem. Commun.*, **2000**, 1247.
[12] E. Peris, J. A. Loch, J. Mata, R. H. Crabtree, *Chem. Commun.*, **2001**, 201.
[13] D. S. McGuinness, K. J. Cavell, *Organometallics*, **2000**, *19*, 741.
[14] J. A. Loch, M. Albrecht, E. Peris, J. Mata, J. W. Faller, R. H. Crabtree, *Organometallics*, **2002**, *21*, 700.
[15] A. Kovacevic, S. Grundemann, J. R. Miecznikowski, E. Clot, O. Eisenstein, T. H. Crabtree, *Chem. Commun.*, **2002**, 2580.
[16] A. J. Arduengo, R. Krafczyk, R. Schmutzler, H. A. Craig, J. R. Goerlich, W. J. Marshall, M. Unverzagt, *Tetrahedron*, **1999**, *55*, 14523.
[17] S. Kleinhenz, A. A. D. Tulloch, A. A. Danopoulos, *Acta Crystallogr. Sect. C-Cryst. Struct. Commun.*, **2000**, *56*, E476.
[18] A. A. Danopoulos, S. Winston, T. Gelbrich, M. B. Hursthouse, R. P. Tooze, *Chem. Commun.*, **2002**, 482.
[19] A. A. Danopoulos, S. Winston, W. B. Motherwell, *Chem. Commun.*, **2002**, 1376.
[20] M. H. Chisholm, J. C. Huffman, I. P. Rothwell, P. G. Bradley, N. Kress, W. H. Woodruff, *J. Am. Chem. Soc.*, **1981**, *103*, 4945.
[21] D. Bourissou, O. Guerret, F. P. Gabbai, G. Bertrand, *Chem. Rev.*, **2000**, *100*, 39.
[22] A. J. Arduengo, R. J. Barsotti, P. H. Corcoran, *US Patent Office No.*, **1992**, 5091498.
[23] A. J. Arduengo, P. H. Corcoran, *US Patent Office No.*, **1992**, 5084542.
[24] A. J. Arduengo, *Acc. Chem. Res.*, **1999**, *32*, 913.
[25] D. J. Williams, D. v. Derveer, L. A. Lipscombe, R. L. Jones, *Inorg. Chim. Acta.*, **1992**, *192*, 51
[26] G. B. Ansell, D. M. Forkey, D. W. Moore, *J. Chem. Soc. D*, **1970**, 56.
[27] A. n. Caballero, E.Dy´ez-Barra, F. A. Jalo´n, S. Merino, J. Tejeda, *J. Organomet. Chem.*, **2001**, *617*, 395.
[28] C. L. Yang, H. M. Lee, S. P. Nolan, *Org. Lett.*, **2001**, *3*, 1511.
[29] P. Jutzi, O. Lorey, *J. Organomet Chem.*, **1976**, *104*, 153
[30] J. Ahman, P. Somfai, *Synth. Commun.*, **1995**, *25*, 2301.
[31] M. E. Haeg, B. J. Whitlock, H. W. W. Jr, *J. Am. Chem. Soc.*, **1989**, *111*, 692.
[32] M. Newcomb, J. M. Timko, D. M. Walba, D. J. Cram, *J. Am. Chem. Soc.*, **1977**, *99*, 6392.
[33] C. M. Hartshorn, P. J. Steel, *Organometallics*, **1998**, *17*, 3487
[34] A. A. D. Tulloch, A. A. Danopoulos, S. Winston, S. Kleinhenz, G. Eastham, *J. Chem. Soc. Dalton. Trans.*, **2000**, 4499.

Chapter 3

N-Heterocyclic Carbene Complexes of Silver

Chapter 3

N-Heterocyclic Carbene Complexes of Silver.

3.1 Introduction.

Silver complexes of *N*-heterocyclic carbenes have shown more interesting properties as their study has recently increased which has been reviewed.[1-5] The first NHC complex of silver to appear in the literature was reported by Arduengo who synthesised a bis-carbene silver (I) complex of the well-known IMes ligand.[6]

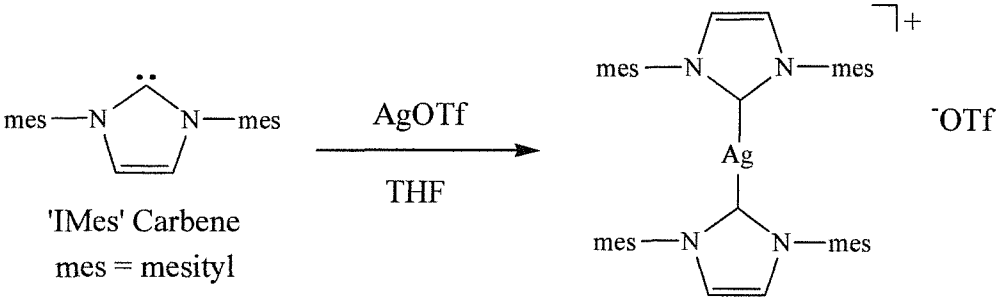

Fig 3.1 Arduengo's silver complex.

This initial synthetic route described the direct reaction of an isolated free carbene with silver triflate, but recently this has not been the common route employed to synthesise silver NHC complexes. Lin and co-workers realised that basic silver acetates are capable of deprotonating imidazolium salts to form silver carbene complexes.[7] If the reaction is performed under basic phase transfer catalysis conditions then the silver carbene complexes are also afforded.

The most significant property of silver imidazol-2-ylidene complexes is the ease in which they can transfer the imidazol-2-ylidene to Group 10 metals forming palladium, platinum and nickel carbene complexes, owing to the labile silver carbene bond.[7-10]

3.2 Results and Discussion.

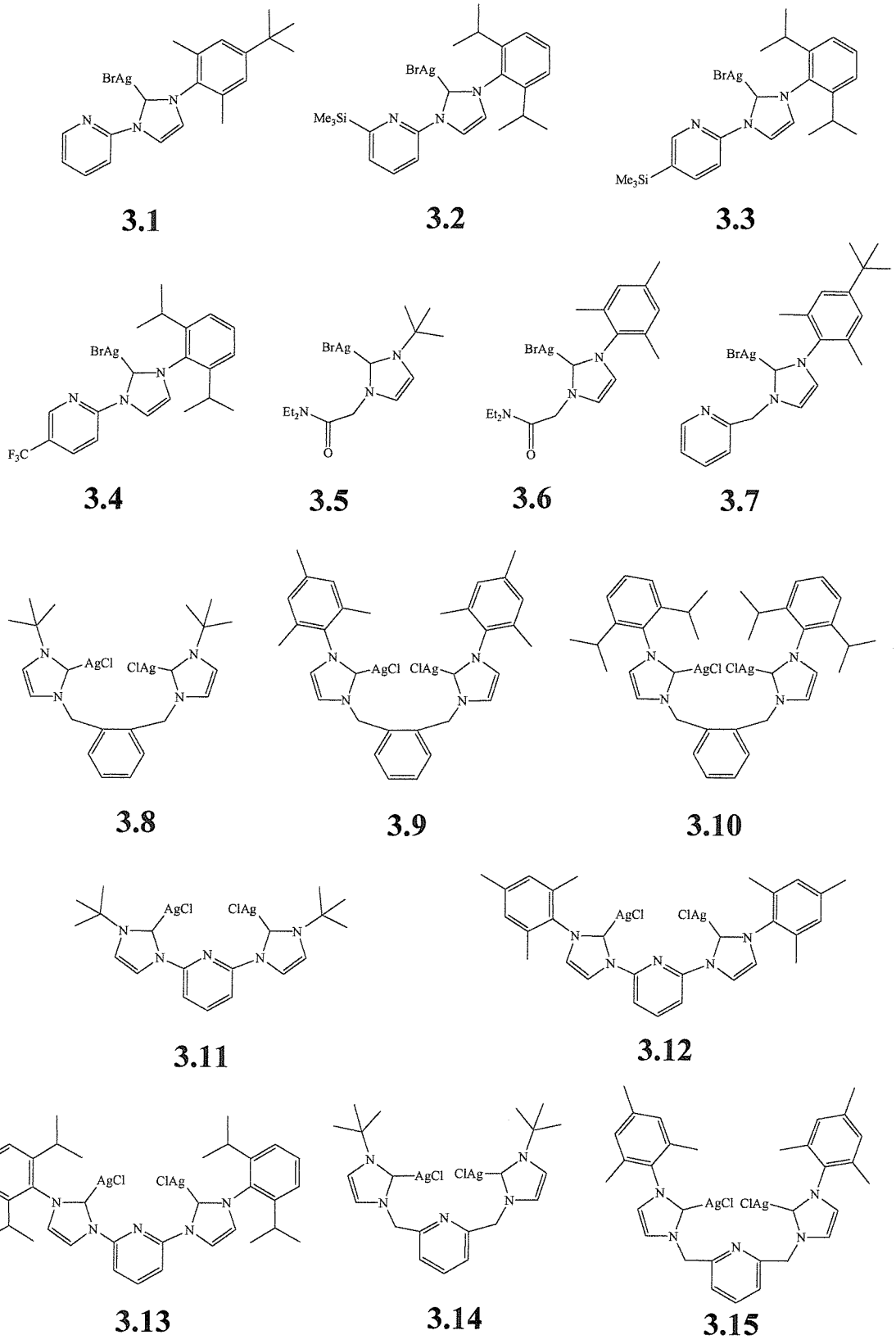

Fig 3.2 Silver (I) imidazol-2-ylidene complexes prepared.

3.2.1 Synthesis of Silver Complexes.

The compounds shown in Fig 3.2 were all synthesised via adaptation of the method reported by Lin and co-workers.[7] The use of silver(I) oxide or silver(I) carbonate to *in situ* deprotonate imidazolium salts has been shown to be a very clean and efficient route to the formation of silver carbene complexes.[1] Previous attempts to use phase transfer methods as reported by Lin were not successful.[11]

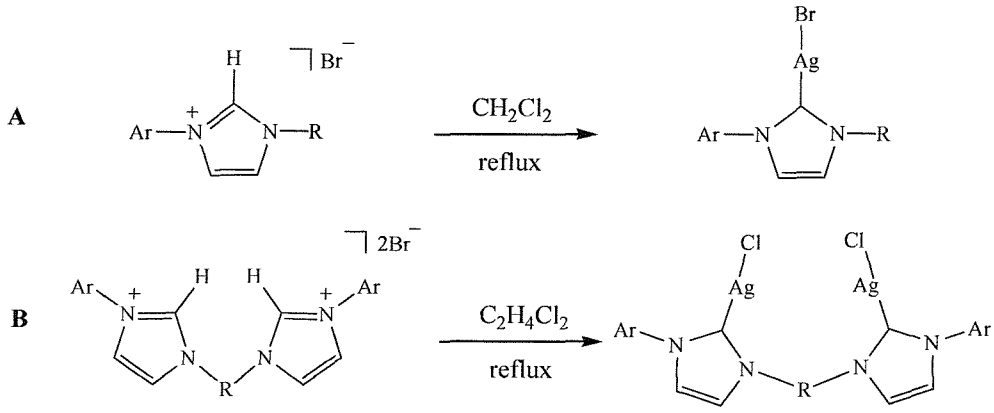

Fig 3.3 Synthesis of silver NHC complexes. Ar = aryl, R = linker group.

The above diagram shows two routes to form the silver NHC complexes; the only difference between the two is the choice of solvent medium. Method **A** shows the formation of mono-imidazol-2-ylidene silver halide complexes and is performed by the refluxing of Ag_2O and imidazolium salt in dichloromethane. Method **B** demonstrates the synthesis of bis-imidazol-2-ylidene complexes and is identical to **A** except for the higher boiling 1,2-dichloroethane is used. The driving force behind this reaction is the production of water, addition of 4 Å molecular sieves to remove the water from the reaction medium helps force the reaction equilibrium to favour the product. The addition of the molecular sieves to these reactions increases the yield by up to 30%. Bis-imidazol-2-ylidene silver complexes do not form if refluxing dichloromethane is used.

This synthetic route poses an identifiable problem, halide exchange. When using dichloromethane, if the imidazolium bromide salt is used then the silver carbene bromide complex ensues. This is not the case when using 1,2-dichloroethane, under refluxing conditions it has been observed that silver chloride complexes are obtained even when using the bromide salts. Arduengo showed that isolated imidazol-2-ylidenes in chlorinated solvents reform the imidazolium salt and other derivatives by attacking the solvent.[12] In the higher

boiling 1,2-dichloroethane it is likely that the hemilabile imidazol-2-ylidene can dissociate from the silver and then reform the imidazolium chloride salt by attacking the solvent. It is then plausible that deprotonation occurs again by a second silver oxide unit giving the silver chloride product. The silver is always in excess in these reactions. This can leave bulk product containing mixed halide, which can be overcome by increasing reaction times and silver excess to ensure that chlorine substitution is predominant.

3.2.2 Characterisation of Silver Complexes.

3.2.2.1 NMR Spectroscopy.

Proton and carbon NMR spectroscopy was used extensively for the confirmation of the identity of the products. Although exact structural identification was not possible without the use of additional forms of spectroscopy there were two key features of the NMR spectra which confirmed that the silver complexes had formed. In the proton NMR spectra the simplest indicator was the loss of the imidazolium proton signal at 10.0 - 11.0 ppm, whilst in the carbon NMR spectra the coordinated imidazol-2-ylidene give resonances in the range 162 – 179 ppm. This signal is further downfield than in the precursor salt show resonances at 145 – 169 ppm, but not as low field as the isolated carbene species at 215 - 222 ppm. No presence of the uncoordinated carbene is observed at room temperature. For the pyridine and picolyl functionalised silver carbene complexes the following characteristic resonances were observed in $CDCl_3$ for these related compounds:

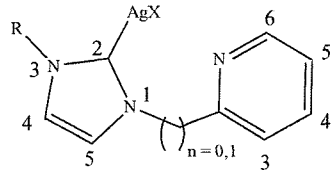

Fig 3.4 Numbering scheme for **3.1** - **3.4**, **3.7**, **3.11** – **3.15**, R = *tert*-butyl, mesityl, 2,6-di-*iso*-propylphenyl or 2,6-dimethyl-4-(*tert*-butyl)phenyl.

- If R = mesityl singlets at 1.8 – 2.3 and 6.8 – 6.9 ppm.
- If R = 2,6-di-*iso*-propylphenyl doublets at 1.1 and 1.3 ppm, a septet at 2.4 ppm and a doublet and triplet or broad singlets at 7.5 – 7.7 ppm.
- If R = 2,6-dimethyl-4-(*tert*-butyl)phenyl singlets at 1.2, 2.1 and 7.1 ppm.
- If R = *tert*-butyl a singlet at 1.3 ppm.
- For the 4- and 5-imidazol-2-ylidene protons two singlets between 7.1 – 7.4 and 8.1 – 8.3 ppm for n = 0 or 6.9 and 7.2 – 7.4 ppm for n = 1.

- If n = 1 then a singlet at 5.4 – 5.5 ppm from the methylene bridge.

Due to the asymmetric nature of the ligand the 4- and 5-imidazol-2-ylidene protons, as in the imidazolium salts and isolated carbenes show a difference in chemical shift of up to 1.0 ppm

For the pyridine ring protons chemical shifts varied depending on the substitution pattern of the ring. If a methylene bridge was incorporated into the ligand then peaks were observed between 7.3 – 8.6 ppm for mono-imidazol-2-ylidene silver complexes (compound **3.7**) and at 7.2 and 7.6 – 7.7 ppm for bis-imidazol-2-ylidene silver complexes (compounds **3.8** – **3.10**, **3.14** and **3.15**). Ligands without a methylene bridge (complexes **3.1** – **3.4** and **3.11** – **3.13**) had peaks in the range 7.4 – 8.7 ppm attributed to the pyridine ring. Depending on whether the compound was a mono- or bis-imidazol-2-ylidene complex the number of peaks varied depending on substitution, either three or four peaks for a mono-imidazol-2-ylidene complex and two peaks for a bis-imidazol-2-ylidene complex. The lowest field pyridine peak observed was in **3.4** on the 3-position of the pyridine ring at 8.7 ppm where the electron withdrawing CF_3 in the 5-position pulls all peaks further downfield as seen in the precursor imidazolium salt.

In the $^{13}C\{^1H\}$ NMR spectra of the pyridine functionalised silver complexes the main diagnostic resonance was the imidazol-2-ylidene appearing in the range 155 – 175 ppm, other signals appear in the following regions; aromatics in the range 124 – 155 ppm, 4- and 5-imidazolium carbons in the range 109 – 121 ppm, methylene bridges at 56 – 58 ppm, aryl substituent peaks from the 3-imidazolium position at 15 – 35 ppm depending on the substitution, i.e. methyl, *iso*-propyl or *tert*-butyl and a trimethylsilyl peak at –1 ppm. These chemical shifts are typical of previously made silver complexes.[11]

For the *N,N*-diethylacetamide (**3.5** and **3.6**) and *o*-phenylene (**3.8** – **3.10**) functionalised silver carbene complexes the following NMR resonances were used to identify the compounds. For **3.5** and **3.6** diastereotopic signals from the ethyl groups as two triplets between 1.1 and 1.4 and two quartets between 3.3 and 3.5 ppm, methylene bridges at 5.2 – 5.6 ppm and 4- and 5-imidazolium proton peaks as two singlets at 7.0 – 7.3 ppm. The aryl/alkyl substituent showed peaks as observed for the pyridine functionalised compounds. In the $^{13}C\{^1H\}$ NMR spectra the imidazol-2-ylidene carbon was observed between 163 – 167 ppm, diethylacetamide peaks between 40 – 42 ppm and other peaks as described for the pyridine functionalised compounds. For the *o*-phenylene (**3.8** – **3.10**) functionalised silver carbene complexes,

resonances in the proton NMR spectra were identified as follows; 4- and 5-imidazol-2-ylidene as two singlets at 6.9 – 7.0 and 7.2 – 7.4 ppm, methylene bridges as singlets at 5.4 – 5.6 ppm, *o*-phenylene protons as two double doublets or multiplets between 6.8 – 7.2 ppm for *tert*-butyl substituted and 7.4 - 7.7 ppm for aryl substituted imidazol-2-ylidenes. The aryl/alkyl substituent showed peaks as observed for the pyridine functionalised compounds. In the $^{13}C\{^1H\}$ NMR spectra the imidazol-2-ylidene carbon gave a peak at 179 ppm where observed and other peaks had similar chemical shifts to the pyridine functionalised compounds.

The NMR data can be used to confirm the presence of the silver carbene complex, but is not useful for structural deduction. The data confirms that a ligand is present in a single coordination mode. However, this does not mean that a mono-carbene complex has formed. There could be a symmetrical bis-imidazol-2-ylidene complex, so further spectroscopic techniques are required before absolute identity can be confirmed.

3.2.2.2 Mass Spectrometry.

Unlike for the characterisation of the imidazolium salts, electrospray mass spectrometry was of low diagnostic value, and at times misleading to elucidation of structural form. The positive electrospray spectrum for compound **3.6** (in MeCN) clearly shows only one peak corresponding to $Ag(Ligand)_2^+$ which would suggest a bis-carbene species, but upon crystallisation the mono-carbene Ag(Ligand)Br is characterised.

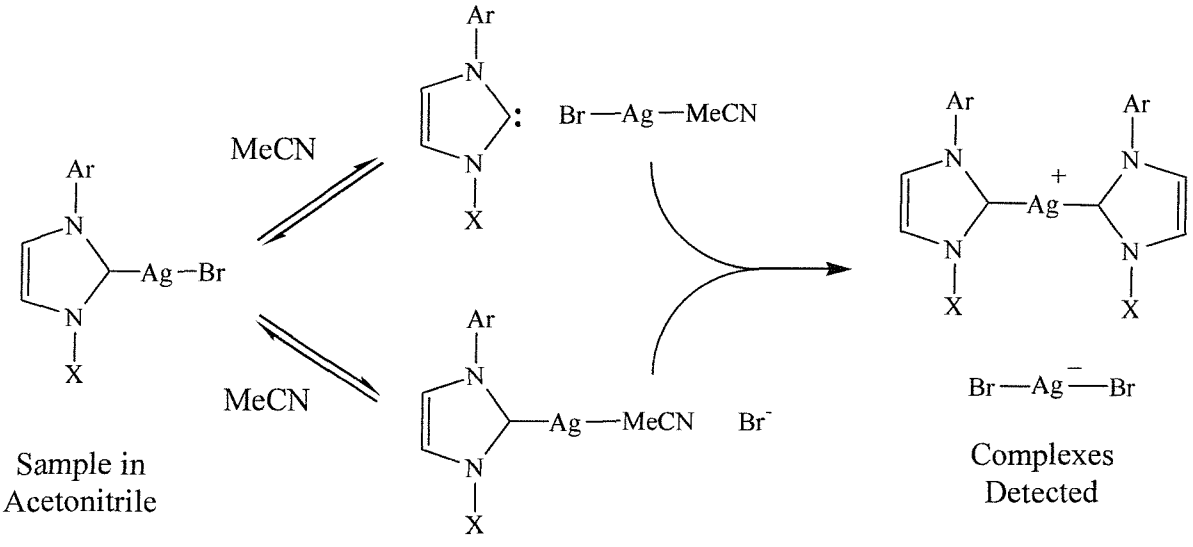

Fig 3.5 Silver complex rearrangement in acetonitrile.

The mass spectrometry samples are prepared in acetonitrile and the misleading results can be explained by acetonitrile displacing the ligands causing rearrangement between Ag(Ligand)Br and $[Ag(Ligand)_2]^+$. This was confirmed when crystalline Ag(Ligand)Br **3.6** was sampled and the only peak observed was $[Ag(Ligand)_2]^+$. The same misleading results were seen for compound **3.9**, only a peak for $[Ag(Ligand)]^+$ suggesting the chelated product, whereas when confirmed by X-ray crystallography the chelated product is not observed but a bis-silver bridged complex is isolated.

3.2.2.3 X-ray Crystallography.

X-ray quality crystals of compounds **3.6** and **3.9** were grown by layering solutions of dichloromethane with diethylether. Compound **3.6** is a mono-carbene silver complex, which in the solid state forms a dimeric species as shown in Fig 3.6. The silver to carbene bond length of 2.099(3) Å is the longest reported, which are usually in the range 2.058 – 2.099 Å, however, it is slightly shorter than known Ag-C single bonds (2.10 – 2.20 Å).

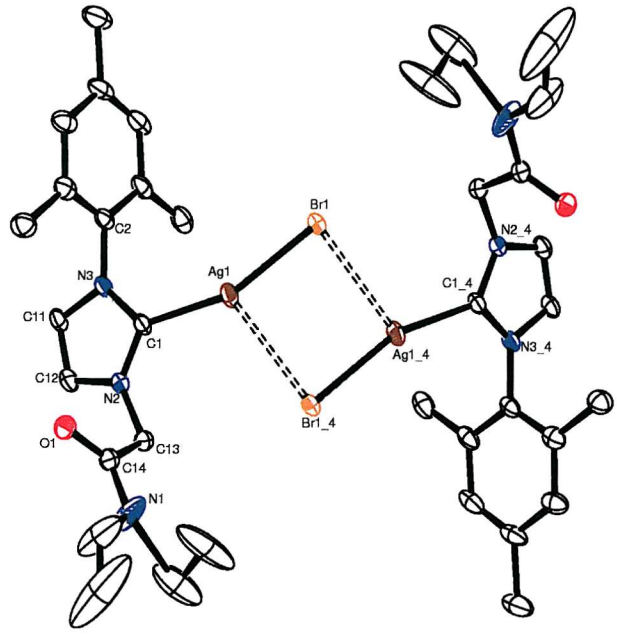

Fig 3.6 Crystal structure of **3.6**, hydrogens removed for clarity.

Table 3.1 Selected bond lengths (Å) and angles (°) for **3.6**

Ag1 – Br1	2.4099(9)	Ag1 – C1	2.099(3)
N3 – C1	1.359(5)	C1 – Ag1 – Br1	157.27(10)
N2 – C1	1.346(4)	N2 – C1 – N3	103.9(3)
C11 – C12	1.346(6)	C12 – N2 – C13 – C14	81.9(3)
Ag1 – Ag1_4	3.721(5)	Br1 – Ag1 – Br1_4	90.1(5)
Ag1 – Br1_4	2.907(5)	Ag1 – Br1 – Ag1_4	88.3(5)

The angle through the N2 – C1 – N3 bonds of 103.9° is typical of other known silver imidazol-2-ylidene complexes that are in the range 103 – 105°. The nitrogen to carbene carbon bond lengths are also typical of other reported complexes.[1] The Ag – Ag distance of 3.721(5) Å is greater than the sum of the van der Waals radii (3.40 Å) and there is no interaction between the two metal centres. In the structure bromine is shown coordinated to the metal centre, however the position is occupied by mixed halides and the bulk structure also incorporates chlorine. The source of this mixed halide, as has been mentioned, is from solvent exchange processes and the presence of different halides occupying this space does not affect the overall geometry. This mixed halide occupation is not unique to this compound and will be noted in other structures. In previous work it had been reported that mono-carbene ligands can lead to bis-carbene complexes and this is the case for complexes analogous to **3.7**.[11] The mesityl analogue of this ligand forms a *trans* bis-carbene silver complex with an associated silver dihalide anion. However the same is not the case for the *tert*-butyl and 2,6-di-*iso*-propylphenyl analogues, which form structures as above. It is still not understood why different structures form preferentially by changing the aromatic group.

The structure of compound **3.9** is a bis-carbene complex, but although designed as a chelating ligand, it behaves in a bridging mode between two silver atoms. The linear complex has the two silvers in an *anti* conformation and again the carbene to silver to halide bond is nearly linear (177.4°).

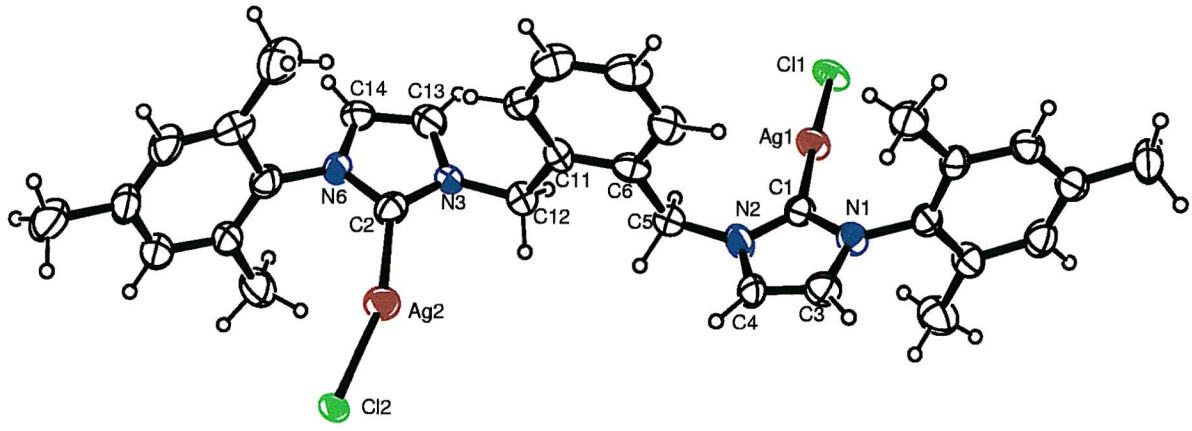

Fig 3.7 Crystal structure of **3.9**.

Table 3.2 Selected bond lengths (Å) and angles (°) for **3.9**

Ag1 – C1	2.061(7)	N3 - C2	1.360(9)
Ag1 – Cl1	2.3419(18)	C2 – Ag2 – Cl2	163.3(2)
Ag2 - C2	2.092(8)	C1 – Ag1 – Cl1	177.4(2)
Ag2 - Cl2	2.3886(15)	N2 – C1 – N1	104.0(6)
N6 - C2	1.321(8)	N6 – C2 – N3	104.5(6)

The silver to carbene bond lengths [2.061(7) and 2.092(8) Å] are comparable to other known silver NHC complexes as are all other bond lengths and angles. By examining the structure in the bulk crystal lattice in the coordination sphere of the silver there is no dimerisation process occurring to a second complex molecule, the Ag – Ag distances between molecules is >3.9 Å, further than in **3.6**. In other known silver NHC complexes that host ligands designed to be chelated to a single metal centre there are no reports of the ligand behaving in the expected fashion. A report by Cavell and co-workers describes a silver bis-NHC complex which has ligands analogous to **3.14** (methyl substituents in place of *tert*-butyl) bridging two silver centres rather than chelating as designed, as observed in the structure of **3.9**,[8] and a recent report of a tri-imidazol-2-ylidene tripodal silver complex shows each carbene bound to a different silver atom.[4]

3.2.2.4 Elemental Analysis

Elemental analysis of the compounds confirmed the composition of the products as containing a silver and halide per imidazol-2-ylidene. Where bis-carbene products had mixed halide substituents it was possible to observe the ratios of halide in the bulk product for that individual batch of product. An example of this is for **3.6** where the ration of Cl:Br was found to be approximately 10:1. Samples sent for elemental analysis had been repeatedly recystallised to remove inorganic salt contamination that was reported in earlier work by us[1] and others,[8] which showed that it was necessary to remove residual $[AgX_2]^-$ from the samples that otherwise persisted as an anion for the silver complexes.

3.3 Conclusions

A range of *N*-functionalised silver(I) mono- and bis-imidazol-2-ylidene complexes can be prepared from basic silver(I) precursors in good yields. It has been shown that a variety of spectroscopic techniques are required to fully characterise these compounds as the presence of donor solvents can alter the structures of the complexes. Crystal structures obtained were from dichloromethane solutions, but by changing solvent to acetonitrile it may be possible to crystallise alternative binding modes of the same ligands due to the hemilability of the ligands. The hemilability of the imidazol-2-ylidene observed with these species may be transferable to other transition metal systems that are catalytically active. The second 'dangling' donor group in conjunction with this hemilability could provide support for active catalytic species.

3.4 Experimental Section.

All experiments were carried out using predried solvents and under a nitrogen atmosphere. Ag_2O was used in all experiments; the use of Ag_2CO_3 gave similar yields and reaction times. The following compounds were made by literature method; 2,6-bis-[3-(2,6-di-*iso*-propylphenyl)-imidazolium]-pyridine dibromide.[11]

General Method 1

Appropriately substituted mono-imidazolium salt was refluxed with an excess of silver(I) oxide or silver(I) carbonate in the presence on 4 Å molecular sieves in dichloromethane (30 – 50 cm^3) for between 5 and 18 hours. After reaction completion the mixture was filtered through Celite, the solvent was removed under reduced pressure and the residual solid washed with diethyl ether before dried *in vacuo*. At this point the silver product complex was generally an analytically pure powder, but crystalline products could be obtained from further layering dichloromethane solutions with diethyl ether.

General Method 2

This method was used for bis-carbene complexes of silver. This is analogous to general method 1 in every aspect except that 1,2-dichloroethane was the solvent of choice due to its higher refluxing temperature.

1-(2-pyridyl)-3-[2,6-dimethyl-4-(*tert*-butyl)phenyl]imidazol-2-ylidene silver bromide 3.1

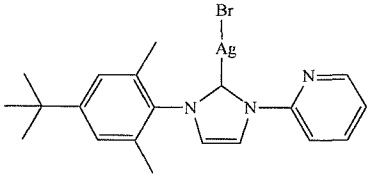

Prepared by general method 1 starting from compound **2.1** (1.50 g, 3.8 mmol) and Ag_2O (1.34 g, 5.8 mmol). Yield 61%. MS (ES+) *m/z* 718 $[Ag(ligand)_2]^+$. NMR $\delta_H(CDCl_3)$ 1.3 [9H, s, $C(CH_3)_3$], 2.0 (6H, s, phenyl-CH_3), 7.1 and 8.1 (2 x 1H, d, 4- and 5-imidazol-2-ylidene), 7.15 (2H, s, phenyl *m*-H), 7.4 (1H, dd, pyr H), 7.9 (1H, dd, pyr H), 8.2 (1H, d, pyr H), 8.5 (1H, d, pyr H). $\delta_C(CDCl_3)$ 18.8 $[C(CH_3)_3]$, 31.8 $[C(CH_3)_3]$, 35.2 (phenyl-CH_3), 116.1, 120.8 (4- and 5-imidazol-2-ylidene), 123.9, 124.5, 126.6, 134.8, 136.0, 140.1, 149.5, 151.2, 155.0 (aromatic), 173.2 (2-ylidene). Found C, 61.78, H, 6.19, N, 10.72, $C_{20}H_{24}N_3Br$ requires C, 62.18, H, 6.26, N, 10.88%.

[1-(6-trimethylsilyl-2-pyridyl)-3-(2,6-di-*iso*-propylphenyl)imidazol-2-ylidene]silver bromide 3.2

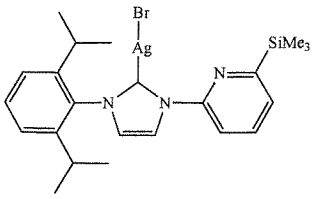

Prepared by general method 1 starting from compound **2.3** (1.00 g, 2.18 mmol) and Ag_2O (0.76 g, 3.2 mmol). Yield 73%. MS (ES+) *m/z* 378 $[Ag(ligand)]^+$. NMR $\delta_H(CDCl_3)$ 0.3 [9H, s, $Si(CH_3)_3$], 1.1, 1.3 [2 x 6H, d, $CH(CH_3)_2$], 2.5 [2H, septet, $CH(CH_3)_2$], 7.1 and 8.2 (2 x 2H, s, 4- and 5-imidazol-2-ylidene), 7.3 (2H, d, $Pr^i_2C_6H_2H$), 7.5 (1H, t, $Pr^i_2C_6H_2H$), 7.6 (1H, d, pyr H), 7.8 (1H, t, pyr H), 8.3 (1H, d, pyr H). $\delta_c(CDCl_3)$ –1.1 [$Si(CH_3)_3$], 25.0 [$CH(CH_3)_2$], 28.9 [$CH(CH_3)_2$], 114.1, 119.9 (4- and 5-imidazol-2-ylidene), 123.9, 124.2, 128.8, 130.6, 134.9, 137.2, 145.5, 150.1 (aromatic *C*), 168.9 (2-imidazol-2-ylidene).

[1-(5-trimethylsilyl-2-pyridyl)-3-(2,6-di-*iso*-propylphenyl)imidazol-2-ylidene]silver bromide 3.3

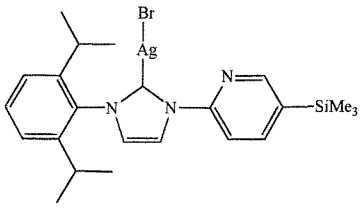

Prepared by general method 1 starting from compound **2.4** (1.50 g, 3.8 mmol) and Ag_2O (1.34 g, 5.8 mmol). Yield 67%. MS (ES+) *m/z* 378 $[Ag(ligand)]^+$. NMR $\delta_H(CDCl_3)$ 0.3 [9H, s, $Si(CH_3)_3$], 1.1, 1.3 [2 x 6H, d, $CH(CH_3)_2$], 2.5 [2H, septet, $CH(CH_3)_2$], 7.2 and 8.1 (2H, s, 4- and 5-imidazol-2-ylidene), 7.3 (2H, d, $Pr^i_2C_6H_2H$), 7.5 (1H, t, $Pr^i_2C_6H_2H$), 8.0 (1H, d, pyr H), 8.2 (1H, d, pyr H), 8.7 (1H, s, pyr H). $\delta_c(CDCl_3)$ –1.3 [$Si(CH_3)_3$], 24.4 [$CH(CH_3)_2$], 28.2 [$CH(CH_3)_2$], 114.7, 119.9 (4- and 5-imidazol-2-ylidene), 124.3, 124.8, 125.2, 130.7, 134.9, 136.0, 144.5, 145.5, 153.1 (aromatic *C*), 168.6 (2-imidazol-2-ylidene).

[1-(5-trifluoromethyl-2-pyridyl)-3-(2,6-di-*iso*-propylphenyl)imidazol-2-ylidene]silver bromide 3.4

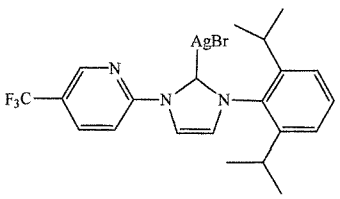

Prepared by general method 1 starting from compound **2.5** (1.50 g, 3.8 mmol) and Ag_2O (1.34 g, 5.8 mmol). Yield 61%. NMR $\delta_H(C_6D_6)$ 1.0, 1.2 [2 x 6H, d, ^iPr $CH(CH_3)_2$], 2.4 [2H, septet, ^iPr $CH(CH_3)_2$], 7.1 and 8.2 (2H, s, 4- and 5-imidazol-2-ylidene), 7.2 (2H, d, $Pr^i_2C_6H_2H$), 7.4 (1H, t, $Pr^i_2C_6H_2H$), 8.4 – 8.7 (3H, br. m, 3 x pyr H). $\delta_C(C_6D_6)$ 23.8, 24.7 [^iPr $C(CH_3)_2$], 28.3 [^iPr $C(CH_3)_2$], 109.2, 114.5 (4- and 5-imidazol-2-ylidene), 120.0, 124.7, 125.0, 130.8, 133.0, 137.1, 145.7, 147.8, 153.2 (aromatic), 162.1 (2-imidazol-2-

ylidene). Trifluoromethyl carbon not observed. Found: C, 44.23; H, 4.16; N, 6.79, $C_{21}H_{22}N_3F_3AgBr$ requires C, 45.35; H, 4.08; N, 7.56%.

[1-(*N,N*-diethylcarbamoylmethyl)-3-(*tert*-butyl)imidazol-2-ylidene] silver bromide 3.5

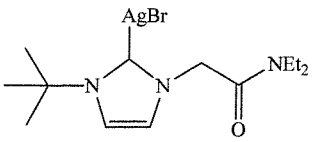

Prepared by general method 1 starting from compound **2.7** (1.00 g, 3.2 mmol) and Ag_2O (1.14 g, 4.9 mmol). Yield 0.54 g, 50%. MS (ES+): *m/z* 584 $[Ag(ligand)_2]^+$. $\delta_H(CDCl_3)$ 1.1, 1.3 (2 x 3H, t, diastereotopic CH_2CH_3), 1.7 [9H, s, $C(CH_3)_3$], 3.35 and 3.45 (2 x 2H, q, diastereotopic CH_2CH_3), 5.6 (2H, s, CH_2), 7.08 and 7.12 (2 x 1H, s, 4- and 5-imidazol-2-ylidene). δ_C 12.9, 13.0, 14.4 and 14.6 (CH_2CH_3), 30.0 and 31.9 $[C(CH_3)_3]$, 41.0, 41.1, 41.9, 42.0 (CH_2CH_3), 57.9 and 60.2 $[C(CH_3)_3]$, 65.8 (CH_2), 118.3, 121.6 (4- and 5-imidazol-2-ylidene), 163.9 (imidazol-2-ylidene), 179.0 (C=O).

[1-(*N,N*-diethylcarbamoylmethyl)-3-(mesityl)imidazol-2-ylidene]silver bromide 3.6

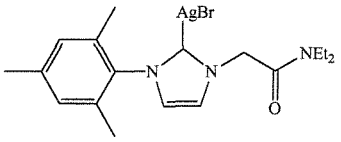

Prepared by general method 1 starting from compound **2.6** (2.00 g, 5.3 mmol) and Ag_2O (1.80 g, 7.9 mmol). Yield quantitative. MS (ES+): *m/z* 707 $[Ag(ligand)_2]^+$. $\delta_H(CDCl_3)$ 1.2, 1.4 (2 x 3H, t, diastereotopic CH_2CH_3), 2.1 (6H, s, *o*-mesityl CH_3), 2.4 (3H, s, *p*-mesityl CH_3), 3.5 (4H, q, NCH_2CH_3), 5.2 (2H, s, CH_2), 6.9 (2H, s, *m*-mesityl H). $\delta_C(CDCl_3)$ 13.9 and 14.7 (CH_2CH_3), 17.8 and 21.2 (*o*-, *p*-mesityl CH_3), 41.0, 41.8 (CH_2CH_3), 52.8 (CH_2), 123.2, 129.5, 135.0 and 139.6 (mesityl, 4- and 5-imidazol-2-ylidene), 167.0 (2-imidazol-2-ylidene). Found: C, 48.37; H, 5.59; N, 9.28, $C_{18}H_{25}N_3OAgCl_{0.92}Br_{0.08}$ requires C, 48.44; H, 5.65; N, 9.42%.

Crystal data for **3.6**: $C_{18}H_{25}N_3OAgCl_{0.92}Br_{0.08}$, clear block, Mw 446.34, Monoclinic, *C2/c* (No. 15), a = 26.539(2) Å, b = 10.448(1) Å, c = 16.885(2) Å, $\alpha = \gamma = 90°$, β = 125.90(1)°, V = 3793.01(6) Å^3, Z = 8, μ = 1.373 mm^{-1}, T = 150 K, Total reflections = 21107, unique reflections = 5526 (R_{int} = 0.0362), Final R indices [$I>2\sigma(I)$] R = 0.0542, R_w = 0.0678 (all data). CCDC Conquest reference code: VIBQOM. Local Code 00skl035.

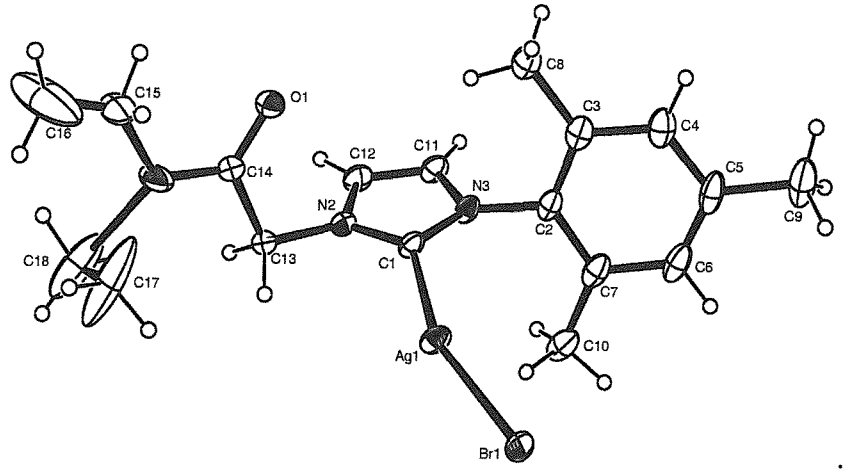

Table 3.3 Selected bond lengths (Å) for **3.6**

Ag1 – C1	2.099(3)	N2 – C13	1.448(5)	C13 – C14	1.536(5)
Ag1 – Br1	2.4099(9)	C11 – C12	1.346(6)	C14 – N1	1.330(6)
O1 – C14	1.208(4)	C17 – C18	1.254(11)	N1 – C15	1.502(9)
N2 – C1	1.346(4)	N3 – C1	1.359(5)	N1 – C17	1.783(15)
N2 – C12	1.381(5)	N3 – C11	1.389(4)	C15 – C16	1.140(14)

Table 3.4 Selected bond angles (°) for **3.6**

C1 – Ag1 – Br1	157.27(10)	N2 – C13 - C14	110.4(3)	C2 – C3 – C8	121.6(4)
C1 – N2 – C12	111.7(3)	C12 – C11 – N3	106.0(3)	C11 – C12 – N2	106.9(3)
C1 – N2 – C13	124.1(3)	O1 – C14 – N1	122.4(4)	C3 – C4 – C5	121.6(5)
C12 – N2 – C13	124.0(3)	O1 – C14 – C13	121.0(3)	N2 – C1 – N3	103.9(3)
C1 – N3 – C11	111.5(3)	N1 – C14 – C13	116.7(3)	N2 – C1 – Ag1	130.5(3)
C1 – N3 – C2	124.6(3)	C2 – C7 – C6	117.0(5)	N3 – C1 – Ag1	123.7(2)
C11 – N3 – C2	123.5(3)	C2 – C7 – C10	121.9(4)	C5 – C6 – C7	122.1(4)
C7 – C2 – C3	122.8(4)	C6 – C7 – C10	121.0(4)	C6 – C5 – C4	118.9(4)
C7 – C2 – N3	119.7(4)	C4 – C3 – C2	117.5(4)	C6 – C5 – C9	121.6(5)
C3 – C2 – N3	117.5(3)	C4 – C3 – C8	120.9(4)	C4 – C5 – C9	119.5(5)

[1-(pyridylmethyl)-3-[2,6-dimethyl-4-(*tert*-butyl)phenyl]imidazol-2-ylidene]silver bromide 3.7

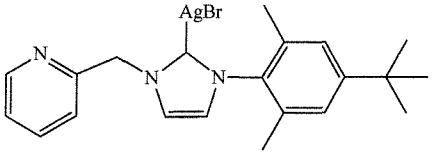

Prepared by general method 1 starting from compound **2.8** (1.50 g, 3.8 mmol) and Ag_2O (1.34 g, 5.8 mmol). Yield 0.91 g, 69%. MS (ES+) *m/z* 455 [Ag(ligand) + MeCN]$^+$. NMR $\delta_H(CDCl_3)$ 1.3 [9H, s, $C(CH_3)_3$], 2.0 (6H, s, phenyl-CH_3), 5.5 (2H, s, CH_2), 6.9 and 7.4 (2 x 1H, s, 4- and 5-imidazol-2-ylidene), 7.1 (2H, s, phenyl H), 7.3 (1H, dd, pyr H), 7.35 (1H, d, pyr H), 8.6 (1H, d, pyr H). $\delta_C(CDCl_3)$ 18.7 [$C(CH_3)_3$], 31.8 [$C(CH_3)_3$], 35.2 (phenyl-CH_3), 57.9 (CH_2), 122.4, 123.1 (4- and 5-imidazol-2-ylidine) 123.6, 124.1, 126.5, 128.3, 134.9, 136.1, 138.2, 150.5, 153.2 (aromatic), 155.7 (2-imidazol-2-ylidene).

Dichloro[3,3'-di-(*tert*-butyl)-1,1'-*o*-phenylenedimethylenebis(imidazol-2-ylidene)] disilver 3.8

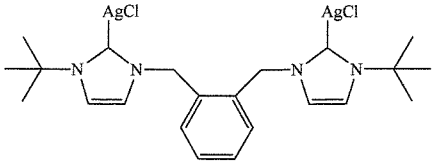

Prepared by general method 2 starting from compound **2.9** (1.00 g, 1.6 mmol) and Ag_2O (0.56 g, 2.4 mmol). Yield 0.89 g, 71%. Mp 152 °C. MS (ES+) *m/z* 458 $[Ag(ligand)]^+$. NMR $\delta_H(CDCl_3)$ 1.6 [18H, s, $C(CH_3)_3$], 5.4 (4H, s, CH_2), 6.8 and 7.3 (2 x 2H, dd, xylene-*H*), 7.0 and 7.2 (2 x 2H, d, 4- and 5-imidazol-2-ylidene). $\delta_C(CDCl_3)$ 31.6 [$C(CH_3)_3$], 53.6 (CH_2), 57.7 [$C(CH_3)_3$], 119.5 and 120.1 (4- and 5-imidazol-2-ylidene), 128.3, 128.8 and 133.9 (xylene-*C*), 179.6 (2-imidazol-2-ylidene).

Dichloro[3,3'-di-(mesityl)-1,1'-*o*-phenylenedimethylenebis(imidazol-2-ylidene)]disilver 3.9

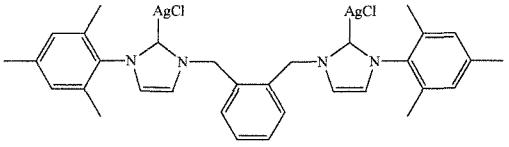

Prepared by general method 2 starting from compound **2.10** (1.0g, 1.6mmol) and Ag_2O (0.56 g, 2.4 mmol). Yield 0.80 g, 66%. X-ray diffraction quality crystals were grown by layering a saturated solution of dichloromethane with diethyl ether. Mp 158°C. MS (ES+): *m/z* 582 $[Ag(ligand)]^+$. $\delta_H(CDCl_3)$ 1.9 (12H, s, *o*-mesityl-CH_3), 2.3 (6H, s, *p*-mesityl-CH_3), 5.6 (4H, s, CH_2), 6.9 (4H, s, *m*-mesityl-*H*), 6.9 and 7.4 (2 x 2H, s, 4- and 5-imidazol-2-ylidene), 7.3 – 7.5 (4H, m, xylene). $\delta_C(CDCl_3)$ 17.6, 20.9 (*o*-, *p*-mesityl CH_3), 52.4 (CH_2), 122.4 and 122.9 (4- and 5-imidazol-2-ylidene), 127.4, 128.7 and 129.1 (xylene), 134.2, 134.4, 135.3 and 139.1 (mesityl). Imidazol-2-ylidene carbon was not observed. Found: C, 48.23; H, 4.33; N, 6.55, $C_{32.5}H_{35}Ag_2Cl_3N_4$ requires C, 48.57; H, 4.39; N, 6.97%. The isolated product contains half a molecule of dichloromethane per formula unit.

Crystal data for **3.8**: $C_{32.5}H_{35}N_4Cl_3Ag_2$, clear block (0.01 x 0.005 x 0.005 mm), Mw 803.73, Monoclinic, $P2_1/a$ (No. 14), a = 17.285(3) Å, b = 12.707(3) Å, c = 18.587(4) Å, $\alpha = \gamma = 90°$, β = 117.407(1)°, V = 3624.7(7) Å^3, Z = 4, μ = 1.327 mm^{-1}, T = 150 K, Total reflections = 35356, unique reflections = 9486 (R_{int} = 0.0821), Final R indices [$I>2\sigma(I)$] R = 0.0734, R_w = 0.1598 (all data). CCDC Conquest reference code: VIBRAZ. Local Code 00skl036.

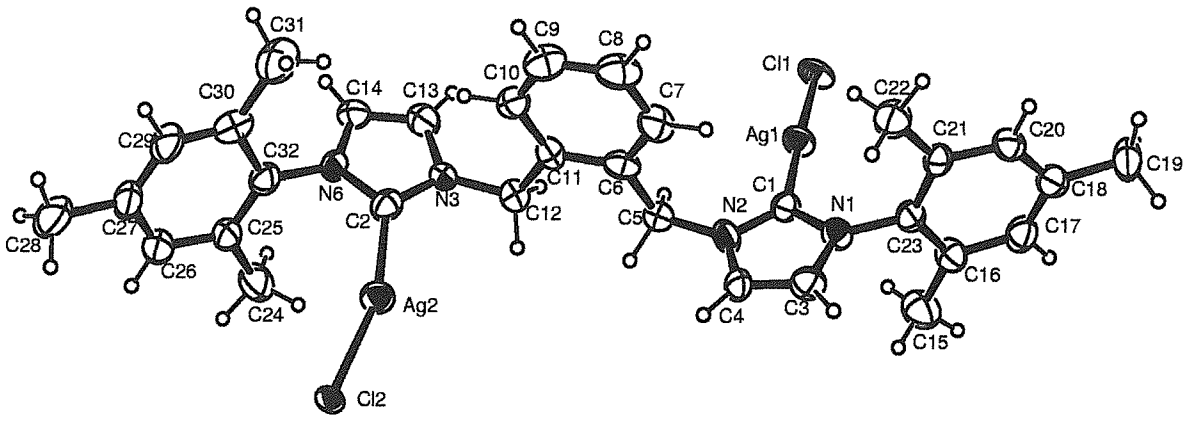

Fig 3.8 Crystal Structure of **3.9**.

Table 3.5 Selected bond lengths (Å) for **3.9**

Ag2 – C2	2.092(8)	N3 – C13	1.397(9)	C4 – C3	1.334(10)
Ag2 – Cl2	2.3886(15)	N3 – C12	1.443(9)	N1 – C3	1.412(9)
Ag1 – C1	2.061(7)	N6 – C2	1.321(8)	N2 – C4	1.365(9)
Ag1 – Cl1	2.3419(18)	N3 – C2	1.360(9)	N2 – C5	1.458(9)
C13 – C14	1.371(11)	N1 – C1	1.355(8)		
N6 - C14	1.368(9)	N2 – C1	1.339(8)		

Table 3.6 Selected bond angles (°) for **3.9**

C2 – Ag2 – Cl2	163.3(2)	C2 – N3 – C12	126.2(6)	N2 – C1 – Ag1	129.3(5)
C1 – Ag1 – Cl1	177.4(2)	C13 – N3 – C12	122.6(6)	N1 – C1 - Ag1	126.6(5)
C2 – N6 – C14	113.1(7)	N6 – C2 – N3	104.5(6)	N2 – C5 – C6	113.4(6)
C2 – N6 – C32	121.8(6)	N6 – C2 – Ag2	125.0(6)	C1 – N2 – C4	112.5(6)
C14 – N6 – C32	125.0(6)	N3 – C2 – Ag2	130.4(5)	C1 – N2 – C5	123.0(6)
C1 – N1 – C3	110.4(6)	C4 – C3 – N1	105.8(6)	C4 – N2 – C5	124.3(6)
C1 – N1 – C23	125.2(5)	N6 – C14 – C13	106.1(7)	C3 – C4 – N2	107.2(6)
C3 – N1 – C23	124.3(6)	N2 – C1 – N1	104.0(6)	C14 – C13 – N3	105.3(7)
C2 – N3 – C13	110.9(6)	N3 – C12 – C11	113.6(6)		

Dichloro[3,3'-di-(2,6-di-*iso*-propylphenyl)-1,1'-*o*-phenylenedimethylenebis(imidazol-2-ylidene)] disilver 3.10

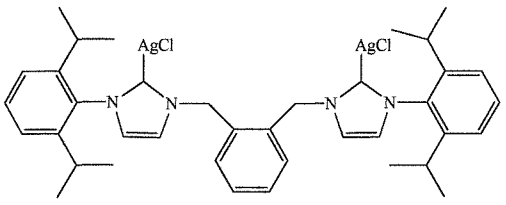

Prepared by general method 2 starting from compound **2.11** (1.00 g, 1.4 mmol) and Ag_2O (0.48 g, 2.1 mmol). Yield 0.92 g, 62%. mp 170°C. MS (ES+): *m/z* 667.6 $[Ag(ligand)]^+$. NMR $\delta_H(CDCl_3)$ 1.1 and 1.2 [2 x 12H, s, $CH(CH_3)_2$], 2.3 [4H, septet, $CH(CH_3)_2$], 5.5 (4H, s, CH_2), 7.0 and 7.2 (2 x 2H, s, 4-, 5-imidazol-2-ylidene), 7.2 and 7.7 (2 x 2H, m, xylyl), 7.4 (4H, m, *m*-$Pr^i_2C_6H_3$), 7.5 (2H, m, *p*-$Pr^i_2C_6H_3$). $\delta_C(CDCl_3)$ 24.4, 24.8 [$CH(CH_3)_2$], 28.4 [$CH(CH_3)_2$], 56.9 (CH_2), 121.7, 122.8, 123.9, 124.4, 130.7, 135.9, 138.8, 145.7, 155.8 (phenyl, xylene, 4- and 5-imidazol-2-ylidene). Carbene carbon was not observed. Found: C, 52.00; H, 5.56; N, 7.58,

$C_{38.5}H_{47}Ag_2Cl_3N_4$ requires C, 52.08; H, 5.34; N, 6.31%. The isolated product contains half a molecule of dichloromethane per formula unit.

2,6-bis[3-(*tert*-butyl)imidazol-2-ylidene]pyridine di-silver dichloride 3.11

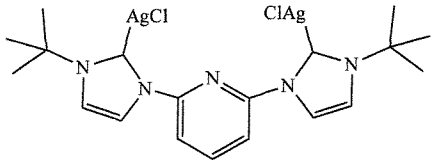

Prepared by general method 2 starting from **2.15** (1.00 g, 2.1 mmol) and Ag_2O (0.71 g, 3.1 mmol). Yield 59%. MS (ES+) *m/z* 431 $[Ag(ligand)]^+$ 162 $[½(ligand)]^{2+}$. NMR $\delta_H(CDCl_3)$ 1.3 [18H, s, $C(CH_3)_3$], 7.4 and 8.2 (2 x 2H, s, 4- and 5-imidazol-2-ylidene), 7.8 (2H, d, pyr-*H*), 8.4 (1H, t, pyr-*H*).

2,6-bis[3-(mesityl)imidazol-2-ylidene]pyridine disilver dichloride 3.12

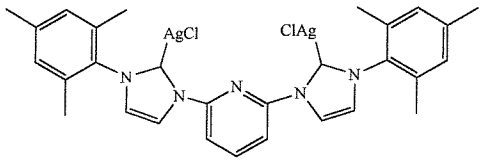

Prepared by general method 2 starting from **2.15** and Ag_2O. Yield: 67%. MS (ES+) *m/z* 555 $[Ag(ligand)]^+$. NMR $\delta_H(CDCl_3)$: 2.00 (12H, s, *o*-CH_3), 2.32 (6H, s, *p*-CH_3), 7.05 (4H, s, $C_6H_2Me_3$), 7.8 - 8.6 (7H, v br. s, aromatic and 4-, 5-imidazol-2-ylidene). $\delta_C(CDCl_3)$ 18.5, 21.7 (mesityl-CH_3), 116.4, 121.9, 124.6, 130.2, 135.0, 136.0, 140.4, 143.5, (aromatic + 4- and 5-imidazol-2-ylidene) 150.8 (2-imidazol-2-ylidene).

[2,6-bis[3-(2,6-di-*iso*-propylphenyl)imidazol-2-ylidene]pyridine disilver dichloride 3.13

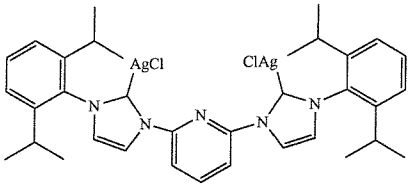

Prepared by general method 2 starting from 2,6-bis-[3-(2,6-di-*iso*-propylphenyl)imidazolium]pyridine dibromide (2.60 g, 4.0 mmol) and Ag_2O (1.80 g, 8.0 mmol) Yield: 2.2 g, 75%. MS (ES+) *m/z* 639 $[Ag(ligand)]^+$. NMR δ_H ($CDCl_3$): 1.2, 1.3 [2 x 12H, d, $CH(CH_3)_2$], 2.5 [4H, septet, $CH(CH_3)_2$], 7.2 and 8.3 (2H, s, 4-,5-imidazol-2-ylidene), 7.3 (4H, d, $Pr^i_2C_6H_3$), 7.5 (2H, t, $Pr^i_2C_6H_3$), 8.1 - 8.2 (3H, br. m, pyridyl). $\delta_c(CDCl_3)$ 24.5, 24.7 [$CH(CH_3)_2$], 28.5 [$CH(CH_3)_2$], 116.2, 121.2 (4-, 5-imidazol-2-ylidene), 124.6, 125.4, 131.0, 134.8, 143.1, 145.6, 150.3 (aromatic *C*), 174.5 (2-imidazol-2-ylidene).

2,6-bis(1-*tert*-butyl-imidazol-2-ylidene)pyridine disilver dichloride 3.14

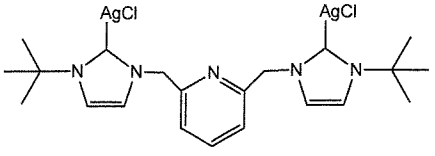

Prepared by general method 2 starting from compound **2.13** (1.0 g, 2.18 mmol) and Ag_2O (0.90 g, 3.27 mmol). Yield 62% (0.782g) MS (ES+) *m/z* 249

[½Ag(ligand).2H_2O]$^{2+}$. (ES-) *m/z* 179 ($AgCl_2$)$^-$, 212 ($AgCl_2.2H_2O$)$^-$. NMR δ_H($CDCl_3$) 1.8 (18H, s, ^{t}Bu), 5.4 (4H, s, CH_2), 7.0 and 7.3 (2 x 2H, s, 4- and 5-imidazolium), 7.2 (2H, d, pyr *m-H*), 7.6 (1H, t, pyr *p-H*).

2,6-bis(1-mesityl-imidazol-2-ylidene)pyridine disilver dichloride 3.15

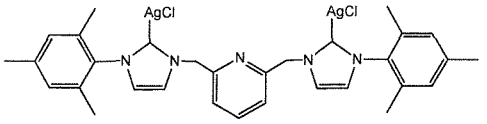

Prepared by general method 2 starting from 2,6-[3-(mesityl)-imidazolium]methyl-pyridine dibromide (1.00 g, 1.57 mmol) and Ag_2O (0.54 g, 2.35 mmol). Yield 73% (0.67 g). MS (ES+) *m/z* 584.6 [Ag(ligand)]$^+$ 322.4 [½(ligand)]$^{2+}$. MS (ES-) *m/z* 179 ($AgCl_2$)$^-$, 212 ($AgCl_2.2H_2O$)$^-$. NMR δ_H($CDCl_3$) 1.9 (12H, s, mesityl *p*-CH_3), 2.3 (6H, s, mesityl *m*-CH_3), 5.5 (4H, s, CH_2), 6.9 (4H, s, mesityl *o*-C*H*), 6.9 and 7.5 (2 x 2H, s, 4-, 5-imidazolium), 7.2 (2H, d, pyr *m-H*), 7.7 (1H, t, *p*-pyr *H*). δ_C($CDCl_3$) 17.6, 20.9 (mesityl-CH_3), 56.7 (CH_2), 120.0, 122.1, 123.0, 123.6, 130.0, 130.5, 135.2, 139.4, 140.2 (4- and 5-imidazol-2-ylidene, aromatic). Imidazol-2-ylidene carbon not observed.

3.5 References

[1] A. A. D. Tulloch, A. A. Danopoulos, S. Winston, S. Kleinhenz, G. Eastham, *J. Chem. Soc. Dalton. Trans.*, **2000**, 4499.

[2] P. L. Arnold, A. C. Scarisbrick, A. J. Blake, C. Wilson, *Chem. Commun.*, **2001**, 2340.

[3] K. M. Lee, H. M. J. Wang, I. J. B. Lin, *J. Chem. Soc. Dalton. Trans.*, **2002**, 2852.

[4] X. Hu, Y. Tang, P. Gantzel, K. Meyer, *Organometallics*, **2003**, *22*, 612.

[5] P. L. Arnold, *Heteroatom Chem.*, **2002**, *13*, 534.

[6] A. J. Arduengo, H. V. R. Dias, J. C. Calabrese, F. Davidson, W. J. Marshall, *Organometallics*, **1993**, *12*, 3405

[7] H. M. Wang, I. J. B. Lin, *Organometallics*, **1998**, *17*, 972.

[8] D. J. Nielsen, K. J. Cavell, B. W. Skelton, A. H. White, *Inorg. Chim. Acta.*, **2002**, *327*, 116.

[9] A. A. D. Tulloch, A. A. Danopoulos, G. J. Tizzard, S. J. Coles, M. B. Hursthouse, R. S. Hay-Motherwell, W. B. Motherwell, *Chem. Commun.*, **2001**, 1270.

[10] A. A. D. Tulloch, A. A. Danopoulos, R. P. Tooze, S. M. Cafferkey, S. Kleinhenz, M. B. Hursthouse, *Chem. Commun.*, **2000**, 1247.

[11] A. A. D. Tulloch, PhD thesis, University of Southampton (Southampton), **2001**.

[12] A. J. Arduengo, F. Davidson, H. V. R. Dias, J. R. Goerlich, D. Khasnis, W. J. Marshall, T. K. Prakasha, *J. Am. Chem. Soc.*, **1997**, *119*, 12742.

Chapter 4

N-Heterocyclic Carbene Complexes of Palladium

Chapter 4

N-Heterocyclic Carbene Complexes of Palladium.

4.1 Introduction.

Since the realisation that *N*-heterocyclic carbenes are easily accessible and have similar metal bonding properties to trialkylphosphines the research into palladium NHC complexes as catalytically active precursors has been immense. There are extensive reviews covering the volumes of literature.[1-5]

As described in the introduction, the imidazol-2-ylidene is a chemical building block that has vast scope for derivatisation, as the literature proves academic research has not missed any opportunities to do this. The first works on palladium *N*-heterocyclic carbenes complexes were reported in the early 1970's by Lappert and co-workers who reported a range of mixed phosphine and *N*-heterocyclic palladium complexes.[6, 7] Aside from the works produced by Lappert, activity in the study of palladium NHC's was slow and steady until the early 1990's when Arduengo's report[8] fuelled huge interest in the area and several groups began research into NHC's complexes and catalysis, especially Herrmann's Group who have made a large contribution to this field.[9]

There has been a great interest in pyridine functionalised imidazol-2-ylidene palladium complexes from us and others as they have proven to be highly active as precatalysts for the Heck C-C coupling reaction.[10, 11]

The quickly developing story starts recently in 1998 when Cavell and co-workers reported novel methyl palladium imidazol-2-ylidene complexes incorporating bidentate chelates including the 2,2'-bipyridyl ligand.[12] Cavell later in 1999 reported the use of Pd(0) bis-carbene complexes containing the 1,3,4,5-tetramethylimidazol-2-ylidene (tmiy) ligand as active Heck and Suzuki precatalysts. During 2000 publications by us,[10] Cavell,[13] and Lin[14] described several palladium complexes bearing pyridine functionalised imidazol-2-ylidenes behaving in a variety of coordination modes, some of which are shown in Fig 4.1.

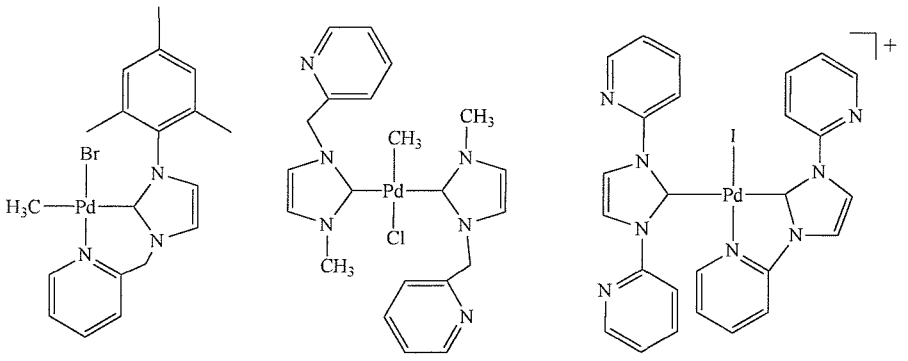

Danopoulos and co-workers | Cavell and co-workers | Lin and co-workers

Fig 4.1 Selection of complexes simultaneously reported in 2000.

From all three groups it could be seen that mono- and bis-imidazol-2-ylidene palladium(II) complexes were accessible and that the pyridine group could be either coordinated or 'dangling'. Cavell later that year reported a decomposition route for imidazol-2-ylidene palladium complexes which will be discussed in Chapter 5.[15] In 2001 interest in the area could be seen to be growing as we communicated chiral chelating 'pincer' imidazol-2-ylidene palladium (II) complexes[16] (fig 4.2) and Crabtree and co-workers reported Heck activity with related systems.[17] This year has also seen similar levels of interest in these pyridine functionalised carbene complexes with several publications by Crabtree reporting complexes analogous to those previously reported by us with their C-C coupling activity,[18] and more reports from Cavell along a similar theme, but with the bulky aryl substituents replaced with simple alkyl chains.[19, 20]

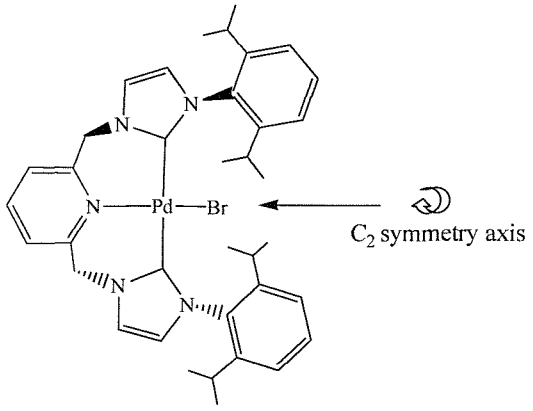

Fig 4.2 Chiral bis-NHC Pd(II) complex.

This chapter describes several palladium complexes, some of which are derived by methodology developed earlier.[11] All have been synthesised in order to understand the mechanism of C-C coupling reactions by studying the effect of varying ligand architecture on catalytic activity.[10, 11]

4.2 Results and Discussion.

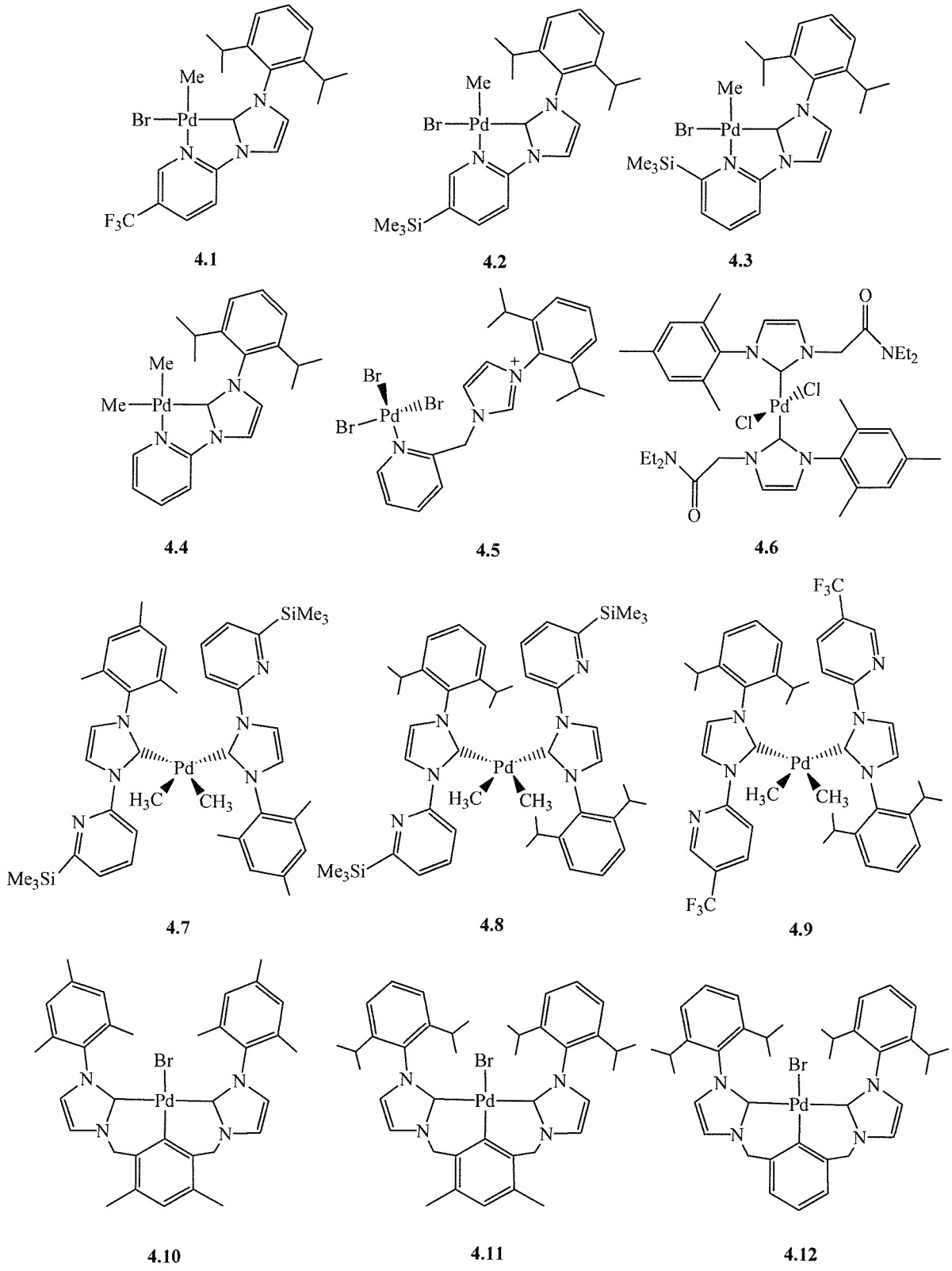

Fig 4.3 Palladium(II) complexes synthesised.

Complexes analogous to **4.1** had been previously prepared and proved to be highly active as Heck catalyst precursors.[11] Compounds **4.1** – **4.3** were synthesised to compare the effect of substitution of the pyridine ring on catalytic activity. The unstable **4.4** was made to establish whether the switch from palladium methyl bromide to palladium dimethyl complexes precursors had an impact on catalytic activity. Compound **4.5** shows that it is necessary to deprotonate the imidazolium salt or different interactions can occur between the imidazolium salt and palladium sources. Compounds **4.6** – **4.12** are all bis-imidazol-2-ylidene palladium complexes, **4.6** – **4.9** contain two non-chelated bidentate ligands, where upon catalytic activation the non-coordinated pyridines could stabilise an active species, which has been observed in related work with rhodium complexes.[21] **4.10** – **4.12** are tridentate chelating bis-carbene ligands, synthesised to study the effect of changing from pyridine-based chelates to a cyclometallated aryl system on catalytic activity.

4.2.1 Synthesis of Palladium Complexes.

The synthesis of the compounds shown in Fig 4.3 proceeded using one of three different routes, depending on the nature of the desired end product, either;

1. *Via* transmetallation from the silver precursor,
2. *Via* reaction with the appropriate isolated imidazol-2-ylidene,
3. *Via in situ* deprotonation of the imidazolium salt with a basic palladium precursor.

Use of methods 1 or 2 mentioned above yielded the same bidentate chelating palladium complexes **4.1** – **4.3**.

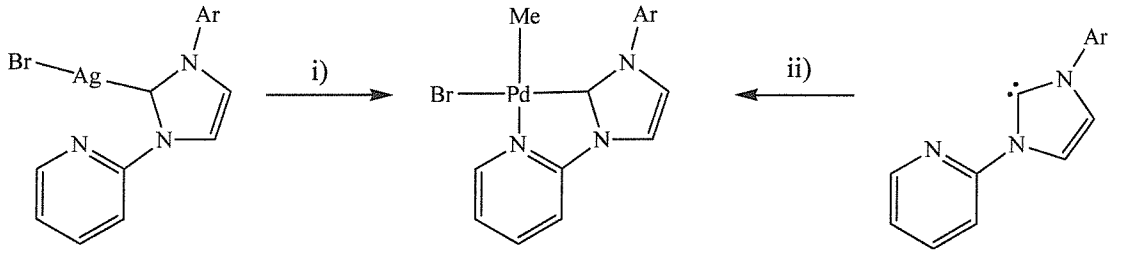

Fig 4.4 Synthesis of compounds **4.1** – **4.3**; i) Pd(COD)MeBr, DCM, reflux; ii) Pd(COD)MeBr, THF, RT.

The transmetallation from the silver imidazol-2-ylidene complexes to Pd(COD)MeBr leads to the Pd(II) mono-imidazol-2-ylidene methyl bromide complexes, which can be crystallised

from the crude reaction mixture after deposited silver halide is removed *via* filtration. The silver deposits that form during the imidazol-2-ylidene transfer process give an approximate visual guide to reaction progression. However, to ensure completion the reactions are left to reflux overnight. The alternative method starting from 'free' imidazol-2-ylidene to obtain these complexes requires the use of Schlenk techniques, but does remove a synthetic step of having to preform the silver complexes, so this has improved atom economy. Both synthetic routes are generally high yielding and the use of the 'free' imidazol-2-ylidene is the preferred method to produce **4.1** – **4.3**.

Compound **4.4** was synthesised using method 2 from compound **2.20** with $Pd(COD)Me_2$ under controlled temperature (-78°C to RT) and moisture free conditions. Upon warming to room temperature the solvent was removed *in vacuo* yielding a white solid that was confirmed by mass spectrometry and proton NMR spectroscopy to be **4.4**. The complex had poor stability and decomposition was observed in the deuterated benzene NMR sample after minutes of being at room temperature and the remainder of the sample decomposed to palladium black from an attempted slow cooling crystallisation in diethylether at –30°C. At this point it cannot be determined if the complex was unstable in the solvents used or was simply thermally unstable for the brief time (10 - 15 mins) that it spent at room temperature. Due to the need of having to use aqueous cyanide solutions to prepare the $Pd(COD)Me_2$ an alternative palladium precursor was sought, as it had been seen that the target molecule was possible to isolate, but an alternative synthesis would be needed.

Method 3 describes the addition of an imidazolium bromide salt to a palladium precursor that has ligands of sufficient basicity to deprotonate the 2-imidazolium proton to form the carbene complex. When the ligands are not of sufficient basicity, complexes such as **4.5** are formed. The addition of 3-(2,6-di-*iso*-propylphenyl)-1-(α-picolyl)imidazolium bromide to $PdCl_2$ in acetonitrile affords crystalline **4.5** in which the imidazolium heterocycle is non-coordinated and 'dangles' freely. There is no interaction of the imidazolium ring with the metal centre.

Compound **4.6** was synthesised using method 1 from the silver precursor and $Pd(COD)Cl_2$ in dichloromethane and forms the bis-carbene complex regardless of stoichiometry used in the reaction. The nitrogen donor is non-coordinated in this Pd(II) complex, however the dangling diethylacetamide group is still available to coordinate to an active Pd(0) species as the N-

donor could provide electronic support if a halide was abstracted. Behaviour of this sort was observed in work using rhodium in which a 'dangling' pyridine became coordinated after halide abstraction.[21]

Complexes **4.7** – **4.9** were initially prepared at NMR experiment scale before being increased to *ca.* half-gram scale. These bis-carbene complexes were obtained after attempting an alternative route to **4.4**, starting with $Pd(TMEDA)Me_2$ instead of $Pd(COD)Me_2$. The use of the silver precursors with the $Pd(TMEDA)Me_2$ led only to palladium black deposition and intractable mixtures. These complexes were therefore synthesised using the isolated ylidenes (method 2) and as with **4.6** the stoichiometry of the reaction did not affect the product. The desired mono-imidazol-2-ylidene chelate complex was not formed; rather the bis-imidazol-2-ylidene complexes, in the fashion of **4.6**, containing the dangling N-donor motif were obtained. X-ray quality crystals of the samples grew rapidly from the deuterated benzene NMR solutions on standing at room temperature. These complexes formed in quantitative yields in less than four hours and by gently heating at 30°C this time could be reduced. Interestingly unlike with the other characterised complexes decomposition occurs at 70°C, this will be discussed further in the NMR spectroscopy section.

The tridentate chelates **4.10** – **4.12** are formed using two different synthetic methods, The first route is based on method 3 using $Pd(OAc)_2$ in DMAC at 160°C, but also involves cyclometallation of **2.18** and **2.19**. In contrast to recent reports by others,[18] this reaction gave good yields of the cyclometallated analogues of **4.10** and **4.11** as air stable white crystalline materials. One reason which could account for the observed difference is the choice of the substitution of the central aromatic ring in **2.18** and **2.19**. The presence of the methyl groups *ortho* to the imidazolium-methyl substituents could promote cyclometallation at the desired position by blocking competing cyclometallations at the 4-position of the aromatic ring. The methyl groups also increase the electron density of the aromatic ring favouring electrophilic attack by the palladium centre.[22] The second method is based on the oxidative addition of the aryl C – Br of **2.17** to $Pd_2(DBA)_3$ leading to **4.12** in good yields. The same approach has been used recently by Crabtree to prepare analogues complexes in which the NHC is substituted by methyls.[17, 18] The mechanism of formation of **4.10** – **4.12** is not clear, especially the nature of the species that undergoes metallation of the imidazolium and the aromatic C-H carbons. The ease of formation of NHC complexes of palladium under the reaction conditions

employed, points to a mono- or *trans* bis-NHC complex as being initially formed, which could further undergo cyclometallation.

4.2.2 Characterisation of Palladium Complexes.

4.2.2.1 NMR Spectroscopy.

Proton NMR spectroscopy was of extremely high diagnostic value with respect to determining not only the number of ligands coordinated, but also the symmetry and structure of the complexes. For compounds **4.1** – **4.3** the following NMR resonances are observed in $CDCl_3$:

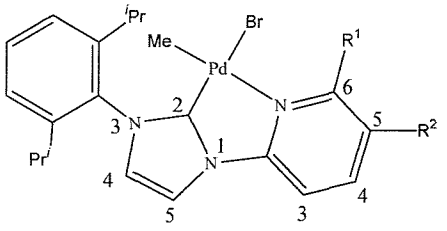

Fig 4.5 Numbering scheme for **4.1** - **4.4**, R = 2,6-di-*iso*-propylphenyl.

- For the palladium methyl group a singlet at 0.1 – 0.3 ppm.
- For the 4- and 5-imidazol-2-ylidene protons two singlets between 6.9 – 7.0 and 7.8 – 7.9 ppm.
- For the pyridine ring three doublets at 7.6 – 7.8, 8.1 – 8.2 and 9.2 – 9.7 ppm.
- For the 2,6-di-*iso*-propylphenyl doublets at 1.1 and 1.3 ppm, a septet at 2.5 - 2.7 ppm and a doublet and triplet at 7.2 – 7.5 ppm.
- When R^1 or $R^2 = SiMe_3$ a singlet at 0.3 ppm.

A resonance is observed at 205 ppm for **4.1** and 177 – 179 ppm for **4.2** and **4.3** in the $^{13}C\{^1H\}$ NMR spectra assignable to the 2-imidazol-2-ylidene carbon. The *iso*-propyl groups showing only two doublets and a septet confirm the presence of one ligand environment and with peaks assignable to the palladium methyl this confirms the proposed structures.

For the palladium dimethyl complex **4.4** decomposition was observed within minutes of collecting the ^1H NMR spectrum, so an extended $^{13}C\{^1H\}$ data collection was not possible. The features used to identify the formation of **4.4** were: a singlet at 0.7 ppm for the palladium methyls, doublets at 1.1 and 1.5 ppm, a septet at 2.9 ppm and a doublet and triplet at 6.2 and

6.4 ppm for the 2,6-di-*iso*-propylphenyl group, two singlets at 6.3 and 6.5 ppm for the 4- and 5- imidazol-2-ylidene protons and two doublets at 7.1 and 8.8 and two double doublets at 6.8 and 7.3 for the pyridine ring protons. Again the *iso*-propyl groups denote a single ligand environment.

The NMR spectrum of the 'dangling' imidazolium compound **4.5** showed similar peak patterns to **4.1** – **4.3**, but contained one additional signal at 10.7 ppm from the 2-imidazolium proton. Due to the lack of solubility of **4.5** in chloroform the data cannot be directly compared to the other complexes reported here as data was collected in d_3-acetonitrile.

The spectrum of complex **4.6** showed slightly broad resonances at room temperature especially at the methylene bridge linking the diethylacetamide group. The peak resonances from the heterocyclic backbone and mesityl group are as expected from the other characterised complexes and the diethylacetamide ethyl groups give. The features used to identify the formation of the palladium complex were: a triplet and quartet at 1.2 and 3.4 ppm from the ethyl groups, a singlet at 5.3 for the methyle bridge, three broad singlets at 2.5, 2.9 and 6.3 ppm for the mesityl group and two singlets at 6.3 and 7.2 ppm for the 4- and 5-imidazol-2-ylidene protons. The presence of only two peaks for the mesityl methyls denoted a single ligand environment, but in this case the complex was a bis-imidazol-2-ylidene complex with a centre of inversion based on the palladium as proven by X-ray crystallography.

Compounds **4.7** – **4.9** all show similar peak resonances as described for **4.1** – **4.4** for the pyridine and imidazol-2-ylidene ring protons. There is a significant change in the peaks caused by the 2,6-di-*iso*-propylphenyl ring and the highly diagnostic value of the *iso*-propyl groups is now shown as where there is a single ligand environment (compounds **4.1** – **4.4**) or two *trans*-bis-imidazol-2-ylidene ligands with a centre of inversion in the complex (i.e compound **4.6** for a mesityl example or compound **6.5**, chapter 6, for 2,6-di-*iso*-propylphenyl) a pair of doublets and one septet is observed for the *iso*-propyl group, however in the *cis*-bis-imidazol-2-ylidene complexes **4.7** – **4.9**, four doublets and two septets are observed (Fig 4.6) as the symmetry in the complex is reduced.

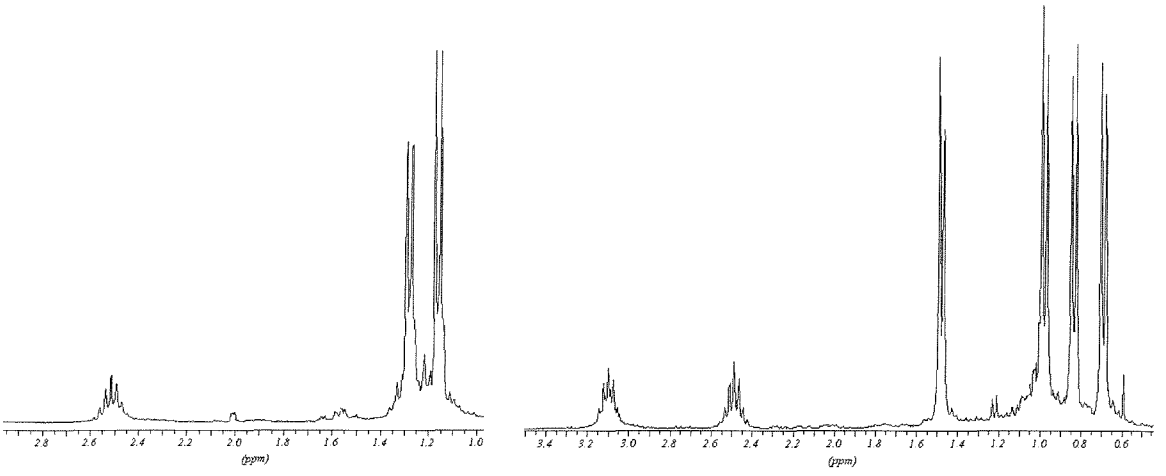

Fig 4.6 Mono/*trans* bis-carbene (left) and *cis*-bis-carbene (right) diagnostic *iso*-propyl ^{1}H NMR peaks.

The left spectrum in Fig 4.6 shows peaks resulting from a complex containing a mirror plane or centre of inversion and the spectrum on the right shows a complex with a C_2 twist as its predominant symmetry element or a *cis*-bis-imidazol-2-ylidene complex. The diagnostic resonances of the *iso*-propyl groups meant quick deduction of solution-phase structure was possible, which could be later confirmed by single crystal X-ray diffraction results. For the mesityl group similar behaviour is observed as the number of singlets from the mesityl methyls increases from two peaks to three upon change of symmetry from a mirror plane to C_2 rotation.

Reports by Cavell have shown that upon heating palladium NHC methyl complexes the methyl-imidazolium species can be ejected from an active catalytic species.[23] To test whether this would occur with complexes of type **4.7** – **4.9**, heating whilst monitoring the ^{1}H NMR spectra was undertaken (Fig 4.8) to see if either of the possible decomposition products depicted in Fig 4.7 could be isolated and characterised.

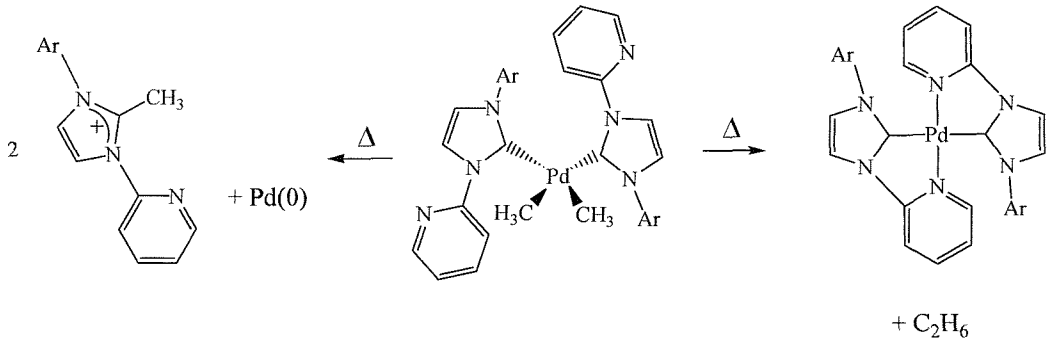

Fig 4.7 Possible decomposition products from heating complexes **4.7** – **4.9**, Ar = 2,6-di-*iso*-propylphenyl.

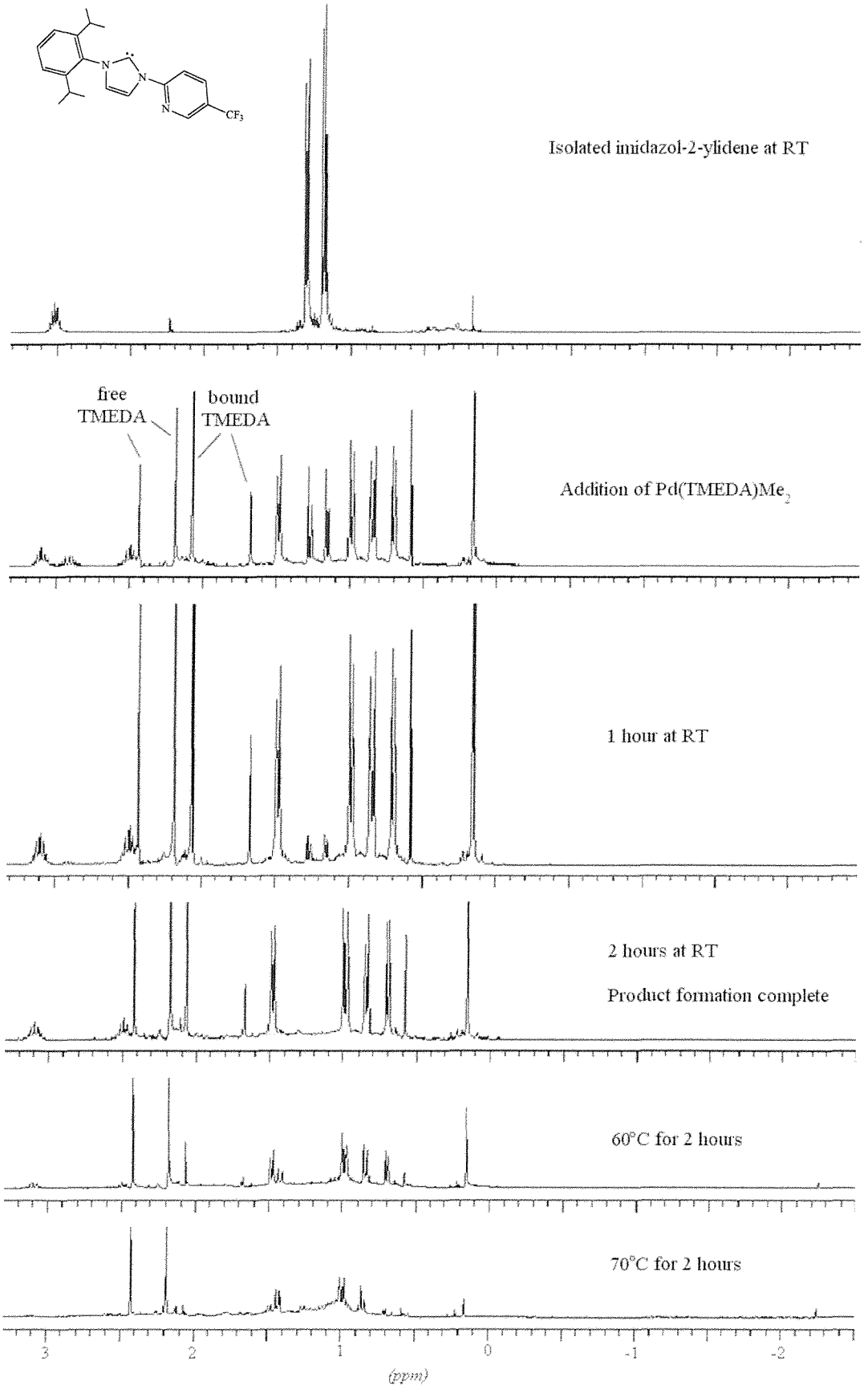

Fig 4.8 High-field ^{1}H NMR showing formation and thermal decomposition of **4.9**.

As can be seen in Fig 4.8 the addition of Pd(TMEDA)Me_2 to the imidazol-2-ylidene **2.22** at room temperature gives complex **4.9** within two hours at room temperature, singlet peaks from the bound/free TMEDA are observed between 2.0 – 2.5 ppm. The complex appears quite stable up to 60°C with no obvious decomposition observed on visual inspection of the sample (remains pale yellow solution) or in the NMR spectrum. Heating to 70°C does cause a change, both visually as the NMR sample takes on a deep red colour without any deposition in the tube and in the NMR spectrum the four *iso*-propyl doublets collapse to two doublets. One more observation is made, two new peaks appear at 11.0 ppm, suggesting an imidazolium proton and a peak at –2.3 ppm. Methyl-imidazolium compounds reported show a peak at around 2.2 ppm for the imidazolium-methyl, which is not observed here. The peak at –2.3 ppm may be due to a hydride species, but this could not be confirmed as no single product could be isolated from the decomposed NMR sample. The change from four to two *iso*-propyl doublets suggests that symmetry is increased, so it may be that there has been elimination of ethane from the complex, or if a hydride has formed elimination of ethene. The change in symmetry would support the presence of a Pd(0) square planar bis-imidazol-2-ylidene complex, especially as there is no sign of palladium black deposited. Without further work the nature of the decomposed compound cannot be confirmed.

The diagnostic value of the appearance of the *iso*-propyl group region of the NMR spectrum was useful when studying complexes **4.10** – **4.12** of the symmetrical imidazolium salts **2.17** – **2.19**. It was observed with the previous analogous pyridine based complexes[16] that four doublets and two septets were observed in the ^{1}H NMR spectra of the palladium complexes, even though there is a mirror plane through the imidazolium salts. This pointed to a desymmetrisation process rendering these groups diastereotopic. An additional feature of high diagnostic value is the appearance of the CH_2 linker peaks, which give rise to an AB coupling pattern (fig 4.9). These features support a non-planar structure in solution, which can be easily rationalised by the bite angles of the two fused six-membered chelate rings resulting in a non-planar helical conformation. Identical behaviour is observed for **4.10** – **4.12** suggesting that there is a helical twist through the complexes, which is confirmed by the X-ray crystal structure. A pair of doublets are observed between 4.7 and 5.5 ppm in the ^{1}H NMR spectrum and a peak observed between 55 and 59

Fig 4.9 AB methylene bridge pattern in tridentate chelate complex **4.12**.

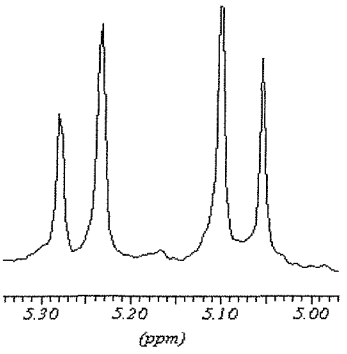

ppm in the $^{13}C\{^1H\}$ NMR spectra, assigned to the protons and the carbons of the methylene bridge of the complexes. The ^1H NMR spectra are very similar for all three complexes, the only difference being the presence of the methyls of the aromatic ring at 2.3 ppm in **4.10** and **4.11**. The appearance of the ^1H-NMR spectrum remains unchanged up to 110°C (toluene-d^8), indicating conformational rigidity. Of high diagnostic value is the $^{13}C\{^1H\}$ NMR spectrum in which the cyclometallated aromatic carbon and the 2-imidazol-2-ylidene carbons appear at 155 and 180 ppm respectively, similar to those observed in analogous compounds.[17]

4.2.2.2 Mass Spectrometry.

Positive ion electrospray mass spectrometry was useful in confirming the presence of the palladium carbene complexes. Samples in acetonitrile showed peaks at mass to charge ratios relating to the parent compounds that could be easily identified, with correct isotopic envelopes. For the bidentate complexes **4.1** – **4.4** the characteristic peak was due to the fragment $[Pd(Ligand)Me + MeCN]^+$. Often a peak corresponding to $(ligand)^+$ was also observed. For the bis-imidazol-2-ylidenes complexes **4.7** – **4.9** the characteristic peak observed corresponded to $[Pd(Ligand)_2Me]^+$ and for compounds **4.10** – **4.12** $[Pd(Ligand) + MeCN]^+$ was observed.

4.2.2.3 X-ray Crystallography.

The majority of the palladium complexes reported here could be isolated as crystalline materials and full structural analysis in the solid state was undertaken by single crystal X-ray diffraction.

The previously characterised structures of pyridine functionalised mono-imidazol-2-ylidene chelates, [3-(aryl)-1-(2-pyridyl)-imidazol-2-ylidene] palladium methyl halide, are isostructural to compounds **4.1** and **4.2**.[11, 24] The X-ray crystal structure of compound **4.1** is shown in Fig 4.10 and **4.2** is described in the experimental section.

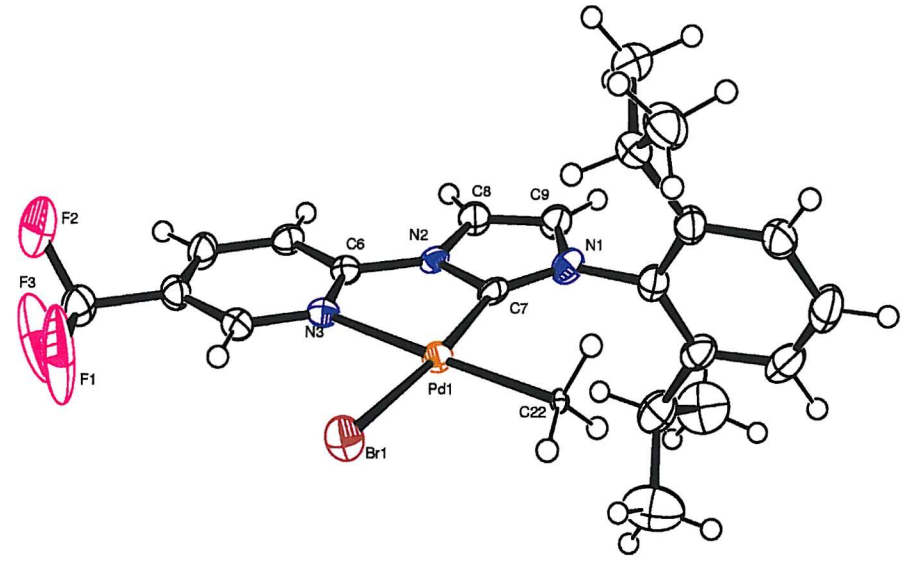

Fig 4.10 Crystal structure of compound **4.1**.

Table 4.1 Comparative bond lengths and angles for **4.1**, **4.2** and [3-(2,6-di-*iso*-propylphenyl)-1-(2-pyridyl)-imidazol-2-ylidene] palladium methyl bromide.

	4.1	**4.2**	**Unsubstituted pyridine**[24]
Pd1 – C7	1.988(4)	1.961(17)	1.970(4)
Pd1 – N3	2.155(4)	2.176(15)	2.166(3)
Pd1 – Br1	2.4605(6)	2.453(3)	2.4528(5)
Pd1 – C22	2.098(3)	2.049(17)	2.034(4)
N3 – Pd1 – C7	79.6(2)	79.0(6)	79.15(13)
N1 – C7 – N2	104.5(4)	103.1(14)	103.5(3)

Complexes **4.1** and **4.2** are mono-imidazol-2-ylidene palladium (II) complexes and both have square planar geometries adopting similar relationships around the metal centre. The ligand behaves as a bidentate chelate bound through the imidazol-2-ylidene and the pyridine nitrogen; a methyl group and bromine complete the coordination sphere. In all structures the halide is always observed to be *trans* to the carbene and the methyl *trans* to the pyridine, reflecting the *trans*-stabilising forces. By examining the variances caused by addition of a functional group onto the pyridine ring of the ligand two conclusions can be drawn. By comparing the trimethylsilylated (**4.2**) to the unsubstituted pyridine complex the two compounds are identical to within the experimental errors of the data, the Pd1 – N3 bond distances being 2.166(3) Å and 2.176(15) Å and the Pd – C7 lengths are at 1.961(17) Å and 1.970(4) Å. There is no structural change by the addition of a bulky substituent with minor electronic effects on the pyridine ring. This is not the case for **4.1** where a highly electron withdrawing trifluoromethyl group has been added to the pyridine ring. All of the ligands in complexes **4.1** – **4.4** have an extended conjugate aromatic system and the effect of withdrawing electron density from one ring causes electronic effects across the whole ligand

system. This is observed in the solid state by variation in bond lengths and angles. The palladium to pyridine bond shortens by 0.01 Å [from 2.166(3) Å to 2.155(4) Å] and the palladium to imidazol-2-ylidene bond extends by 0.02 Å [from 1.970(4) Å to 1.988(4) Å]. The heterocycle N-C-N bond angle also opens by a 1° [from 103.5(3)° to 104.5(4)°] showing how the electron stabilisation from the imidazol-2-ylidene nitrogens is reduced as the electron density is drawn into stabilising the aromatic pyridine ring. These very subtle effects are outside of the experimental errors. This shows an interesting feature that the electron withdrawal from the pyridine is effectively weakening the palladium carbene bond, which could have dramatic effect on an active catalytic species.

Compound **4.5** is a square planar palladium(II) complex in which the imidazolium bromide ligand has interacted with palladium(II) chloride. The coordination sphere of the square planar metal comprises three chloride ligands and the imidazolium pyridine group. There is no interaction of the dangling imidazolium with any other atom in the unit cell. Although chlorides are depicted in Fig 4.11 the structure contains mixed halide substitution at the three-halide sites, but are predominantly occupied by chlorine. The imidazolium bromide being mixed with the palladium chloride can explain the source of this mixture.

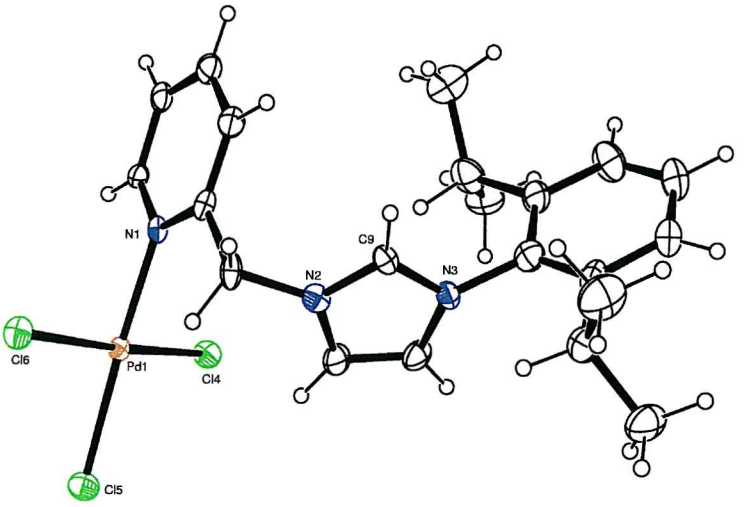

Fig 4.11 Crystal structure of compound **4.5**.

Compounds **4.6** – **4.9** are all square planar bis-carbene palladium complexes of which compounds **4.6** and **4.8** have been characterised by X-ray crystallography. Four ligands, two ylidenes and two halides or methyl groups coordinate each metal centre. The structures of **4.6** and **4.8** are shown below with selected bond lengths and angles.

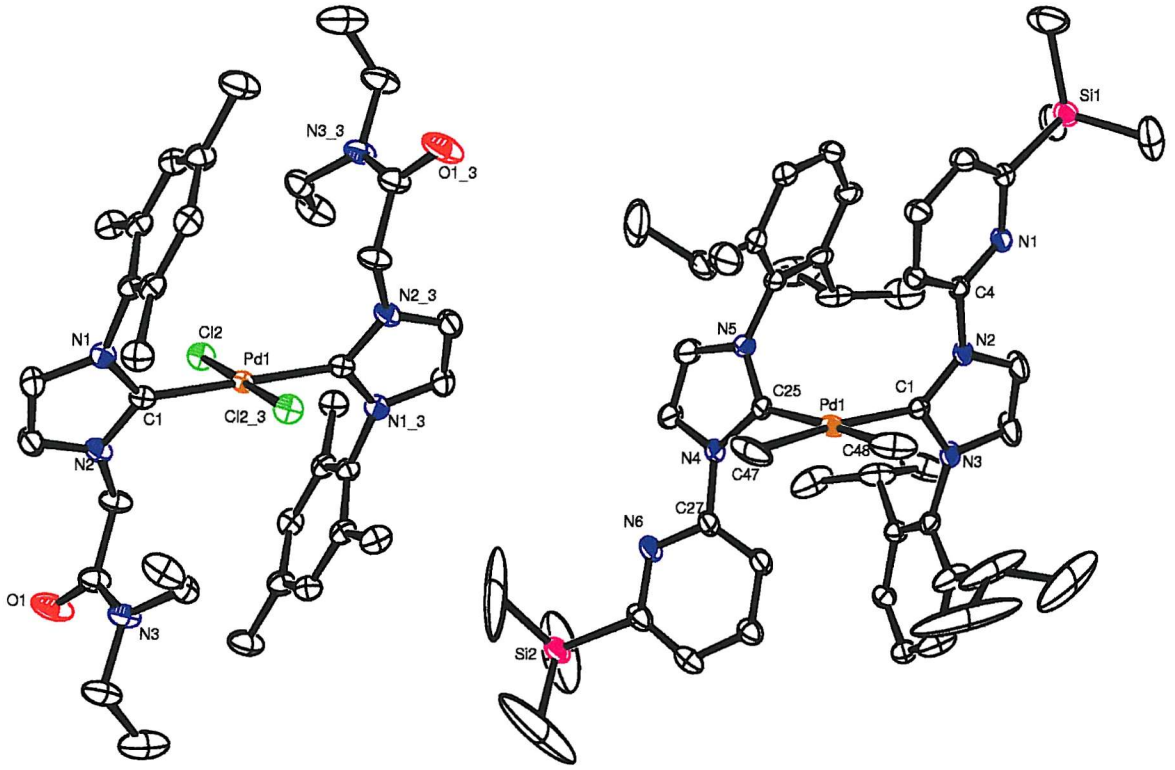

Fig 4.12 Crystal structures of **4.6** (left) and **4.8** (right). Hydrogens removed for clarity.

Table 4.2 Selected bond lengths (Å) and angles (°) for compounds **4.6** (left) and **4.8** (right).

4.6		**4.8**	
Pd1 – Cl2	2.3164(6)	Pd1 – C47	2.083(5)
Pd1 – C1	2.015(2)	Pd1 – C1	2.054(4)
N1 – C1 – N2	104.9(2)	N2 – C1 – N3	102.7(3)
C1 – Pd1 – Cl2	87.9(7)	C1 – Pd1 – C48	87.8(2)

By comparing the structures of the two compounds, the strength of the *trans*-effect can be seen to influence the structure of the complexes. When halides complete the coordination sphere and the weak-donor N-group is non-coordinated then a *trans* bis-carbene complex is formed, but when methyls complete the coordination sphere the imidazol-2-ylidenes take a *cis* geometry with respect to each other. The palladium to ylidene bond lengths are all comparable to other known Pd(II) complexes and both of these geometries have been observed for Pd(II) bis-carbene complexes.[10, 14]

Compounds **4.10** – **4.12** are all tridentate bis-carbene complexes with the third bound atom being a cyclometallated aryl carbon incorporated into the ligand backbone, of which compounds **4.11** and **4.12** have been characterised by X-ray crystallography. The structure of **4.12** is shown in fig 4.5 and **4.11** is listed in the experimental section.

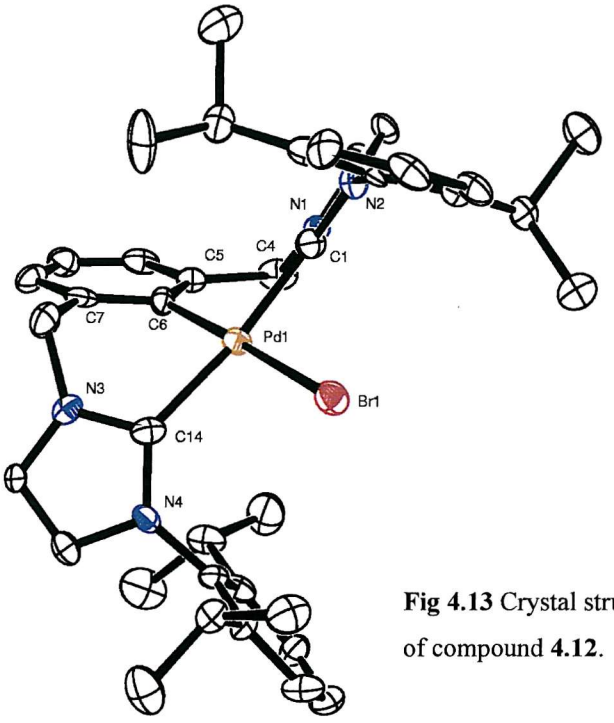

Fig 4.13 Crystal structure of compound **4.12**.

Table 4.3 Selected bond lengths (Å) and angles (°) for **4.12**.

Pd1 – C6	2.021(9)
Pd1 – C1	2.057(10)
Pd1 – C14	2.039(10)
Pd1 – Br1	2.5154(13)
N3 – C14 – N4	103.5(7)
N1 – C1 – N2	105.8(7)
C6 – Pd1 – C14	85.0(4)

This helical twisted motif observed in **4.11** and **4.12** is isostructural to the related pyridine linked complexes.[16] The Pd(II) square planar complexes have bond lengths and angles that are typical of analogous complexes.[17] The molecule adopts a C_2 symmetric structure, in which the extended system of the five linked aromatic rings of the 'pincer' ligand wraps around the square planar palladium centre. The fused six-membered chelate rings adopt boat conformations similar to that observed in the pyridine based complexes previously reported.[16] The palladium – carbene bond lengths are Pd1 – C1 of 2.057(10) Å and Pd1 – C14 of 2.039(10) Å are identical to the pyridine analogues (within experimental error) and the palladium aryl bond 2.021(9) Å is 0.05 Å shorter than the pyridine analogues (in the range 2.065 – 2.071 Å). The complexes exist in the crystal lattice as a racemate and do not have a chiral space group.

4.3 Conclusions

A variety of palladium(II) mono- and bis-imidazol-2-ylidene complexes have successfully been isolated and characterised. Several different techniques were utilized to produce these complexes; *via* the use of the 'free' imidazol-2-ylidenes described in chapter 2 (for complexes **4.4** and **4.7 – 4.9**); the use of the precursor silver complexes as transmetallation reagents described in chapter 3 (for complexes **4.1 – 4.3** and **4.6**) or *via* in situ deprotonation of the imidazolium salt precursor (for complexes **4.10 – 4.12**) and C-H/C-Br activation.

Compounds **4.7** – **4.9** containing the 'dangling' pyridine structural motif have potential to be easily reduced to a catalytically active Pd(0) state if simply heating the complexes will eliminate ethane, as no evidence of a methyl-imidazolium species was observed.

Compounds **4.1** – **4.3** are derivatives of previously studied complexes[11] and the additional substitution of the pyridine ring allows study of different structural and electronic effects on C-C coupling activity. The bis-carbene systems **4.6** – **4.12** also represent a good array of structurally and electronically diverse complexes. These compounds allow a study of subtle variations of the molecular structure of a catalytic precursor on activity in an active catalytic system for example:

1. Mono- vs. bis-carbene systems (**4.1** – **4.3** and **4.7** – **4.9**).
2. The effect of the 'dangling' donor on catalytic activity/stability (**4.6** – **4.9**).
3. Enforcing a less flexible active site, Pd-aryl vs Pd-pyridine donation (**4.10** – **4.12**).
4. The effect of steric bulk (**4.10** – **4.12**).

As has been previously observed complexes bearing pyridine functionalised imidazol-2-ylidenes are highly active precatalysts for the Heck reaction and the novel complexes described here might help gain information on a possible mechanism of the Heck reaction with these ligand systems.

4.4 Experimental Section.

The following palladium starting materials were synthesised from literature method from the Aldrich purchased precursor $PdCl_2$; $Pd(OAc)_2$,[25] $Pd(COD)Cl_2$,[26] $Pd(COD)Br_2$,[26] $Pd(COD)MeBr$,[27] $CuMe_2Li$,[28] $Pd(COD)Me_2$,[29] $Pd(TMEDA)Cl_2$,[30] $Pd(TMEDA)Me_2$.[31]

General method 1:

A dichloromethane solution of the corresponding silver carbene complex was added dropwise to a solution of Pd(COD)MeBr and stirred at room temperature for 12-24h. After completion, the precipitated silver halide was removed by filtration, and the filtrate was evaporated to dryness. The remaining solid residue was washed with diethylether and dried under vacuum. The products were obtained as pale yellow solids, which in most cases were spectroscopically and analytically pure. If necessary, further purification was carried out by recrystallisation from a saturated solution of dichloromethane and layered with diethylether.

General method 2:

Under an inert atmosphere to a solution of Pd(COD)MeBr or $Pd(TMEDA)Me_2$ in predried toluene was added dropwise *via* cannula to a solution of the appropriate imidazol-2-ylidene in the same solvent. The precipitated product was isolated by filtration, washed with petroleum ether (40/60) and dried under vacuum. Recrystallisation from a saturated solution of dichloromethane layered with diethylether gave spectroscopically and analytically pure products.

[3-(2,6-di-*iso*-propylphenyl)-1-(5-trifluoromethyl)-2-pyridyl)-imidazol-2-ylidene] palladium methyl bromide 4.1

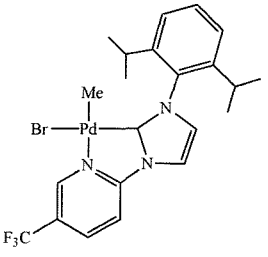

This was prepared by following general method 1 from {3-(2,6-di-*iso*-propylphenyl)-1-[(5-trifluoromethyl)-2-pyridyl)] imidazol-2-ylidene} silver bromide (0.28 g, 0.5 mmol) and Pd(COD)MeBr (0.16 g, 0.5 mmol). X-ray quality crystals were obtained by layering dichloromethane solutions with petroleum. Yield 0.31g, 85%. MS (ES): *m/z* 535, $[Pd(ligand)Me + MeCN]^+$. $\delta_H(CDCl_3)$: 0.1 (3H, s, $PdCH_3$), 1.1, 1.3 [2 x 6H, d, $CH(CH_3)_2$], 2.7 [2H, septet, $CH(CH_3)_2$], 7.0 and 7.9 (2 x 1H, d, 4- and 5-imidazol-2-ylidene), 7.2 (2H, d, $Pr^i_2C_6H_2H$), 7.5 (1H, t, $Pr^i_2C_6H_2H$), 7.8 (1H, d, pyr), 8.2 (1H, d, pyr), 9.7 (1H, br. d, pyr). $\delta_C(CDCl_3)$: 0.0 ($PdCH_3$), 22.3, 23.6 [$CH(CH_3)_2$], 27.5 [$CH(CH_3)_2$], 29.9 (CF_3), 109.5

(3-pyridyl *C*H), 109.5, 114.5 (4- and 5-imidazol-2-ylidene), 122.9, 123.1, 125.6, 129.9, 133.2, 136.8, 143.5, 143.9, 151.1 (aromatics) 205.9 (2-imidazol-2-ylidene). Found: C, 44.84; H, 4.42; N, 6.95. $C_{22}H_{25}F_3N_3PdBr$ requires: C, 45.97; H, 4.38; N, 7.31%.

Crystal data for **4.1**: $C_{24}H_{29}BrCl_4F_3N_3Pd$, colourless plate, Mw 1489.22, Monoclinic, *C*2/*C* (No. 15), a = 23.6757(10) Å, b = 13.4251(7) Å, c = 18.6251(8) Å, $\alpha = \gamma = 90$ °, β = 90.269(3)°, V = 5919.9(5) Å^3, Z = 4, μ = 2.376 mm^{-1}, T = 150 K, Total reflections = 22245, unique reflections = 6703 (R_{int} = 0.0803), Final R indices [$I>2\sigma(I)$] R = 0.0496, R_w = 0.1028 (all data). CCDC Code 194161. X-ray Local Code 01sw044. Unit cell contains complex and 2 molecules of dichloromethane.

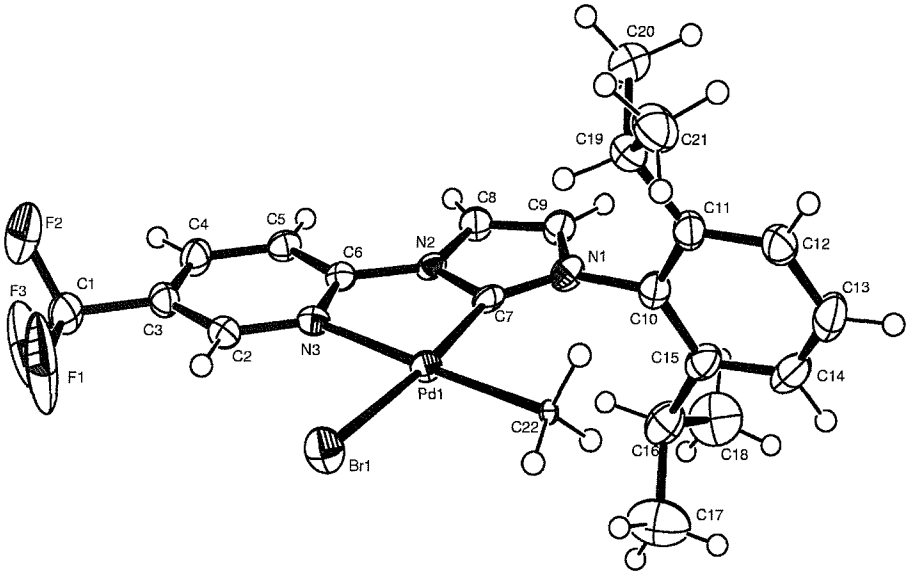

Fig 4.14 X-ray crystal structure of **4.1**.

Table 4.4 Bond lengths (Å) for **4.1**.

C1 – F1	1.271(6)	C6 – N3	1.350(6)	C10 – C11	1.417(7)	C16 – C17	1.545(8)
C1 – F3	1.307(6)	C6 – N2	1.402(6)	C10 – N1	1.450(6)	C19 – C20	1.522(7)
C1 – F2	1.322(6)	C7 – N1	1.323(6)	C11 – C12	1.379(7)	C19 – C21	1.532(7)
C1 – C3	1.500(7)	C7 – N2	1.377(5)	C11 – C19	1.531(7)	C22 – Pd1	2.098(3)
C2 – N3	1.338(6)	C7 – Pd1	1.988(4)	C12 – C13	1.388(8)	N3 – Pd1	2.155(4)
C2 – C3	1.379(6)	C8 – C9	1.335(7)	C13 – C14	1.352(8)	Pd1 – Br1	2.4605(6)
C3 – C4	1.384(7)	C8 – N2	1.389(6)	C14 – C15	1.399(7)		
C4 – C5	1.389(7)	C9 – N1	1.402(6)	C15 – C16	1.516(8)		
C5 – C6	1.384(6)	C10 – C15	1.398(7)	C16 – C18	1.514(8)		

Table 4.5 Bond angles (°) for **4.1**.

F1 – C1 – F3	108.3(5)	C9 – C8 – N2	106.7(4)	C20 – C19 – C21	110.8(4)
F1 – C1 – F2	106.3(5)	C8 – C9 – N1	106.7(4)	C11 – C19 – C21	112.4(4)

F3 – C1 – F2	100.9(5)	C15 – C10 – C11	123.0(4)	C7 – N1 – C9	111.7(4)
F1 – C1 – C3	114.8(4)	C15 – C10 – N1	118.2(4)	C7 – N1 – C10	127.6(4)
F3 – C1 – C3	113.3(4)	C11 – C10 – N1	118.7(4)	C9 – N1 – C10	120.8(4)
F2 – C1 – C3	112.1(4)	C12 – C11 – C10	116.9(5)	C7 – N2 – C8	110.6(4)
N3 – C2 – C3	121.9(4)	C12 – C11 – C19	121.8(5)	C7 – N2 – C6	121.7(3)
C2 – C3 – C4	120.0(4)	C10 – C11 – C19	121.2(4)	C8 – N2 – C6	127.7(4)
C2 – C3 – C1	119.5(4)	C11 – C12 – C13	120.9(5)	C2 – N3 – C6	118.2(4)
C4 – C3 – C1	120.4(4)	C14 – C13 – C12	120.9(5)	C2 – N3 – Pd1	128.9(3)
C3 – C4 – C5	118.6(4)	C13 – C14 – C15	121.9(5)	C6 – N3 – Pd1	112.9(3)
C6 – C5 – C4	118.1(4)	C10 – C15 – C14	116.3(5)	C7 – Pd1 – C22	96.5(2)
N3 – C6 – C5	123.2(4)	C10 – C15 – C16	122.2(5)	C7 – Pd1 – N3	79.6(2)
N3 – C6 – N2	113.0(4)	C14 – C15 – C16	121.5(5)	C22 – Pd1 – N3	175.77(14)
C5 – C6 – N2	123.9(4)	C18 – C16 – C15	111.5(5)	C7 – Pd1 – Br1	173.04(12)
N1 – C7 – N2	104.5(4)	C18 – C16 – C17	110.0(5)	C22 – Pd1 – Br1	90.49(10)
N1 – C7 – Pd1	142.7(3)	C15 – C16 – C17	110.3(5)	N3 – Pd1 – Br1	93.52(10)
N2 – C7 – Pd1	112.8(3)	C20 – C19 – C11	111.5(4)		

[3-(2,6-di-*iso*-propylphenyl)-1-(5-trimethylsilyl)-2-pyridyl)-imidazol-2-ylidene] palladium methyl bromide 4.2

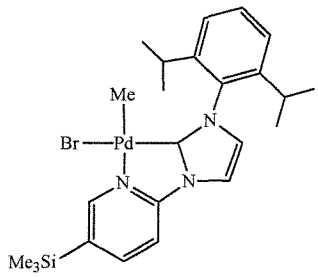

This was prepared by following general method 1 from {3-(2,6-di-*iso*-propylphenyl)-1-[(6-trimethysilyl)-2-pyridyl)] imidazol-2-ylidene} silver chloride (0.25 g, 0.5 mmol) and Pd(COD)MeBr (0.16 g, 0.5 mmol). Yield: 0.22g, 75%. MS(ES+): *m/z* 525, [Pd(ligand)Me + Na]$^+$. $\delta_H(CDCl_3)$: 0.1 (3H, s, PdCH_3), 0.3 [9H, s, Si$(CH_3)_3$], 1.1, 1.3 [2 x 6H, d, CH(CH_3)$_2$], 2.7 [2H, septet, CH(CH$_3$)$_2$], 6.9 and 7.8 (2 x 1H, d, 4- and 5-imidazol-2-ylidene), 7.2 (2H, d, Pr$^i_2$C$_6H_2$H), 7.5 (1H, t, Pr$^i_2$C$_6$H$_2$*H*), 7.6 (1H, d, pyr H), 8.1 (1H, d, pyr H), 9.5 (1H, br. d, pyr H). $\delta_C(CDCl_3)$: -1.3 (PdCH_3), 1.1 [Si(CH_3)$_3$], 23.3, 24.7 [CH(CH_3)$_2$], 28.0 [CH(CH$_3$)$_2$], 109.4, 114.9 (4- and 5-imidazol-2-ylidene), 123.3, 124.0, 125.8, 128.7, 130.7, 134.6, 135.8, 145.1, 150.1, 154.2 (aromatic), 179.5 (2-imidazol-2-ylidene). Found: C, 50.62; H, 6.31; N, 6.42. (Calculated for $C_{24}H_{34}SiN_3PdBr$: C, 49.79; H, 5.92; N, 7.26%).

Crystal data for **4.2**: $C_{25}H_{35}N_3OSiBrPd$, yellow plate, Mw 607.96, Orthorhombic, *Pbca* (No. 61), 15.7372(5) Å, b = 11.6927(3) Å, c = 30.0256(9) Å, $\alpha = \beta = \gamma = 90°$, V = 5525.0(3) Å^3, Z = 8, μ = 2.182 mm^{-1}, T = 150 K, Total reflections = 19397, unique reflections = 6273 (R_{int} = 0.0910), Final R indices [$I>2\sigma(I)$] R = 0.0801, R_w = 0.1548 (all data). X-ray Local Code 02sw026. Unit cell contains complex and a molecule of methanol. Symmetry transformations used to generate equivalent atoms: -x, -y, -z + 1.

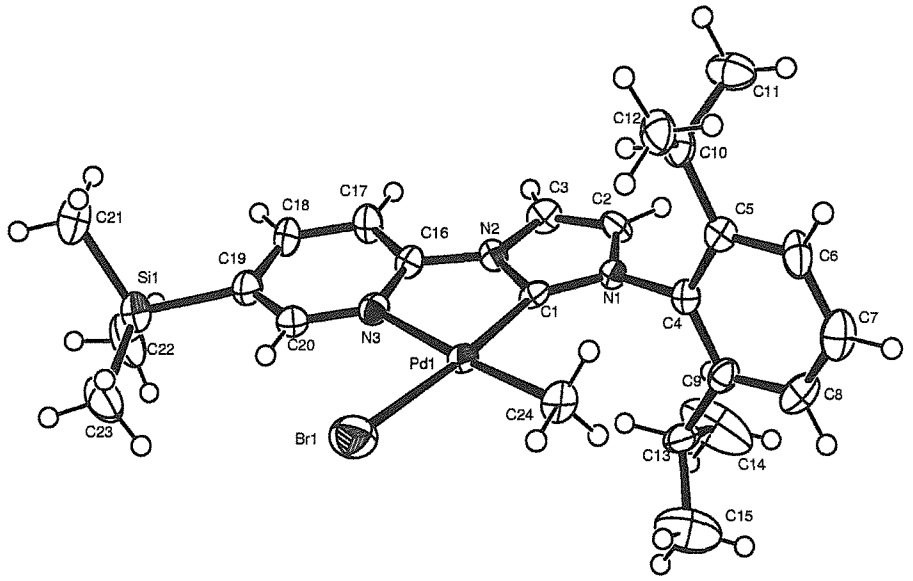

Fig 4.15 X-ray crystal structure of **4.2**.

Table 4.6 Bond lengths (Å) for **4.2**

C1 – N1	1.361(10)	C5 – C6	1.373(13)	C13 – C14	1.512(16)	C21 – Si1	1.825(12)
C1 – N2	1.373(11)	C5 – C10	1.508(12)	C16 – N3	1.314(11)	C22 – Si1	1.880(12)
C1 – Pd1	1.959(8)	C6 – C7	1.400(14)	C16 – C17	1.392(12)	C23 – Si1	1.859(11)
C2 – C3	1.314(12)	C7 – C8	1.382(14)	C16 – N2	1.401(10)	C24 – Pd1	2.042(8)
C2 – N1	1.398(10)	C8 – C9	1.385(13)	C17 – C18	1.398(13)	N3 – Pd1	2.178(7)
C3 – N2	1.395(11)	C9 – C13	1.533(13)	C18 – C19	1.397(14)	Br1 – Pd1	2.4525(13)
C4 – C5	1.392(12)	C10 – C11	1.524(13)	C19 – C20	1.385(13)		
C4 – C9	1.414(12)	C10 – C12	1.527(13)	C19 – Si1	1.902(9)		
C4 – N1	1.441(10)	C13 – C15	1.525(16)	C20 – N3	1.346(11)		

Table 4.7 Bond angles (°) for **4.2**.

N1 – C1 – N2	102.9(7)	C5 – C10 – C12	111.1(8)	C1 – N2 – C16	120.2(7)
N1 – C1 – Pd1	142.8(6)	C11 – C10 – C12	112.3(8)	C3 – N2 – C16	128.1(7)
N2 – C1 – Pd1	114.3(6)	C15 – C13 – C14	110.4(10)	C16 – N3 – C20	118.7(8)
C3 – C2 – N1	107.8(8)	C15 – C13 – C9	112.5(8)	C16 – N3 – Pd1	112.4(6)
C2 – C3 – N2	106.4(7)	C14 – C13 – C9	109.9(9)	C20 – N3 – Pd1	128.9(6)
C5 – C4 – C9	122.8(8)	N3 – C16 – C17	123.5(8)	C21 – Si1 – C23	110.6(6)
C5 – C4 – N1	117.9(7)	N3 – C16 – N2	114.2(7)	C21 – Si1 – C22	108.3(7)
C9 – C4 – N1	119.1(7)	C17 – C16 – N2	122.2(8)	C23 – Si1 – C22	113.1(6)
C6 – C5 – C4	117.6(8)	C16 – C17 – C18	117.0(9)	C21 – Si1 – C19	110.6(5)
C6 – C5 – C10	119.6(8)	C19 – C18 – C17	120.4(9)	C23 – Si1 – C19	107.9(5)
C4 – C5 – C10	122.7(8)	C20 – C19 – C18	116.8(8)	C22 – Si1 – C19	106.3(5)
C5 – C6 – C7	121.5(9)	C20 – C19 – Si1	122.7(7)	C1 – Pd1 – C24	96.0(3)
C8 – C7 – C6	119.6(9)	C18 – C19 – Si1	120.5(7)	C1 – Pd1 – N3	78.8(3)
C7 – C8 – C9	121.4(9)	N3 – C20 – C19	123.3(9)	C24 – Pd1 – N3	174.8(3)
C8 – C9 – C4	117.1(9)	C1 – N1 – C2	111.1(7)	C1 – Pd1 – Br1	173.6(2)
C8 – C9 – C13	122.7(8)	C1 – N1 – C4	127.1(7)	C24 – Pd1 – Br1	90.4(2)
C4 – C9 – C13	120.2(8)	C2 – N1 – C4	121.8(7)	N3 – Pd1 – Br1	94.81(19)
C5 – C10 – C11	111.8(8)	C1 – N2 – C3	111.7(7)		

{3-(2,6-di-*iso*-propylphenyl)-1-[(6-trimethylsilyl)-2-pyridyl)]-imidazol-2-ylidene} palladium methyl bromide 4.3

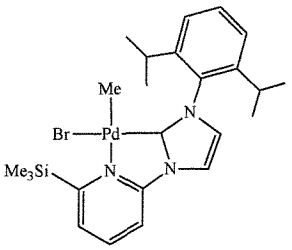

This was prepared by following general method 1 from {3-(2,6-di-*iso*-propylphenyl)-1-[(6-trimethysilyl)-2-pyridyl)] imidazol-2-ylidene} silver chloride (0.25 g, 0.5 mmol) and Pd(COD)MeBr (0.16 g, 0.5 mmol). Yield: 0.18g, 60%. MS (ES): m/z 907, $[Pd(ligand)_2Me]^+$. $\delta_H(CDCl_3)$: 0.3 (3H, s, $PdCH_3$), 0.4 [9H, s, $Si(CH_3)_3$], 1.2, 1.3 [2 x 6H, d, $CH(CH_3)_2$], 2.5 [2H, septet, $CH(CH_3)_2$], 7.0 and 7.8 (2 x 1H, d, 4- and 5-imidazol-2-ylidene), 7.3 (2H, d, $Pr^i_2C_6H_2H$), 7.4 (1H, t, $Pr^i_2C_6H_2H$), 7.7 (1H, d, pyr H), 8.1 (1H, t, 4-pyridyl H), 9.2 (1H, d, pyr *H*). Found: C, 50.23; H, 6.09; N, 7.35. $C_{24}H_{34}Br_1N_3Pd_1Si_1$ requires C, 49.79; H, 5.92; N, 7.26%.

[3-(2,6-di-*iso*-propylphenyl)-1-(2-pyridyl)-imidazol-2-ylidene] palladium dimethyl 4.4

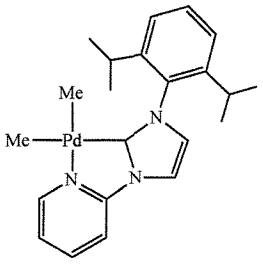

To a precooled (-78°C) solution of $Pd(COD)Me_2$ (0.045g, 0.18 mmol) dissolved in THF ($10cm^3$) was added a precooled (-78°C) solution of **2.20** (0.056 g, 0.18 mmol) in the same solvent. The mixture was stirred at and allowed to rise to 0°C and at this point the solvent was removed *in vacuo* to yield a white micro-crystalline solid. Attempts to crystallise **4.4** from diethylether saw only decomposition on standing at –30°C. MS(ES+) *m/z* 882 $[Pd(Ligand)Me_2]_2^+$, 467 $[Pd(Ligand)(Me)MeCN]^+$, 426 $[Pd(Ligand)Me]^+$. NMR $\delta_H(C_6D_6)$: 0.7 (6H, s, Pd-Me_2), 1.1, 1.5 [2 x 6H, d, $CH(CH_3)_2$], 2.9 [2H, septet, $CH(CH_3)_2$], 6.2 (2H, d, $Pr^i_2C_6H_2H$), 6.3 and 6.5 (1H, d, 4- and 5-imidazol-2-ylidene), 6.4 (1H, t, $Pr^i_2C_6H_2H$), 6.8 (1H, dd, pyr H), 7.1 (1H, d, pyr H), 7.3 (1H, dd, pyr H), 8.8 (1H, d, pyr H). Sample decomposed rapidly in benzene on standing.

[3-(2,6-di*iso*propylphenyl)-1-(α -picolyl)imidazolium] palladium trichloride/bromide 4.5

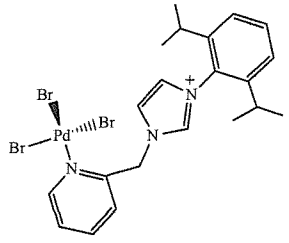

To a solution of $PdCl_2$ (0.04 g, 0.25 mmol) dissolved in acetonitrile (10 cm^3) was added a solution of 3-(2,6-di-*iso*-propylphenyl)-1-(α -picolyl)imidazolium bromide (0.09 g, 0.25 mmol) in the same solvent. The mixture was stirred at room temperature until yellow **4.5** precipitated as a microcrystalline powder. Recrystallisation from acetonitrile yielded yellow X-ray quality crystals. $\delta_H(CD_3CN)$: 2.0, [2 x 6H, d, $CH(CH_3)_2$], 3.3 [2H, septet, $CH(CH_3)_2$], 6.4 (2H, br. s, CH_2), 7.7 and 8.4 (2 x 1H, d, 4- and 5-imidazol-2-

ylidene), 8.5 (2H, br. d, $Pr^i_2C_6H_2H$), 8.8 (1H, m, 5-picolyl *H*), 9.0 (1H, t, $Pr^i_2C_6H_2H$), 10.0 (2H, br., 3,4-picolyl), 10.1 (1H, d, 6-picolyl *H*), 10.7 (1H, s, imidazol-2-ylidene).

Crystal data for **4.5**: $C_{96}H_{122}Br_{5.54}Cl_{6.46}N_{18}Pd_4$, colourless plate, Mw 2625.42, Triclinic, *P*-1 (No. 15), a = 12.515(5) Å, b = 15.993(5) Å, c = 16.428(5) Å, α = 114.512(5), β = 108.155(5)°, γ = 96.941(5) °, V = 2721.3(16) Å^3, Z = 1, μ = 2.894 mm^{-1}, T = 150 K, Total reflections = 15113, unique reflections = 7785 (R_{int} = 0.0421), Final R indices [$I>2\sigma(I)$] R = 0.0665, R_w = 0.1017 (all data). CCDC Code 194162. X-ray Local Code 02sw091. Unit cell contains two complex units and 3 molecules of acetonitrile.

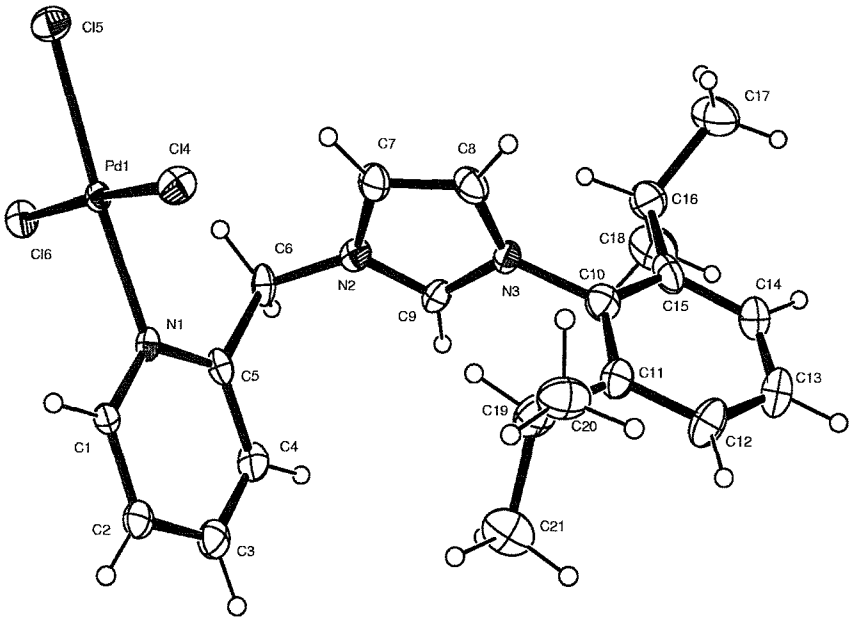

Fig 4.16 X-ray crystal structure of **4.5**.

Table 4.8 Bond lengths (Å) for **4.5**.

Pd1 – N1	2.048(7)	N2 – C6	1.469(12)	C5 – C6	1.509(13)	C13 – C14	1.399(19)
Pd1 – Cl5	2.331(2)	N3 – C9	1.328(13)	C7 – C8	1.354(15)	C14 – C15	1.369(16)
Pd1 – Cl4	2.371(2)	N3 – C8	1.373(13)	C10 – C15	1.356(15)	C15 – C16	1.527(17)
Pd1 – Cl6	2.3968(19)	N3 – C10	1.463(13)	C10 – C11	1.400(15)	C16 – C17	1.531(17)
N1 – C1	1.331(11)	C1 – C2	1.369(14)	C11 – C12	1.363(16)	C16 – C18	1.547(18)
N1 – C5	1.348(12)	C2 – C3	1.359(15)	C11 – C19	1.539(16)	C19 – C20	1.495(17)
N2 – C9	1.330(12)	C3 – C4	1.365(15)	C12 – C13	1.362(18)	C19 – C21	1.557(17)
N2 – C7	1.394(13)	C4 – C5	1.375(14)				

Table 4.9 Bond angles (°) for **4.5**.

N1 – Pd1 – Cl5	176.3(2)	N1 – C1 – C2	121.6(9)	C12 – C11 – C19	120.2(11)
N1 – Pd1 – Cl4	87.1(2)	C3 – C2 – C1	119.5(10)	C10 – C11 – C19	123.2(10)
Cl5 – Pd1 – Cl4	92.60(7)	C2 – C3 – C4	119.1(10)	C13 – C12 – C11	121.8(13)
N1 – Pd1 – Cl6	90.0(2)	C3 – C4 – C5	120.1(10)	C12 – C13 – C14	119.6(12)

Cl5 – Pd1 – Cl6	90.45(7)	N1 – C5 – C4	120.1(9)	C15 – C14 – C13	120.5(12)
Cl4 – Pd1 – Cl6	175.63(6)	N1 – C5 – C6	118.7(9)	C10 – C15 – C14	117.6(12)
C1 – N1 – C5	119.7(8)	C4 – C5 – C6	121.2(9)	C10 – C15 – C16	122.8(11)
C1 – N1 – Pd1	119.3(6)	N2 – C6 – C5	109.6(8)	C14 – C15 – C16	119.6(11)
C5 – N1 – Pd1	121.0(6)	C8 – C7 – N2	106.6(9)	C15 – C16 – C17	110.6(11)
C9 – N2 – C7	108.2(9)	C7 – C8 – N3	107.4(10)	C15 – C16 – C18	110.2(10)
C9 – N2 – C6	124.9(9)	N3 – C9 – N2	109.0(9)	C17 – C16 – C18	110.7(10)
C7 – N2 – C6	126.6(8)	C15 – C10 – C11	123.8(11)	C20 – C19 – C11	112.5(11)
C9 – N3 – C8	108.8(9)	C15 – C10 – N3	120.3(10)	C20 – C19 – C21	110.5(10)
C9 – N3 – C10	123.2(8)	C11 – C10 – N3	115.9(9)	C11 – C19 – C21	111.3(10)
C8 – N3 – C10	125.9(9)	C12 – C11 – C10	116.6(12)		

Bis-{1-[3-(mesityl)-imidazol-2-ylidene]-1-diethylcarbamoylmethyl} palladium dichloride 4.6

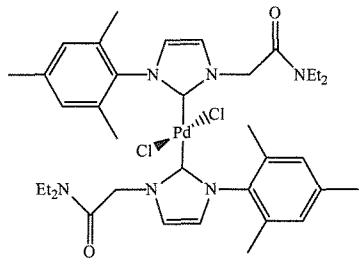

This was prepared following the general method 1 from **3.6** (0.20 g, 0.45 mmol) and $Pd(COD)Cl_2$ (0.13 g, 0.45 mmol) in dichloromethane (50 cm^3) by stirring at room temperature for 12 h. The crude product was washed with methanol, dissolved in dichloromethane and passed through a short silica gel column. Evaporation of the volatiles gave spectroscopically pure product. X-ray quality crystals were obtained by layering a saturated dichloromethane solution with diethylether. NMR $\delta_H(CDCl_3)$ 1.2 [6H, t, $N(CH_2CH_3)$], 2.5 (6H, bs, mesityl CH_3), 2.9 (12H, bs, mesityl CH_3), 3.4 [4H, q, $N(CH_2CH_3)$], 5.3 (4H, s, CH_2), 6.3 (6H, bs, mesityl H and 4-imidazol-2-ylidene), 7.2 (2H, s, 5-imidazol-2-ylidene). Found: C, 55.29; H, 6.21; N, 10.49. (Calculated for $C_{36}H_{50}Cl_2N_6O_2PdCl_2$: C, 55.71; H, 6.49; N, 10.82%).

Crystal data for **4.6**: $C_{18}H_{25}N_3OClPd_{0.5}$, yellow plate, Mw 388.06, Monoclinic, $P2_1/c$ (No. 14), a = 11.448(2) Å, b = 10.010(2) Å, c = 16.985(3) Å, $\alpha = \gamma = 90°$, β = 103.99(3)°, V = 1888.7(7) $Å^3$, Z = 4, μ = 0.672 mm^{-1}, T = 150 K, Total reflections = 15398, unique reflections = 4301 (R_{int} = 0.0781), Final R indices [$I>2\sigma(I)$] R = 0.0431, R_w = 0.0529 (all data). Symmetry transformations used to generate equivalent atoms: -x + 1, -y + 1, -z. CCDC Code 194165. X-ray Local Code 01sot040.

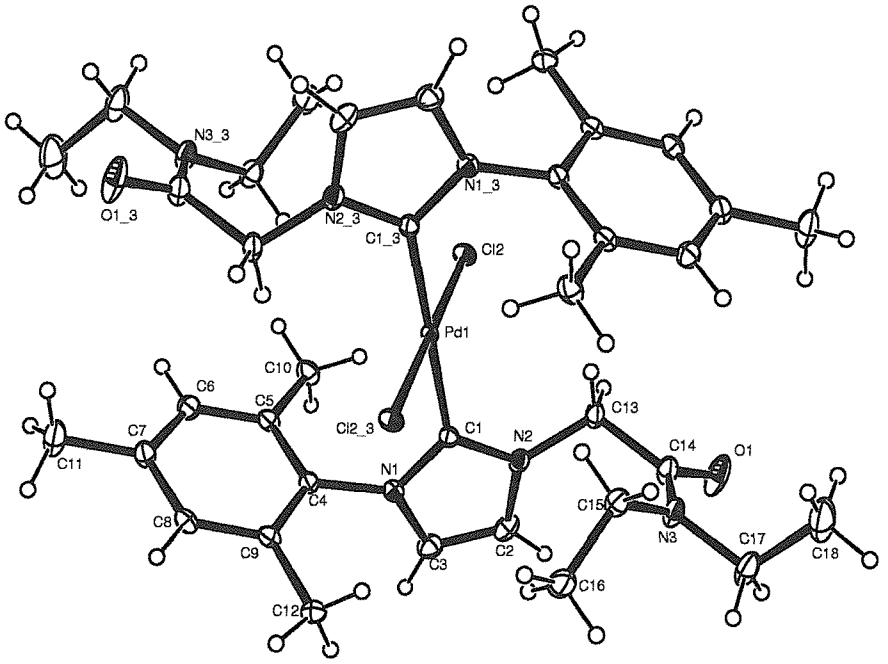

Fig 4.17 X-ray crystal structure of **4.6**.

Table 4.10 Bond lengths (Å) for **4.6**.

C1 – N1	1.352(3)	C4 – C9	1.402(3)	C8 – C9	1.392(3)	C15 – C16	1.504(4)
C1 – N2	1.355(3)	C4 – N1	1.445(3)	C9 – C12	1.502(3)	C17 – N3	1.470(3)
C1 – Pd1	2.015(2)	C5 – C6	1.391(3)	C13 – N2	1.464(3)	C17 – C18	1.510(5)
C2 – C3	1.341(4)	C5 – C10	1.504(3)	C13 – C14	1.532(3)	Cl2 – Pd1	2.3164(6)
C2 – N2	1.388(4)	C6 – C7	1.388(3)	C14 – O1	1.224(3)	Pd1 – C1_3	2.015(2)
C3 – N1	1.392(3)	C7 – C8	1.399(4)	C14 – N3	1.338(3)	Pd1 – Cl2_3	2.3164(6)
C4 – C5	1.400(3)	C7 – C11	1.505(4)	C15 – N3	1.471(3)		

Table 4.11 Bond angles (°) for **4.6**.

N1 – C1 – N2	104.9(2)	C6 – C7 – C11	120.7(2)	C1 – N1 – C4	122.00(19)
N1 – C1 – Pd1	127.80(17)	C8 – C7 – C11	120.8(2)	C3 – N1 – C4	127.0(2)
N2 – C1 – Pd1	127.19(19)	C9 – C8 – C7	121.7(2)	C1 – N2 – C2	110.6(2)
C3 – C2 – N2	107.0(2)	C8 – C9 – C4	117.7(2)	C1 – N2 – C13	124.7(2)
C2 – C3 – N1	106.6(2)	C8 – C9 – C12	120.7(2)	C2 – N2 – C13	124.3(2)
C5 – C4 – C9	122.2(2)	C4 – C9 – C12	121.6(2)	C14 – N3 – C17	117.9(2)
C5 – C4 – N1	118.8(2)	N2 – C13 – C14	114.2(2)	C14 – N3 – C15	125.7(2)
C9 – C4 – N1	119.0(2)	O1 – C14 – N3	123.0(2)	C17 – N3 – C15	116.2(2)
C6 – C5 – C4	117.5(2)	O1 – C14 – C13	117.7(2)	C1_3 – Pd1 – C1	180.00(5)
C6 – C5 – C10	120.5(2)	N3 – C14 – C13	119.3(2)	C1_3 – Pd1 – Cl2	92.09(7)
C4 – C5 – C10	121.9(2)	N3 – C15 – C16	113.0(2)	C1 – Pd1 – Cl2	87.91(7)
C7 – C6 – C5	122.2(2)	N3 – C17 – C18	112.1(3)	Cl2 – Pd1 – Cl2_3	180.00(3)
C6 – C7 – C8	118.5(2)	C1 – N1 – C3	110.8(2)		

Di-{3-(mesityl)-1-[(6-trimethylsilyl)2-pyridyl]-imidazol-2-ylidene} palladium dimethyl 4.7 NMR Scale only.

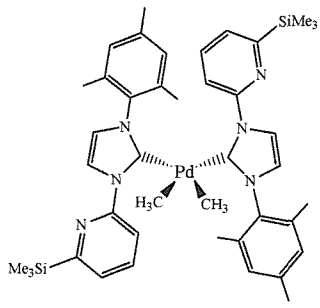

This was prepared following the general method 2 from **2.19** (0.03 g, 0.08 mmol) and Pd(TMEDA)Me_2 (0.01 g, 0.04 mmol). MS (ES+): *m/z* 867 $[Pd(Ligand)_2Me]^+$. NMR $\delta_H(C_6D_6)$ 0.3 (6H, s, Pd-CH_3), 0.4 [18H, bs, $Si(CH_3)_3$], 2.1, 2.2 (2 x 6H, s, mesityl *o*-CH_3), 2.3, (6H, s, mesityl *p*-CH_3), 6.0 and 6.1 (2 x 2H, s, mesityl H), 6.8 and 8.6 (2 x 2H, s, 4- and 5-imidazol-2-ylidene), 7.0 (2H, d, Pyr H), 7.1 (2H, d, Pyr H), 10.2 (2H, d, Pyr H).

Di-{3-(2,6-di-*iso*-propylphenyl)-1-[(6-trimethylsilyl)2-pyridyl]-imidazol-2-ylidene} palladium dimethyl 4.8

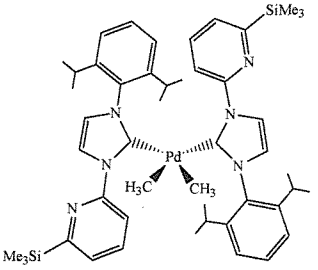

This was prepared following the general method 2 from **2.21** (0.30 g, 0.8 mmol) and Pd(TMEDA)Me_2 (0.10 g, 0.4 mmol). Yield 0.35 g, 81%. MS (ES+): *m/z* 875 $[Pd(Ligand)_2Me]^+$. NMR $\delta_H(C_6D_6)$ 0.2 [18H, s, $Si(CH_3)_3$], 0.6, 0.8, 0.9, 1.5 [4 x 6H, d, $CH(CH_3)_2$], 2.5, 3.1 [2 x 2H, septet, $CH(CH_3)_2$], 6.3 and 7.0 (2 x 2H, br.d 4-, 5-imidazol-2-ylidene), 6.4 (4H, d, $Pr^i_2C_6H_2H$), 6.7 (2H, t, $Pr^i_2C_6H_2H$), 6.9 (2H, dd, Pyr H), 8.3 (2H, d, Pyr H), 9.4 (2H, d, Pyr H). $\delta_C(C_6D_6)$ –1.5 (Pd-CH_3), 1.5 [$Si(CH_3)_3$], 116.1, 118.6 (4- and 5-imidazol-2-ylidene), 123.3, 124.2, 124.6, 126.7, 130.1, 136.1, 138.4, 145.1, 148.0, 151.7, 164.3 (aromatic) 174.4 (2-imidazol-2-ylidene).

Crystal data for **4.8**: $C_{48}H_{68}N_6PdSi_2$, yellow plate, Mw 891.66, Monoclinic, $P2_1/c$ (No. 14), a = 20.4334(5) Å, b = 10.1594(2) Å, c = 23.8809(5) Å, $\alpha = \gamma = 90°$, β = 100.8020(10)°, V = 4869.6(2) Å^3, Z = 4, μ = 0.468 mm^{-1}, T = 150 K, Total reflections = 19837, unique reflections = 10836 (R_{int} = 0.0378), Final R indices [$I>2\sigma(I)$] R = 0.0629, R_w = 0.0882 (all data). X-ray Local Code 02sw004.

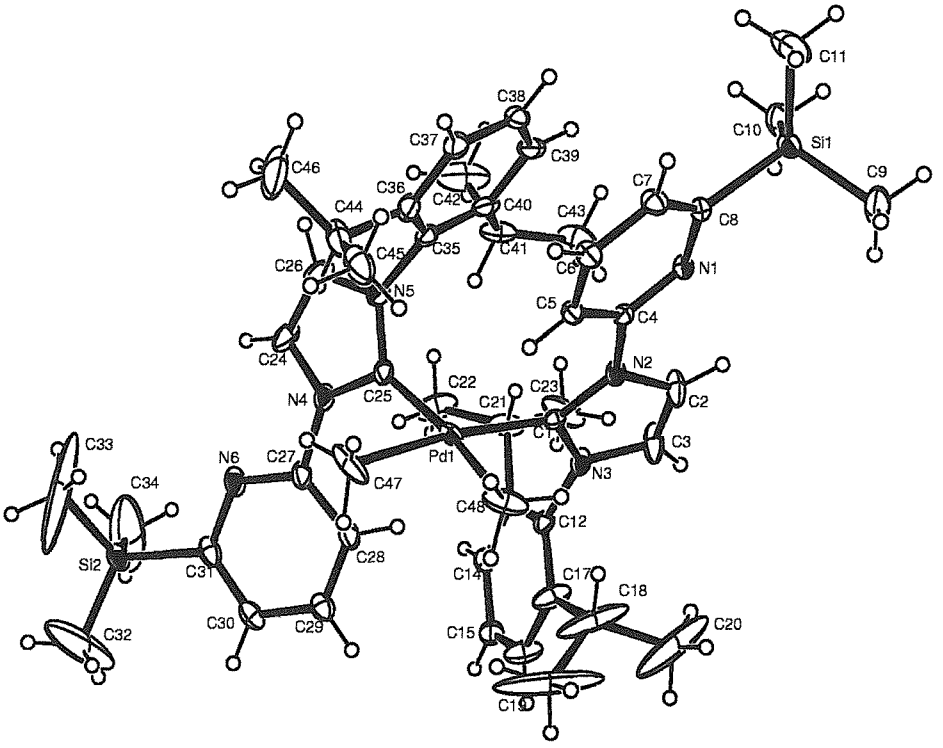

Fig 4.18 X-ray crystal structure of **4.8**.

Table 4.12 Bond lengths (Å) for **4.8**.

C1 – N3	1.365(5)	C11 – Si1	1.873(6)	C25 – N5	1.365(5)	C35 – C36	1.400(7)
C1 – N2	1.374(5)	C12 – C17	1.383(6)	C25 – N4	1.376(5)	C35 – N5	1.442(5)
C1 – Pd1	2.054(4)	C12 – C13	1.390(6)	C25 – Pd1	2.052(4)	C36 – C37	1.397(6)
C2 – C3	1.327(6)	C12 – N3	1.445(5)	C26 – N5	1.391(6)	C36 – C44	1.505(7)
C2 – N2	1.394(5)	C13 – C14	1.393(5)	C27 – N6	1.327(5)	C37 – C38	1.374(6)
C3 – N3	1.394(6)	C13 – C21	1.508(6)	C27 – C28	1.376(6)	C38 – C39	1.376(6)
C4 – N1	1.324(5)	C14 – C15	1.372(6)	C27 – N4	1.437(5)	C39 – C40	1.398(6)
C4 – C5	1.378(5)	C15 – C16	1.363(7)	C28 – C29	1.373(6)	C40 – C41	1.513(7)
C4 – N2	1.432(5)	C16 – C17	1.388(7)	C29 – C30	1.392(6)	C41 – C43	1.514(8)
C5 – C6	1.378(5)	C17 – C18	1.510(7)	C30 – C31	1.389(7)	C41 – C42	1.536(8)
C6 – C7	1.385(6)	C18 – C19	1.51(2)	C31 – N6	1.356(6)	C44 – C45	1.531(9)
C7 – C8	1.382(6)	C18 – C20	1.54(2)	C31 – Si2	1.891(4)	C44 – C46	1.532(8)
C8 – N1	1.360(5)	C21 – C22	1.519(8)	C32 – Si2	1.717(9)	C47 – Pd1	2.083(5)
C8 – Si1	1.882(4)	C21 – C23	1.539(8)	C33 – Si2	1.744(10)	C48 – Pd1	2.087(5)
C9 – Si1	1.841(5)	C24 – C26	1.325(7)	C34 – Si2	1.680(10)		
C10 – Si1	1.840(5)	C24 – N4	1.387(7)	C35 – C40	1.395(7)		

Table 4.13 Selected bond angles (°) for **4.8**.

N3 – C1 – N2	102.7(3)	C12 – C13 – C14	117.3(4)	C1 – N2 – C4	128.4(3)
N3 – C1 – Pd1	126.1(3)	C12 – C13 – C21	122.6(3)	C2 – N2 – C4	119.9(3)
N2 – C1 – Pd1	130.6(3)	C14 – C13 – C21	120.0(4)	C1 – N3 – C3	111.7(3)
C3 – C2 – N2	106.8(4)	C15 – C14 – C13	121.7(4)	C1 – N3 – C12	128.3(3)
C2 – C3 – N3	107.1(4)	C16 – C15 – C14	119.4(4)	C3 - N3 – C12	119.8(3)
N1 – C4 – C5	124.3(3)	C15 – C16 – C17	121.5(4)	C25 – Pd1 – C1	102.34(15)

N1 – C4 – N2	113.8(3)	C12 – C17 – C16	118.0(4)	C25 – Pd1 – C47	86.8(2)
C5 – C4 – N2	121.8(3)	C12 – C17 – C18	122.4(5)	C1 – Pd1 – C47	170.7(2)
C6 – C5 – C4	117.3(3)	C16 – C17 – C18	119.5(5)	C25 – Pd1 – C48	169.7(2)
C5 – C6 – C7	119.7(4)	C17 – C18 – C19	111.6(9)	C1 – Pd1 – C48	87.8(2)
C8 – C7 – C6	119.6(4)	C17 – C18 – C20	108.8(8)	C47 – Pd1 – C48	83.1(3)
N1 – C8 – C7	120.6(3)	C19 – C18 – C20	113.8(9)	C10 – Si1 – C9	112.4(3)
N1 – C8 – Si1	113.7(3)	C13 – C21 – C22	113.1(4)	C10 – Si1 – C11	109.5(3)
C7 – C8 – Si1	125.7(3)	C13 – C21 – C23	110.4(4)	C9 – Si1 – C11	110.0(3)
C17 – C12 – C13	122.0(4)	C22 – C21 – C23	110.1(4)	C10 – Si1 – C8	107.8(2)
C17 – C12 – N3	119.2(4)	C4 – N1 – C8	118.5(3)	C9 – Si1 – C8	107.9(2)
C13 – C12 – N3	118.5(4)	C1 – N2 – C2	111.7(3)	C11 – Si1 – C8	109.2(2)

Di-{3-(2,6-di-*iso*-propylphenyl)-1-[(5-trifluoromethyl)2-pyridyl]-imidazol-2-ylidene} palladium dimethyl 4.9 NMR Scale only.

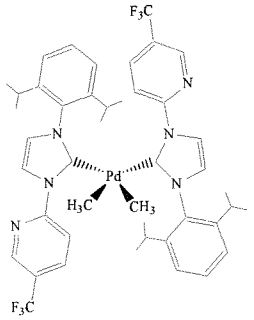

This was prepared following the general method 2 from **2.22** (0.03 g, 0.08 mmol) and Pd(TMEDA)Me_2 (0.01 g, 0.04 mmol). MS (ES+): *m/z* 867 $[Pd(Ligand)_2Me]^+$. NMR $\delta_H(C_6D_6)$ 0.1 (6H, s, Pd-CH_3), 0.6, 0.7, 0.9, 1.4 [4 x 6H, d, $CH(CH_3)_2$], 2.5, 3.1 [2 x 2H, septet, $CH(CH_3)_2$], 6.3 and 8.2 (2 x 2H, s, 4-, 5-imidazol-2-ylidene), 6.4 and 6.9 (2 x 2H, d, $Pr^i_2C_6H_2H$), 6.9 (2H, t, $Pr^i_2C_6H_2H$), 7.4 (2H, d, Pyr H), 8.4 (2H, s, Pyr H), 10.0 (2H, d, Pyr H). Very fine plate crystals grew from the NMR sample however, from X-ray diffraction studies poor quality data was obtained only allowing connectivity to be confirmed, which showed complex **4.9** to be isostructural to **4.8**. Due to the weakness of the data it is not presented here.

1,3-{bis[3-(mesityl)imidazol-2-ylidene]methyl}-4,6-dimethylbenzene palladium bromide 4.10

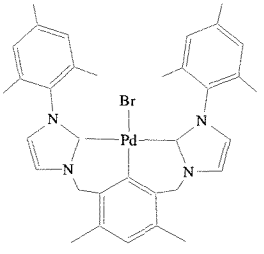

A mixture of $Pd(OAc)_2$, (0.07 g, 0.31 mmol), **2.19** (0.5 g, 0.75 mmol), $NaOOCCH_3$ (0.303 g, 3.7 mmol) and N, N-dimethylacetamide (20 cm^3) was heated in a sealed rotaflo ampoule at 160°C for 24 h, giving a dark–red purple mixture. After removal of the volatiles under reduced pressure at 70-80°C, the residue was extracted into ether (3 x 30 cm^3), the extracts were passed through a short alumina pad deactivated with THF, and concentrated to *ca* 5 cm^3, to give the product as white crystalline material. X-ray quality crystals were obtained from diethylether solutions by slow evaporation. Yield 0.12g, 60%. MS(ES+) *m/z* 650.0, $[Pd(ligand)(MeCN)]^+$. NMR $\delta_H(CDCl_3)$, 1.8 (6H, s, phenyl CH_3) 2.2, 2.3 (2 x 6H, s,

mesityl CH_3), 2.4 (6H, s, mesityl CH_3), 5.1, 5.3 (2 x 2H, d, CH_2 AB pattern), 6.6 (3H, bs, 5-imidazol-2-ylidene and *p*-phenyl H), 6.9 (4H, s, mesityl *H*), 7.1 (2H, s, 4-imidazol-2-ylidene). $\delta_C(CDCl_3)$ 18.6, 19.3, 19.9, 21.0 (CH_3), 53.7 (CH_2), 119.4, 121.5 (4- and 5-imidazol-2-ylidene), 127.0, 128.5, 128.7, 130.7, 134.6, 136.0, 136.4, 136.9, 137.6, 156.2 (aromatic), 180.9 (2-imidazol-2-ylidene). Found: C, 58.55 H, 5.65; N, 8.05, $C_{34}H_{37}N_4Br_1Pd_1$ requires: C, 59.36; H, 5.42; N, 8.14.

1,3-[bis{3-(2,6-di-*iso*-propylphenyl)imidazol-2-ylidene)methyl}-4,6-dimethylbenzene palladium bromide 4.11

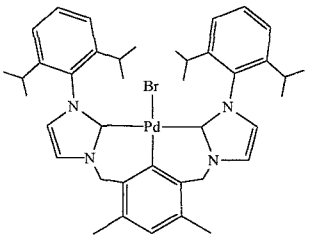

A mixture of $Pd(OAc)_2$, (0.07 g, 0.31 mmol), **2.18** (0.23 g, 0.31 mmol), $NaOOCCH_3$ (0.26 g, 3.5 mmol) and N, N'-dimethylacetamide (20 cm^3) was heated in a sealed rotaflow ampoule at 160°C for 24 h, giving a dark–red purple mixture. After removal of the volatiles under reduced pressure at 70 - 80°C, the residue was extracted into ether (3 x 30 cm^3), the extracts were passed through a short alumina pad deactivated with THF, and concentrated to *ca* 5 cm^3, to give the product as white crystalline material. X-ray quality crystals were obtained from ether solutions by slow evaporation. Yield: 0.12 g, 52%. MS (ES): *m/z* 732.0, $[Pd(ligand)(MeCN)]^+$. $\delta_H(CDCl_3)$ 0.6, 1.0, 1.2, 1.3 [24H, 4 x d, $CH(CH_3)_2$], 2.2, 2.8 [4H, 2 x septet, $CH(CH_3)_2$], 2.3 (6H, s, *o*-CH_3), 4.9, 5.2 (4H, 2 x d, CH_2 AB pattern), 6.4 (1H, s, aromatic *H*), 6.5 (2H, d, 5-imidazol-2-ylidene *H*), 6.9 (2H, d, 4-imidazol-2-ylidene *H*), 7.0, 7.1 (4H, 2 x d, $Pr^i_2C_6H_2H$), 7.3 (2H, t, $Pr^i_2C_6H_2H$). $\delta_C(CDCl_3)$ 18.9 (CH_3-phenyl), 22.2, 22.6, 23.4, 23.7 [$CH(CH_3)$], 26.9, 27.6 [$CH(CH_3)$], 52.9 (CH_2), 117.9, 121.9 (4- and 5-imidazol-2-ylidene), 122.6, 122.7, 125.6, 127.9, 129.4, 135.3, 136.1, 144.2, 145.3, 155.5 (aromatic), 180.9 (imidazol-2-ylidene). Found: C, 62.06; H, 6.45; N, 6.91. $C_{40}H_{49}N_4Br_1Pd_1$ requires: C, 62.06; H, 6.64; N, 7.24 %.

Crystal data for **4.11**: $C_{40}H_{49}BrN_4Pd$, colourless block, Mw 772.14, Monoclinic, $P2_1/c$ (No. 14), a = 12.0839(2) Å, b = 15.3863(3) Å, c = 20.9393(5) Å, $\alpha = \gamma = 90°$, β = 90.3890(10)°, V = 3893.08(14) Å^3, Z = 4, μ = 1.534 mm^{-1}, T = 150 K, Total reflections = 14984, unique reflections = 8760 (R_{int} = 0.0264), Final R indices [$I>2\sigma(I)$] R = 0.0567, R_w = 0.0733 (all data). CCDC Code 194844. X-ray Local Code 01sw048.

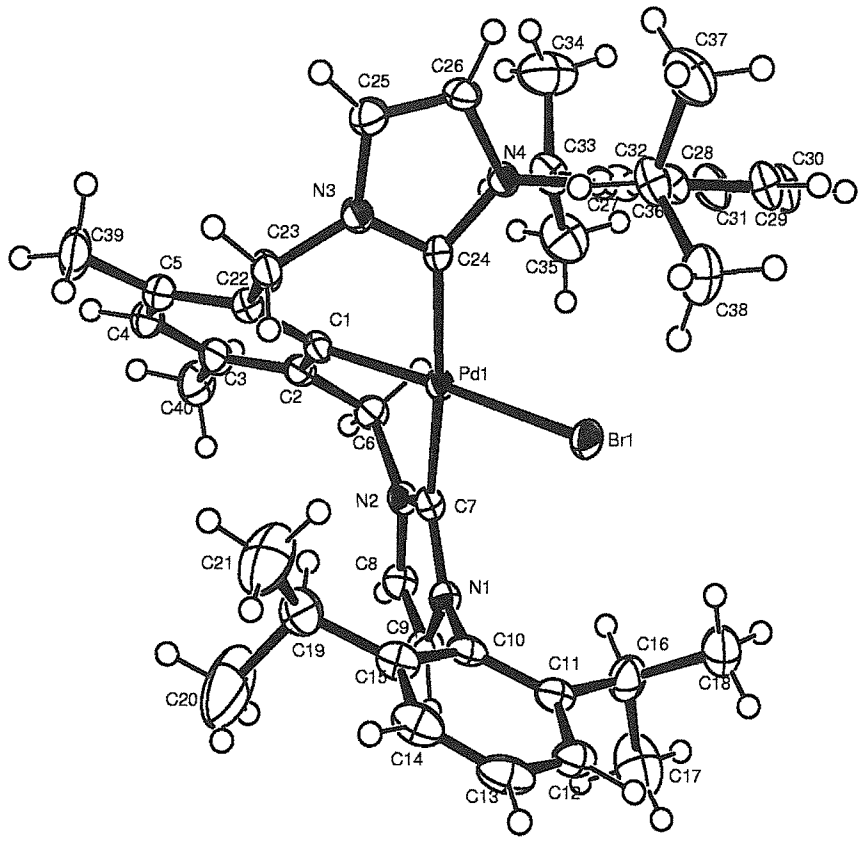

Fig 4.19 X-ray crystal structure of **4.11**.

Table 4.14 Bond lengths (Å) for **4.11**.

C1 – C22	1.400(7)	C7 – Pd1	2.033(5)	C16 – C17	1.517(9)	C27 – C28	1.407(7)
C1 – C2	1.413(7)	C8 – C9	1.351(7)	C16 – C18	1.534(8)	C27 – N4	1.433(6)
C1 – Pd1	2.032(4)	C8 – N2	1.374(6)	C19 – C21	1.503(9)	C28 – C29	1.400(7)
C2 – C3	1.415(7)	C9 – N1	1.388(6)	C19 – C20	1.517(11)	C28 – C36	1.510(7)
C2 – C6	1.508(7)	C10 – C11	1.387(7)	C22 – C23	1.514(7)	C29 – C30	1.388(8)
C3 – C4	1.391(8)	C10 – C15	1.399(7)	C23 – N3	1.477(6)	C30 – C31	1.385(8)
C3 – C40	1.510(8)	C10 – N1	1.442(6)	C24 – N3	1.351(6)	C31 – C32	1.392(7)
C4 – C5	1.383(8)	C11 – C12	1.411(7)	C24 – N4	1.371(6)	C32 – C33	1.516(7)
C5 – C22	1.411(7)	C11 – C16	1.529(8)	C24 – Pd1	2.014(5)	C33 – C35	1.506(8)
C5 – C39	1.515(8)	C12 – C13	1.376(9)	C25 – C26	1.346(7)	C33 – C34	1.531(8)
C6 – N2	1.475(6)	C13 – C14	1.382(9)	C25 – N3	1.383(6)	C36 – C38	1.528(8)
C7 – N2	1.355(6)	C14 – C15	1.409(7)	C26 – N4	1.386(6)	C36 – C37	1.540(8)
C7 – N1	1.369(6)	C15 – C19	1.522(8)	C27 – C32	1.394(7)	Br1 – Pd1	2.5059(6)

Table 4.15 Selected bond angles (°) for **4.11**.

C(22)-C(1)-C(2)	118.4(4)	N(1)-C(7)-Pd(1)	135.2(3)	C(7)-N(2)-C(8)	112.2(4)
C(22)-C(1)-Pd(1)	120.1(4)	C(9)-C(8)-N(2)	106.5(4)	C(7)-N(2)-C(6)	121.7(4)
C(2)-C(1)-Pd(1)	121.1(3)	C(8)-C(9)-N(1)	106.8(4)	C(8)-N(2)-C(6)	125.8(4)
C(1)-C(2)-C(3)	121.0(5)	C(1)-C(22)-C(5)	121.0(5)	C(24)-N(3)-C(25)	111.9(4)
C(1)-C(2)-C(6)	118.7(4)	C(1)-C(22)-C(23)	119.4(4)	C(24)-N(3)-C(23)	121.5(4)
C(3)-C(2)-C(6)	120.3(4)	C(5)-C(22)-C(23)	119.6(5)	C(25)-N(3)-C(23)	126.5(4)
C(4)-C(3)-C(2)	118.4(5)	N(3)-C(23)-C(22)	111.1(4)	C(24)-N(4)-C(26)	110.7(4)

C(4)-C(3)-C(40)	119.2(5)	N(3)-C(24)-N(4)	103.9(4)	C(24)-N(4)-C(27)	126.6(4)
C(2)-C(3)-C(40)	122.3(5)	N(3)-C(24)-Pd(1)	121.3(3)	C(26)-N(4)-C(27)	122.7(4)
C(5)-C(4)-C(3)	122.0(5)	N(4)-C(24)-Pd(1)	134.6(3)	C(24)-Pd(1)-C(1)	86.7(2)
C(4)-C(5)-C(22)	119.1(5)	C(26)-C(25)-N(3)	106.4(4)	C(24)-Pd(1)-C(7)	173.0(2)
C(4)-C(5)-C(39)	118.4(5)	C(25)-C(26)-N(4)	107.0(4)	C(1)-Pd(1)-C(7)	86.8(2)
C(22)-C(5)-C(39)	122.5(5)	C(32)-C(27)-C(28)	122.5(4)	C(24)-Pd(1)-Br(1)	92.95(13)
N(2)-C(6)-C(2)	109.8(4)	C(7)-N(1)-C(9)	110.9(4)	C(1)-Pd(1)-Br(1)	174.50(13)
N(2)-C(7)-N(1)	103.7(4)	C(7)-N(1)-C(10)	127.6(4)	C(7)-Pd(1)-Br(1)	93.78(13)
N(2)-C(7)-Pd(1)	121.1(3)	C(9)-N(1)-C(10)	121.1(4)		

1,3-[bis{3-(2,6-di*iso*propylphenyl)imidazol-2-ylidene)methyl}benzene palladium bromide 4.12

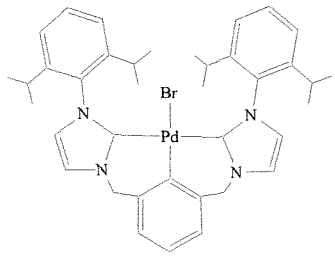

A mixture of $Pd_2(DBA)_3$, (0.08 g, *ca* 0.1 mmol), **2.17** (0.16 g, 0.2 mmol). NaOAc (0.25 g, excess) and N, N-dimethylacetamide (20 cm^3) was heated in a sealed rotaflo ampoule at 160°C for 24 h, giving a dark–red brown mixture. After removal of the volatiles under reduced pressure at 70 - 80°C, the residue was extracted into ether (3 x 30 cm^3), the extracts were passed through a short alumina pad deactivated with THF, and concentrated to *ca* 5 cm^3, to give the product. Crystals were grown by slowly evaporating ether solutions. The compound is soluble in hot toluene and chlorinated solvents. Yield: 0.1g, *ca* 65%. $\delta_H(CDCl_3)$ 0.6, 1.1, 1.3, 1.4 [24H, 4 x d, $CH(CH_3)_2$], 2.2, 2.9 [4H, 2 x septet, $CH(CH_3)_2$], 3.0 (6H, s, *o*-CH_3), 4.7, 5.5 (4H, 2 x d, CH_2 AB pattern), 6.7 and 8.0 (2H, d, 4- and 5-imidazol-2-ylidene), 7.1, 7.2 (4H, 2 x d, $Pr^i_2C_6H_2H$), 7.3 (2H, t, $Pr^i_2C_6H_2H$), 7.5 (2H, d, aromatic), 7.7(1H, t, aromatic).

Crystal data for **4.12**: $C_{118}H_{145}Br_3N_{12}OPd_3$, colourless block, Mw 2306.39, Triclinic, *P*-1 (No. 2), a = 16.0118(6) Å, b = 16.4652(6) Å, c = 23.5036(10) Å, α = 110.001(2)°, β = 96.4400(10)°, γ = 93.111(2)°, V = 5757.4(4) $Å^3$, Z = 2, μ = 1.556 mm^{-1}, T = 150 K, Total reflections = 75870, unique reflections = 25634 (R_{int} = 0.2459), Final R indices [$I>2\sigma(I)$] R = 0.0925, R_w = 0.2895 (all data). CCDC Code 194845. X-ray Local Code 01sw049. Unit cell contains 3 molecules of complex and one molecule of diethylether.

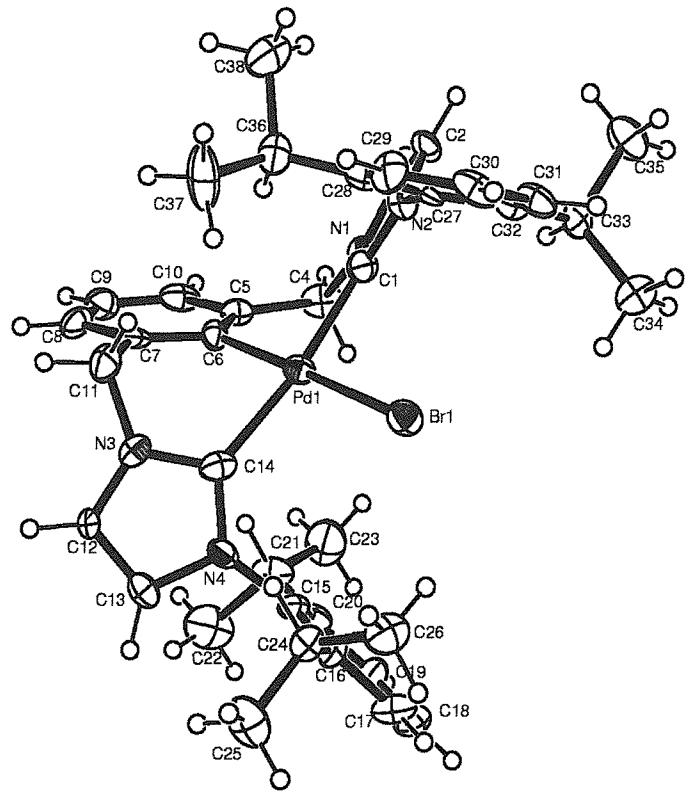

Fig 4.20 X-ray crystal structure of **4.12**.

Table 4.16 Selected bond lengths (Å) for **4.12**

C1 – N1	1.348(10)	C7 – C11	1.512(14)	C16 – C17	1.379(14)	C28 – C29	1.403(14)
C1 – N2	1.346(10)	C8 – C9	1.388(14)	C16 – C24	1.520(14)	C28 – C36	1.515(14)
C1 – Pd1	2.057(10)	C9 – C10	1.382(15)	C17 – C18	1.371(14)	C29 – C30	1.382(14)
C2 – C3	1.324(13)	C11 – N3	1.472(10)	C18 – C19	1.373(14)	C30 – C31	1.379(14)
C2 – N2	1.412(9)	C12 – N3	1.348(9)	C19 – C20	1.383(14)	C31 – C32	1.396(14)
C3 – N1	1.379(10)	C12 – C13	1.368(13)	C20 – C21	1.506(14)	C32 – C33	1.509(13)
C4 – N1	1.453(10)	C13 – N4	1.384(9)	C21 – C23	1.475(14)	C33 – C34	1.522(13)
C4 – C5	1.518(14)	C14 – N4	1.360(9)	C21 – C22	1.547(15)	C33 – C35	1.545(13)
C5 – C10	1.396(13)	C14 – N3	1.368(10)	C24 – C25	1.521(14)	C36 – C37	1.511(14)
C5 – C6	1.405(13)	C14 - Pd1	2.039(10)	C24 – C26	1.522(13)	C36 – C38	1.542(13)
C6 – C7	1.392(13)	C15 – C16	1.393(13)	C27 – C28	1.397(13)	Pd1 – Br1	2.5154(13)
C6 – Pd1	2.021(9)	C15 – C20	1.410(13)	C27 – C32	1.405(13)		
C7 – C8	1.401(13)	C15 – N4	1.445(10)	C27 – N2	1.424(9)		

Table 4.17 Selected bond angles (°) for **4.12**

N1 – C1 – N2	105.8(7)	C20 – C15 – N4	117.5(8)	C31 – C32 – C33	120.7(9)
N1 – C1 – Pd1	120.8(6)	C17 – C16 – C15	116.5(10)	C27 – C32 – C33	123.3(9)
N2 – C1 – Pd1	133.1(6)	C17 – C16 – C24	120.5(9)	C32 – C33 – C34	112.9(8)
C3 – C2 – N2	107.7(8)	C15 – C16 – C24	123.0(9)	C32 – C33 – C35	110.7(8)
C2 – C3 – N1	106.7(8)	C18 – C17 – C16	122.4(11)	C34 – C33 – C35	109.5(8)
N1 – C4 – C5	109.5(7)	C19 – C18 – C17	119.5(11)	C37 – C36 – C28	115.7(9)
C10 – C5 – C6	119.7(9)	C18 – C19 – C20	122.2(11)	C37 – C36 – C38	109.1(10)
C10 – C5 – C4	120.3(9)	C19 – C20 – C15	116.1(9)	C28 – C36 – C38	110.2(9)

C6 – C5 – C4	120.0(9)	C19 – C20 – C21	121.1(9)	C1 – N1 – C3	111.0(6)
C7 – C6 – C5	118.0(9)	C15 – C20 – C21	122.8(10)	C1 – N1 – C4	123.9(5)
C7 – C6 – Pd1	120.2(7)	C23 – C21 – C20	114.0(10)	C3 – N1 – C4	125.0(6)
C5 – C6 – Pd1	121.8(7)	C23 – C21 – C22	110.1(9)	C1 – N2 – C2	108.8(6)
C6 – C7 – C8	121.9(10)	C20 – C21 – C22	110.0(9)	C1 – N2 – C27	125.5(5)
C6 – C7 – C11	118.3(9)	C16 – C24 – C25	111.8(9)	C2 – N2 – C27	125.4(6)
C8 – C7 – C11	119.6(10)	C16 – C24 – C26	112.1(8)	C12 – N3 – C14	113.0(6)
C9 – C8 – C7	119.3(10)	C25 – C24 – C26	110.8(9)	C12 – N3 – C11	126.9(6)
C8 – C9 – C10	119.3(10)	C28 – C27 – C32	123.3(9)	C14 – N3 – C11	118.6(6)
C9 – C10 – C5	121.6(10)	C28 – C27 – N2	118.6(8)	C14 – N4 – C13	110.4(6)
N3 – C11 – C7	108.5(8)	C32 – C27 – N2	118.0(8)	C14 – N4 – C15	128.6(6)
N3 – C12 – C13	105.7(8)	C27 – C28 – C29	117.5(10)	C13 – N4 – C15	120.2(6)
C12 – C13 – N4	107.2(8)	C27 – C28 – C36	122.8(9)	C6 – Pd1 – C14	85.0(4)
N4 – C14 – N3	103.5(7)	C29 – C28 – C36	119.7(9)	C6 – Pd1 – C1	84.8(4)
N4 – C14 – Pd1	135.3(7)	C30 – C29 – C28	120.6(10)	C14 – Pd1 – C1	169.8(4)
N3 – C14 – Pd1	120.9(6)	C31 – C30 – C29	120.0(10)	C6 – Pd1 – Br1	177.7(3)
C16 – C15 – C20	123.4(9)	C30 – C31 – C32	122.3(11)	C14 – Pd1 – Br1	92.9(3)
C16 – C15 – N4	118.7(8)	C31 – C32 – C27	116.0(9)	C1 – Pd1 – Br1	97.3(3)

4.5 References

[1] W. A. Herrmann, *Angew. Chem. Int. Ed. Engl.*, **2002**, *41*, 1290
[2] W. A. Herrmann, C. Köcher, *Angew. Chem. Int. Ed. Engl.*, **1997**, *36*, 2163.
[3] M. Regitz, *Angew. Chem. Int. Ed. Engl.*, **1996**, *35*, 725.
[4] A. C. Hillier, G. A. Grasa, M. S. Viciu, H. M. Lee, C. L. Yang, S. P. Nolan, *J. Organomet. Chem.*, **2002**, *653*, 69.
[5] D. Bourissou, O. Guerret, F. P. Gabbai, G. Bertrand, *Chem. Rev.*, **2000**, *100*, 39.
[6] D. J. Cardin, B. Cetinkaya, E. Cetinkaya, M. F. Lappert, *J. Chem. Soc. Dalton. Trans.*, **1973**, *5*, 514.
[7] D. J. Cardin, B. Cetinkaya, E. Cetinkaya, M. F. Lappert, L. J. Manojlovic-Muir, K. W. Muir, *J. Organomet. Chem.*, **1972**, *44*, c59
[8] A. J. Arduengo, R. L. Harlow, M. Kline, *J. Am. Chem. Soc.*, **1991**, *113*, 361.
[9] D. Milhalios, P. W. Roesky, M. Elison, J. Fischer, G. R. J. Artus, C.-P. Reisinger, C. Kocher, M. Steinbeck, L. J. Gooben, O. Runte, T. Weskamp, J. Schwarz, V. P. W. Bohm, F. J. Kohl, M. Prinz, *Thesis filed under W.A. Herrmann*, **1992 - 2001**, *Munchen*, Technische Universistat.
[10] A. A. D. Tulloch, A. A. Danopoulos, R. P. Tooze, S. M. Cafferkey, S. Kleinhenz, M. B. Hursthouse, *Chem. Commun.*, **2000**, 1247.
[11] A. A. D. Tulloch, PhD thesis, University of Southampton (Southampton), **2001**.
[12] M. J. Green, K. J. Cavell, B. W. Skelton, A. H. White, *J. Organomet. Chem.*, **1998**, *554*, 175.
[13] D. S. McGuinness, K. J. Cavell, *Organometallics*, **2000**, *19*, 741.
[14] J. C. C. Chen, I. J. B. Lin, *Organometallics*, **2000**, *19*, 5113
[15] D. S. McGuinness, K. J. Cavell, *Organometallics*, **2000**, *19*, 4918.
[16] A. A. D. Tulloch, A. A. Danopoulos, G. J. Tizzard, S. J. Coles, M. B. Hursthouse, R. S. Hay-Motherwell, W. B. Motherwell, *Chem. Commun.*, **2001**, 1270.
[17] S. Grundemann, M. Albrecht, J. A. Loch, J. W. Faller, R. H. Crabtree, *Organometallics*, **2001**, *20*, 5485.
[18] J. A. Loch, M. Albrecht, E. Peris, J. Mata, J. W. Faller, R. H. Crabtree, *Organometallics*, **2002**, *21*, 700.
[19] D. J. Nielsen, K. J. Cavell, B. W. Skelton, A. H. White, *Inorg. Chim. Acta.*, **2002**, *327*, 116.
[20] D. J. Nielsen, A. M. Magill, B. F. Yates, K. J. Cavell, B. W. Skelton, A. H. White, *Chem. Commun.*, **2002**, 2500.
[21] A. A. Danopoulos, S. Winston, M. B. Hursthouse, *J. Chem. Soc. Dalton. Trans.*, **2002**, 3090.
[22] C. M. Hartshorn, P. J. Steel, *Organometallics*, **1998**, *17*, 3487
[23] D. S. McGuinness, N. Saendig, B. F. Yates, K. J. Cavell, *J. Am. Chem. Soc.*, **2001**, *123*, 4029.
[24] A. A. D. Tulloch, S. Winston, A. A. Danopoulos, G. Eastham, M. B. Hursthouse, *J. Chem. Soc. Dalton. Trans.*, **2003**, 699.
[25] T. A. Stephenson, S. M. Morehouse, A. R. Powell, J. P. Heffer, G. Wilkinson, *J. Chem. Soc.*, **1965**, 3632.
[26] D. Drew, J. R. Doyle, *Inorg. Synth.*, **1972**, *13*, 53.
[27] R. Rulke, J. Ernsting, A. Spek, C. Elsevier, P. V. Leeuwen, K. Vrieze, *Inorg. Chem.*, **1993**, *32*, 5769.
[28] H. L. Goering, S. S. Kantner, *J. Org. Chem.*, **1983**, *48*, 721.
[29] M. Rudler-Chauvin, H. Rudler, *J. Organomet. Chem.*, **1977**, *134*, 115.

[30] W. d. Graaf, J. Boersma, W. J. J. Smeets, A. L. Spek, G. V. Koten, *Organometallics*, **1989**, *8*, 2907

[31] H. Alper, P. Arya, S. C. Bourque, G. R. Jefferson, L. E. Manzer, *Can. J. Chem.*, **2000**, *78*, 920

Chapter 5

The Heck Reaction

Chapter 5

The Heck Reaction.

5.1 Introduction.

The development of new methodology for the formation of C-C and C-N bonds is the crux of all organic research chemistry. Many palladium complexes, especially palladium NHC complexes have proven active precatalysts in accelerating these bonds creation.[1, 2]

As briefly described in the Chapter 1 the Mizoroki or Heck reaction[3, 4] is the process of coupling alkyl or more widely used aryl halides with terminal alkenes, as shown below.

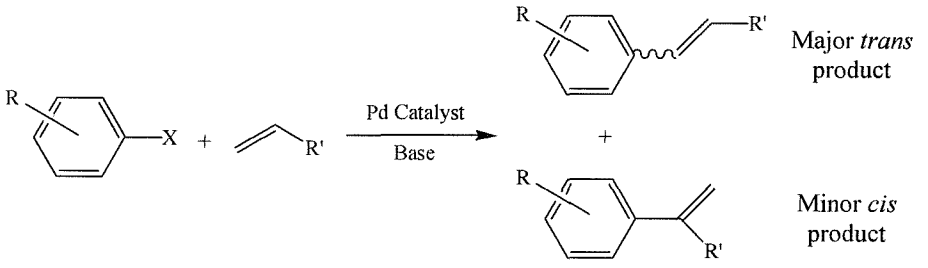

Fig 5.1 The Heck Reaction, R = halide, R' = alkyl, aryl.

The scope for coupling a wide variety of monomers (limited at the moment to non-β-hydrogen containing species) not only by the Heck reaction, but also by other closely related coupling processes, for example Suzuki (boronic acids),[5] Kumada (Grignard reagents),[6] Sonogashira (alkynes),[7] and Stille (tin reagents) couplings[8] has driven incredible volumes of research into palladium based precatalysts.[2, 9-11] The interest in the use of the cheaper aryl chlorides has been hindered by the low activity of palladium catalysts towards aryl chlorides. This has been attributed to the strength of the C-Cl bond (bond dissociation energy 96 kcal mol^{-1}) whereas the weaker bonded but more expensive bromides (81 kcal mol^{-1}) and iodides (65 kcal mol^{-1}) are more readily coupled.[12] This reluctance for aryl chlorides to add oxidatively to Pd(0) centres, the common initial step in palladium catalysed reactions, means that ligand tuning effects must facilitate this process.[2]

Heck catalysis can be performed either homogeneously using complexes such as palladium acetate, or heterogeneously using polymer-supported palladium complexes or palladium

supported on inorganic oxides. Heterogeneous Heck coupling has been recently reviewed and will not be discussed here.[10]

Early work into the homogeneous Heck reaction was held back by the problem of catalyst lifetime, palladium black rapidly precipitated from active systems. This was overcome when it was realised that the addition of an excess of trialkylphosphine to the system stabilised the resting catalyst state and greatly lengthened lifetimes.[13] Later it was shown that use of $P(^tBu)_3$, enabled the coupling of the less reactive aryl chlorides, but industrial attraction was low due to the necessity for an inert environment to use this phosphine.[14] Other σ-donating trialkylphosphines provided highly electron rich, underligated, metal centres capable of activating the C-Cl bond. Interest in moving away from the more classical and highly productive approach of using trialkylphosphines as supporting ligands came from the possible economical and chemical benefits. Good excess of unrecoverable toxic phosphine ligands are required to support active palladium species, which when scaled up to industrial processing quantities means the expense of the unrecoverable excess ligand may at least equal the cost of the recyclable palladium being used. Phosphines can also fully ligate the coordination sphere of palladium giving $Pd(L)_3$ or $Pd(L)_4$ species which causes partial deactivation and reduces activity. In order to avoid this high catalyst loadings are required to maintain activity, again increasing costs. In light of this, shortly after the discovery of the stable *N*-heterocyclic carbene the first Heck active NHC palladium precatalyst complexes were reported by Herrmann (Fig 5.2).[15] These new NHC complexes had equally high activity in the Heck reaction as the phosphine supported catalysts but proved to have higher thermal stability, be stable to oxygen and stoichiometric amounts of ligands can be used rather than a large excess.

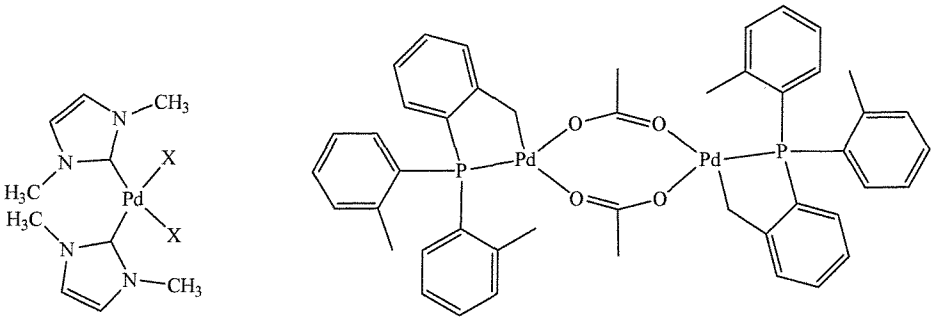

Fig 5.2 The first Heck active NHC precatalyst (left) Hermann's palladacycle (right). X = halide.

Reports of palladacycles further increased catalytic lifetimes and systems that were active for millions of turnovers were described,[16, 17] the most successful palladacycle being $Pd_2[P(o-$

tol)$_3$]$_2$(μ-OAc)$_2$ reported by Herrmann[18] (Herrmann's catalyst, Fig 5.2). These catalysts had the added advantage of being recyclable, extremely easy to handle and active for a variety of different coupling reactions

The turnover number (TON) and turnover frequency (TOF) are the universally applied measure of activity. One turnover is classed as the coupling of one pair of monomers by a single catalytic molecule, calculated by moles of product per mole of catalyst (TON) or moles of product per mole of catalyst per hour (TOF). This measurement can be misleading however as it assumes that 100% of the precatalyst applied is active which is often not the case.

Many different ligand systems have been explored to compete with the activities of the phosphine-based systems, many still incorporate a phosphine donor or derivative. Notably Milstein's,[19] Shibasaki's[17] and later Jensen's[20] reports of tridentate phosphine and phosphite 'pincer' palladium systems (Fig 5.3) showed high activity for the Heck coupling of aryl chlorides.

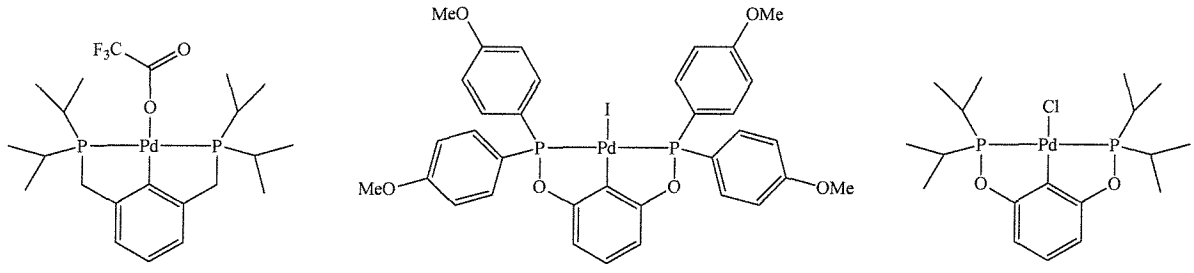

Milstein's Precatalyst | Shibasaki's Precatalyst | Jensen's Precatalyst

Fig 5.3 Phosphine derived palladium precatalysts.

Since Herrmann's disclosure of the first active palladium NHC precatalyst other NHC based systems have been reported mimicking ligand architectures of known phosphine systems as shown in this report and the literature allowing direct comparison of activity to be drawn between the phosphines and NHCs as supports for Heck coupling.[11, 21-25]

5.2 Mechanism of the Heck Reaction

One of the most debated points around the Heck Reaction is that of the mechanism, how can so many differently architectured precatalysts all showing high activities with a wide variety of substrates still be operating with the same mechanism? Heck proposed a widely favoured mechanism involving a Pd(II)/Pd(0) pathway[4] with an activation step being required before the catalytic cycle can begin, Shaw however suggested that a Pd(II)/Pd(IV) pathway[26] is also plausible with certain ligands (palladacycle) which had been recently supported by Jensen.[20]

Fig 5.4 depicts the popular Pd(II)/Pd(0) mechanism which consists of several independent steps. The first is the generation of a palladium(0) species, which can be performed by reducing a palladium(II) precursor or by starting with a palladium(0) species. The active palladium then undergoes oxidative addition of an aryl halide, simultaneously rupturing the organic bond and forming two new metal ligand bonds. Once this has occurred an alkene substrate must coordinate to the palladium. Depending on the nature of the supporting ligands a vacant site will have to be created before this occurs, so hemilabile ligands are preferable. After coordination a concerted migratory insertion of the aryl group takes place and this is rapidly followed by a β-hydride elimination, generating the double bond and forming the product. Dissociation then occurs leaving a palladium hydride species that is scavenged by base reductively eliminating HX to regenerate the initial palladium(0) species.

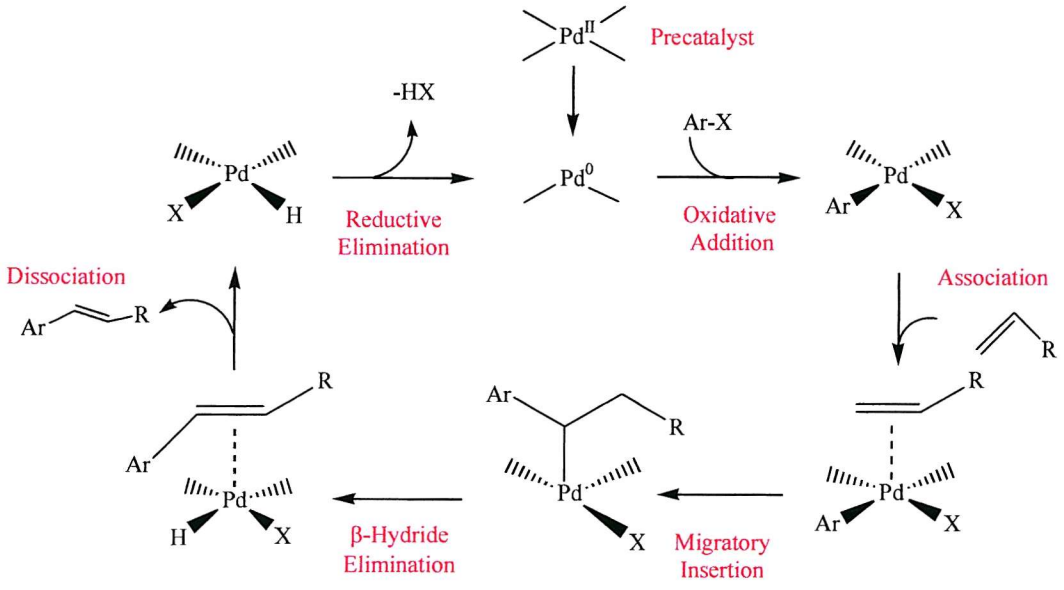

Fig 5.4 General Pd(II)/Pd(0) Heck pathway.

Many catalyst systems report an induction period before any activity is observed, which supports this mechanism as for certain systems the reduction to a zero oxidation state may not be facile. This induction period can be shortened by the addition of reducing agents.[15] Recently in related work by Cloke and co-workers a palladium (0) bis-NHC complex that had oxidatively added 4-chlorotoluene was isolated and structurally characterised, the first step of the Pd(II)/Pd(0) pathway adding further weight to the argument supporting this mechanism.[27]

The second pathway, a Pd(II)/Pd(IV) mechanism,[20] as proposed by Jensen has a very different route as shown in Fig 5.5.

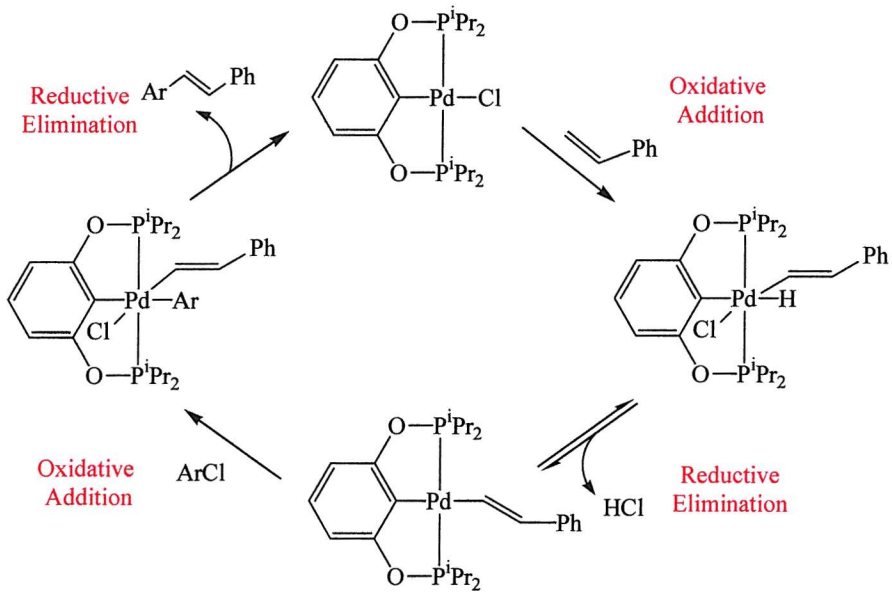

Fig 5.5 Proposed Pd(II)/Pd(IV) Heck pathway.

Due to the nature of the ligand system it is proposed that it would not be viable for an aryl chloride to oxidatively add as the initial step as this would generate a highly stable 18 electron species which would then not continue to participate in a coupling reaction. Therefore firstly an oxidative addition of the vinyl C-H to the palladium, which then undergoes a reductive elimination of HCl is proposed. A second oxidative addition of the aryl halide then occurs and reductive elimination of the product regenerates the Pd (II) catalyst. In these systems an induction period was not observed.

These two mechanisms represent only two possibilities for homogeneous Heck catalysts and do not allow for a heterogeneous system based on a colloidal metal species or any suggestion of how systems such as palladium on carbon might operate. All that is clear is that there is no single mechanism for the Heck reaction; each class of catalyst that actively couples aryl

halides to terminal alkenes must, to an extent, have its own mode of operation. A recent review concluded that even heterogeneous precatalysts can become homogeneous whilst active through metal leeching from the inorganic supports, casting more doubts on the mechanism of the Heck reaction.[10]

As mentioned in Chapter 1 it has recently been reported by Cavell and co-workers that a facile decomposition route exists (Fig 5.6) through which active palladium complexes can pass.[28-30] Further work into this process has shown that the decomposition occurs when an active species is held at elevated temperatures in the resting state, ie at completion of a catalytic run. This has clear implications for uses of carbenes as living catalysts.

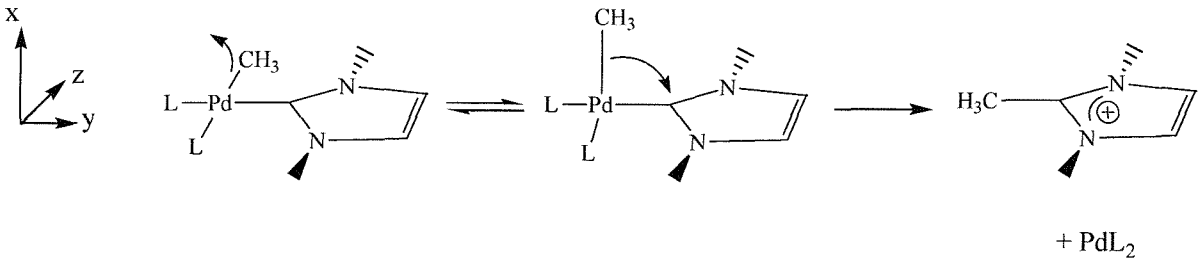

Fig 5.6 Decomposition route for NHCs.

By examining Fig 5.6 it can be seen that for this decomposition route to occur the square planar palladium complex must allow a small alkyl group to first rotate through 90° to get into a position such as a migration from the palladium to imidazol-2-ylidene can take place due to overlap of the out-of-plane p_x-orbital with the metal d-orbitals. It has been shown by Cavell that two different processes can heavily retard this process; the first having bulky substituents on the heterocyclic nitrogens or having the imidazol-2-ylidene placed into a chelating system, both methods physically stopping the flexibility of the coordinated ligands to get into the required position to undergo the reductive elimination

This chapter describes the observed Heck activity for some of the palladium complexes synthesised in this project and compares the effect of electronic and structural variation between these and previously prepared complexes on C-C coupling activity.

5.3 Results and Discussion

Catalytic testing of the previously prepared complexes **A**, **B** and **C**, Fig 5.7, showed that pyridine functionalised NHC Pd(II) complexes are highly active precursors for the Heck coupling of aryl iodides and activated aryl bromides with activated alkenes.[31] Both mono- and bis-carbene pyridine systems show excellent coupling activity for the bidentate ligand systems. The presence of a methylene linker between the pyridine and heterocyclic ring (**B**) was observed to alter initial reaction rates, with more favourable activity coming from the larger 6-membered chelating ligand. This behaviour was not observed for the tridentate ligands but high activities were maintained.[31]

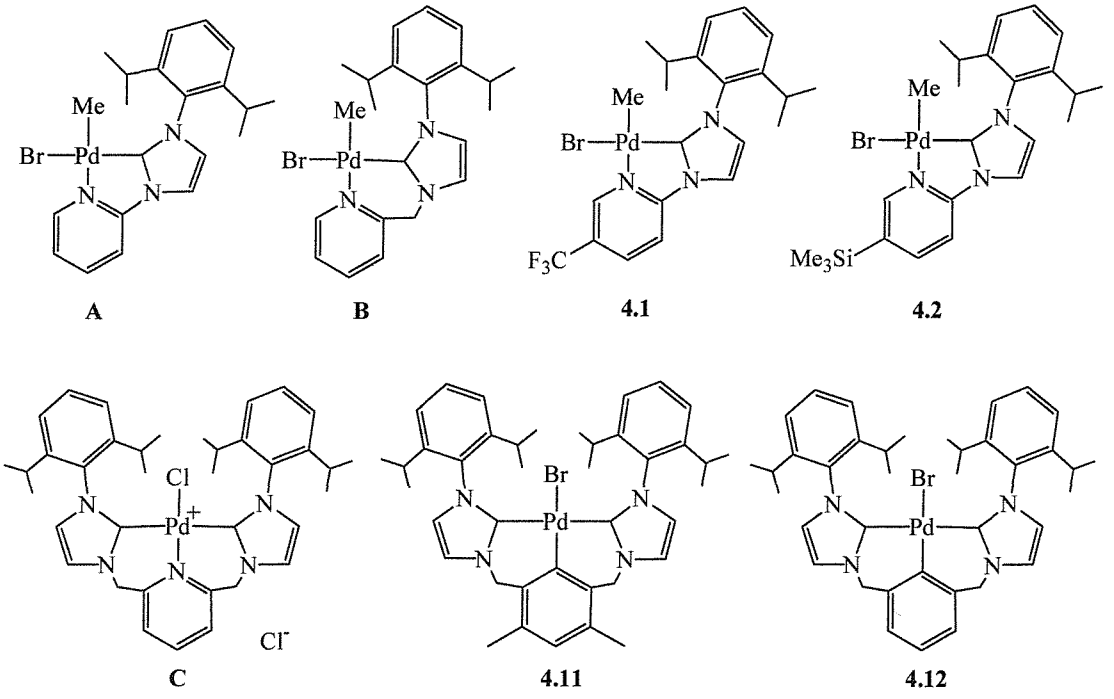

Fig 5.7 Compounds used in Heck catalytic comparison.

With the previous knowledge that these types of compounds are extremely active Heck precursors the functionalisation of the pyridine ring in complexes **4.1** and **4.2** would allow the study of the presence of an electron-withdrawing group (complex **4.1**) or additional structural bulk (complex **4.2**) on catalytic activity. The larger tridentate complexes **4.11** and **4.12** where the pyridine has been exchanged for a cyclometallated aryl group would test the difference of placing a more rigid donor that is unable to disassociate from the metal, into the ligand backbone.

The previously used reaction medium of *N*-methylpyrrolidone (NMP) was used for all catalytic runs as trials in 1,4-dioxane and *N*,*N*-dimethylacetamide (DMAc) showed slightly less activity. Similarly the base triethylamine was exclusively used for all of the following experiments after tests with sodium carbonate, potassium phosphate and sodium acetate did not improve results.

Due to the nature of the procedures, to maximise the reproducibility of results each reaction was completed in duplicate and where possible triplicate, with two independent runs carried out for each test to ensure reproducibility; averaged results are included here. No reducing agents were employed to drive the oxidation state of palladium from two to zero as they proved unnecessary; in contrast to trialkylphosphine based systems no induction period was observed. Due to the rigorous procedures being utilized to ensure reproducibility, substrates that were liquids at room temperature were favoured for the work to allow more rapid catalytic testing as all measurements could be carried out using gas-tight syringes. Catalyst amounts were accurately measured to within 0.05 of a milligram and used from freshly prepared stock solutions in NMP, which were diluted to the required concentration. It was noted that a stock solution left for 6 - 7 days would begin to lose activity and after four weeks had lost over 60% of catalytic activity. The inert GC standard di(ethyleneglycol)dibutylether was added before the reaction.

5.3.1 Activity of Mono-Carbene Supported Precatalysts.

Initial activity testing of compounds **4.1**, **4.2**, **4.11** and **4.12** is detailed in the following table. The complexes were tested with 4-bromoacetophenone coupled with methylacrylate at 140°C.

Table 5.1 Catalytic reactions with bidentate supported precatalysts.

Complex	Conc. (mol)	Loading (mol%)	Solvent	Base	Time (hr)	TON	Yield (%)
4.1	1.0×10^{-5}	0.2	NMP	NEt_3	18	500	100
4.1	1.0×10^{-7}	0.002	NMP	NEt_3	18	35,289	71
4.1	1.0×10^{-9}	0.00002	NMP	NEt_3	18	3,087,723	62
4.2	1.0×10^{-7}	0.002	NMP	NEt_3	18	38,319	76
4.2	1.0×10^{-9}	0.00002	NMP	NEt_3	18	3,411,780	68
A	1.0×10^{-7}	0.002	NMP	NEt_3	18	27,850	55
B	1.0×10^{-7}	0.002	NMP	NEt_3	18	32,421	65

The results for **4.1** and **4.2** in Table 5.1 show excellent activities. In normal organometallic complex catalysed reactions catalyst loadings are in the range of 0.1 – 1.0 mol% of the substrates. In these reactions loadings as low as 0.00002 mol% were producing extremely high activities within 18 hours giving turnovers in the millions. Two general conclusions can be drawn from these results; firstly that the mono-carbene complexes show very high activities for coupling of activated aryl bromides; secondly moderate activity (50 – 60% yield in 18 hours) is maintained with the reduction in volume of catalyst of up to 1000 fold. By comparing the activity of the functionalised **4.1** and **4.2** to the previously studied **A** and **B** there is no appreciable difference in activity observed after 18 hrs with 0.002 mol% of catalyst.

Very poor yields were only observed when the catalyst concentration was dropped further to 2×10^{-7} mol%. This could be explained by the incredibly small amount of catalyst experiencing problems with decomposition that a higher concentration of catalyst can withstand without significant loss of activity. Catalytic activity was still observed when temperatures were dropped from 140°C to 100°C but the levels of activity reduced by almost half.

The GC traces indicate there are two products produced from the reactions, in ratio between 95:5 to 99:1 which when characterised by NMR shows the major peak to be the desired *trans*-alkene product and the lesser peak to be the *cis*-alkene. These ratios were similar to those observed by others studying the Heck reaction with NHCs.[11] There is no evidence of the bis-aryl species.

Further testing at low concentrations (2×10^{-5} mol%) of coupling with bromobenzene led comparatively to very low activity over 18 hrs of reaction, yielding only between 1 and 3%. Experiments with activated aryl chlorides had slightly improved results but only yielded a maximum of 5 - 8% product in 18 hrs at low concentration.

It had been observed during initial testing that the bulk of activity was during the initial two hours of any given run, with it accordingly tailing off as the concentrations of coupling substrates reduced due to product formation. Regardless of the catalyst concentration all experiments with activated aryl bromides would reach completion within 24 – 30 hours even for the lowest concentration of catalyst, most completing in 6 – 8 hours. As has been

described no appreciable difference in overall activity between the complexes had been detected which insinuates that the supporting ligand does not affect overall activity. To observe the differences in structure on activity, instead of continuing testing the catalysts at higher concentrations with a wider variety of halide and alkene substrates as had been previously done,[31] more focus was placed on studying the effect of the structural variations on initial activity, as no induction period was being observed for these complexes.[11]

By making use of the moderate activity at low concentrations it was possible to study the initial activity over a four-hour period by using a catalyst concentration that would allow good yield of product in this time period but not completion, i.e. 2 x 10^{-5} mol%. Reaction sampling was carried out at constant intervals over a four-hour period and from this a graph of yield against time was constructed and different ligands were directly compared for activity. Continuous sampling from one-pot was not the chosen method to acquire data as it was observed that results from this technique with the available equipment were not reproducible. Instead data was collected by simultaneously starting 12 – 15 independent runs in sealed Rotaflow ampoules and terminating a batch of 2 - 3 reactions at a given time point. Experiments were carried out at 140°C in NMP as before with similar volumes of substrates and each catalyst was run three times to ensure the reproducibility of the results.

The graph depicted in Fig 5.8 is a comparison between the activity of **4.1**, **4.2**, **A** and **B**. Interestingly it is observed that although in the previous tests that show all of the catalysts have the same general catalytic activity, under scrutiny of the initial coupling activity, complex **4.1** is considerably more active.

Initial results from studying these catalyst systems at the ESRF synchrotron source in Grenoble has shown that the catalytic species is not colloidal palladium in solution and that the pyridine dissociates rapidly and is replaced by NMP.[32] It was also observed that only a small percentage of the catalyst was activated during the catalytic run, most remained as Pd(II), which hindered further data collection.[32]

As the pyridine has been observed to 'dangle' in active catalytic species, the presence of the electron-withdrawing CF_3 may allow a more rapid dissociation of the pyridine from the palladium, reducing time in the resting state, increasing activity. It was noted that certain phosphines could retard activity by binding too strongly to the resting palladium causing

problems in reactivation. Whether this extra electron-withdrawing group is enough to cause an increase in activity due to this reasons is hard to confirm without further study.

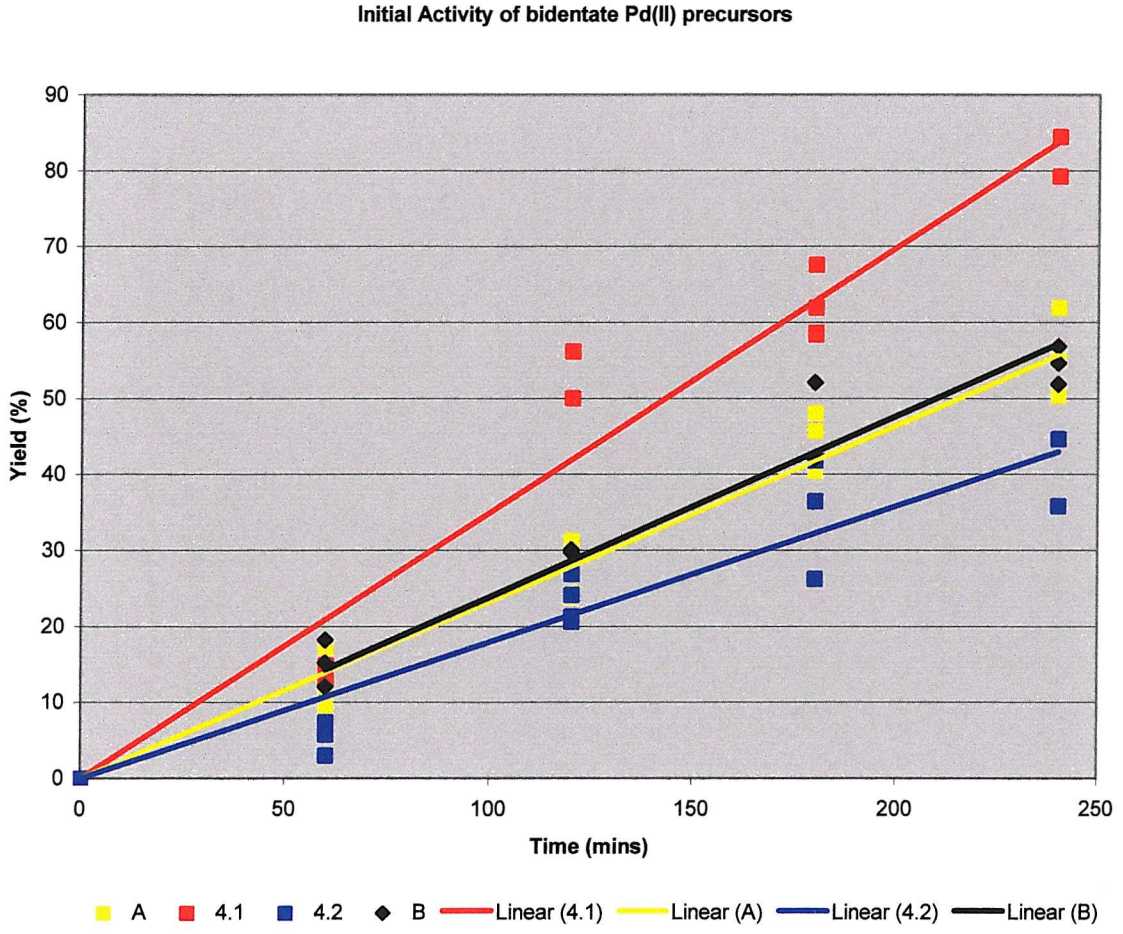

Fig 5.8 Comparative activities of bidentate ligands on catalytic activity.

Attempts to carry out competitive catalysis between **A**, **B** and **4.1** was unfortunately hampered by the incredible complexity of the GC-traces of the products. The procedures were carried out by taking a fixed amount of alkene substrate (1.0 mmol) and to this adding not one aryl halide, but a variety of four substrates, in this case 4-bromoacetophenone, 4-bromoanisole, 4-bromotoluene and bromobenzene in equal excess (5 mmol each). These different substrates have varied electronic differences reflecting activation of the aryl bromide bond, 4-bromoacetophenone being the most activated. The catalyst could preferentially couple one of the products due to these differences in bond activation, which might give some insight to a possible mechanism. Problems arose when trying to analyse the products from these reactions, peaks in the GC and GCMS chromatograms allowed for

recognition of the multiple products but the peaks could not be resolved to a sufficient quality to allow quantitative analysis.

Experiments to test whether these bidentate systems undergo decomposition on completion of reaction as described by Cavell were carried out at a simple level by examining if the complexes display any 'living' behaviour. At the end of a catalytic experiment for all complexes no sign of palladium black was observed at any level of catalyst concentration, suggesting no decomposition had occurred. When taking complex **4.1** and **4.12** at 0.002 mol% concentration in NMP with 4-bromoacetophenone and methylacrylate and running the reaction for 24 hours, allowing completion (monitored by GC), and then adding additional substrates to the reaction mixture, the catalyst continued to produce product. This behaviour is not uncommon for these types of Heck precursor and, as observed by Cavell, the decomposition does not occur with bulky and chelating ligands.

5.3.2 Activity of Bis-Carbene Supported Precataiysts.

A similar study of comparing the effect of a potentially labile nitrogen donor (complex **C**) versus a cyclometallated aryl group (complexes **4.11** and **4.12**) was undertaken for the tridentate complexes. It is important to note that in these complexes for the central linkage to become hemilabile it would require dissociation of an imidazol-2-ylidene to break the rigid chelation holding the linker group in place. For this type of ligand architecture previous work has shown that variation of the bulky aryl group substituents did alter Heck activity to a significant extent, substitution of a mesityl group had increased activity over a 2,6-di-*iso*-propylphenyl ring, presumable due to less steric congestion around the active site. The presence of a methylene linkage increasing the chelating ring-size from 5 to 6 had little to no effect on activity unlike with the bidentate ligands.[31] In general the tridentate pyridine based complexes showed higher activity for the coupling of aryl chlorides than the bidentate complexes. This study tests the effect (if any) of the central linking group between the NHC donors. Complex **C** contains an unsubstituted pyridine ring, complex **4.11** has an aryl group with increased electron density due to the dimethyl substitution and **4.12** has an unsubstituted aromatic ring.

Table 5.2 Catalytic reactions with tridentate supported precatalysts, 140°C, methylacrylate, 4-bromoacetophenone.

Catalyst	Conc. (mol)	Loading (mol%)	Solvent	Base	Time (hr)	TON	Yield (%)
4.11	1.0×10^{-5}	0.2	NMP	NEt_3	18	294	100
4.11	1.0×10^{-7}	0.002	NMP	NEt_3	18	16730	57
4.11	1.0×10^{-9}	0.00002	NMP	NEt_3	18	1,564,906	53
4.12	1.0×10^{-5}	0.2	NMP	NEt_3	18	294	100
4.12	1.0×10^{-7}	0.002	NMP	NEt_3	18	16273	55
4.12	1.0×10^{-9}	0.00002	NMP	NEt_3	18	1,786,680	61
C	1.0×10^{-7}	0.002	NMP	NEt_3	18	16301	55

Comparison of **C** to **4.11** and **4.12** when coupling activated aryl bromides to methyl acrylate shows no significant difference in activity between the two different ligand types, all three catalyst precursors show very high TON's. The presence of methyl substituents on the cyclometallated aryl ring slightly reduces the activity of the complex, the additional electron density these provide appear to slightly hinder activity. Attempted coupling of bromobenzene and methyl acrylate using **4.11** and **4.12** again yielded poor results at low catalyst loadings as with the bidentate supporting ligands. More success was seen with coupling of the activated chloride, 4-chloroacetophenone. With the mono-carbene supported centres very low TON's were observed, but for the bis-carbene species this was slightly increased to 10 – 12% yield in four hours, but two product peaks were observed in the GC traces, in a ratio of 2:1 in favour of the *trans*-isomer, which is still very poor when compared with the bromides. Others studying related precatalysts have reported that these cyclometallated catalysts are active for chloride substrates but longer reaction times (19 hrs) were required to get a 70% yield at 0.2 mol% catalyst loadings.[33]

The investigation into initial 4 hr coupling activity of **4.11**, **4.12** and **C** at low concentrations as completed with the bidentate supported ligands did not show any significant difference in the activity between pyridine chelating compounds and the cyclometallated species. A slight increase in activity was observed for the cyclometallated species but this was not of a sufficient enough increase to substantiate definite increased activity above associated experimental errors for this procedure.

5.4 Conclusions

The newly prepared complexes tested as catalysts for Heck reactions show excellent activities for the coupling of aryl bromides, as expected from previous work with their analogues. The low loadings of catalyst used for these reactions would make these complexes ideal for industrial use, as the reduced volumes of catalyst may balance the price of using bromide substrates over chlorides.

For the bidentate supported complexes the presence of a highly electron–withdrawing group dramatically increases initial coupling activity having a larger effect than increasing chelate ring size or adding steric bulk. This could be due to electron withdrawal assisting pyridine dissociation, reducing the catalysts resting time.

For the tridentate supported complexes the exchange of the pyridine functional group with a cyclometallated aryl group linking the two *N*-heterocyclic rings does not have a substantial effect on the coupling of activated bromides. The tridentate supported systems show increased activity over the bidentate systems for the coupling of activated aryl chlorides, but further study is required to optimise conditions for this coupling which shows only low activity at the desired catalyst loading levels.[31]

From these and previous studies it is clear that different ligand systems are required for the coupling of different substrates and that one ligand system is not universally employable under 'standard' conditions that will cover an infinite variety of substrates – the goal of all catalysts.

5.5 Experimental Section.

In a typical run, a Rotaflo ampoule (50 cm^3) was charged with the corresponding aryl halide (5 mmol), alkene (6 mmol), base (7 mmol), internal standard (500 µl) and solvent (5 cm^3). A solution of the catalyst in solvent (1 cm^3) was added to the reaction mixture, the vessel placed under a partial vacuum before being sealed and rapidly heated to reaction temperature. After the desired time the reaction mixture was rapidly cooled to room temperature and quenched with water (2 cm^3) and products extracted into dichloromethane (5 cm^3). The organic layer was analysed by gas chromatography.

So an example run is, a 50ml Rotoflo ampoule was charged with 4-bromoacetophenone (995µl, 5 mmol), methylacrylate (622 µl, 6 mmol), triethylamine (1066 µl, 7 mmol), di(ethyleneglycol)dibutylether (500 µl) and N-methylpyrrolidone (5 cm^3). A solution of **4.1** (1 x 10^{-9} mol) in *N*-methylpyrrolidone (1 cm^3) was added to the reaction mixture, the vessel placed under partial vacuum and rapidly heated to 140°C. After 18 hours, the reaction mixture was rapidly cooled to room temperature, quenched with water (2 cm^3) and products extracted into dichloromethane (5 cm^3). The organic layer was analysed by gas chromatography.

GC and Analyzer: Varian 3400 fitted with Varian 1200 Autosampler and using a 30m Megabore column with Hewlett Packard 1600 Integrator/Detector, column program: 5 mins at 100°C then ramp to 220°C at 20°/min and hold at 220°C for 4 mins. Column max. 250 °C.

5.6 References

[1] W. A. Herrmann, *Applied Homogeneous Catalysis with Organometallic Compounds*, Wiley-VCH, Weinheim, **2000**.
[2] A. C. Hillier, G. A. Grasa, M. S. Viciu, H. M. Lee, C. L. Yang, S. P. Nolan, *J. Organomet. Chem.*, **2002**, *653*, 69.
[3] T. Mizoroki, K. Mori, A. Ozaki, *Bull. Chem. Soc. Jpn.*, **1971**, *44*, 581.
[4] R. F. Heck, J. P. Nolley, *J. Org. Chem.*, **1972**, *37*, 2320.
[5] N. Miyaura, A. Suzuki, *Chem. Rev.*, **1995**, *95*, 2457.
[6] K. Tamao, K. Sumitani, M. Kumada, *J. Am. Chem. Soc.*, **1972**, *94*, 4374.
[7] K. Sonogashira, Y. Tohda, N. Hagihara, *Tetrahedron Lett.*, **1975**, 4467.
[8] J. K. Stille, *Angew. Chem. Int. Ed. Engl.*, **1986**, *25*, 508.
[9] A. F. Littke, G. C. Fu, *Angew. Chem. Int. Ed. Engl.*, **2002**, *41*, 4176.
[10] A. Biffis, M. Zecca, M. Basato, *J. Mol. Catal. A - Chem.*, **2001**, *173*, 249.
[11] I. P. Beletskaya, A. V. Cheprakov, *Chem. Rev.*, **2000**, *100*, 3009.
[12] V. V. Grushin, H. Alper, *Chem. Rev.*, **1994**, *94*, 1047
[13] H. A. Dieck, R. F. Heck, *J. Am. Chem. Soc.*, **1974**, *96*, 1133.
[14] A. F. Littke, G. C. Fu, *J. Org. Chem.*, **1999**, *64*, 10.
[15] W. A. Herrmann, M. Elison, J. Fischer, C. Köcher, G. R. J. Artus, *Angew. Chem. Int. Ed. Engl.*, **1995**, *34*, 2371.
[16] M. Ohff, A. Ohff, D. Milstein, *Chem. Commun.*, **1999**, 357.
[17] F. Miyazaki, K. Yamaguchi, M. Shibasaki, *Tetrahedron Lett.*, **1999**, *40*, 7379.
[18] W. A. Herrmann, C. Brossmer, K. Ofele, C.-P. Reisinger, T. Priermeier, M. Beller, H. Fischer, *Angew. Chem. Int. Ed. Engl.*, **1995**, *34*, 1844.
[19] M. Ohff, A. Ohff, M. E. v. D. Boom, D. Milstein, *J. Am. Chem. Soc.*, **1997**, *119*, 11687.
[20] D. Morales-Morales, R. Redon, C. Yung, C. M. Jensen, *Chem. Commun.*, **2000**, 1619.
[21] W. A. Herrmann, *Angew. Chem. Int. Ed. Engl.*, **2002**, *41*, 1290
[22] J. A. Loch, M. Albrecht, E. Peris, J. Mata, J. W. Faller, R. H. Crabtree, *Organometallics*, **2002**, *21*, 700.
[23] A. A. D. Tulloch, A. A. Danopoulos, G. J. Tizzard, S. J. Coles, M. B. Hursthouse, R. S. Hay-Motherwell, W. B. Motherwell, *Chem. Commun.*, **2001**, 1270.
[24] D. J. Nielsen, K. J. Cavell, B. W. Skelton, A. H. White, *Inorg. Chim. Acta.*, **2002**, *327*, 116.
[25] W. A. Herrmann, V. P. W. Bohm, C. W. K. Gstottmayr, M. Grosche, C. P. Reisinger, T. Weskamp, *J. Organomet. Chem.*, **2001**, *617*, 616.
[26] B. L. Shaw, S. D. Perera, E. A. Staley, *Chem. Commun.*, **1998**, 1361.
[27] S. Caddick, F. G. N. Cloke, P. B. Hitchcock, J. Leonard, A. K. d. K. Lewis, D. McKerrecher, L. R. Titcomb, *Organometallics*, **2002**, *21*, 4318
[28] D. J. Nielsen, A. M. Magill, B. F. Yates, K. J. Cavell, B. W. Skelton, A. H. White, *Chem. Commun.*, **2002**, 2500.
[29] D. S. McGuinness, N. Saendig, B. F. Yates, K. J. Cavell, *J. Am. Chem. Soc.*, **2001**, *123*, 4029.
[30] D. S. McGuinness, K. J. Cavell, *Organometallics*, **2000**, *19*, 4918.
[31] A. A. D. Tulloch, PhD thesis, University of Southampton (Southampton), **2001**.
[32] S. G. Fiddy, Personnal Communication, **2002**.
[33] S. Grundemann, M. Albrecht, J. A. Loch, J. W. Faller, R. H. Crabtree, *Organometallics*, **2001**, *20*, 5485.

Chapter 6

N-Heterocyclic Carbene Complexes of Nickel

Chapter 6

N-Heterocyclic Carbene Complexes of Nickel.

6.1 Introduction.

With the ever-growing volumes of evidence that palladium NHC complexes make strong precatalysts for use in C-C coupling reactions[1, 2] the search for superior analogues of these complexes begins to take form. Aside from making ligand derivatisations the next step is to examine the other metals in Group 10 and their abilities to host NHCs and test their catalytic activity.

The use of platinum has similar restraints to palladium, mainly the cost. Platinum(II) chloride (98% purity) retails at £54 per gram and palladium(II) chloride (98% purity) is only slightly cheaper at £44 per gram, however, this is not the case for nickel as nickel(II) chloride (98% purity) costs only £0.39 per gram, which is over 100 times cheaper.[3] In addition platinum(II) and (0) complexes also show good stability once formed so generally will not proceed into a catalytic cycle due to this stability.

The cost of coupling substrates also has its part to play. In a typical coupling reaction alkyl/aryl halides are used and by comparing prices, 4-iodoacetophenone costs approx. £150 per litre, 4-bromoacetophenone £25 per litre and 4-chloroacetophenone just £10 per litre.[3] It is clearly more economical to use chlorinated analogues.

It is has been observed that Pd(0) complexes have difficulties in activating the carbon-chlorine bond[4] in catalytic cycles involving oxidative addition, but the organic chlorides are the most attractive, from an economical point of view, for industrial applications. Nickel catalysts do not suffer this same problem[4] and so to this end nickel is traditionally the first metal turned to in group 10 when making analogues of palladium precatalysts. Nickel catalysts are known to be active in polymerisation reactions as well as C-C coupling reactions.[5-7]

After Lappert first reported nickel NHC complexes,[8, 9] it was much later in 1992 that Sellman fully characterised sulphur bridged nickel imidazolin-2-ylidene complexes.[10]

Hermann reported structures of mono- and bis-imidazol-2-ylidene nickel carbonyl complexes.[11] Later Arduengo described the first Ni(0) complex containing the bis-Imes ligand.[12] Since these early reports only few NHC complexes of nickel have been described[12-14] considering the wealth of research in the area of NHC transition metal chemistry.[15-18] These have included a chiral bis imidazol-2-ylidene chelate Ni(II) complex[19] (Fig 6.1) and simpler bis-carbene chelates.[20, 21]

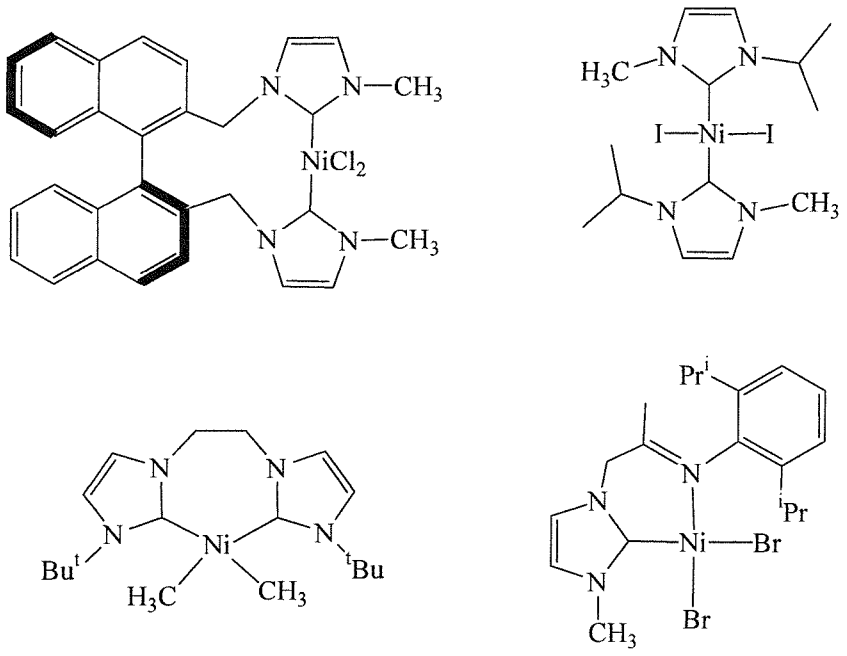

Fig 6.1 Chiral Ni(II) NHC complex (top left), chelating Ni(II) NHC dimethyl complex (bottom left), Cavell's active Ni(II) precatalyst (top right), patented ethylene precatalyst (bottom left).

Nickel imidazol-2-ylidene complexes (Fig 6.1, top right) have been studied as catalysts in butadiene dimerisation in imidazolium salt based ionic liquids. They are twice as active as the trialkylphosphine analogue $Ni(PCy_3)_2I_2$ which was tested for comparison.[22] Imine functionalised imidazol-2-ylidene complexes have also recently been patented as ethylene polymerisation catalysts.[23]

This chapter describes novel pyridine and picolyl functionalised imidazol-2-ylidene complexes of nickel, the only other known picolyl functionalised imidazol-2-ylidene nickel complex was described previously by us.[24]

6.2 Results and Discussion

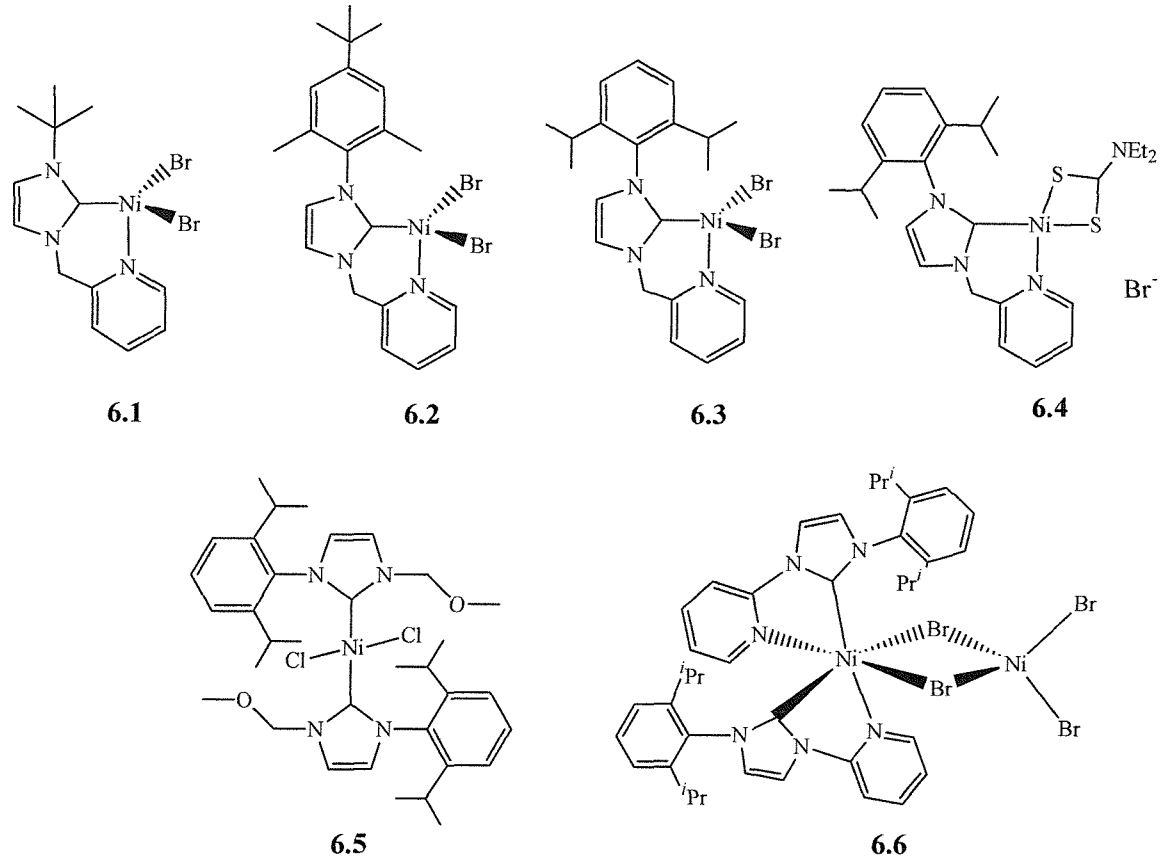

Fig 6.2 Nickel (II) imidazol-2-ylidene complexes prepared.

Compounds **6.1** – **6.3** are analogous to a complex previously prepared[24] and were synthesised with the intention to study the effect of the aryl/alkyl nature on the catalytic activity in C-C forming reactions. The halide substituted **6.4** was formed during attempts to derivatise complexes of type **6.1** – **6.3**. Compound **6.5** was synthesised in order to study the effect of the nature of the heteroatom donor on the structure adopted. The unusual mixed geometry complex **6.6** was isolated after attempting to introduce a ligand with a smaller bite angle.

6.2.1 Synthesis of Nickel (II) Complexes

The nickel(II) complexes shown in Fig 6.2 were all prepared from the same nickel(II) precursor, nickel dibromide dimethoxyethane (DME). The use of the labile DME allows easy substitution by the imidazol-2-ylidene or other classical donors.

The synthesis was based on the methodology using the silver(I) imidazol-2-ylidene complexes as transfer reagents to nickel (Fig 6.3), as had been successfully employed with the Pd(II) complexes in chapter 4 and previous work.[24]

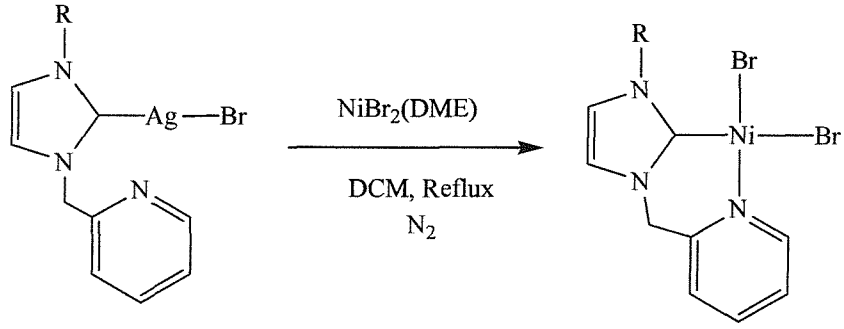

Fig 6.3 Synthesis of Ni(II) complexes. R = *tert*-butyl, 2,6-di-*iso*-propylphenyl or 2,6-dimethyl-4-*tert*-butylphenyl.

Unlike the mono-carbene palladium (II) complexes the formation of the analogous nickel complexes was not straightforward. Decomposition of the nickel-NHC complexes in air was noted if they were left standing over the period of 7 – 10 days, or in wet solvents within 30 – 40 hours possibly due to the weaker nickel carbene bond. This meant that unlike for the palladium complexes there was reduction in the driving force of the transfer from the silver to nickel.

For compounds **6.1** – **6.3** the addition of one equivalent of the precursor silver carbene complex to $Ni(DME)Br_2$ in refluxing dichloromethane afforded the nickel(II) mono-carbene complex in only low yields (15 - 25%). Crystalline product from this reaction was obtained directly from the crude reaction mixture, as on cooling the purple reaction mixture, purple crystals instantaneously formed in the silver deposits. Redissolving the complex and filtering whilst hot through an oven dried frit allowed the isolation of the pure nickel complex. Recrystallisation from dichloromethane gave X-ray quality crystals.

Unlike the palladium complexes, very poor yields were observed for these reactions even when refluxing the dichloromethane. Increasing the yield of product by changing the reaction solvent to the higher boiling 1,2-dichloroethane was successful, as observed with the silver 'pincer' carbene complexes. After 3 – 4 hours of refluxing, a purple solution had formed with substantial silver deposit. Subsequent filtration of the solution and cooling to

allow collection of the crystalline product yielded a fine purple powder albeit in a much higher yield (60 – 80%). Attempts to recrystallise the powder by slow cooling from chlorinated solutions failed with only a few isolated crystals being collected from powdered material. The reason for the change of the state of the solid form of the complexes was resolved by elemental analysis and single crystal X-ray diffraction. The use of 1,2-dichloroethane was causing halide exchange at elevated temperatures and the powdered product was a mixed bromide/chloride complex. This behaviour has been discussed earlier. Although this introduces ambiguity in exact yield determination when going on to use these complexes as precatalysts in reactions where Ni(0) is postulated the catalytic species, the precise composition for preliminary catalyst testing is not a significant issue.

Syntheses were carried out under an inert atmosphere, however the products are stable enough in air for quick synthetic manipulations. In one case the decomposition product of [1-(mesityl)-3-(α-picolyl)-imidazol-2-ylidene]nickeldibromide was fully characterised and shown to be a complex with a dangling imidazolium, where the pyridine remains coordinated and a third halide completes the metal coordination sphere.[24] This product is isostructural to compound **4.5** in chapter 4. When the silver reagent was used in the ratio 2:1 Ag:Ni, a mixture of products was obtained, the majority was the mono-imidazol-2-ylidene complex [1-(mesityl)-3-(α-picolyl)-imidazol-2-ylidene] nickel dibromide, but after recrystallisation from slow evaporation of DCM, a second crystalline material was formed, which is depicted in fig 6.4. This was characterised by X-ray crystallography but attempts to collect NMR data failed as it was impossible to isolate enough of the crystals from the mixture to obtain a spectrum. Complete separation of the paramagnetic mono-imidazol-2-ylidene was impossible. Further attempts to isolate pure bis-imidazol-2-ylidene complex were not successful; the major component was the mono-imidazol-2-ylidene product and not the bis-carbene complex targeted. This complex is analogous to palladium NHC complexes observed by others.[25]

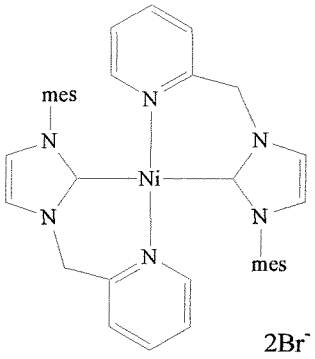

Fig 6.4 Bis-imidazol-2-ylidene Ni(II) complex.

The use of the 'free' carbene (compound **2.24**) in place of the silver reagent in THF gave the same nickel (II) mono-imidazol-2-ylidene complexes as confirmed by unit cell determination of the crystalline material isolated. The yields were good and comparable to

those obtained when using the 1,2-dichloroethane at reflux. The additional advantage in this case is the isolation of well-defined complexes with only one type of halide associated with the product; the reaction can be carried out in polar rather than chlorinated solvents. Attempts to isolate the Ni(II) bis-imidazol-2-ylidene complex using the 'free' carbene route were not undertaken due to time constraints.

Complex **6.4** was obtained whilst preparing derivatives of complexes **6.1** – **6.3**. Taking one equivalent of sodium diethyldithiocarbamate and refluxing in dichloromethane with **6.3** gave **6.4**. Only one halide was substituted by the diethyldithiocarbamate group (determined from X-ray data) even when a 3:1 excess dithiocarbamate:bromine was employed. This complex was isolated in its crystalline form in moderate to good yields (62%). Leaving a solution of **6.4** in dichloromethane open to air for a week yielded crystals of nickel bis-diethyldithiocarbamate and a white powder, presumably the imidazolium salt formed from decomposition.

Attempts to alkylate the compound **6.3** with Grignard or zinc reagents such as $MgMe_2$, $MgEt_2$ and $ZnEt_2$ resulted in colour changes from purple to brown but unfortunately no well-defined complexes could be identified by NMR or isolated by crystallisation. The addition of $AlMe_3$ was also to no avail, addition at –78°C and warming to –40°C resulted in the solution changing from purple to brown and at –10°C black paramagnetic nickel deposited. Nickel(II) dimethyl chelating bis-imidazol-2-ylidene complexes have been characterised although they had poor thermal stabilities above room temperature as by 50°C evolution of methane and ethane is detected.[20]

Complex **6.5** was prepared from the precursor silver reagent **3.6** in a 2:1 ratio of Ag:Ni giving the corresponding bis-carbene complex. It is interesting to note that the methoxy oxygen does not bind to the nickel centre (determined from X-ray data) however, in the pyridine functionalised bis- imidazol-2-ylidene product from the reactions with **6.1** – **6.3** the pyridine nitrogen is bound and not 'dangling'. The 'dangling' mode of the methoxy oxygen is unlikely to be due to steric strain on the methoxy ligand, but rather due to the fact that Ni(II) is a borderline hard Lewis acid and hence preferentially binds hard bases; chlorine is a harder lewis base than the methoxy group, therefore it remains bound to the metal. This complex is isostructural to the analogous palladium species.[26] Several attempts to coordinate

the oxygen donors by abstraction and exchange of the halides with the non-coordinating anion BF_4^- gave only intractable mixtures or **6.5** was recovered unmodified.

Complex **6.6** was synthesised in an attempt to introduce the smaller chelating ligands to nickel as had been completed with the palladium complexes described earlier. The difference of introducing a six-member to five-member chelate ring was very apparent, as the target mono-imidazol-2-ylidene dihalide complex was not formed. On refluxing the $Ni(DME)Br_2$ with one equivalent of silver precursor a deep purple solution formed similar to that observed with complexes **6.1** - **6.3** indicating that the desired product was forming. As the completed reaction was allowed to cool from the deep purple solution dropped a light blue powder **6.7** and not a purple product as was expected. On redissolving the powder a deep purple solution was again obtained. Similar behaviour was observed when using the analogous silver complex **3.1** for this reaction. After filtering whilst hot, followed by slow cooling, X-ray quality crystals were obtained.

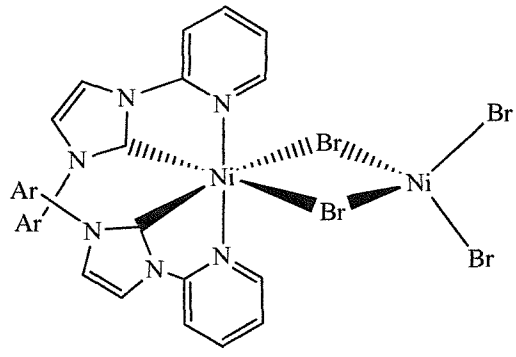

Fig 6.5 Complex **6.7** as characterised by X-ray crystallography. Ar = 2,6-di-*iso*-propylphenyl.

The product in the solid state consists of two-nickel centres in different geometries (Fig 6.5). The first is tetrahedral, coordinated by two terminal and two bridging bromines and the second is an octahedral centre hosting two ligands and bridged to the other nickel through the two halides. It is proposed that the reason for the formation of the bis-carbene species is relative solubility. $Ni(DME)Br_2$ is poorly soluble in non-coordinating solvents such as dichloromethane. After an initial transfer of an imidazol-2-ylidene has occurred the mono-NHC nickel complex, having better solubility in dichloromethane, will react faster than the $Ni(DME)Br_2$ with a second silver reagent. By changing the reaction medium to a donor solvent such as THF there is no change in product. Upon dissolving the complex the colour

change from bright blue to purple suggests that this compound does not retain the dimeric form in solution. Attempts to isolate a mono-nuclear product were carried out by adding trimethylphosphine. It was hoped that the phosphine would coordinate to the nickel, cleaving the halide bridges and obtain either as a pair $[NiBr_2(PMe_3)_3][Ni(Lig)_2Br_2]$ or $[NiBr_4]^{2-}[Ni(Ligand)_2(PMe_3)_2]^{2+}$. This resulted exclusively in the isolation of $NiBr_2(PMe_3)_3$ and a white precipitate was observed. It is assumed that the trimethylphosphine displaced the imidazol-2-ylidenes, as phosphines have been observed to exist in equilibrium with NHC's,[27] and the white precipitate was an imidazolium derivative. It was not possible to isolate enough of the small amounts of ultra fine white powder to characterise it by NMR spectroscopy and mass spectrometry of the powder showed no identifiable peaks.

An alternative route to the desired mono-carbene using the isolated imidazol-2-ylidene **2.19** in preference to the silver reagent was instigated with partial success. Due to the instability of the 'free' carbenes in chlorinated solvents the reaction was performed in THF, in which the $Ni(DME)Br_2$ has some solubility but not as good as DCM. A brown crystalline product was obtained from the crude reaction mixture that was identified using X-ray crystallography. The data showed three products, the desired mono-carbene species, a bis-carbene species comparable to **6.6** and $[NiBr_4]^{2-}$ (Fig 6.6). This gives an overall oxidation state of Ni(II), but does prove it is possible to obtain the desired mono-carbene target. Attempts to separate each of the three species using different crystallisation methods in the hope that they may crystallise separately were not successful.

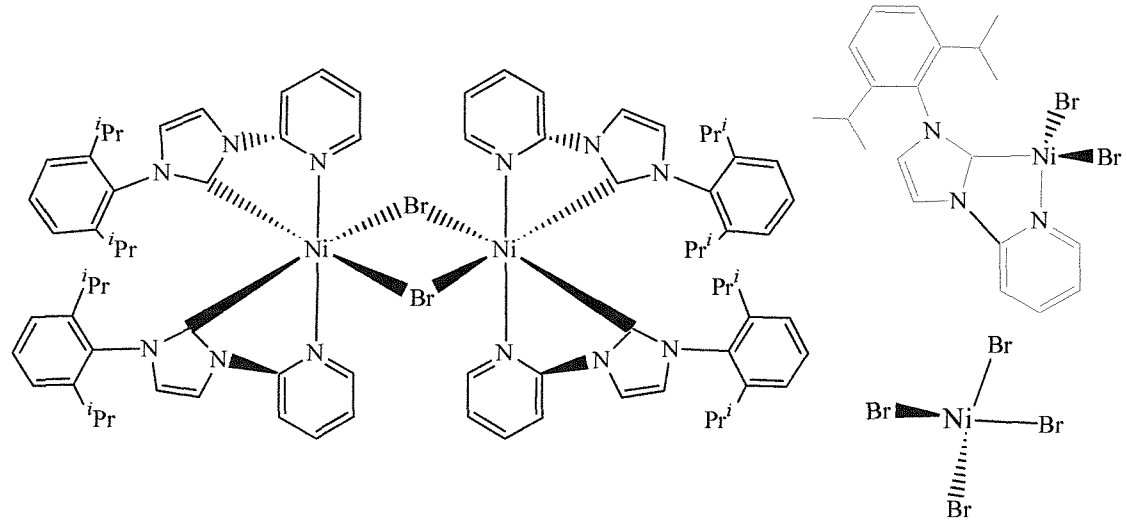

Fig 6.6 Three complexes co-crystallised from 'free' carbene method.

From these the information given above two conclusions can be drawn; firstly, the smaller biting ligand leads preferentially to a bis-carbene species and secondly, alternative more soluble nickel (II) sources are required to continue this work as this is still believed to be the primary reason for the formation of the bis-carbene complexes.

6.2.2 Characterisation of Nickel Complexes

With the exception of compound **6.5**, NMR spectroscopy was ruled out because of the paramagnetic nature of these complexes. Mass spectrometry was also to no avail (except for **6.5**) as the complexes were undetectable by electrospray methods or other forms of mass spectrometry. Elemental analysis was used to confirm chemical composition; structural information was determined for all compounds *via* single crystal X-ray diffraction as all complexes could be crystallised by dissolving in dichloromethane and layering this with diethylether or petroleum ether.

Compounds **6.1** – **6.5** all are readily soluble in chlorinated solvents, and are partially soluble in polar solvents such as toluene, THF and acetonitrile, **6.5** also has good solubility in diethylether. All compounds are insoluble in non-polar solvents. Compound **6.6** is only soluble in refluxing, high boiling, chlorinated solvents and precipitates rapidly on cooling.

6.2.2.1 NMR Spectroscopy and Mass Spectrometry

The diamagnetic complex **6.5** was the only compound that NMR studies were possible for. Resonances in the ^{1}H NMR spectrum were assigned as follows to confirm the identity of **6.5**; for the 2,6-di-*iso*-propylphenyl group doublets at 0.9 and 1.5 ppm, a septet at 3.0 ppm, a doublet at 7.3 ppm and a triplet at 7.4 ppm, for the methoxy methyl a singlet at 3.3 ppm, for the methylene bridge a singlet at 6.2 ppm and the 4- and 5-imidazol-2-ylidene protons at 6.3 and 6.5 ppm. These chemical shifts were only slightly different from the corresponding peaks of palladium bromide analogue.[24] The presence of only one environment for the *iso*-propyl groups (two doublets, one septet) suggests that this is a *trans*-carbene complex rather than *cis*-carbene and has a centre of inversion. Electrospray mass spectrometry showed an ion peak representing $[Ni(Ligand)_2Cl + MeCN]^+$ and $[Ni(Ligand)_2Cl]^+$ supporting the NMR spectroscopy observations.

6.2.2.2 X-ray Crystallography

Due to the inherent paramagnetic nature of these compounds identification by single crystal X-ray crystallography was the primary diagnostic tool. All of the complexes were isolated as crystalline samples (solvents of crystallisation contained no colouration after crystallisation) and so it is believed that these structures represent the bulk of the sample and are not just one unique crystal.

Compounds **6.1** – **6.3** are all isostructural to the mesityl analogue previously prepared.[24] They all contain a tetrahedral nickel centre that is ligated by the bidentate ligand and two halides or the diethyldithiocarbamate. The structure of compound **6.2** is shown below and all others are shown in the experimental section.

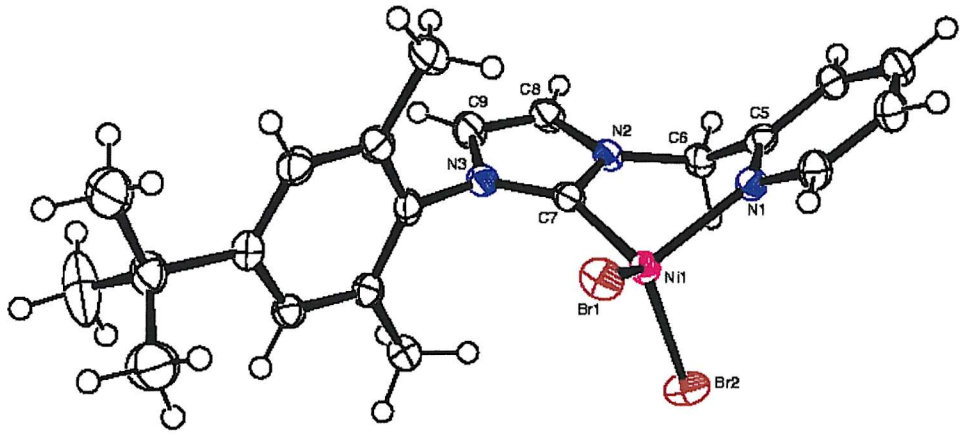

Fig 6.7 Crystal structure of **6.2**. Ellipsoids shown at 50% probability.

Table 6.1 Comparative bond lengths (Å) and angles (°) for **6.1** – **6.4**.

R – Group	**6.1**	**6.2**	**6.3**	Mesityl	**6.4**
Ni1 – C7	1.991(3)	1.961(3)	1.955(4)	1.961(2)	1.879(4)
Ni1 – N1	2.026(3)	2.012(3)	2.026(4)	2.030(2)	1.941(3)
Ni1 – Br1	2.2914(7)	2.3405(7)	2.3749(9)	2.3677(4)	-
Ni1 – Br2	2.3376(11)	2.3948(7)	2.3551(8)	2.3585(4)	-
N3 – C7 – N2	104.9(2)	104.8(3)	104.1(4)	104.64(19)	104.4(3)
C7 – Ni1 – N1	92.29(11)	93.38(12)	92.55(16)	92.74(9)	90.66(14)

By comparing the nickel to carbene carbon bond lengths (Table 6.1) it can be seen that there is a slight shortening of the bond of *ca.* 0.05 Å when an aromatic group is positioned on the 3-imidazol-2-ylidene nitrogen [1.991(3) Å for a *tert*-butyl substituent, 1.955 – 1.961 Å for an aryl substituent]. As was observed with the palladium complexes the strength of this bond effects catalytic activity. This shortening is caused by delocalisation of the electron density across the two-ring system giving more stabilisation to the ylidene, which in turn forms a stronger Ni – C bond. These nickel carbene bond lengths (1.955 – 1.991 Å) are towards the

higher end of the range of known bond lengths (1.828 – 1.986 Å). The nickel pyridine bond length remains unaffected by the change of alkyl substituent on the heterocyclic ring. It is proposed that these complexes retain their structures in solution as no change in colour is observed. There are only two other pyridine NHC nickel complexes that have been previously structurally characterised, one is the mesityl analogue by us,[24] the other is a saddle shaped cyclophane complex[28] having a similar shaped structure to the metal TAAB complexes described in chapter 7.

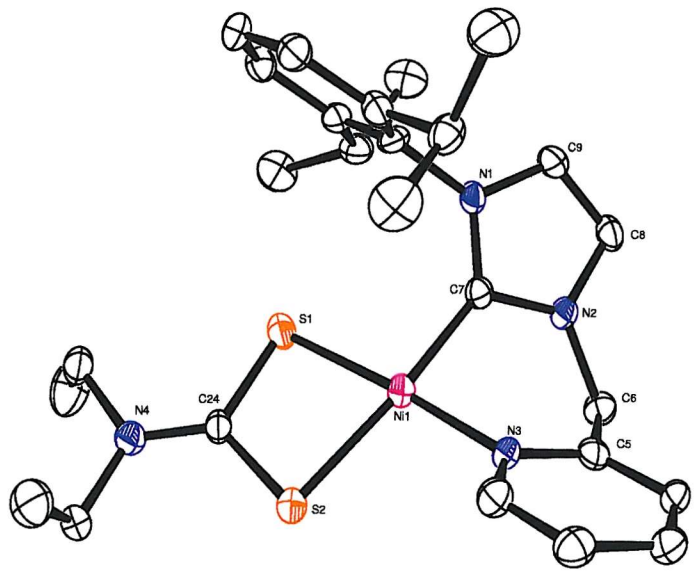

Fig 6.8 Crystal structure of **6.4**, hydrogen's and bromide anion removed for clarity, ellipsoids shown at 50% probability.

Complex **6.4** containing the diethyldithiocarbamate group is a square planar complex unlike the tetrahedral complexes **6.1** – **6.3**, it is common for nickel dithiocarbamate complexes to have square planar geometries as has been observed with nickel phosphine complexes.[29] The exchange of the electron-withdrawing halides with the dithiocarbamate group causes the nickel carbene bond to shorten further by *ca.* 0.08 Å, [from 1.955(4) Å to 1.879(4) Å] as less electron density is drawn from the nickel carbon bond by the removal of the halides. The nickel pyridine bond is also shortened by 0.08 Å [from 2.026(4) Å to 1.941(3) Å] by the substitution of the halides. Bond angles around the metal centre are only affected by the change in sterics from exchanging the halides with the bulkier diethyldithiocarbamate.

The bis-imidazol-2-ylidene complex (fig 6.9) characterised as the minor product from its attempted synthesis is a centrosymmetric square planar nickel (II) complex. Two imidazol-2-ylidene groups coordinate the nickel and in this structure the pendant arm pyridines are

also bound to the metal centre completing the coordination sphere. Two non-coordinated bromides balance the oxidation state. Selected bond lengths and angles are shown in table 6.2.

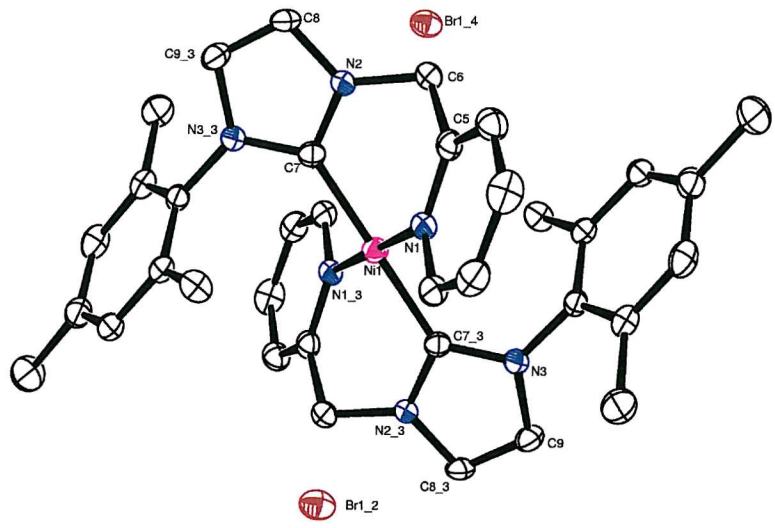

Table 6.2 Selected bond lengths (Å) and angles (°) for bis-imidazol-2-ylidene Ni complex.

Ni1 – N1	1.928(3)
Ni1 – C7	1.907(3)
N2 – C7	1.345(4)
N3_3 – C7	1.365(4)
N2 – C8	1.380(4)
N3_3 – C9_3	1.391(4)
C8 – C9_3	1.350(4)
C7 – Ni1 – N1	87.26(11)
C7 – Ni1 – N1_3	92.74(11)
N2 – C7 – N3_3	104.5(2)
N2 – C7 – Ni1	120.6(2)
N3_3 – C7 – Ni1	134.6(2)

Fig 6.9 Crystal structure of bis-imidazol-2-ylidene Ni complex. Ellipsoids shown at 50% probability, hydrogen's have been removed for clarity.

The nickel to carbene bond length of 1.907(3) Å is well within the range of reported nickel carbene bond lengths. There appears to be no specific interaction of the halides with any specific sections of the complex by examination of the bulk structure. The closest related complex to this is the reported Ni(II) cyclophane complex that is ligated by the two pyridine rings and two imidazol-2-ylidenes, which are cyclically linked through methylene bridges. In the cyclophane the nickel to carbene bond lengths are slightly shorter than in this complex (average cyclophane is 1.85 Å compared to 1.90 Å) but the pyridine bond lengths are similar. The lengthening of the bond in the complex described here may be due to steric hindrance of the mesityl groups.

Complex **6.5** (fig 6.10) is a centrosymmetric square planar nickel(II) complex coordinated by two chlorides and two imidazol-2-ylidene groups. The halides and imidazol-2-ylidene groups are mutually *trans* to one another. The methoxy functional groups do not interact with the metal centre and are 'dangling'. In this structure the imidazol-2-ylidene ligands are related through the centre of inversion, however the rotamer of this complex has also been characterised, although the quality of the data allowed only connectivity to be established and so is not presented here. The nickel carbene bond length 1.9100(14) Å is typical of

known distances. This complex is isostructural to the reported palladium analogue.[26] Selected bond lengths and angles are shown in table 6.3.

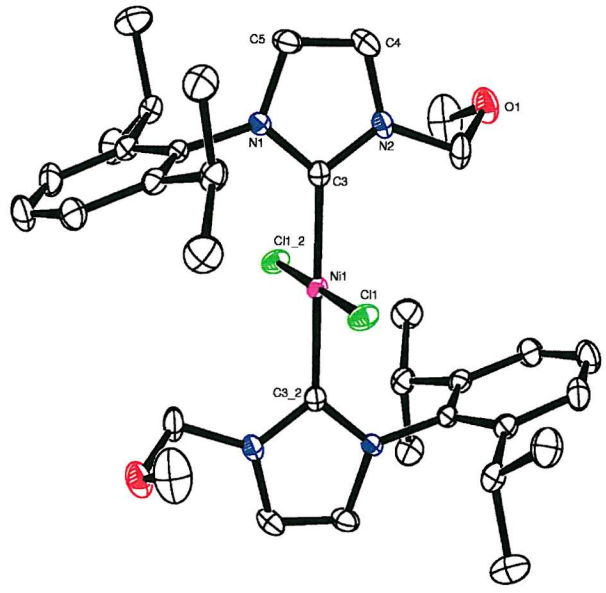

Table 6.3 Selected bond lengths (Å) and angles (°) for **6.5**.

Ni1 – C3	1.9100(14)
Ni1 – Cl1	2.1850(8)
N2 – C3	1.350(2)
N1 – C3	1.356(2)
N2 – C4	1.384(2)
N1 – C5	1.395(2)
C4 – C5	1.344(2)
C3 – Ni1 – C3_2	180
C3 – Ni1 – Cl1	89.21(5)
N2 – C3 – N1	104.42(12)
N2 – C3 – Ni1	125.96(10)
N1 – C3 – Ni1	129.59(10)

Fig 6.10 Crystal structure of **6.5**. Ellipsoids shown at 50% probability, hydrogen's removed for clarity.

The structure of compound **6.7** is a rare example of where two different geometries of the same element coexist in the same complex. There are examples of mixed geometry nickel complexes of extended Schiff base ligands, and mixed metal systems, but these are generally based on multi-dentate ligands designed to coordinate multiple metal centres[30, 31] unlike **6.7** where the ligand is designed as a bidentate chelate for a single metal centre. A second data collection related to this reaction where the 'free' carbene was used in preference to the silver transfer reagent was obtained. A dimeric species is again produced (fig 6.11) however, this complex is part of a multi-component structure in which three products co-crystallised to give the targeted mono-carbene nickel dibromide, the bis-carbene nickel bromide dimer and $[NiBr_4]^{2-}$, the full structure of this is detailed in the experimental section.

On first inspection it appears that **6.7** is the halfway stage to the product elucidated from the free carbene route, it contains nickel in both a tetrahedral and slightly distorted octahedral geometry (most angles within 10° of a right angle). In both structures the pyridine functionalities are mutually *trans* whilst the imidazol-2-ylidenes are mutually *cis*, being *trans* to a bromine. The nickel carbene bonds [2.00(3) – 2.022(8) Å] represent the longest known bonds of this type and the slight lengthening is due to the *trans*-effects around the nickel centre. The bridging bromine to nickel bonds are 0.03 Å longer than the terminal

bonds which is typical. The tetrahedral mono-carbene nickel dibromide has co-crystallised with the bis-carbene dimer and is comparable to compounds **6.1** – **6.3**. The nickel carbene bond length of *ca.* 1.97 Å is in the range observed for **6.1** – **6.3** [1.955(4) Å – 1.991(3) Å] and the nickel pyridine bond length of *ca.* 2.04 Å is also comparable [2.012(3) – 2.030(2) Å]. Unfortunately the quality of the data from the low quality crystals only allowed bond lengths accurate to two decimal places.

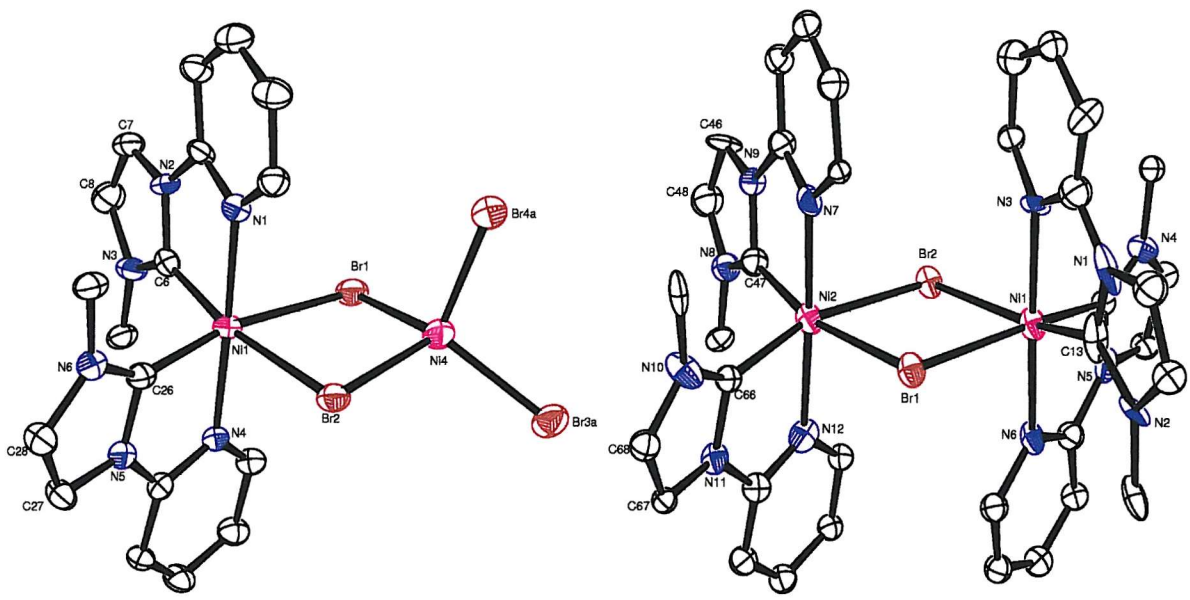

Fig 6.11 Crystal structure of **6.6** (left) and part of the product with 'free'carbene (right). 2,6-di-*iso*-propylphenyl groups partially and hydrogens removed for clarity.

Table 6.4 Comparative bond lengths (Å) and angles (°) of **6.6** and free carbene product.

6.6		**Carbene Product**	
Ni1 – C6	2.022(8)	Ni2 – C47	2.00(3)
Ni1 – C26	2.005(7)	Ni2 – C66	2.05(3)
Ni1 – N1	2.102(6)	Ni2 – N7	2.10(2)
Ni1 – N4	2.100(6)	Ni2 – N12	2.16(2)
Ni1 – Br1	2.6649(13)	Ni2 – Br1	2.622(5)
Ni1 – Br2	2.6881(13)	Ni2 – Br2	2.632(4)
Br1 – Ni1 – Br2	83.50(4)	Br1 – Ni2 – Br2	84.81(13)
N2 – C6 – N3	104.1(6)	N9 – C47 – N8	104.2(11)
C6 – Ni1 – N1	78.9(3)	C47 – Ni2 – N7	80.5(12)
C6 – Ni1 – C26	101.4(3)	C47 – Ni2 – C66	109.2(10)

6.2.3 'Pincer' Nickel (II) and Ni(0) Imidazol-2-ylidene Complexes.

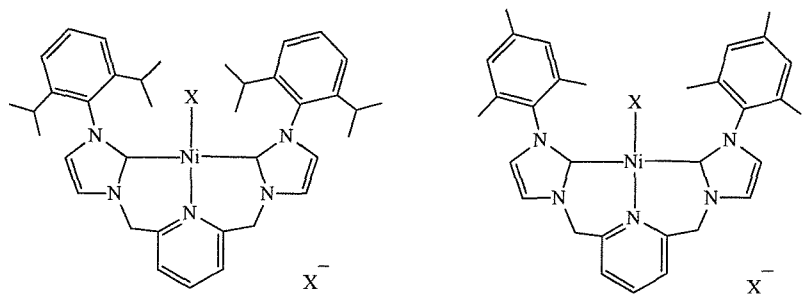

A B

Fig 6.12 Proposed Ni (II) 'pincer' bis-imidzol-2-ylidene complexes. X = halide

Initial efforts to isolate Ni(II) 'pincer' imidazol-2-ylidene (**A** and **B**, Fig 6.12) complexes analogous to the palladium complexes previously reported[32] have shown that they can be prepared. The reaction of the precursor silver reagent **3.15** or the previously reported 2,6-di-*iso*-propylphenyl analogue with $Ni(DME)Br_2$ in 1,2-dichloroethane under reflux gives an air-stable brown powder of **A** or **B**. The ^1H NMR ($CDCl_3$) of **A** is similar to the palladium analogue reported previously. Peaks assignable to two *iso*-propyl environments were observed, i.e. four doublets (0.9, 1.0, 1.1 and 1.4 ppm) and two septets (2.6 and 3.1 ppm) for the *iso*-propyl groups and two doublets were observed for the methylene bridge. Elemental analysis of **B** showed that after allowing for a 1:1 mixed Br/Cl complex which is not unprecedented for reactions involving 1,2-dichloroethane then the following elemental analysis results support the formation of a complex of stoichiometry Ni(Ligand)BrCl (Found; C, 56.94, H, 5.34, N, 10.57, $C_{31}H_{33}N_5Ni_1Cl_1Br_1$ requires C, 57.31, H, 5.12, N, 10.78 %). Unfortunately further investigation into these complexes was not possible due to time restraints but from these initial results it is clear it is possible to isolate these 'pincer' complexes.

Investigations into Ni(0) complexes was instigated after the realisation that 'free' carbenes could be isolated. $Ni(COD)_2$ was chosen as the primary starting material as work with palladium(II) COD complexes had shown that COD is a good leaving group when used with NHCs. A new and vastly improved route to $Ni(COD)_2$ had been reported[33] which made this a viable starting material. Initial reactions of the free-carbene **2.19** with $Ni(COD)_2$ in precooled THF (-78°C) in a 1:1 ratio led instantly to a deep purple complex. Attempts to grow crystals from this solution by slow cooling failed. The purple complex was extremely air sensitive and rapidly decomposed within seconds of being in contact with air. A sample

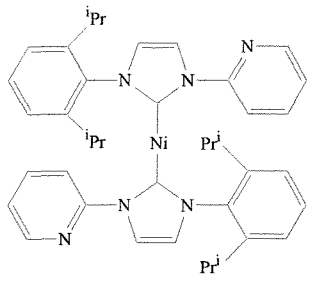

Fig 6.13 Proposed Ni(0) bis-imidazol-2-ylidene

was prepared for ^{1}H NMR studies and from this two conclusions were drawn; firstly there was a single ligand environment based on the *iso*-propyl group signals of two doublets at 1.1 and 1.3 ppm and a septet at 3.0 ppm, suggesting a bis-carbene complex from previous work. Residual peaks for COD remained however even when pumped on under vacuum and it is not possible to determine if these are from residual $Ni(COD)_2$ or a Ni(Ligand)COD complex which would also show only one ligand environment. Further investigation into this product is needed before one of the two possible structures can be confirmed, although from the amount of excess starting material recovered the structure shown in Fig 6.13 is believed to have been formed.

6.3 Conclusions

It has been shown that chelating picolyl functionalised mono-imidazol-2-ylidene Ni(II) dihalide complexes (**6.1** – **6.3**) have been isolated *via* transmetallation from the silver precursors or *via* reaction with the 'free' imidazol-2-ylidene. When using the silver precursors choice of chlorinated solvent must reflect the desired use of the end product as halide exchange processes occur in higher boiling solvents. An example of anion exchange (**6.4**) with one of the complexes has been described. The methoxy bis-imidazol-2-ylidene Ni(II) dihalide complex **6.5** shows how it is possible to design a precatalyst with dangling functional groups that could provide electronic support for a catalytically active complex.

Attempts to isolate pyridine functionalised mono-imidazol-2-ylidene Ni(II) dihalide complexes led to the bis-imidazol-2-ylidene complexes (**6.6**) regardless of which of the two synthetic routes were utilized. An interesting mixed geometry complex was isolated from the transmetallation and three complexes were isolated from the 'free' carbene route. It is clear that with further work the targeted complexes can be isolated.

Initial studies into pincer chelates and Ni(0) species have shown that further work on the synthetic routes is required to confirm the identity of these species, especially with the unstable Ni(0) products.

These complexes provide a good array of precatalysts that could be tested for C-C coupling activity, which was not undertaken in this project due to time constraints.

6.4 Experimental Section.

Sodium diethyldithiocarbamate was purchased from Aldrich and dried azeotropically prior to use. The following chemicals were prepared from literature method, $Ni(DME)Br_2$,[34] $Ni(DME)I_2$,[34] $Ni(COD)_2$,[33] $NiBr_2(PMe_3)_3$,[35] $Ni(S_2CNEt_2)_2$,[36] $Mg(TMEDA)Me_2$,[37] $Ni(TMEDA)Me_2$,[38] $Ni(BIPY)Et_2$,[39] $Ni(BIPY)Me_2$,[40] [1-(*tert*-butyl)-3-(α-picolyl)-imidazol-2-ylidene] silver bromide,[41] [1-(mesityl)-3-(α-picolyl)-imidazol-2-ylidene] silver bromide,[41] [1-(2,6-di-*iso*-propylphenyl)-3-(α-picolyl)-imidazol-2-ylidene] silver bromide,[41] 1-(2,6-di-*iso*-propylphenyl)-3-(pyridin-2-yl)-imidazol-2-ylidene silver bromide.[41]

General Method 1

Under an inert atmosphere, to the appropriate imidazol-2-ylidene silver halide precursor in pre-dried dichloromethane (100 cm^3), was added a slight excess of nickel dimethoxyethane dibromide and the mixture refluxed for 6 – 12 hours. Silver halide deposits were observed as the reaction progressed. On completion the reaction mixture was allowed to cool before the solution was filtered through a frit and the solvent removed *in vacuo* to yield product. Recrystallisation of samples from dichloromethane layered with petroleum ether generally yielded X-ray quality crystals.

[1-(*tert*-butyl)-3-(α-picolyl) imidazol-2-ylidene] nickel dibromide 6.1

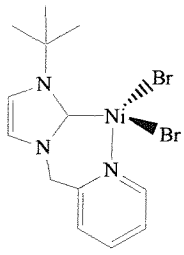

Following general method 1 using [1-(*tert*-butyl)-3-(α-picolyl)imidazol-2-ylidene] silver bromide (0.30 g, 0.7 mmol) and $Ni(DME)Br_2$ (0.23 g, 0.8 mmol). Yield 56%, 0.18 g. Found C, 40.10, H, 4.40, N, 10.79, $C_{13}H_{17}N_3Br_2Ni$ requires C, 35.99, H, 3.95, N, 9.69%. The X-ray crystal structure shows mixture of chlorine and bromine at the two halide occupying sites. As the crystals were used for the elemental analysis this can explain the poor agreement in the elemental analysis results.

Crystal data for **6.1**: $C_{13}H_{17}Br_{0.72}Cl_{1.28}N_3Ni$, purple block, Mw 376.81, Monoclinic, $P2_1/c$ (No. 14), a = 14.021(3) Å, b = 9.2265(18) Å, c = 12.237(2) Å, $\alpha = \gamma = 90°$, β = 105.21(3)°, V = 1527.6(5) $Å^3$, Z = 4, μ = 3.360 mm^{-1}, T = 150 K, Total reflections = 8931, unique reflections = 3425 (R_{int} = 0.0514), Final R indices [$I>2\sigma(I)$] R = 0.0403, R_w = 0.0553 (all data). X-ray Local Code 01sw005.

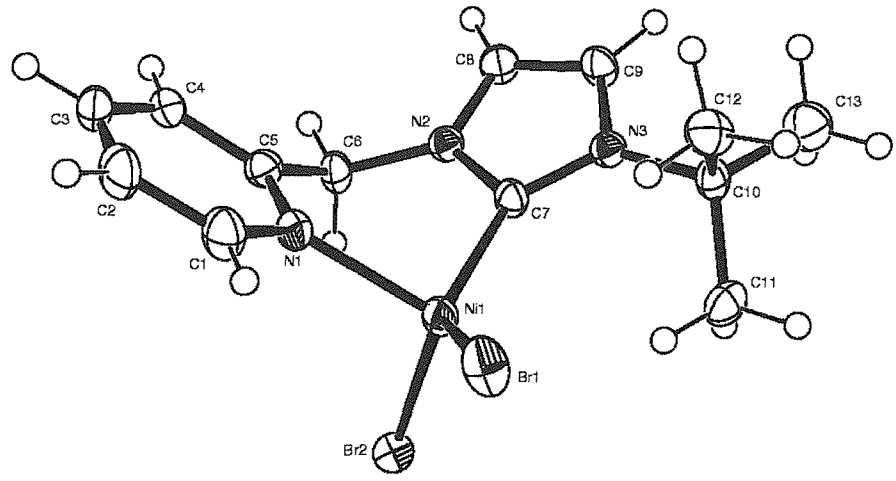

Fig 6.14 Crystal structure of **6.1**.

Table 6.5 Bond lengths (Å) for **6.1.**

C1 – N1	1.349(4)	C5 – C6	1.506(4)	C8 – C9	1.341(4)	C10 – C12	1.519(4)
C1 – C2	1.386(5)	C6 – N2	1.463(4)	C8 – N2	1.375(4)	C10 – C13	1.527(5)
C2 – C3	1.378(5)	C7 – N3	1.347(4)	C9 – N3	1.386(4)	N1 – Ni1	2.026(3)
C3 – C4	1.380(5)	C7 – N2	1.355(4)	C10 – N3	1.509(4)	Ni1 – Br1	2.2914(7)
C5 – N1	1.346(4)	C7 – Ni1	1.991(3)	C10 – C11	1.516(4)	Ni1 – Br2	2.337(1)

Table 6.6 Bond angles (°) for **6.1**.

N1 – C1 – C2	122.2(3)	C9 – C8 – N2	106.5(3)	C7 – N2 – C8	111.1(2)
C3 – C2 – C1	118.6(3)	C8 – C9 – N3	107.3(3)	C7 – N2 – C6	123.5(2)
C3 – C4 – C5	119.4(3)	N3 – C10 – C11	109.0(2)	C8 – N2 – C6	125.4(2)
N1 – C5 – C4	121.5(3)	N3 – C10 – C12	108.0(2)	C7 – N3 – C9	110.3(2)
N1 – C5 – C6	117.1(3)	C11 – C10 – C12	111.5(3)	C7 – N3 – C10	125.0(2)
C4 – C5 – C6	121.4(3)	N3 – C10 – C13	108.9(2)	C9 – N3 – C10	124.6(2)
N2 – C6 – C5	112.5(2)	C11 – C10 – C13	109.4(3)	C7 – Ni1 – N1	92.29(11)
N3 – C7 – N2	104.9(2)	C12 – C10 – C13	109.9(3)	C7 – Ni1 – Br1	125.26(9)
N3 – C7 – Ni1	138.2(2)	C1 – N1 – C5	118.8(3)	N1 – Ni1 – Br1	104.81(8)
N2 – C7 – Ni1	116.6(2)	C1 – N1 –Ni1	119.8(2)	C7 – Ni1 – Br2	107.24(9)
Br1 – Ni1 – Br2	119.01(3)	C5 – N1 - Ni1	121.3(2)	N1 – Ni1 – Br2	101.47(8)

[1-[3,5-dimethyl-4-(*tert*-butyl)phenyl]-3-(α-picolyl)imidazol-2-ylidene] nickel dibromide 6.2

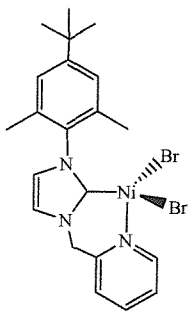

Following general method 1 using compound **3.7** (0.15 g, 0.3 mmol) and Ni(DME)Br_2 (0.10 g, 0.3 mmol). Yield 61%, 0.10 g. MS(ES+) *m/z* 306 $(Ligand)^+$, Found C, 46.73, H, 4.57, N, 7.79 $C_{21}H_{25}Br_2N_3Ni$ requires C, 46.89, H, 4.68, N, 7.81 %.

Crystal data for **6.2**: $C_{21}H_{25}Br_2N_3Ni$, purple block, Mw 537.97, Monoclinic, $P2_1/n$ (No. 14), a = 7.0347(14) Å, b = 23.581(5) Å, c = 13.633(3) Å, $\alpha = \gamma =$ 90 °, β = 92.98(3)°, V = 2258.5(8) Å^3, Z = 4, μ = 4.408 mm^{-1}, T = 150 K, Total reflections =

17862, unique reflections = 5115 (R_{int} = 0.0673), Final R indices [$I>2\sigma(I)$] R = 0.0415, R_w = 0.0790 (all data). X-ray Local Code 01sw017.

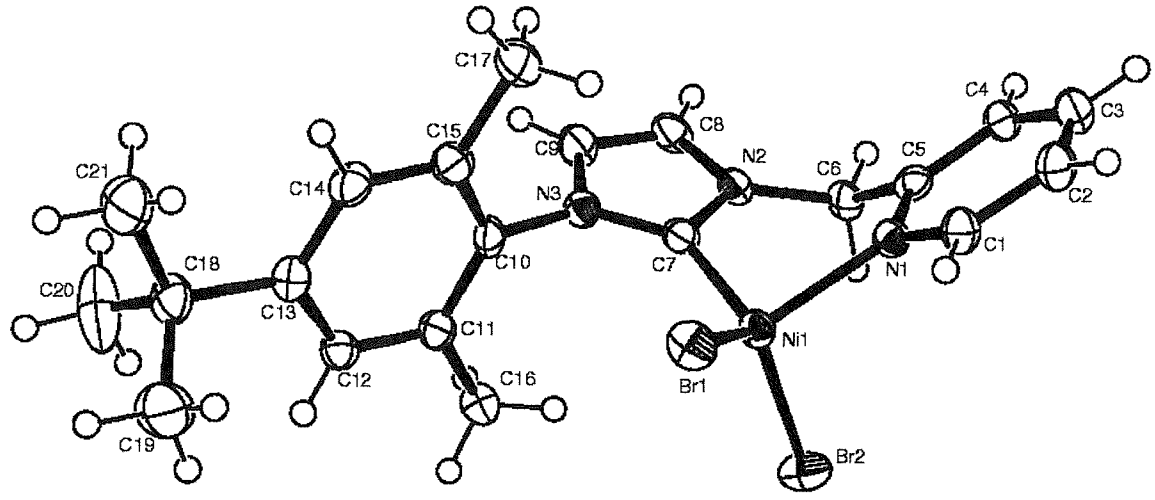

Fig 6.15 Crystal Structure of **6.2**.

Table 6.7 Bond lengths (Å) for **6.2**.

C1 – N1	1.349(4)	C7 – N3	1.341(4)	C10 – N3	1.457(4)	C15 – C17	1.511(5)
C1 – C2	1.385(5)	C7 – N2	1.352(4)	C11 – C12	1.396(5)	C18 – C21	1.514(6)
C2 – C3	1.374(5)	C7 – Ni1	1.961(3)	C11 – C16	1.506(5)	C18 – C20	1.528(6)
C3 – C4	1.378(5)	C8 – C9	1.334(5)	C12 – C13	1.388(5)	C18 – C19	1.533(6)
C4 – C5	1.389(5)	C8 – N2	1.384(4)	C13 – C14	1.400(5)	N1 – Ni1	2.012(3)
C5 – N1	1.354(4)	C9 – N3	1.398(4)	C13 – C18	1.543(5)	Ni1 – Br1	2.3405(7)
C5 – C6	1.503(5)	C10 – C15	1.383(5)	C14 – C15	1.395(5)	Ni1 – Br2	2.3948(7)
C6 – N2	1.467(4)	C10 – C11	1.385(5)				

Table 6.8 Bond angles (°) for **6.2**.

N1 – C1 – C2	122.5(3)	C15 – C10 – N3	117.6(3)	C1 – N1 – C5	118.8(3)
C3 – C2 – C1	118.7(3)	C11 – C10 – N3	118.9(3)	C1 – N1 – Ni1	120.1(2)
C2 – C3 – C4	119.2(3)	C10 – C11 – C12	116.8(3)	C5 – N1 – Ni1	121.1(2)
C3 – C4 – C5	120.2(3)	C10 – C11 – C16	121.8(3)	C7 – N2 – C8	111.0(3)
N1 – C5 – C4	120.6(3)	C12 – C11 – C16	121.4(3)	C7 – N2 – C6	123.5(3)
N1 – C5 – C6	118.5(3)	C13 – C12 – C11	122.9(3)	C8 – N2 – C6	125.3(3)
C4 – C5 – C6	120.7(3)	C12 – C13 – C14	117.3(3)	C7 – N3 – C9	110.9(3)
N2 – C6 – C5	114.1(3)	C12 – C13 – C18	120.8(3)	C7 – N3 – C10	126.2(3)
N3 – C7 – N2	104.8(3)	C14 – C13 – C18	121.8(3)	C9 – N3 – C10	122.8(3)
N3 – C7 - Ni1	136.7(2)	C15 – C14 – C13	122.0(3)	C7 – Ni1 – N1	93.38(12)
N2 – C7 – Ni1	118.5(2)	C10 – C15 – C14	117.4(3)	C7 – Ni1 – Br1	117.80(10)
C9 – C8 – N2	106.9(3)	C10 – C15 – C17	121.8(3)	N1 – Ni1 – Br1	110.22(8)
C8 – C9 – N3	106.5(3)	C14 – C15 – C17	120.8(3)	C7 – Ni1 – Br2	102.71(10)
C15 – C10 – C11	123.4(3)	Br1 – Ni1 – Br2	125.92(2)	N1 – Ni1 – Br2	100.93(8)

[1-(2,6-di-*iso*-propylphenyl)-3-(α-picolyl) imidazol-2-ylidene] nickel dibromide 6.3

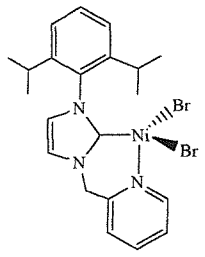

Following general method 1 using [1-(2,6-di-*iso*-propylphenyl)-3-(α-picolyl)imidazol-2-ylidene] silver bromide (0.16 g, 0.32 mmol) and Ni(DME)Br_2 (0.10 g, 0.3 mmol). Yield 0.10 g, 59%. Found C, 46.76, H, 4.59, N, 7.36, $C_{21}H_{25}N_3Br_2Ni$ requires C, 46.89, H, 4.68, N, 7.81%.

Crystal data for **6.3**: $C_{21}H_{25}Br_2N_3Ni$, purple plate, Mw 537.97, Monoclinic, $P2_1/n$ (No. 14), a = 9.7116(19) Å, b = 15.417(3) Å, c = 15.243(3) Å, $\alpha = \gamma = 90$ °, β = 105.81(3)°, V = 2195.9(8) Å^3, Z = 4, μ = 4.533 mm^{-1}, T = 150 K, Total reflections = 29973, unique reflections = 5008 (R_{int} = 0.0900), Final R indices [$I>2\sigma(I)$] R = 0.0479, R_w = 0.0895 (all data). X-ray Local Code 00sw002.

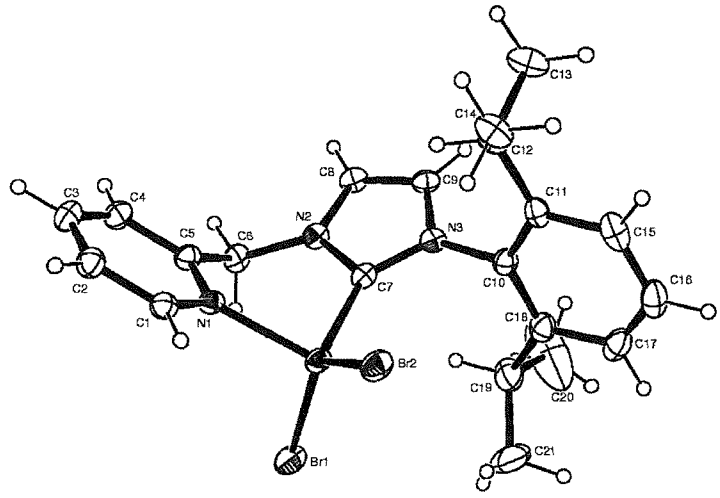

Table 6. 9 Bond lengths (Å) for **6.3**.

C16 – C17	1.363(9)	C3 – C4	1.375(8)	C8 – C9	1.339(6)	C11 – C12	1.502(7)
C16 – C15	1.381(8)	C4 – C5	1.385(7)	C8 – N2	1.372(6)	C12 – C14	1.528(7)
C20 – C19	1.539(11)	C5 – N1	1.352(5)	C9 – N3	1.385(6)	C17 – C18	1.389(7)
C21 – C19	1.487(10)	C5 – C6	1.496(7)	C10 – C18	1.389(7)	C18 – C19	1.525(8)
C13 – C12	1.534(7)	C6 – N2	1.459(6)	C10 – C11	1.403(7)	N1 – Ni1	2.026(4)
C1 – N1	1.340(6)	C7 – N3	1.351(6)	C10 – N3	1.442(5)	Br1 – Ni1	2.3749(9)
C1 – C2	1.374(7)	C7 – N2	1.361(5)	C11 – C15	1.392(7)	Br2 – Ni1	2.3551(8)
C2 – C3	1.378(7)	C7 – Ni1	1.955(4)				

Table 6.10 Bond angles (°) for **6.3**.

N1 – C1 – C2	123.0(4)	C11 – C10 – N3	117.9(4)	C1 – N1 – C5	118.5(4)
C1 – C2 – C3	118.6(5)	C15 – C11 – C10	116.9(5)	C1 – N1 – Ni1	121.2(3)
C4 – C3 – C2	119.0(5)	C15 – C11 – C12	120.2(5)	C5 – N1 – Ni1	120.3(3)
C3 – C4 – C5	119.8(5)	C10 – C11 – C12	122.9(4)	C7 – N2 – C8	111.4(4)
N1 – C5 – C4	121.0(5)	C11 – C12 – C14	112.6(4)	C7 – N2 – C6	122.0(4)
N1 – C5 – C6	117.7(4)	C11 – C12 – C13	110.9(4)	C8 – N2 – C6	126.5(4)
C4 – C5 – C6	121.3(4)	C14 – C12 – C13	110.7(4)	C7 – N3 – C9	110.7(4)

N2 – C6 – C5	112.7(4)	C16 – C15 – C11	121.0(5)	C7 – N3 – C10	125.2(4)
N3 – C7 – N2	104.1(4)	C16 – C17 – C18	121.6(5)	C9 – N3 – C10	124.1(4)
N3 – C7 – Ni1	137.5(3)	C17 – C18 – C10	117.1(5)	C7 – Ni1 – N1	92.55(16)
N2 – C7 – Ni1	118.1(3)	C17 – C18 – C19	120.5(5)	C7 – Ni1 – Br2	111.33(13)
C9 – C8 – N2	106.6(4)	C10 – C18 – C19	122.4(4)	N1 – Ni1 – Br2	105.49(11)
C8 – C9 – N3	107.2(4)	C21 – C19 – C18	112.9(7)	C7 – Ni1 – Br1	105.48(13)
C18 – C10 – C11	123.0(4)	C21 – C19 – C20	112.0(8)	N1 – Ni1 – Br1	103.77(10)
C18 – C10 – N3	119.1(4)	C18 – C19 – C20	108.3(5)	Br2 – Ni1 – Br1	131.13(3)

[1-(2,6-di-*iso*-propylphenyl)-3-(α-picolyl)imidazol-2-ylidene] nickel diethyldithiocarbamate bromide 6.4

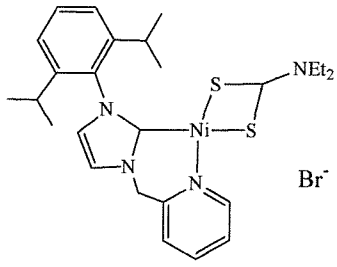

To a solution of **6.3** (0.25 g, 0.46 mmol) in dichloromethane (dry, 30 cm^3) was added sodium diethyldithiocarbamate (0.87 g, 0.51 mmol) and the solution refluxed overnight. The purple solution changed to pale brown and salt deposits were observed. The supernatant was removed *in vacuo* and the product extracted into ether, filtered through a frit and concentrated to *ca.* 5 cm^3 from which X-ray quality crystals formed at room temperature on standing. Yield 62%, 0.17 g. MS (ES+) *m/z* 525 $[Ni(Ligand)(S_2CNEt_2)]^+$, 320 $(Ligand)^+$. Found C, 50.24, H, 5.32, N, 9.72 % $C_{25}H_{35}BrN_4NiS_2$ requires C, 50.53, H, 5.94, N, 9.43 %.

Crystal data for **6.4**: $C_{27}H_{37}N_4S_2BrCl_2Ni$, orange shard, Mw 691.25, Monoclinic, $P2_1/n$ (No. 14), a = 9.8969(3) Å, b = 24.1705(10) Å, c = 14.6443(6) Å, $\alpha = \gamma = 90°$, β = 109.1690(10)°, V = 3308.9(2) $Å^3$, Z = 4, μ = 2.104 mm^{-1}, T = 150 K, Total reflections = 20675, unique reflections = 7345 (R_{int} = 0.0811), Final R indices [$I>2\sigma(I)$] R = 0.0528, R_w = 0.0992 (all data). X-ray Local Code 01sw036.

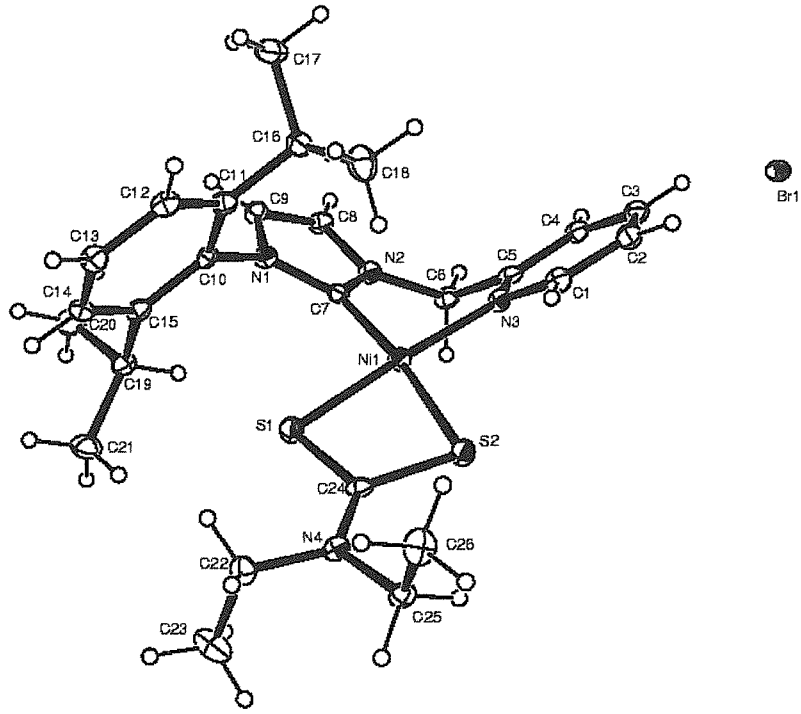

Fig 6.16 Crystal structure of **6.4**.

Table 6.11 Bond lengths (Å) for **6.4**.

Ni1 – C7	1.879(4)	N2 – C7	1.349(4)	C2 – C3	1.379(5)	C12 – C13	1.376(5)
Ni1 – N3	1.941(3)	N2 – C8	1.388(5)	C3 – C4	1.374(5)	C13 – C14	1.388(5)
Ni1 – S1	2.1723(11)	N2 – C6	1.458(4)	C4 – C5	1.395(5)	C14 – C15	1.389(5)
Ni1 – S2	2.2323(10)	N3 – C1	1.339(5)	C5 – C6	1.498(5)	C15 – C19	1.524(5)
S1 – C24	1.715(4)	N3 – C5	1.360(4)	C8 – C9	1.340(5)	C16 – C18	1.526(6)
S2 – C24	1.726(4)	N4 – C24	1.306(4)	C10 – C15	1.393(5)	C16 – C17	1.531(5)
N1 – C7	1.363(4)	N4 – C25	1.472(5)	C10 – C11	1.398(5)	C19 – C21	1.531(5)
N1 – C9	1.392(4)	N4 – C22	1.474(5)	C11 – C12	1.393(5)	C19 – C20	1.535(6)
N1 – C10	1.454(4)	C1 – C2	1.387(5)	C11 – C16	1.510(5)	C22 – C23	1.503(5)

Table 6.12 Bond angles (°) for **6.4**.

C7 – Ni1 – N3	90.66(14)	C1 – N3 – C5	117.9(3)	C9 – C8 – N2	106.4(3)
C7 – Ni1 – S1	94.21(11)	C1 – N3 – Ni1	119.9(2)	C8 – C9 – N1	107.1(3)
N3 – Ni1 – S1	174.60(10)	C5 – N3 – Ni1	122.2(3)	C15 – C10 - C11	123.6(3)
C7 – Ni1 – S2	172.90(11)	N3 – C1 – C2	123.4(3)	C15 – C10 – N1	119.1(3)
N3 – Ni1 – S2	96.14(9)	C3 – C2 – C1	118.5(4)	C11 – C10 – N1	117.3(3)
S1 – Ni1 – S2	79.08(4)	C4 – C3 – C2	119.2(4)	C12 – C11 – C10	117.0(3)
C24 – S1 – Ni1	86.88(13)	C3 – C4 – C5	119.7(3)	C13 – C12 – C11	121.1(4)
C24 – S2 – Ni1	84.74(12)	N3 – C5 – C4	121.3(4)	C12 – C13 – C14	120.1(3)
C7 – N1 – C9	110.5(3)	N3 – C5 – C6	117.0(3)	C13 – C14 – C15	121.4(3)
C7 – N1 – C10	125.1(3)	C4 – C5 – C6	121.6(3)	C14 – C15 – C10	116.7(3)
C9 – N1 – C10	124.0(3)	N2 – C6 – C5	110.3(3)	N4 – C24 – S1	124.8(3)
C7 – N2 – C8	111.6(3)	N2 – C7 – N1	104.4(3)	N4 – C24 – S2	126.0(3)
C7 – N2 – C6	121.9(3)	N2 – C7 – Ni1	120.3(3)	S1 – C24 – S2	109.2(2)
C8 – N2 – C6	126.4(3)	N1 – C7 – Ni1	135.3(3)		

Bis-[1-(2,6-di-*iso*-propylphenyl)-3-(methylmethoxy)imidazol-2-ylidene] nickel dichloride 6.5

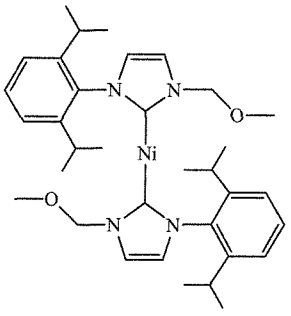

Following general method 1 using [1-(2,6-di-*iso*-propylphenyl)-3-(methylmethoxy)-imidazol-2-ylidene] silver bromide (0.75 g, 1.8 mmol) was added to a solution of $NiBr_2DME$ (0.28 g, 0.9 mmol) in dichloromethane (30 cm^3) and refluxed overnight. Silver bromide precipitated from the light orange solution. The mixture was filtered via a frit and the resulting orange solution was concentrated to *ca.* 5 cm^3 and cooled to –30°C from which X-ray quality crystals were obtained. Yield 81%, 0.49 g. MS(ES+): *m/z* 678 $[Ni(ligand)_2Cl(MeCN)]^+$, 637 $[Ni(ligand)_2Cl]^+$, 273 $[Ligand]^+$. $\delta_H(CDCl_3)$ 0.9 and 1.5 [2 x 12H, d, $CH(CH_3)_2$], 3.0 [4H, septet, $CH(CH_3)_2$], 3.3 (6H, s, OCH_3), 6.2 (4H, s, CH_2), 6.3 and 6.5 (2 x 2H, s, 4- and 5-imidazol-2-ylidene), 7.3 (4H, d, $^iPrC_6H_2H$), 7.4 (2H, t, $^iPrC_6H_2H$).

Crystal data for **6.5**: $C_{34}H_{48}N_4O_2Cl_2Ni$, orange cube, Mw 674.37, Triclinic, *P*-1 (No. 2), a = 8.008(2) Å, b = 9.261(2) Å, c = 12.410(3) Å, α = 74.25(3)°, β = 78.06(3)°, γ = 80.02(3)°, V = 859.9(3) Å^3, Z = 1, μ = 0.755 mm^{-1}, T = 150 K, Total reflections = 3927, unique reflections = 3927 (R_{int} = 0.0), Final R indices [$I>2\sigma(I)$] R = 0.0290, R_w = 0.0379 (all data). Symmetry transformations used to generate equivalent atoms: -x,-y,-z. X-ray Local Code 01sw025.

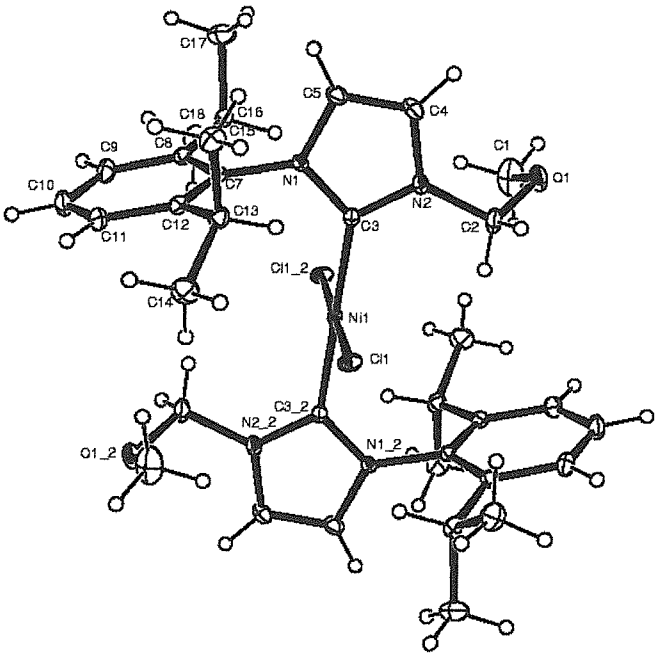

Fig 6.17 Crystal structure of **6.5**.

Table 6.13 Bond lengths (Å) for **6.5**.

Ni1 – C3	1.9100(14)	N2 – C2	1.467(2)	C7 – C12	1.404(2)	C12 – C13	1.522(2)
Ni1 – Cl1	2.1850(8)	N1 – C3	1.356(2)	C8 – C9	1.395(2)	C13 – C14	1.529(2)
O1 – C2	1.393(2)	N1 – C5	1.395(2)	C8 – C16	1.520(2)	C13 – C15	1.540(2)
O1 – C1	1.405(2)	N1 – C7	1.446(2)	C9 – C10	1.386(2)	C16 – C18	1.528(2)
N2 – C3	1.350(2)	C4 – C5	1.344(2)	C10 – C11	1.384(2)	C16 – C17	1.533(2)
N2 – C4	1.384(2)	C7 – C8	1.403(2)	C11 – C12	1.396(2)		

Table 6.14 Bond angles (°) for **6.5**

C3 – Ni1 – C3_2	180	N2 – C3 – N1	104.42(12)	C11 – C10 – C9	120.35(15)
C3 – Ni1 – Cl1	89.21(5)	N2 – C3 – Ni1	125.96(10)	C10 – C11 – C12	121.27(15)
C3 – Ni1 – Cl1_2	90.79(5)	N1 – C3 – Ni1	129.59(10)	C11 – C12 – C7	116.86(14)
Cl1 –Ni1 – Cl1_2	180	C5 – C4 – N2	106.37(13)	C11 – C12 – C13	121.02(14)
C2 – O1 – C1	113.16(14)	C4 – C5 – N1	106.84(13)	C7 – C12 – C13	122.00(13)
C3 – N2 -C4	111.71(12)	C8 – C7 – C12	123.30(13)	C12 – C13 – C14	114.06(13)
C3 – N2 – C2	124.84(13)	C8 – C7 – N1	118.38(13)	C12 – C13 – C15	110.04(12)
C4 – N2 – C2	123.45(13)	C12 – C7 – N1	118.32(13)	C14 – C13 – C15	109.51(13)
C3 – N1 – C5	110.66(12)	C9 – C8 – C7	117.00(14)	C8 – C16 – C18	113.54(13)
C3 – N1 – C7	123.97(11)	C9 – C8 – C16	120.89(14)	C8 – C16 – C17	110.01(13)
C5 – N1 – C7	125.33(12)	C7 – C8 – C16	122.01(13)	C18 – C16 – C17	109.70(14)
O1 – C2 – N2	111.17(13)	C10 – C9 – C8	121.11(15)		

Bis-[1-(mesityl)-3-(α-picolyl) imidazol-2-ylidene] nickel dibromide.

Following general method 1 using [1-(mesityl)-3-(α-picolyl)-imidazol-2-ylidene] silver bromide (0.15 g, 0.33 mmol) was added to a solution of $Ni(DME)Br_2$ (0.05 g, 0.16 mmol) in dichloroethane (30 cm^3) and refluxed overnight. Silver precipitated from the green solution. The mixture was filtered via a frit and the resulting pale yellow/green solution was concentrated to *ca.* 5 cm^3 and cooled to –30°C from which X-ray quality crystals were obtained. Yield 74% 0.09 g. $\delta_H(CDCl_3)$ 2.1 (12H, s, *o*-mesityl CH_3), 2.5 (6H, s, *p*-mesityl CH_3), 5.5 (2H, s, CH_2), 6.7 and 7.3 (2 x 2H, s, 4-and 5-imidazol-2-ylidene), 6.9 (2H, s, mesityl *H*), 7.3 (1H, m, pyr H), 7.5 (1H, d, pyr H), 7.8 (1H, d, pyr H), 8.5 (1H, d, pyr H).

Crystal data for **6.6**: $C_{19}H_{21}BrCl_2N_3Ni_{0.5}$, yellow cube, Mw 471.55, Monoclinic, $P2_1/n$ (No. 14), a = 10.669(2) Å, b = 10.221(2) Å, c = 19.561(4) Å, $\alpha = \gamma = 90$ °, β = 105.41(3)°, V = 2056.3(7) $Å^3$, Z = 4, μ = 2.710 mm^{-1}, T = 150 K, Total reflections = 12692, unique reflections = 4525 (R_{int} = 0.0524), Final R indices [$I>2\sigma(I)$] R = 0.0413, R_w = 0.0734 (all data). Unit contains one molecule of DCM. Symmetry transformations used to generate equivalent atoms: 1) -x, -y, -z ; 2) -x, -y-1, -z. X-ray Local Code 01sw010.

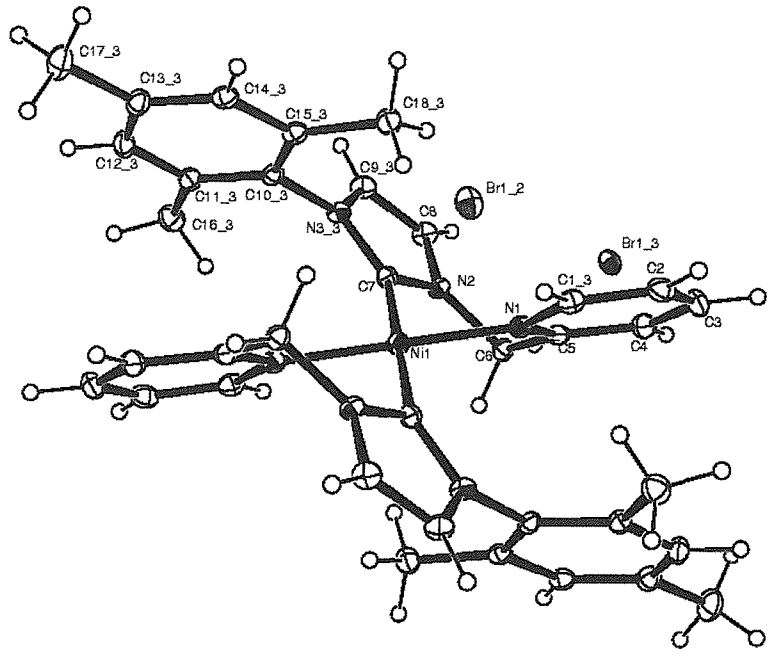

Fig 6.18 Crystal structure of bis-[1-(mesityl)-3-(α-picolyl)imidazol-2-ylidene] nickel dibromide.

Table 6.15 Bond lengths (Å) for Bis-[1-(mesityl)-3-(α-picolyl)imidazol-2-ylidene] nickel dibromide.

C1_3 – N1	1.347(4)	C7 – N3_3	1.365(4)	C11_3 – C12_3	1.391(5)
C2 – C1_3	1.378(4)	C7 – Ni1	1.907(3)	C11_3 – C16_3	1.511(4)
C2 – C3	1.380(5)	C8 – C9_3	1.350(4)	C12_3 – C13 _3	1.391(5)
C3 – C4	1.383(5)	C8 – N2	1.380(4)	C13_3 – C14 _3	1.389(4)
C4 – C5	1.390(4)	C9 – N3	1.391(4)	C13_3 – C17 _3	1.507(4)
C5 – N1	1.355(4)	C10 – C11	1.396(4)	C14_3 – C15 _3	1.401(4)
C6 – N2	1.470(3)	C10 – C15	1.402(4)	C15_3 – C18_3	1.502(4)
C7 – N2	1.345(4)	C10 – N3	1.438(4)	N1 – Ni1	1.928(3)

Table 6.16 Bond angles (°) for Bis-[1-(mesityl)-3-(α-picolyl) imidazol-2-ylidene] nickel dibromide.

N1 – C1_3 – C2	122.1(3)	C11 – C10 – C15	122.3(3)	C10_3 – C15_3 – C18_3	123.4(3)
C1_3 – C2 – C3	119.9(3)	C11 – C10 – N3	119.2(3)	C1_3 – N1 – C5	118.3(3)
C2 – C3 – C4	118.4(3)	C15 – C10 – N3	118.5(3)	C1_3 – N1 – Ni1	119.6(2)
C3 – C4 – C5	119.4(3)	C12 – C11 – C10	117.8(3)	C5 – N1 – Ni1	122.0(2)
N1 – C5 – C4	121.8(3)	C12 – C11 – C16	120.1(3)	C7 – N2 – C8	112.1(2)
N1 – C5 – C6	117.8(3)	C10 – C11 – C16	122.1(3)	C7 – N2 – C6	121.0(2)
C4 – C5 – C6	120.4(3)	C13 – C12 – C11	122.2(3)	C8 – N2 – C6	126.8(2)
N2 – C6 – C5	108.1(2)	C14 – C13 – C12	118.2(3)	C7 – N3_3 – C9_3	110.1(2)
N2 – C7 – N3_3	104.5(2)	C14 – C13 – C17	120.7(3)	C7 – N3_3 – C10_3	123.5(2)
N2 – C7 – Ni1	120.6(2)	C12 – C13 – C17	121.0(3)	C9_3 – N3_3 – C10	126.4(2)
N3_3 – C7 – Ni1	134.6(2)	C13 – C14 – C15	122.3(3)	C7 – Ni1 – N1_3	92.74(11)
C9_3 – C8 – N2	106.0(3)	C14 – C15 – C10	117.1(3)	C7 – Ni1 – N1	87.26(11)
C8 – C9_3 – N3	107.3(3)	C14 – C15 – C18	119.5(3)		

Compound 6.6

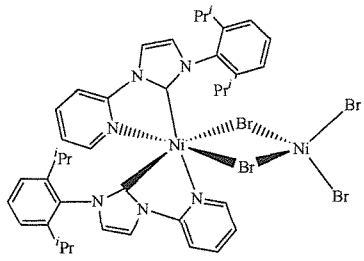

Following general method 1 using 1-(2,6-di-*iso*-propylphenyl)-3-(pyridin-2-yl)-imidazol-2-ylidene silver bromide (0.20 g, 0.4 mmol) and Ni(DME)Br_2 (0.12 g, 0.4 mmol). Yield 0.10 g. Found C, 44.26, H, 5.09, N, 7.26, $C_{40}H_{46}N_6Br_4Ni_2$ requires C, 45.85, H, 4.42, N, 8.02%.

Crystal data for **6.6**: $C_{40}H_{46}Br_4N_6Ni_2$, blue shard, Mw 1047.89, Tetragonal, *P*4(2)/*n* (No. 86), $a = 20.548(3)$ Å, $b = 20.548(3)$ Å, $c = 27.667(6)$ Å, $\alpha = \beta = \gamma = 90°$, $V = 11681.9(33)$ Å^3, $Z = 8$, $\mu = 3.407$ mm^{-1}, $T = 150$ K, Total reflections = 33550, unique reflections = 10594 (R_{int} = 0.1089), Final R indices [$I>2\sigma(I)$] R = 0.0652, R_w = 0.1599 (all data). Symmetry transformations used to generate equivalent atoms: 1) -x, -y, -z; 2) -x, -y-1, -z. X-ray Local Code 01sw006.

Table 6.17 Bond lengths (Å) for **6.6**.

C1 – N1	1.318(9)	C9 – N3	1.455(10)	C24 – C25	1.386(10)	C32 – C33	1.412(14)
C1 – C2	1.384(10)	C10 – C11	1.394(12)	C25 – N4	1.339(8)	C33 – C34	1.398(12)
C1 – N2	1.417(9)	C10 – C18	1.514(12)	C25 – N5	1.394(9)	C34 – C35	1.484(12)
C2 – C3	1.365(11)	C11 – C12	1.406(12)	C26 – N6	1.342(9)	C35 – C37	1.558(13)
C3 – C4	1.350(11)	C12 – C13	1.326(12)	C26 – N5	1.381(8)	C35 – C36	1.561(11)
C4 – C5	1.415(10)	C13 – C14	1.406(12)	C26 – Ni1	2.005(7)	C38 – C40	1.530(11)
C5 – N1	1.324(9)	C14 – C15	1.515(12)	C27 – C28	1.326(11)	C38 – C39	1.540(11)
C6 – N3	1.333(9)	C15 – C16	1.529(11)	C27 – N5	1.403(9)	N1 – Ni1	2.102(6)
C6 – N2	1.352(9)	C15 – C17	1.562(12)	C28 – N6	1.415(9)	N4 – Ni1	2.100(6)
C6 – Ni1	2.022(8)	C18 – C20	1.524(13)	C29 – C30	1.387(11)	Ni1 – Br1	2.6649(13)
C7 – C8	1.302(11)	C18 – C19	1.534(13)	C29 – C34	1.400(12)	Ni1 – Br2	2.6881(13)
C7 – N2	1.406(9)	C21 – N4	1.321(9)	C29 – N6	1.451(10)	Ni4 – Br4A	2.363(8)
C8 – N3	1.418(10)	C21 – C22	1.419(10)	C30 – C31	1.397(12)	Ni4 – Br3A	2.384(6)
C9 – C10	1.364(12)	C22 – C23	1.375(10)	C30 – C38	1.523(13)	Ni4 – Br1	2.4089(14)
C9 – C4	1.397(11)	C23 – C24	1.355(10)	C31 – C32	1.335(14)	Ni4 – Br2	2.4188(13)

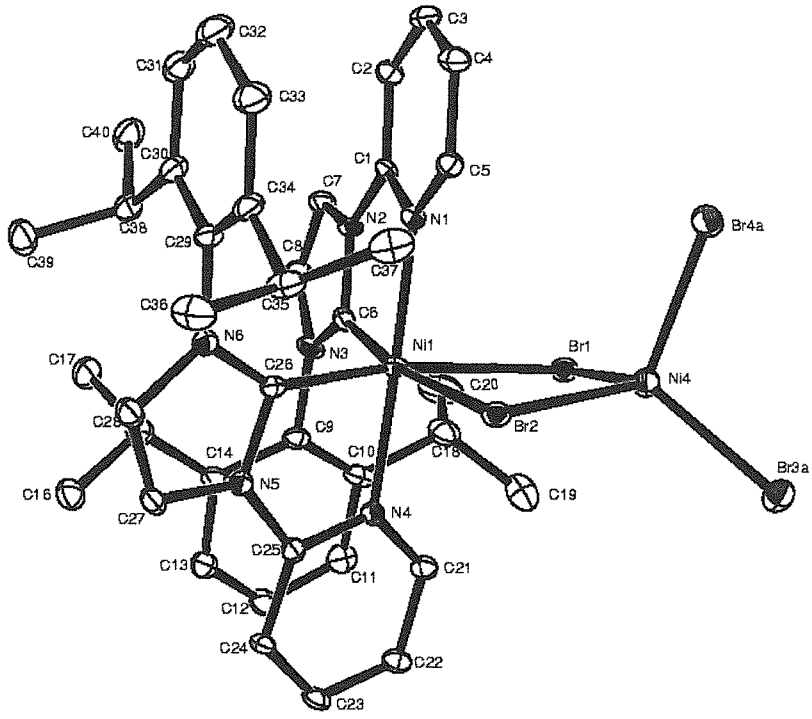

Fig 6.19 Crystal structure of **6.6.**

Table 6.18 Bond angles (°) for **6.6**

N1 – C5 – C4	121.5(7)	C14 – C15 – C17	109.1(8)	N4 – Ni1 – N1	177.8(2)
N3 – C6 – N2	104.1(6)	C16 – C15 – C17	108.5(7)	C26 – Ni1 – Br1	167.9(2)
N3 – C6 – Ni1	142.8(6)	C10 – C18 – C20	113.7(9)	C6 – Ni1 – Br1	89.5(2)
N2 – C6 – Ni1	113.0(6)	C10 – C18 – C19	113.7(8)	N4 – Ni1 – Br1	93.2(2)
C8 – C7 – N2	105.8(7)	C20 – C18 – C19	109.2(9)	N1 – Ni1 – Br1	87.8(2)
C7 – C8 – N3	107.8(8)	C1 – N1 – C5	117.3(6)	C26 – Ni1 – Br2	86.2(2)
C10 – C9 – C14	124.5(8)	C1 – N1 – Ni1	114.6(5)	C6 – Ni1 – Br2	170.5(2)
C10 – C9 – N3	118.1(7)	C5 – N1 – Ni1	128.2(5)	N4 – Ni1 – Br2	87.6(2)
C14 – C9 – N3	117.4(8)	C6 – N2 – C7	111.8(6)	N1 – Ni1 – Br2	94.4(2)
C9 – C10 – C11	116.3(9)	C6 – N2 – C1	119.5(6)	Br1 – Ni1 – Br2	83.50(4)
C9 – C10 – C18	124.0(8)	C7 – N2 – C1	128.7(6)	Br4A – Ni4 – Br3A	104.9(6)
C11 – C10 – C18	119.7(10)	C6 – N3 – C8	110.5(7)	Br4A – Ni4 – Br1	108.5(4)
C10 – C11 – C12	121.3(10)	C6 – N3 – C9	126.9(7)	Br3A – Ni4 – Br1	127.4(4)
C13 – C12 – C11	119.7(9)	C8 – N3 – C9	122.4(7)	Br4A – Ni4 – Br2	107.4(3)
C12 – C13 – C14	122.2(9)	C26 – Ni1 – C6	101.4(3)	Br3A – Ni4 – Br2	112.06(15)
C9 – C14 – C13	115.9(9)	C26 – Ni1 – N4	79.8(3)	Br1 – Ni4 – Br2	95.18(5)
C9 – C14 – C15	122.8(8)	C6 – Ni1 – N4	99.2(3)	Ni4 – Br1 – Ni1	90.17(4)
C13 – C14 – C15	121.3(8)	C26 – Ni1 – N1	99.5(3)	Ni4 – Br2 – Ni1	89.41(4)
C14 – C15 – C16	115.9(8)	C6 – Ni1 – N1	78.9(3)		

Free Carbene Method.

To a solution of 1-(2,6-di-*iso*-propylphenyl)-3-(pyridin-2-yl)-imidazol-2-ylidene (0.20 g, 0.65 mmol) in DME (dry, 30 cm^3) at –78°C, $Ni(DME)Br_2$ (0.22 g, 0.72 mmol) was added

and the reaction stirred for 30 mins before being allowed to rise to room temp. Colour changed from orange through green to brown. The solvent was removed *in vacuo* and resulting brown solid was washed with petroleum ether (2 x 10 cm^3). Yield 0.10 g. Found C, 44.26, H, 5.09, N, 7.26, $C_{40}H_{46}N_6Br_4Ni_2$ requires C, 45.85, H, 4.42, N, 8.02%. X-ray quality crystals were afforded by slow cooling THF solutions (green). Product decomposed rapidly in $CDCl_3$ and is insoluble in C_6D_6.

Crystal data: $C_{112}H_{121}Br_8N_{15}Ni_4O_3$, brown shard, Mw 2599.36, Monoclinic, $P2_1/n$ (No. 14), a = 14.4071(11) Å, b = 23.5511(16) Å, c = 36.789(3) Å, $\alpha = \gamma = 90$ °, β =98.795(3)°, V = 12336.0(17) $Å^3$, Z = 4, μ = 3.244 mm^{-1}, T = 150 K, Total reflections = 15931, unique reflections = 6883 (R_{int} = 0.0634), Final R indices [$I>2\sigma(I)$] R = 0.0910, R_w = 0.1542 (all data). Unit cell contains 3 independent nickel complexes and 3 molecules of THF. Local Code 02sw048.

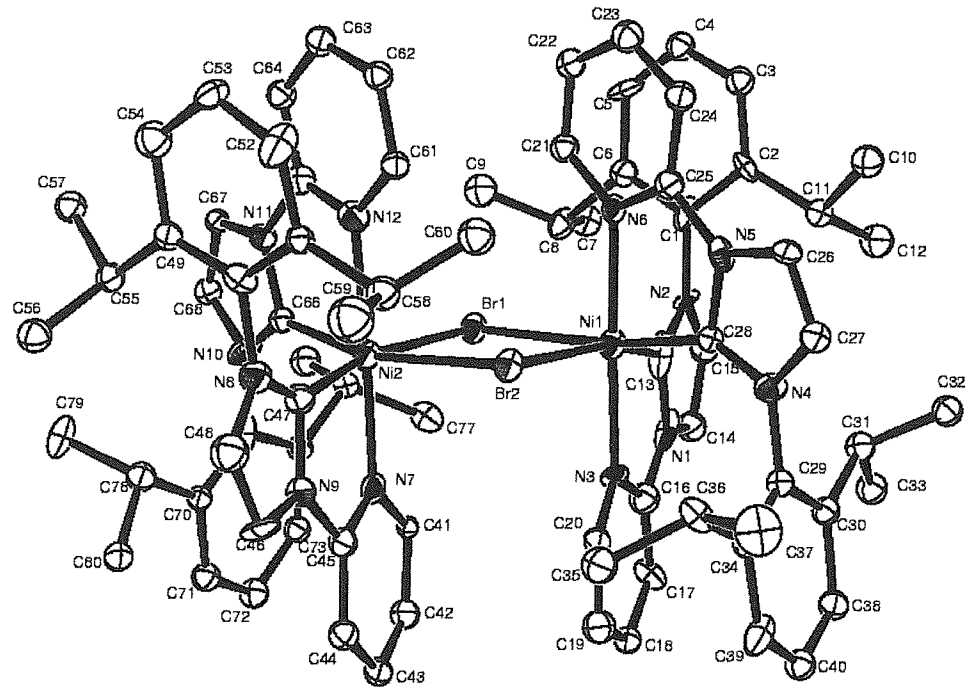

Fig 6.20 Bis-carbene nickel dimer component.

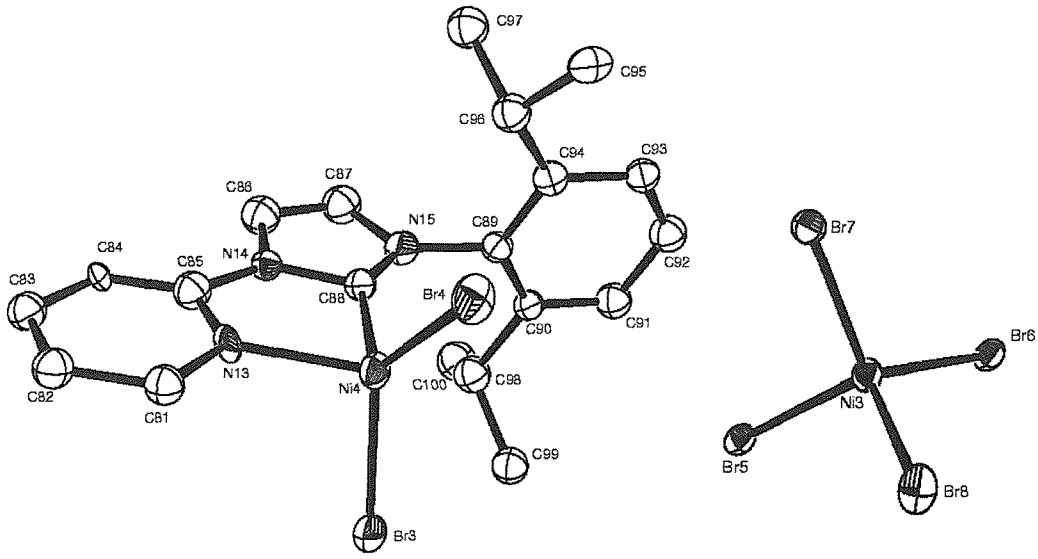

Fig 6.21 Crystal structures of mono-carbene component and $NiBr_4$ isolated from 'free' carbene route.

Table 6.19 Bond lengths (Å) for nickel tetrabromide.

Ni3 – Br8	2.380(5)	Ni3 – Br6	2.409(4)	Ni3 – Br7	2.382(4)	Ni3 – Br5	2.415(6)

Table 6.20 Bond angles (°) for nickel tetrabromide.

Br8 – Ni3 – Br7	121.7(2)	Br7 – Ni3 – Br6	109.77(17)	Br7 – Ni3 – Br5	101.58(17)
Br8 – Ni3 – Br6	105.76(17)	Br8 – Ni3 – Br5	106.67(19)	Br6 – Ni3 – Br5	111.21(19)

Table 6.21 Bond lengths (Å) for mono-carbene component.

C81 – N13	1.36(3)	C86 – C87	1.36(4)	C89 – N15	1.45(3)	C95 – C96	1.55(3)
C81 – C82	1.47(3)	C87 – N15	1.44(3)	C90 – C91	1.39(3)	C96 – C97	1.63(4)
C83 – C84	1.39(4)	C88 – N15	1.31(3)	C90 – C98	1.53(4)	C98 – C100	1.50(4)
C84 – C85	1.33(4)	C88 – N14	1.39(3)	C91 – C92	1.44(3)	C98 – C99	1.55(4)
C85 – N13	1.33(4)	C88 – Ni4	1.97(4)	C92 – C93	1.34(3)	N13 – Ni4	2.04(2)
C85 – N14	1.37(4)	C89 – C90	1.37(3)	C93 – C94	1.44(3)	Ni4 – Br4	2.330(4)
C86 – N14	1.36(3)	C89 – C94	1.41(3)	C94 – C96	1.49(3)	Ni4 – Br3	2.367(5)

Table 6.22 Bond angles (°) for mono-carbene component.

N13 – C81 – C82	121(3)	C89 – C90 – C91	120(2)	C88 – Ni4 – N13	79.5(13)
C83 – C82 – C81	115(3)	C89 – C90 – C98	122(3)	C88 – Ni4 – Br4	113.2(8)
C84 – C83 – C82	120(3)	C91 – C90 – C98	117(3)	N13 – Ni4 – Br4	114.5(7)
C85 – C84 – C83	121(4)	C90 – C91 – C92	116(3)	C88 – Ni4 – Br3	111.2(7)
C84 – C85 – N13	123(4)	C93 – C92 – C91	124(3)	N13 – Ni4 – Br3	99.4(7)
C84 – C85 – N14	130(4)	C92 – C93 – C94	120(3)	Br4 – Ni4 – Br3	127.6(2)
N13 – C85 – N14	107(3)	C89 – C94 – C93	115(3)	C85 – N13 – C81	120(3)
N14 – C86 – C87	111(3)	C89 – C94 – C96	122(3)	C85 – N13 – Ni4	119(2)
C86 – C87 – N15	102(3)	C93 – C94 – C96	123(3)	C81 – N13 – Ni4	121(2)
N15 – C88 – N14	106(3)	C94 – C96 – C95	113(2)	C86 – N14 – C85	126(3)

N15 – C88 – Ni4	145(2)	C94 – C96 – C97	108(3)	C86 – N14 – C88	108(3)
N14 – C88 – Ni4	109(3)	C95 – C96 – C97	105(2)	C85 – N14 – C88	125(3)
C90 – C89 – C94	125(3)	C100 – C98 – C90	116(3)	C88 – N15 – C87	113(3)
C90 – C89 – N15	119(2)	C100 – C98 – C99	108(3)	C88 – N15 – C89	126(3)
C94 – C89 – N15	117(2)	C90 – C98 – C99	112(2)	C87 – N15 – C89	121(3)

Table 6.23 Selected bond lengths (Å) for bis-carbene nickel dimer component.

C1 – C2	1.39(3)	C13 – Ni1	1.96(3)	C24 – C25	1.41(3)	C31 – C33	1.52(3)
C1 – N2	1.42(4)	C14 – C15	1.36(4)	C25 – N6	1.31(3)	C38 – C40	1.37(4)
C1 – C6	1.47(4)	C14 – N1	1.39(4)	C25 – N5	1.42(3)	C39 – C40	1.33(3)
C2 – C3	1.40(3)	C15 – N2	1.41(3)	C26 – C27	1.32(3)	C34 – C39	1.38(4)
C2 – C11	1.57(3)	C16 – N3	1.34(4)	C26 – N5	1.38(3)	C34 – C36	1.52(3)
C3 – C4	1.33(3)	C16 – C17	1.36(4)	C27 – N4	1.37(3)	C35 – C36	1.58(3)
C4 – C5	1.36(3)	C16 – N1	1.38(4)	C28 – N4	1.34(3)	C36 – C37	1.48(3)
C5 – C6	1.41(3)	C17 – C18	1.38(3)	C28 – N5	1.38(3)	N3 – Ni1	2.11(2)
C6 – C8	1.56(3)	C18 – C19	1.37(3)	C28 – Ni1	2.02(3)	N6 – Ni1	2.13(2)
C7 – C8	1.56(3)	C19 – C20	1.40(4)	C29 – C34	1.40(4)	N7 – Ni2	2.10(2)
C8 – C9	1.51(3)	C20 – N3	1.29(3)	C29 – C30	1.44(3)	N12 – Ni2	2.16(2)
C10 – C11	1.51(3)	C21 – C22	1.37(3)	C29 – N4	1.45(3)	Ni1 – Br1	2.604(4)
C11 – C12	1.52(3)	C21 – N6	1.38(3)	C30 – C38	1.45(3)	Ni1 – Br2	2.631(5)
C13 – N1	1.35(4)	C22 – C23	1.36(3)	C30 – C31	1.51(4)	Ni2 – Br1	2.622(5)
C13 – N2	1.46(4)	C23 – C24	1.36(3)	C31 – C32	1.51(3)	Ni2 – Br2	2.632(4)

Table 6.24 Selected bond angles (°) for bis-carbene nickel dimer component.

C2 – C1 – N2	121(3)	N1 – C13 – Ni1	118(4)	C16 – N3 – Ni1	118(3)
C2 – C1 – C6	120(3)	N2 – C13 – Ni1	136(4)	C13 – Ni1 – C28	108.5(10)
N2 – C1 – C6	119(3)	C15 – C14 – N1	106(3)	C13 – Ni1 – N3	75.1(18)
C1 – C2 – C3	119(3)	C14 – C15 – N2	111(3)	C28 – Ni1 – N3	97.9(10)
C1 – C2 – C11	119(3)	N3 – C16 – C17	129(4)	C13 – Ni1 – N6	105.1(18)
C3 – C2 – C11	122(2)	N3 – C16 – N1	110(4)	C28 – Ni1 – N6	80.3(10)
C4 – C3 – C2	121(3)	C17 – C16 – N1	121(4)	N3 – Ni1 – N6	178.2(7)
C3 – C4 – C5	123(3)	C16 – C17 – C18	114(3)	C13 – Ni1 – Br1	84.0(8)
C4 – C5 – C6	121(3)	C19 – C18 – C17	121(3)	C28 – Ni1 – Br1	165.8(7)
C5 – C6 – C1	117(3)	C18 – C19 – C20	117(3)	N3 – Ni1 – Br1	91.8(5)
C5 – C6 – C8	124(3)	N3 – C20 – C19	126(3)	N6 – Ni1 – Br1	90.1(5)
C1 – C6 – C8	120(3)	C13 – N1 – C16	118(4)	C13 – Ni1 – Br2	162.6(13)
C9 – C8 – C7	109(2)	C13 – N1 – C14	112(4)	C28 – Ni1 – Br2	84.4(7)
C9 – C8 – C6	112(2)	C16 – N1 – C14	129(4)	N3 – Ni1 – Br2	91.9(8)
C7 – C8 – C6	108(2)	C15 – N2 – C1	126(3)	N6 – Ni1 – Br2	88.2(6)
C10 – C11 – C12	111(2)	C15 – N2 – C13	105(3)	Br1 – Ni1 – Br2	84.81(13)
C10 – C11 – C2	114(2)	C1 – N2 – C13	129(3)	Ni1 – Br1 – Ni2	95.77(15)
C12 – C11 – C2	108(2)	C20 – N3 – C16	113(3)	Ni1 – Br2 – Ni2	94.88(14)
N1 – C13 – N2	106(3)	C20 – N3 – Ni1	129(2)		

6.5 References

[1] A. Biffis, M. Zecca, M. Basato, *J. Mol. Catal. A - Chem.*, **2001**, *173*, 249.
[2] A. F. Littke, G. C. Fu, *Angew. Chem. Int. Ed. Engl.*, **2002**, *41*, 4176.
[3] *Prices taken from Aldrich 2003 - 2004 catalogue.*
[4] T. S. Lee, J. H. An, J. Kim, J. Y. Bae, *Bull. Korean. Chem. Soc.*, **2001**, *22*, 375.
[5] W. Klaui, J. Bongards, G. Reis, *Angew. Chem. Int. Ed. Engl.*, **2000**, *39*, 3894.
[6] M. Taguchi, I. Tomita, T. Endo, *Angew. Chem. Int. Ed. Engl.*, **2000**, *39*, 3667.
[7] M. D. Leatherman, M. Brookhart, *Macromol*, **2001**, *34*, 2748.
[8] M. F. Lappert, P. L. Pye, *J. Chem. Soc. Dalton. Trans.*, **1977**, 2172.
[9] M. F. Lappert, P. L. Pye, *J. Chem. Soc. Dalton. Trans.*, **1978**, 837.
[10] D. Sellmann, W. Prechtel, F. Knoch, M. Moll, *Organometallics*, **1992**, *11*, 2346.
[11] K. Ofele, W. A. Herrmann, D. Mihalios, M. Elison, E. Herdtweck, W. Scherer, J. Mink, *J. Organomet. Chem.*, **1993**, *459*, 177.
[12] A. J. Arduengo, S. F. Gamper, C. J. Calabrese, F. Davidson, *J. Am. Chem. Soc.*, **1994**, *116*, 4391.
[13] P. L. Arnold, F. G. N. Cloke, T. Geldbach, P. B. Hitchcock, *Organometallics*, **1999**, *18*, 3228.
[14] W. A. Herrmann, G. Gerstberger, M. Spiegler, *Organometallics*, **1997**, *16*, 2209.
[15] W. A. Herrmann, C. Köcher, *Angew. Chem. Int. Ed. Engl.*, **1997**, *36*, 2163.
[16] W. A. Herrmann, *Angew. Chem. Int. Ed. Engl.*, **2002**, *41*, 1290
[17] M. Regitz, *Angew. Chem. Int. Ed. Engl.*, **1996**, *35*, 725.
[18] D. Bourissou, O. Guerret, F. P. Gabbai, G. Bertrand, *Chem. Rev.*, **2000**, *100*, 39.
[19] D. S. Clyne, J. Jin, E. Genest, J. C. Gallucci, T. V. RajanBabu, *Org. Lett.*, **2000**, *2*, 1125.
[20] R. E. Douthwaite, M. L. H. Green, P. J. Silcock, P. T. Gomes, *Organometallics*, **2001**, *20*, 2611
[21] R. E. Douthwaite, D. Haussinger, M. L. H. Green, P. J. Silcock, P. T. Gomes, A. M. Martins, A. A. Danopoulos, *Organometallics*, **1999**, *18*, 4584.
[22] D. S. McGuinness, W. Mueller, P. Wasserscheid, K. J. Cavell, B. W. Skelton, A. H. White, U. Englert, *Organometallics*, **2002**, *21*, 175.
[23] M. Tilset, O. Andell, A. Dhindsa, M. Froseth, WO2001-GB5699, Borealis Technology Oy, Finland, **2002**.
[24] A. A. D. Tulloch, PhD thesis, University of Southampton (Southampton), **2001**.
[25] D. S. McGuinness, K. J. Cavell, *Organometallics*, **2000**, *19*, 741.
[26] A. A. D. Tulloch, S. Winston, A. A. Danopoulos, G. Eastham, M. B. Hursthouse, *J. Chem. Soc. Dalton. Trans.*, **2003**, 699.
[27] L. R. Titcomb, S. Caddick, F. G. N. Cloke, D. J. Wilson, D. McKerrecher, *Chem. Commun.*, **2001**, 1388
[28] M. V. Baker, B. W. Skelton, A. H. White, C. C. Williams, *Organometallics*, **2002**, *21*, 2674.
[29] A. Manohar, K. Ramalingham, R. Thiruneelakandan, G. Bocelli, L.Righi, *Z. Anorg. Allg. Chem.*, **2001**, *627*, 1103.
[30] K. K. Nanda, R. Das, K. Ventatsubramanian, P. Paul, K. Nag, *J. Chem. Soc. Dalton. Trans.*, **1993**, 2515.
[31] S. Brooker, P. D. Croucher, T. C. Davidson, G. S. Dunbar, C. U. Beck, S.Subaramanian, *Eur. J. Inorg. Chem.*, **2000**, 169.
[32] A. A. D. Tulloch, A. A. Danopoulos, G. J. Tizzard, S. J. Coles, M. B. Hursthouse, R. S. Hay-Motherwell, W. B. Motherwell, *Chem. Commun.*, **2001**, 1270.

[33] M. J. Tenorio, M. C. Puerta, I. Salcedo, P. Valerga, *J. Chem. Soc. Dalton. Trans.*, **2001**, 653.
[34] L. G. L. Ward, *Inorg. Synth.*, *13*, 156.
[35] O. Dahl, *Acta Chem. Scand.*, **1969**, *23*, 2342.
[36] T. H. Randle, T. J. Cardwell, R. J. Magee, *Aust. J. Chem.*, **1976**, *29*, 1191.
[37] W. Kaschube, K. R. Porschke, K. Angermund, C. Kruger, G. Wilke, *Chem. Ber.-Recl.*, **1988**, *121*, 1921.
[38] K. Porschke, G. Wilke, W. Kaschube, *J. Organomet. Chem.*, **1988**, *355*, 525.
[39] T. Saito, Y. Uchida, A. Misono, A. Yamamoto, K. Morifuji, S. Ikeda, *J. Am. Chem. Soc.*, **1966**, *88*, 5198
[40] G. Wilke, G. Herrmann, *Angew. Chem. Int. Ed. Engl.*, **1966**, *5*, 581.
[41] A. A. D. Tulloch, A. A. Danopoulos, S. Winston, S. Kleinhenz, G. Eastham, *J. Chem. Soc. Dalton. Trans.*, **2000**, 4499.

Chapter 7

Amido / Imino Mixed Donor Ligand Systems and their Titanium and Zirconium Complexes

Chapter 7

Amido / Imino Mixed Donor Ligand Systems and their Titanium and Zirconium complexes

7.1 Introduction

7.1.1 Single Site Catalysts for Olefin Polymerisation

During the early 1980's the way industrial production of polymers such as polyethylene and polypropylene was performed dramatically changed due to the development of new organotransition metal catalysts.[1] The introduction of single-site catalysts over heterogeneous Ziegler-Natta systems allowed for better control over the microstructure and consequently the mechanical properties of the polymers, by tuning of the catalyst structures. These developments were very quickly put into large-scale use, especially for the production of speciality polymers and engineering plastics. [2-4]

Most single-site catalysts are currently based on metallocenes of the general type shown in fig 7.1.

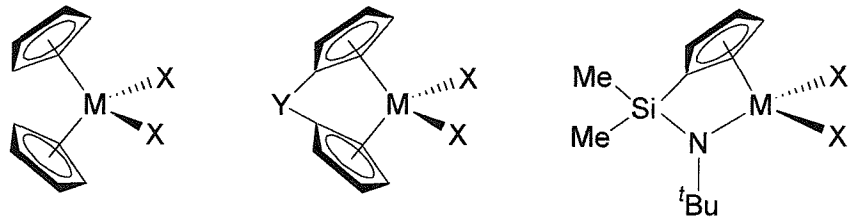

Fig 7.1 Group 4 bent metallocene (**A**), ansa metallocene (**B**) and a constrained-geometry metallocene (**C**) X = halide, Y= bridging group.

The group 4 metallocenes in combination with an activator [e.g. methylalumoxane (MAO) or tris(pentafluorophenylborane) (BARF)] are highly active polymerisation catalysts;[5] furthermore, the stereochemistry of metallocenes of type (**B**) can easily be tuned by the proper choice of Cp-ligands and bridging groups, which transfers efficiently onto the metal catalytic site. These catalysts have been reviewed.[6-8] Constrained-geometry catalysts (**C**) based on titanium show good polymerisation activities,[9] especially

for the polymerisation of ethylene due to the higher electrophilicity of the metal centre and its accessibility by a substrate molecule. It has now been realised that while all of these catalysts are highly efficient at specific reactions, there is no catalyst, or class of catalyst, that will universally polymerise all types of olefin substrates. The study of single site polymerisation catalysts has now begun to diverge both academically[10] and industrially[1] towards non-metallocene, early transition metal complexes[11] such as amides,[12] amidinate/amide mixed donors[13] and imino/oxygen donors,[14] as well as to late transition metal (Ni, Pd, Fe, Co) catalysts[5] in the search for a system that can provide greater activity and control of the polymer structure, in a wider range of applications.

7.1.2 Mechanism of Polymerisation

There are two mechanisms proposed for alkene polymerisation by transition metals, the Cossee-Arlman[15-17] mechanism and the Green-Rooney mechanism.[18]

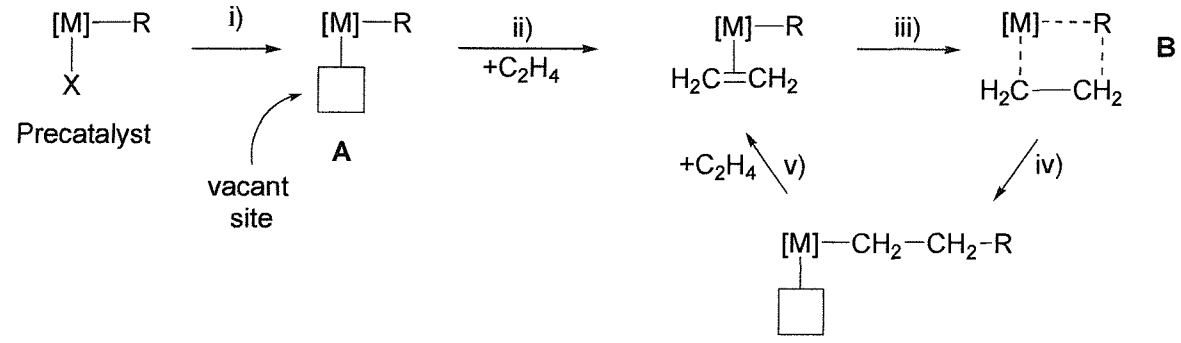

Fig 7.2 Mechanism of olefin polymerisation.

It is generally agreed that the catalytically active species in olefin polymerisation is a coordinatively unsaturated $14e^-$ cationic electrophilic complex **A** (fig 7.2), involving a loosely coordinate four centred transition (**B**), by examination of fig 7.2 the mechanism involves:

i) *Activation* of the precatalyst to create the active species,

ii) *Coordination* of the substrate to the active catalyst,

iii) *Insertion* of the coordinated monomer into the growing polymer chain,

iv) *Regeneration* of an unsaturated coordination sphere,

v) *Coordination* of substrate and further growth of the chain.

The difference in the two proposed mechanisms (Fig 7.3) occurs in step iii), in the Cossee-Arlman route it is proposed a direct insertion occurs from the four-centred transition state, whereas the Green-Rooney method proposes the formation of a metal carbene complex *via* α-hydrogen activation of the substrate, before a second hydrogen elimination step to propagate chain growth.

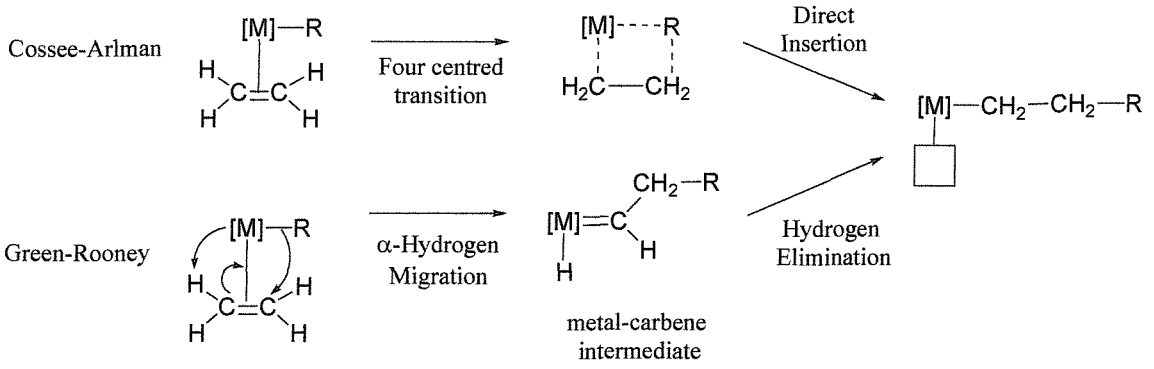

Fig 7.3 Cosse-Arlman and Green-Rooney proposed insertion steps.

Experimental evidence exists supporting both Cossee-Arlman and Green-Rooney mechanisms for different metal and ligand architectures.[19-21]

7.1.3. Activation of Pre-Catalyst.

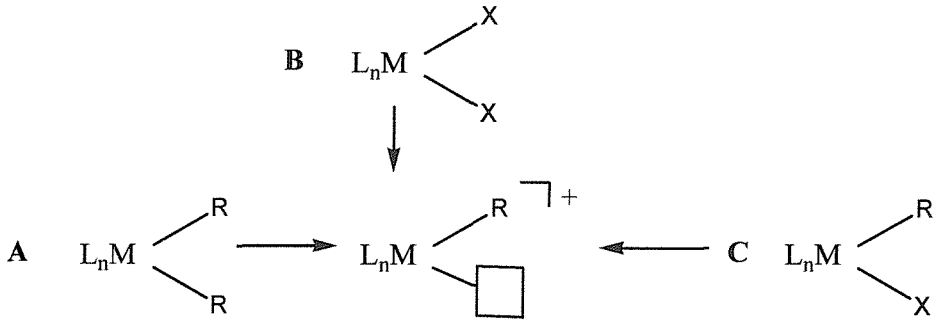

Fig 7.4 Methods to activating precatalyst. X = halide, R = alkyl.

The activation of the precatalyst to form the 14e⁻ active complex can be performed *via*:

A. Abstraction of an alkyl ligand,

B. Abstraction of an anionic ligand,

C. Combination of both alkylation and abstraction.

Method **A** (fig 7.4) involves the abstraction of an alkyl ligand, or alkyl anion from a neutral alkyl complex. Reagents for this purpose are typically trityl salts [$C(Ph)_3^+$], BARF or Brookhart's acid.[22] They work by different mechanisms including protonation of an alkyl ligand (Brookhart's acid), or abstraction in the case of the trityl and BARF.

Method **B** involves the abstraction of an anionic ligand typically a halide by salt elimination and its substitution by a weakly coordinating anion. Common reagents for this are $NaBF_4$ or silver salts such as $AgPF_6$ or $AgOSO_2CF_3$ for the late transition metals.

Method **C** is a combination of both alkylation and abstraction, generally involving a dihalide precursor being treated with an alkylating and then alkyl-abstracting reagent, for this a trialkylaluminium compound followed by BARF could be used or the addition of MAO,[23] which performs both alkylation and abstraction.

7.1.4 Ligand Design

There is an interest in the study of non-metallocene supporting ligands incorporating amido functional groups into ligand systems, especially in organometallic complexes of the early transition metals.[11] The well-known electronic characteristics of the amido group (Fig 7.6) and its integration into tunable ligand backbones provides the opportunities for the design of metal complexes with catalytic activity.[5, 24] Significant contributions in this field have shown the capability of single site polymerisation catalysts based on chelating or functionalised amido ligands.[5]

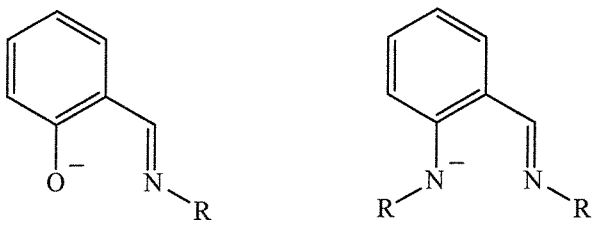

Fig 7.5 Salicyladimine (left) and amido analogue (right) ligand systems, R = functional groups.

Organometallic complexes with Schiff bases, mainly salicylaldimines (fig 7.5) and their derivatives have been well explored.[10, 25] Group 4 complexes of the salicyladimine ligands exhibit high activity and living behaviour in polymerisation reactions.[14, 26-28] The desirable features of these ligands are their easy synthetic accessibility and the opportunity to sterically

and electronically tune the system by substitution of the aromatic ring or at the imine carbon or nitrogen with functional groups.[14, 27-29] In contrast, the coordination chemistry of the anionic ligands that formally originate by replacement of the PhO^- group with the isoelectronic $PhNR^-$ have received less attention even though the tuning opportunities in this case are even greater. The exchange of the oxygen by nitrogen provides an extra tuning site on the ligand system by choice of the substituents for the amine.

These systems, as ligands, are isoelectronic to the cyclopentadienyl (Cp^-) 6-electron system as the amido functionality (R_2N^-) is a σ- and π-donor (Fig 7.6) contributing $4e^-$ and the imino functionality (R-C=N-R) is a 2-electron π-donor.

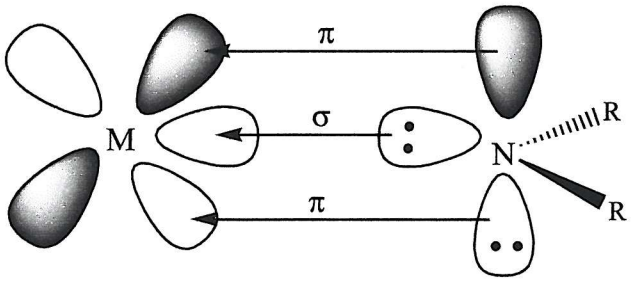

Fig 7.6 Amido functionality bonding model to metal centres.

The lack of current research in this mixed N-donor is possibly due to the synthetic difficulties associated with the synthesis of this ligand system (see Results and Discussion).

7.1.5 Metal Complexes

Wilkinson and co-workers had previously studied manganese, iron and cobalt complexes of the amido analogues of salicylaldimino ligands.[30, 31] Reaction of two equivalents of the lithiated amine with the appropriate metal halide precursor yielded the bis-salicylaldiminato complexes *via* salt elimination (Fig 7.7). The iron, cobalt and manganese complexes were fully characterised and single crystal X-ray diffraction showed distorted tetrahedral geometries around the metal centre in all cases.

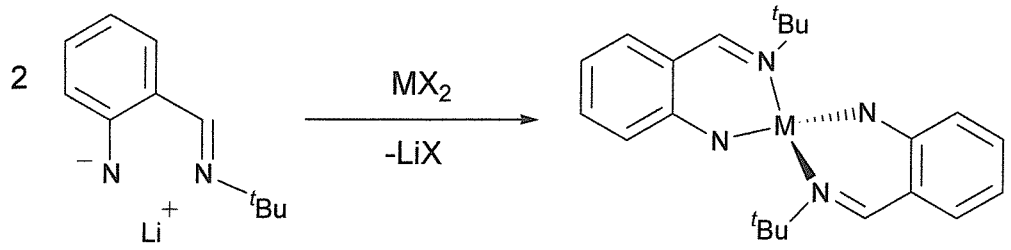

Fig 7.7 Synthesis of bis-salicylaldiminato spiro complexes. M = Mn, Fe, Co.

By changing the metal precursor from metal halide to the metal bis-trimethylsilylamide and the addition of only one equivalent of the aryl amine, not the lithium salt, a mono-chelate complex was formed *via* transamination and was characterised by single crystal X-ray diffraction methods confirming the structure depicted in Fig 7.8. This mono-chelate complex shows the anionic ligand can adopt a bridging mode through the amine to stabilise two metal centres. All of these complexes, in toluene, proved to be inert to H_2, CO, and C_2H_4 at room temperatures and pressures of up to 7 bar. The reason for this inertness may be due to the coordination sphere of the metal being rigidly filled by the ligands, giving too much steric protection.

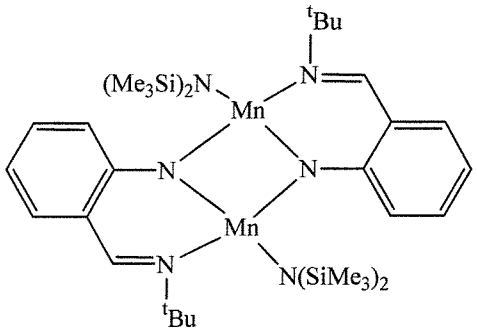

Fig 7.8 Manganese mono - salicylaldiminato complex

To challenge the catalytic ability of the widely used metallocenes efforts were guided towards Group 4 of the periodic table and to zirconium and titanium mixed donor complexes. Initial work performing salt eliminations with zirconium tetrachloride and the lithiated salicylaldiminato ligands gave the products shown in Fig 7.9.

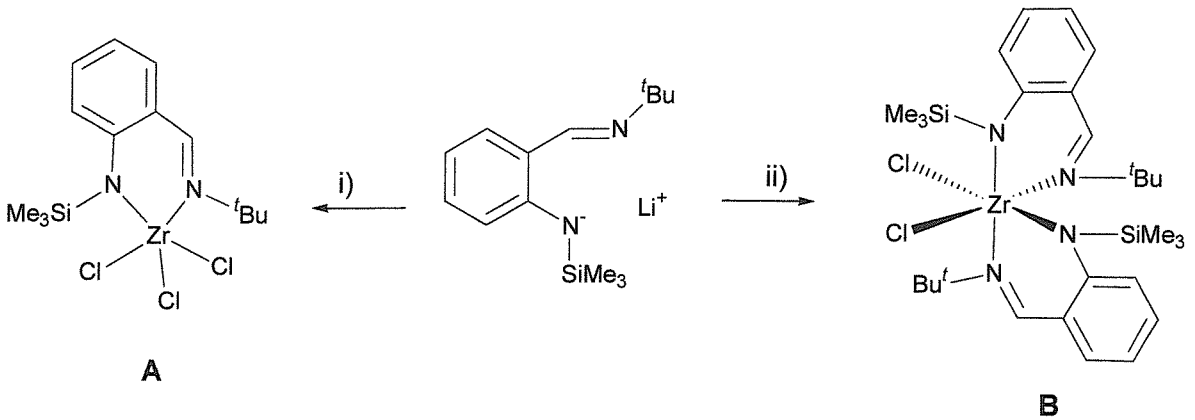

Fig 7.9 Zirconium salicylaldiminato complexes synthesised; i) $ZrCl_4(THT)_2$, diethyl ether, -78 °C to RT; ii) $ZrCl_4$, toluene, -78 °C to RT.

These complexes were fully characterised and their crystal structures obtained (Fig 7.10). Selected bond lengths and angles for these two structures are given in table 7.1. The structure of **A** is a five-coordinate complex with distorted trigonal bipyramidal geometry with the imine (N2) and chloride (Cl1) functionalities occupying the axial positions, the equatorial positions are filled with a silylamide and the remaining chlorides. The Zr – N1 of 2.029(7) Å is typical of a planar amido nitrogen, while the Zr1 – N2 of 2.336(9) Å is longer than the amido bond, but slightly shorter than that found in the known analogous salicylaldimines which are in the range 2.40 – 2.45 Å.[32]

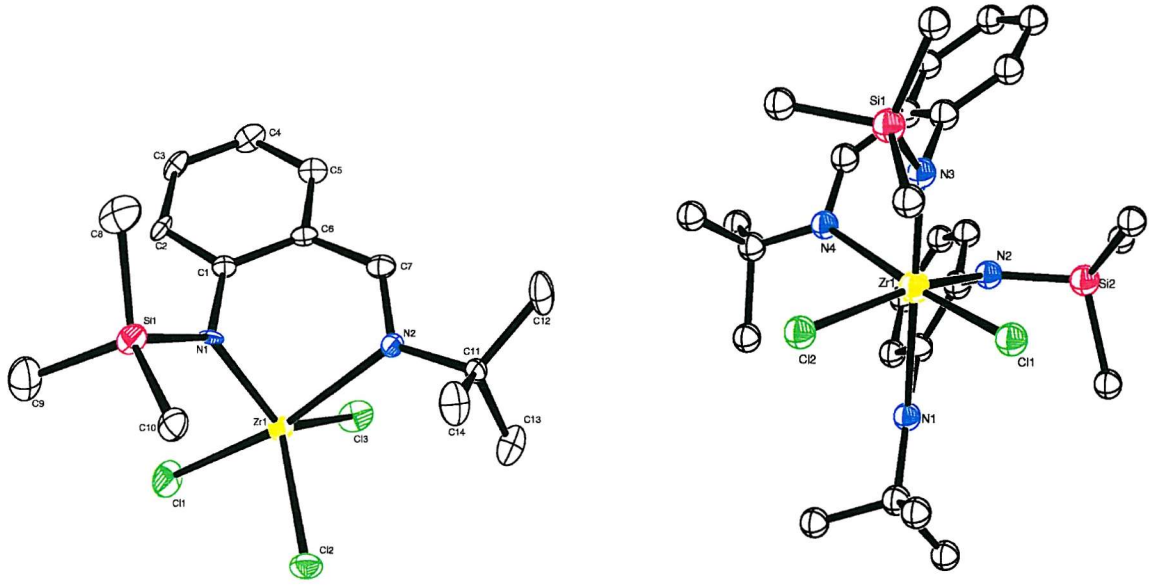

Fig 7.10 Crystal structures of **A** (left) and **B** (right). Hydrogens removed for clarity.

Table 7.1 Selected bond lengths (Å) and angles (°) for **A** and **B**.

A				**B**			
Zr1 - N1	2.029 (7)	Zr1 - N2 - C7	108.12 (5)	Zr1 - N1	2.486 (6)	Cl1 - Zr1 - N1	90.14 (2)
Zr1 - N2	2.336 (9)	Zr1 - N1 - C1	101.03 (5)	Zr1 - N2	2.103 (5)	Cl1 - Zr1 - N2	95.22 (2)
Zr1 - Cl1	2.434 (6)	Cl1 - Zr1 - Cl2	95.49 (2)	Zr1 - N3	2.043 (5)	Cl1 - Zr1 - N3	92.63 (2)
Zr1 - Cl2	2.386 (6)	Cl1 - Zr1 - Cl3	91.13 (14)	Zr1 - N4	2.456 (6)	Cl1 - Zr1 - N4	173.61(2)
Zr1 - Cl3	2.415 (8)	Cl2 - Zr1 - Cl3	112.9 (2)	Zr1 - Cl1	2.414 (5)	Cl2 - Zr1 - N2	161.73(1)
				Zr1 - Cl2	2.490 (4)	Cl1 - Zr1 - Cl2	94.31 (2)

The structure of **B** comprises of an octahedral zirconium centre with *cis* chlorides, due to the arrangement of the two ligands there is a low C_1 geometry as one chloride is *trans* to an imino group whereas the other is *trans* to an amido functionality, leaving one amido group *trans* to an imino group (Fig 7.9). The bond lengths around the zirconium centre reflect the various *trans* influences on the atoms, i.e. Zr1 – Cl1 of 2.414(5) Å (*trans* to imine) is almost 0.1 Å shorter than Zr1 – Cl2 at 2.490(4) Å (*trans* to amido). The unit cell of 2 contains two independent zirconium units, both showing the same geometry around the zirconium.

7.1.6 Aza-Macrocycles

The *o*-aminobenzaldehyde on storage is known, especially upon acidification, to undergo self-condensation to form assorted anhydrooligomers, which are now known to consist of at least the three products shown in Fig 7.11.

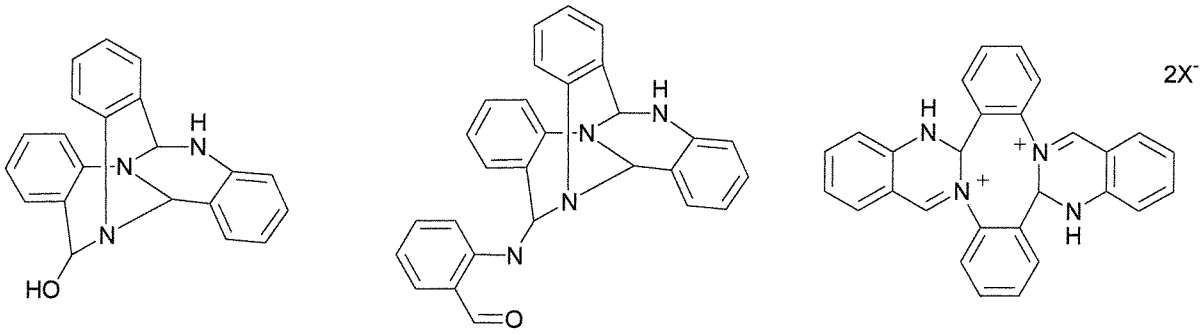

Fig 7.11 Self-condensed forms of *o*-aminobenzaldehyde.

These species however, when added to transition metal precursors, will undergo self-rearrangement to form tri- and tetrameric macrocycles, more commonly known as the tris-anhydrotrimer (TRI) and tetra-anhydrotetramer (TAAB) of *o*-aminobenzaldehyde, and generate metal complexes of the type shown in Fig 7.12.[33]

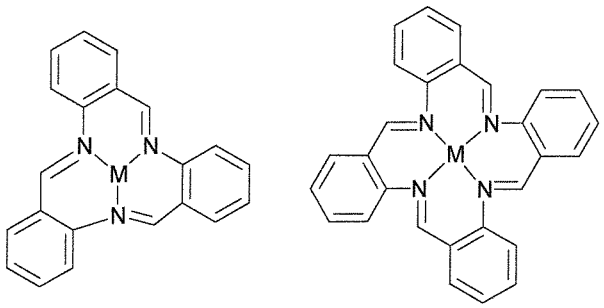

Fig 7.12 Metal complexes of the TRI (left) and TAAB (right) ligand.

In 1937 Pfeiffer and co-workers[34] formed metal complexes from *o*-aminobenzaldehyde using precursor metal amino complexes and in doing, so unbeknown to them, isolated the first TAAB metal complexes, but reported bis-*o*-aminobenzaldimine complexes as they had no structural data at that time. Seventeen years later Eichhorn and Latif were working on self-condensation around metal centres and also isolated TAAB complexes but incorrectly assigned open chain structures to their compounds, but realised that the complexes are inert

to ligand- and metal-exchange reactions.[35] By 1964 Busch developed the 'template hypothesis' for the formation of these macrocyclic complexes and proposed structures for the work that were later confirmed by X-ray crystallography.[36-38] To date the free macrocyclic ligand does not appear to exist and all attempts to demetallate the TRI and TAAB complexes, or form the free tri- and tetrameric species by deprotonation or dehydrogenation of the self-condensed forms of *o*-aminobenzaldehyde have failed.[39]

The main factors affecting the formation of the trimeric ligand over the tetramer on a metal centre, or the ratio of one to the other, generally involve the coordination geometry of the metal. For typically octahedral metal ions the final step of the cyclisation may occur on either a trigonal face or a tetragonal perimeter, so a mixture of compounds can be seen. The size of the templating ion in the synthesis is also an important factor, small metal ions simply cannot coordinate the larger tetrameric macrocycle. Comparative solubility of the TRI and TAAB complexes also has an effect as if the TRI species has very poor solubility, on formation precipitation occurs so the tetramer simply cannot form.[40] TRI and TAAB complexes are known for mainly the mid to late transition metals with complexes of Fe^{2+}, Co^{2+}, Ni^{2+}, Cu^{2+}, Zn^{2+}, Pd^{2+} and Pt^{2+} having been characterised.[41-51]

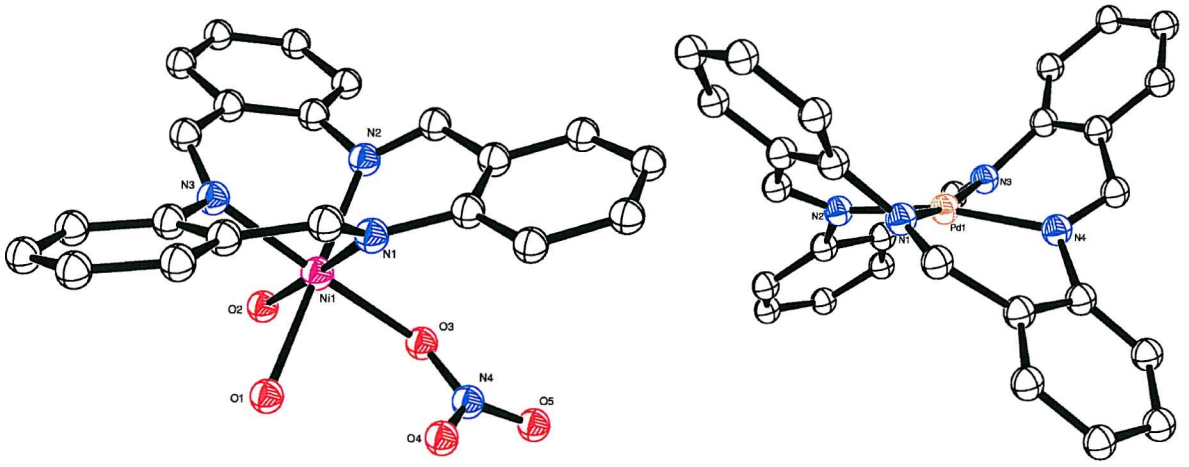

Fig 7.13 Crystal structures of $Ni(TRI)(H_2O)_2NO_3$ (left) and $Pd(TAAB)^{2+}$ (right) complexes. The counter ions and hydrogens have been removed for clarity.

In the octahedral nickel complex[37] shown in Fig 7.13 it can be seen that the macrocycle sits as a flat cap on top of the metal which is a common structural trait of the TRI complexes. In the TAAB complexes, the larger central hole in the ring allows metal ions to become centrally coordinated and the complexes typically take on a saddle type shape (Fig 7.13).

7.2 Results and Discussion

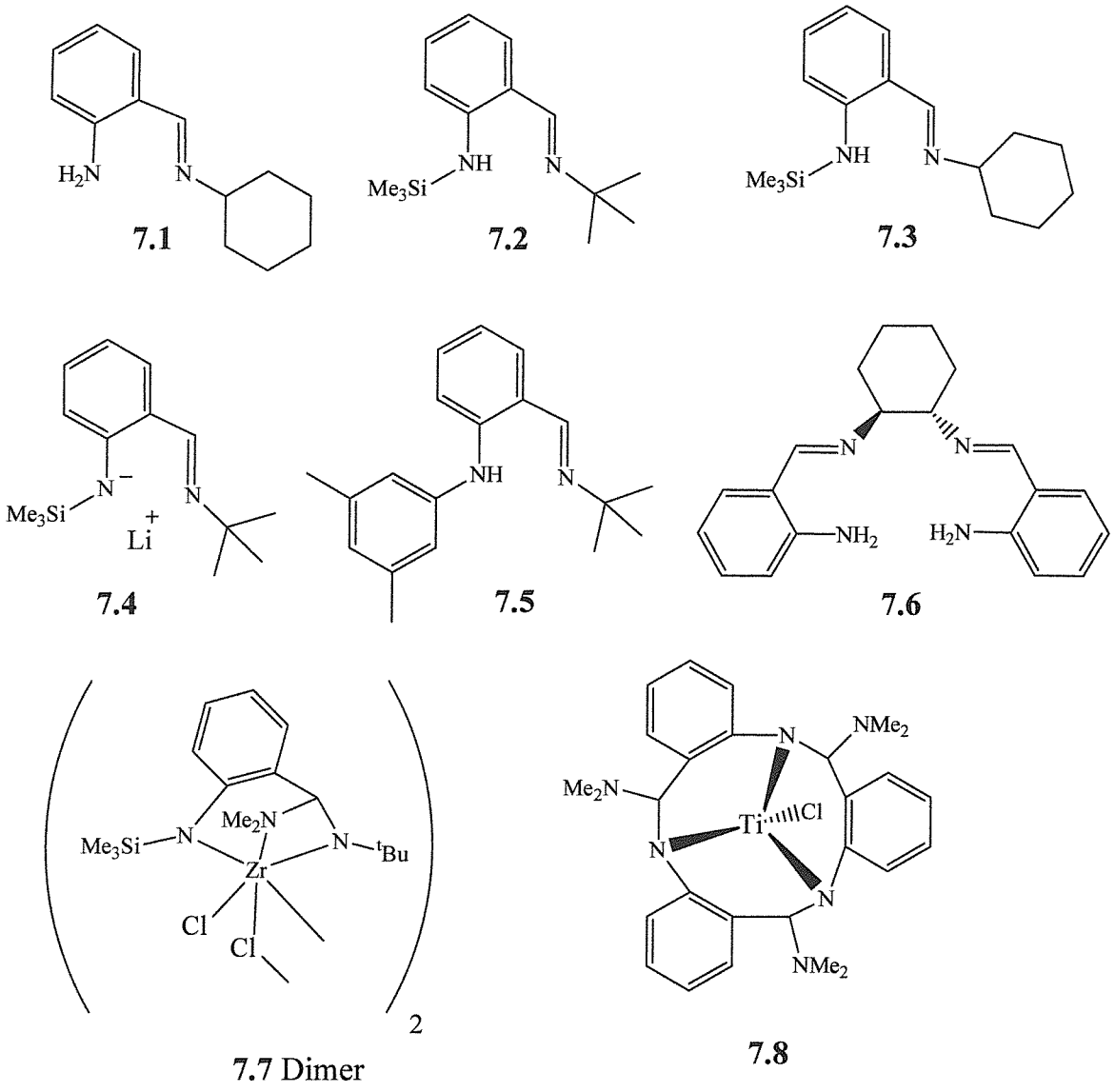

Fig 7.14 Mixed donor ligands and metal complexes prepared.

7.2.1 Ligand Syntheses

The amido/imino mixed donor ligands were all developed from a common organic building block, *o*-aminobenzaldehyde. These ligands are highly versatile as both of the functional groups are available for modification; furthermore the aromatic ring is also available for substitution. The only obstacle is the large-scale production of the unstable *o*-aminobenzaldehyde (Fig 7.15).

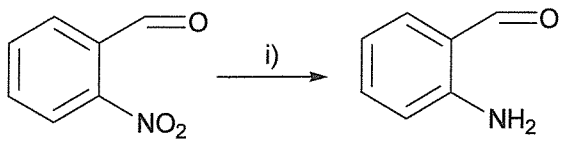

Fig 7.15 Synthesis of o-aminobenzaldehyde; i) $FeSO_4.7H_2O$, NH_4OH or Pd/C (50% wt), H_2.

The reported synthesis of *o*-aminobenzaldehyde requires an iron sulfate reduction of the *o*-nitrobenzaldehyde (Fig 7.15) to the amine followed by *in situ* steam distillation.[52] Due to the unstable nature of the product this is done on a small-scale batch process (0.5 – 1.0 g) and the procedure repeated 8 - 10 times to acquire sufficient quantities of the product. This process is highly time dependant and the steam distillation must be completed within 4 - 6 minutes of the reduction otherwise the reactive *o*-aminobenzaldehyde begins to undergo a series of self-condensation reaction as described. Each batch cycle takes no more than 15 –20 minutes to complete. When the initial work on this ligand system was undertaken there had been a house supply of steam, which provided the necessary volume of steam to complete the reaction with acceptable loss of product. This supply was no longer available, nor was equipment to provide the required volumes of steam to complete the distillation step with acceptable product loss. It was conceded that the low yields obtained before self-condensation occurred made the existing synthetic method unsuitable.

An alternative reduction method was pursued involving hydrogenation of the nitro group with palladium on carbon.[53] This process appeared advantageous in that it could be scaled up, which was unfeasible with the iron reduction method due to the time constraint on the steam distillation. The iron sulphate reductions were performed at 95°C whereas the hydrogenation could be completed at room temperature or lower to retard the self-condensation. Monitoring hydrogen consumption could also approximate the reaction progression. Unfortunately after separation of the product from the hydrogenation an oil was obtained, which could not be crystallised or purified by column chromatography. This meant that the problematic steam distillation would still be needed to acquire the pure crystalline product that was sought. The proton NMR of this product appeared to show the correct product however the compounds lack of crystalline form was treated as suspicious. On comparison the yields between the two methods were similar and the advantages of the palladium-catalysed hydrogenation were clear, although the residual impurity from the reaction made this route problematic.

Once the *o*-aminobenzaldehyde had been isolated, it was rapidly converted to the 2-(R)-iminomethylaniline, where R = *tert*-butyl or cyclohexyl, by refluxing the *o*-aminobenzaldehyde with a large excess of alkylamine (25 fold) in Dean-Stark apparatus with catalytic hydrochloric acid. The acid assisted protonation of the aldehyde to form water, which was azeotropically removed from the reaction driving the equilibrium to the right. This gave the known 2-*tert*-butyliminomethylaniline[31] or **7.1**. Silylation of the amine gives **7.2** or **7.3**, completed *via* deprotonation of the amine to form the lithium salt, then addition of trimethylsilylchloride (Fig 7.16). The lithium salt of **7.2** was prepared using n-BuLi giving **7.4**. These synthetic procedures are high yielding, the condensation and silylation both >75%, the lithiation quantitative. The analogous formation of the cyclohexylimine analogue follows the same procedures as the *tert*-butyl functionalised compounds with similarly high yields.

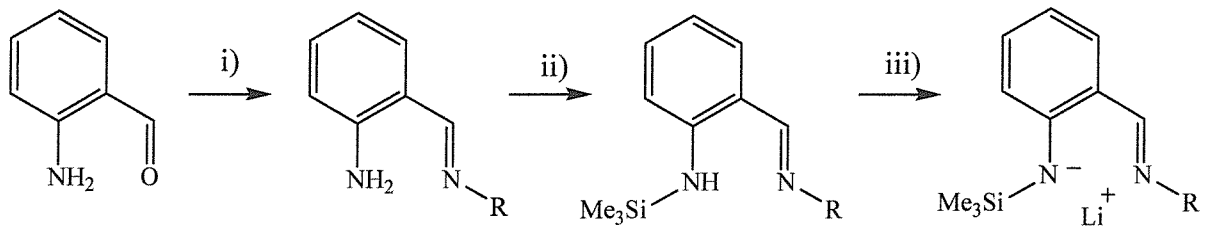

Fig 7.16 i) x25 equivs R-NH_2, C_6H_6, Dean-Stark, reflux; ii) n-BuLi, -78°C, $SiMe_3Cl$; iii) n-BuLi, petrol, -78°C; R = *tert*-butyl, cyclohexyl.

To vary the amido functionality **7.5** was synthesised to see the difference of a dialkyl amide versus a silylamide on coordination and catalytic activity. Compound **7.5** was successfully prepared by taking the *o*-(*tert*-butyl)iminoaniline in toluene and performing a palladium catalysed amination[54, 55] using $Pd(DBA)_2$ and racemic BINAP as the catalyst, sodium *tert*-butoxide as base and 3,5-dimethylbromobenzene as second substrate. **7.5** was isolated in moderate yields (*ca.* 40%) from this coupling which was performed on only a small scale to establish the viability of the route and refinement of catalytic conditions is required to increase this yield.

Compound **7.6** was prepared to study the effect of more rigid chelation in comparison to having a more flexible bis-ligand complex. The preparation of **7.6** was not as trivial as would have been hoped, in following a similar methodology to the preparation of **7.1**, two equivalents of *o*-aminobenzaldehyde were placed in the dean stark apparatus with 1,2-*trans*-diaminocyclohexane, but the yield was low with only 28% conversion to di-substituted

product. A second mono-substituted cyclohexyl amine was detected by MS and both ^{1}H and ^{13}C NMR, confirming the presence of a second product. This low yield of product can be explained by the loss of *o*-aminobenzaldehyde, the self-condensation proving to be more favourable than the condensation with 1,2-*trans*-diaminocyclohexane. Steric hindrance may also attribute to the low yield after the first condensation has occurred on the 1,2-*trans*-diaminocyclohexane. Repeated recrystallisation from high boiling petroleum ether (80-100) yielded pure **7.6**.

7.2.2 Characterisation of Ligands

7.2.2.1 NMR Spectroscopy

For all of the ligand precursors the most indicative analysis was the ^{1}H and ^{13}C NMR spectra. General characteristic peaks in the proton NMR used to identify **7.1 – 7.4** and **7.6** ($CDCl_3$) were:

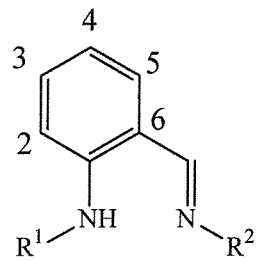

Fig 7.17 Numbering scheme for **7.1 – 7.6,** R^1 = trimethylsilyl, R^2 = *tert*-butyl, cyclohexyl.

- If R^1 = trimethylsilyl, a singlet at 0.3 ppm,
- If R^1 = hydrogen, a broad singlet at 6.2 – 6.4 ppm,
- If R^1 = 3,5-dimethylphenyl, singlets at 2.4 and 7.2 – 7.5 ppm,
- If R^2 = *tert*-butyl, a singlet at 1.2 – 1.3 ppm,
- If R^2 = cyclohexyl, a multiplet at 1.2 – 1.7 ppm and a quintet at 2.6 – 3.1 ppm.

When R^1 is a functional group the residual amine proton gives a low-field peak at 9.8 - 9.9 ppm in C_6D_6 or 9.2 ppm in $CDCl_3$. The imino methyl proton is observed as a singlet between 8.2 and 8.4 ppm in the ^{1}H NMR and a corresponding peak from the carbon is observed at 158 – 174 ppm in the ^{13}C spectrum.

Peaks assignable to the aromatic protons for the 2-, 3-, 4- and 5-positions on the aromatic ring backbone for all compounds appear as overlapping multiplets between 6.5 – 6.8 and 7.2 – 7.5 ppm and full assignment of peaks was not possible.

For **7.6** the ^{1}H and ^{13}C NMR are simplified by the presence of a plane of symmetry through the compound, the NMR peaks for this compound were as observed for the other reported compounds.

7.2.2.2 Mass Spectrometry

For compounds **7.1**, **7.5** and **7.6** a combination of positive ion electrospray mass spectrometry (MS), gas chromatography (GC) and gas chromatography mass spectroscopy (GC-MS, using chemical ionisation) could be used to identify parent ion peaks in the MS, the elution of only a single peak from the GC corresponding to the product which was confirmed by GCMS. For **7.2**, **7.3** and **7.4** the moisture sensitivity of the silicon nitrogen bond and the lithium salt did not allow the use of the GC and MS systems as the products rapidly decomposed on the columns of the machines.

7.2.3 Metal Complex Synthesis.

7.2.3.1 Reactions with Zirconium Halide and Amido Complexes.

Previous unreported work had involved the isolation and characterisation of the mono- and bis-ligand-zirconium complexes of **7.2**, as shown in Fig 7.9. These products were formed *via* salt metathesis routes from the lithium reagents and so work progressed by attempting to transaminate the ligands onto zirconium.

Reaction of **7.2** with $Zr(NMe)_4$ in toluene at 80°C did not lead to the formation of an identifiable metal complex. However, from the reaction of **7.2** with $ZrCl_2(NMe)_2THF_2$ the unexpected **7.7** (Fig 7.18) was isolated as a low yielding yellow crystalline solid.

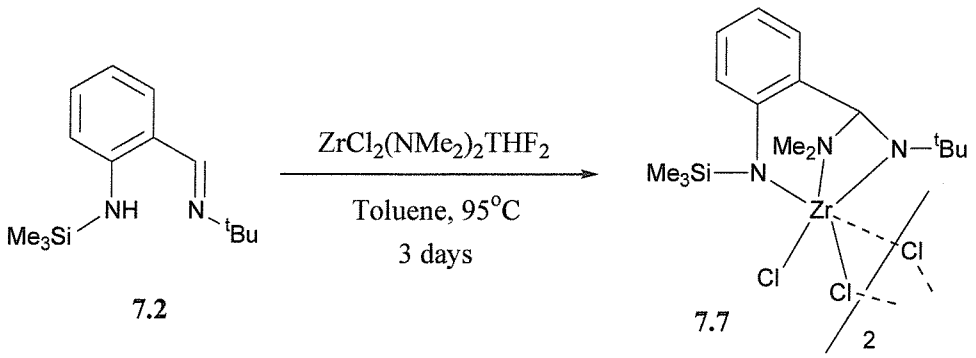

Fig 7.18 Transamination leading to insertion product **7.7**.

The exact mechanism of formation of **7.7** is unclear. The ligand system in complex **7.7** has undergone an insertion of the iminomethyl into a dimethylamido group. Transamination of one of the dimethylamido groups by the silylamide, followed by insertion of the imine into the second dimethylamido ligand is one possible route however an intermolecular pathway involving nucleophilic attack of dimethylamide followed by transamination cannot be ruled out. Insertion reactions, especially of cumulenes (CO_2, CS_2, RNCO *etc.*) are common in early transition metal amido complexes,[56] yet insertion of imines into metal–amido bonds is rare.

From the proton NMR data obtained from the yellow crystals isolated it was quickly observed that the ligand was coordinated to the zirconium as the low-field at peak from the precursor amine proton at 9.9 ppm was missing and peaks assignable to the dimethyl amide (1.5 ppm) were present.

The crystals obtained were studied by X-ray crystallography and the structure is shown in Fig 7.19 with selected bond lengths and angles in Table 7.2. Only one half of the dimer is shown for clarity. Complex **7.7** is a chloride-bridged dimer with one terminal and two bridging chlorides. Each zirconium centre is six-coordinate with distorted octahedral geometry one face is occupied by the tripodal ligand. The Zr–nitrogen bond lengths and the bond angles around the nitrogens support the presence of two monoanionic amido groups, Zr1 – N1 of 2.0882(18) Å and Zr1 – N2 is 2.0122(17) Å (typically 2.0 – 2.1 Å) and one dative amine functional group, Zr1 – N3 at 2.3582(17) Å (typically 2.3 – 2.4 Å). This makes the ligand a ten-electron, dianionic donor with one amido and one asymmetrically trisubstituted amidinato functional group. Functionalised amidinato complexes have appeared in the literature.[57-59] This observed reactivity of the imino group in the presence of highly

electrophilic early transition metals has to be taken into account when using salen type ligands as supports for catalysis.

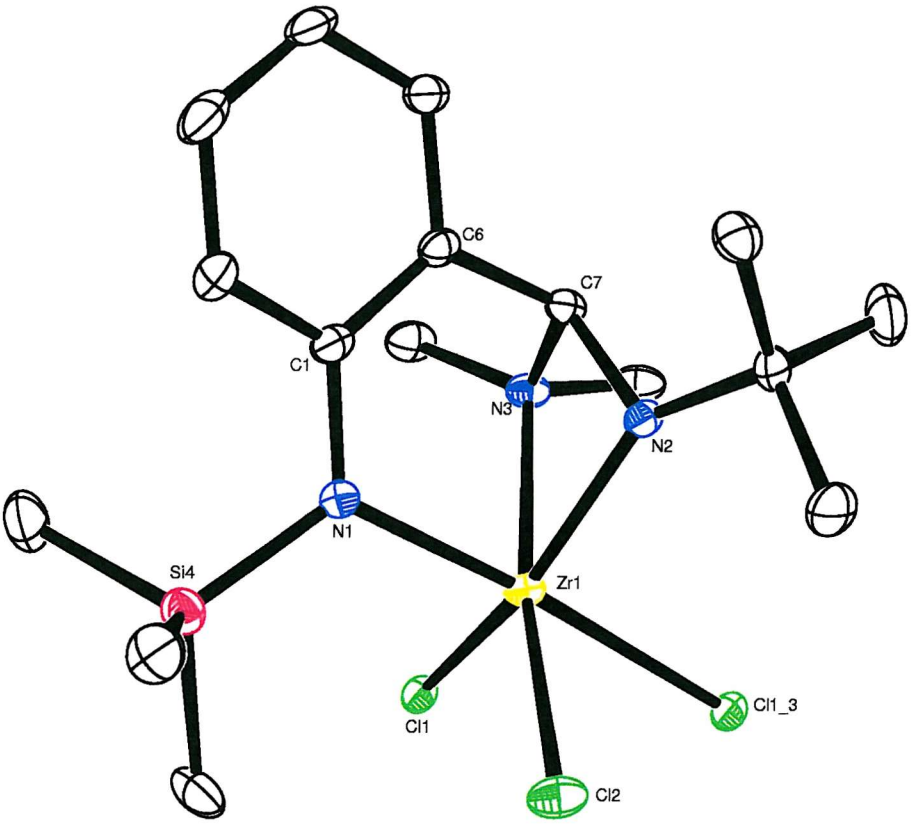

Fig 7.19 Crystal structure of **7.7**. Hydrogens removed for clarity, only half of dimer displayed. The full structure is described in the experimental section.

Table 7.2 Selected bond lengths (Å) and angles (°) for **7.7**.

Zr1 - Cl1	2.6142(7)	N2 – Zr1 – N3	63.07(7)
Zr1 - Cl2	2.4395(7)	N2 – Zr1 – N1	92.01(7)
Zr1 - Cl1_3	2.7067(8)	N1 – Zr1 – N3	84.70(7)
Zr1 - N1	2.0882(18)	N3 – Zr1 – Cl2	169.92(5)
Zr1 - N2	2.0122(17)	N2 – Zr1 – Cl1	142.23(5)
Zr1 - N3	2.3582(17)	N1 – Zr1 – Cl1_3	172.23(5)

7.2.3.2 Reactions with Titanium Halide and Amido Complexes.

Attempts to introduce **7.2** onto $Ti(NMe)_4$ and $Ti(NMe)_2Cl_2$ *via* transamination were unsuccessful. Another unanticipated result was obtained by reaction of $Ti(NMe)_2Cl_2$ with the previously synthesised 2-*tert*-butyliminomethylaniline[31] to give **7.8**, again showing the reactivity of the iminomethyl functionality.

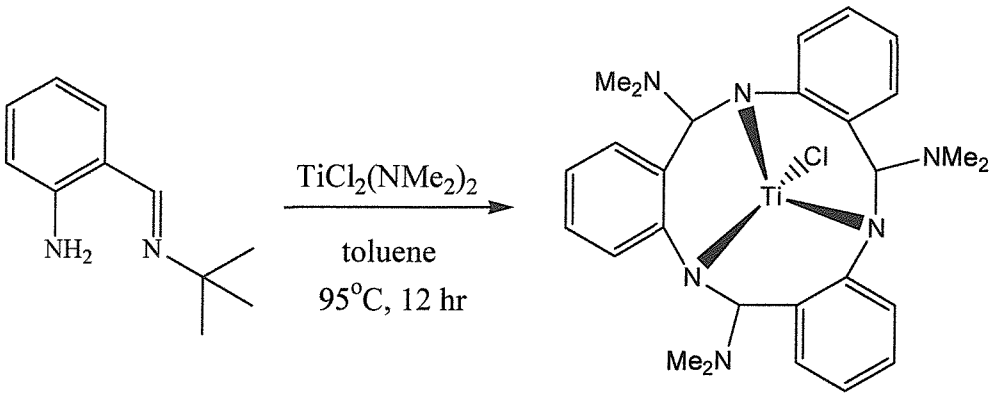

Fig 7.20 Synthesis of macrocyclic **7.8**.

Although the mechanism of the formation of **7.8** is not clear, there is evidence that it involves a metal directed condensation similar to other known complexes that are formed following Busch's template hypothesis. Pre-coordination of the *o-tert*-butyliminomethylaniline is necessary for the reaction to occur. This is shown by the inertness of the electronically richer $Ti(NMe_2)_4$ which fails to produce **7.8** by heating at 100°C with *o-tert*-butyliminomethylaniline, possibly due to its reduced nucleophilicity. This is also shown by the fact that in earlier work with metal halides, the Wilkinson group did not observe this behaviour even when working with Fe and Co, both known to form these aza-macrocycles. The stoichiometry of the reaction is also unclear, **7.8** is always isolated as a low yielding (30 – 37%) red crystalline solid even when the ratio of ligand to metal is varied from 2:1 to 4:1 in favour of the ligand. During the course of the templating mechanism *tert*-butylamine must be eliminated from the ligand system, dimethylamide must be incorporated into the and a chlorine dissociate. Without further study there is not enough evidence to propose a mechanism at this point.

Complex **7.8** was characterised by X-ray crystallography and the structure is shown in Fig 7.21, with selected bond lengths and angles in Table 7.3. The coordination geometry around the titanium can be best described as a tricapped trigonal pyramid. The macrocyclic ligand adopts a cone conformation similar to that of the cone conformation found in calixarenes. The three shorter titanium–nitrogen distances (Ti1 – N11, Ti1 – N21 and Ti1 – N31, average 1.978 Å) fall in the long end of the bond range characteristic of titanium (IV) amido bonds. The geometry of these nitrogens is almost planar (average angle sum 354.4°). The slight

deviation from planarity can be ascribed to competition of N–C and N–Ti π-bonding, or due to constraints imposed by the ligand backbone.

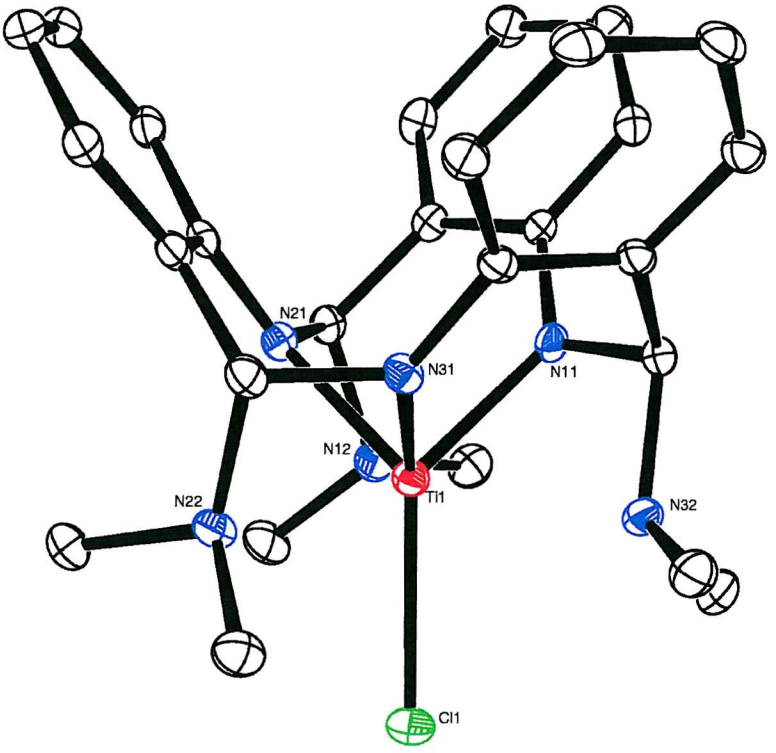

Fig 7.21 Crystal Structure of **7.8**, hydrogens removed for clarity.

Table 7.3 Selected bond lengths (Å) and angles (°) for **7.8**

Ti1 – N11	1.975(2)	N11 – Ti1 – N31	87.35(9)
Ti1 – N31	1.979(2)	N11 – Ti1 – N21	87.18(9)
Ti1 – N21	1.981(2)	N31 – Ti1 – N21	87.75(9)
Ti1 – N32	2.366(2)	N12 – Ti1 – N22	119.45(8)
Ti1 – N12	2.385(2)	N12 – Ti1 – N32	118.48 (9)
Ti1 – N22	2.380(2)	N22 – Ti1 – N32	119.58 (8)
Ti1 – Cl1	2.3722(10)	N11 – Ti1 – Cl1	127.23(7)

One significant difference from **7.8** compared to other reported macrocycles is the presence of the dimethylamido functionalities on the bridging sections, which have not previously been seen on analogous macrocyclic complexes made *via* trimerisation. The pyramidal nitrogen atoms of the dimethylamino groups (N12, N22, N32) interact weakly with the metal centre (average Ti1 – N distance 2.37 Å) to cause a change in shape of the capping ligand, from a near planar cap (Fig 7.13) to a conical cap (Fig 7.21). Functionalisation of the bridges have only been observed on the TAAB macrocycles, and these functional groups have been additions to the preformed complex by nucleophilic attack and are not part of the templating mechanism and can be removed through acidification. This complex does differ in one

significant way from the 'Busch' macrocycles in that the three imino donors (C=N) have been reduced to an amido (C-N) donors making the macrocycle a trianionic ligand at some point during the templating.

Attempts to liberate the macrocycle *via* hydrolysis from the titanium met with limited success, it is known with other 'Busch' macrocycles that the ligands have never successfully been removed from the metals nor independently synthesised.[60] **7.8** is indefinitely stable in air but upon hydrolysis over a period of 12 hr, when layered with ether, decolourisation occurred from dark red to yellow. ^{1}H NMR analysis of the yellow ether extract gave a complicated spectrum, with the formation of a many low field proton signals between 6.0 ppm and 10.7 ppm, which could be due to the partial liberation of the macrocycle, but was too complex to fully assign.

7.3 Conclusions

The initial problems of a reliable synthesis of the *o*-aminobenzaldehyde have still not been remedied, although more synthetic options have been developed, it is important that this problem be resolved for this chemistry to continue, as reliable ligand syntheses are vital.

The salicylaldiminato ligand system is one that has vast scope for study due to the range of structural and electronic tuning that is available. It has been shown the amine can be arylated as well as silylated, which has led to a variety of ligand precursors.[61]

The interesting group 4 complexes isolated with these compounds shows how this ligand system is not simply a spectator ligand; it has interesting properties undergoing reactions at the imine before it reaches a state where it is a supporting ligand for catalysis. Due to the unexpected complexes obtained catalytic activity was not tested during this project.

The development of a new synthetic route to aza-macrocycle formation throws up several new avenues of study and provides more questions than answers. The insertion of the imine into group 4 metal amido bonds is an important area to study, as it is a relatively unexplored phenomenon.

7.4 Experimental

All experiments were carried out under N_2 or partial vacuum unless stated. All solvents were degassed and distilled from appropriate drying agents before use. Commercial chemicals were purchased from Aldrich, Avocado or Acros and used without further purification unless stated. The following were prepared from literature methods; *o*-aminobenzaldehyde,[52,53] $ZrCl_2(NMe_2)_2(THF)_2$,[62] [(trimethylsilyl)methyl]lithium,[63] dibenzylmagnesium,[64] dichlorodibenzylzirconium,[65] 6-(tertbutyliminomethyl)aniline.[31]

7.4.1 Synthesis of Ligands

o-Cyclohexyliminomethylaniline 7.1.

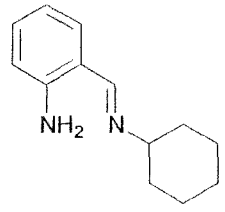

To a solution of *o*-aminobenzaldehyde (1.38 g, 0.011 mol) in benzene (100 cm^3), cyclohexylamine (19.5 cm^3, 15 fold excess) and concentrated hydrochloric acid (5 drops) were added, giving a yellow solution. The solution was refluxed overnight in Dean-Stark apparatus, the benzene removed under vacuum and the resulting solid was extracted with petroleum ether (3 x 20 cm^3). The petrol was removed *in vacuo* and the resulting oil was sublimed onto a cold finger to yield pure product, 76%, 1.76 g. Mp 48°C, MS (ES+): *m/z* 203 $(M)^+$, GC-MS (CIMS): one peak 11.2 mins, *m/z* 203 $(M)^+$. NMR δ_H ($CDCl_3$) 1.2 - 1.7 (10H, m, cyclohexyl ring *H*), 3.1 (1H, quintet, cyclohexyl *H* adjacent N), 6.4 (2H, bs, NH_2), 6.55 (2H, t, aromatic), 7.15 (2H, m, aromatic), 8.4 (1H, s, imino *H*). δ_C($CDCl_3$) 24.7, 25.7, 35.0, 69.9 (cyclohexyl), 115.6, 116.1, 130.5, 133.2, 148.5, 161.5 (aromatic) 174.1 (imino methyl).

[o-(*tert*-Butyl)iminomethyl]-*N*-(trimethylsilyl)aniline 7.2.

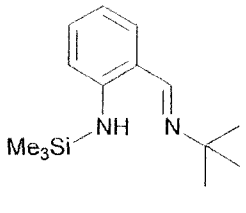

To a precooled (–78°C) solution of o-(*tert*-butyl)iminomethylaniline (5.0 g, 28.5 mmol) in diethylether (200 cm^3) was added dropwise a solution of n-BuLi (12.8 cm^3 of a 2.45 M solution in hexanes, 31.3 mmol). The mixture was stirred for 15 min then allowed to reach room temperature and stirred for 2 h. The resulting yellow suspension was cooled again to -30°C and a solution of Me_3SiCl (3.40 g, 31.3 mmol) in diethylether (10 cm^3) was added dropwise from a syringe. After stirring at room temperature for 12 hr the majority of the ether was removed under reduced pressure, the resulting residue was extracted with petroleum ether (2 × 100 cm^3), the organic extracts were filtered through Celite and evaporated to dryness. The remaining oily

residue gave after vacuum distillation (bp 68 – 70 °C, 0.05 mmHg) product as colourless oil Yield: 4.6 g, 65%. δ_H (C_6D_6) 0.25 [9H, s, $Si(CH_3)_3$], 1.2 [9H, s, $C(CH_3)_3$], 6.6 – 7.2 (4H, m, aromatic), 8.2 (1H, s, imino), 9.9 (1H, s, NH). δ_C (C_6D_6) 0.1 [$Si(CH_3)_3$], 30.0 [$C(CH_3)_3$], 56.9 [$C(CH_3)_3$], 116.1, 116.2, 120.4, 130.7, 134.6, 150.7 (aromatic), 159.6 (imino methyl).

[o-(cyclohexyl)iminomethyl]-*N*-(trimethylsilyl)aniline 7.3.

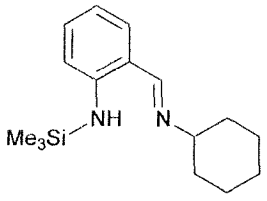

To a precooled (–78°C) solution of **7.1** (1.76 g, 8.7 mmol) in diethyl ether (80 cm^3) was added *n*-BuLi (3.5 cm^3, 2.5 M solution, 8.75 mmol) and stirred until the temperature had risen to room temperature. Trimethylsilylchloride (0.75 cm^3, 8.7 mmol) was added and the reaction stirred overnight. The resulting suspension was filtered, the solvent removed *in vacuo,* and the resulting solid extracted into petroleum ether (2 x 15 cm^3) and recrystallised at -78°C giving dark yellow crystalline product. Yield 68%, 1.62 g. Mp. 18 - 20°C. NMR δ_H ($CDCl_3$) 0.3 [9H, s, $Si(CH_3)_3$], 1.3 - 1.7 (11H, m, cyclohexyl *H*), 6.65 (1H, d, aromatic *H*), 6.75 (1H, t, aromatic *H*), 7.15 (2H, m, aromatic *H*), 8.35 (1H, s, imino C-*H*), 9.2 (1H, s, N-*H*). δ_C($CDCl_3$) 24.2, 25.8, 34.7, 68.9 (cyclohexyl), 115.5, 116.0, 130.1, 133.7, 149.1, 161.7 (aromatic), 168.0 (imino methyl).

Lithium [*o*-(*tert*-butyl)iminomethyl]-*N*-(trimethylsilyl)anilide 7.4.

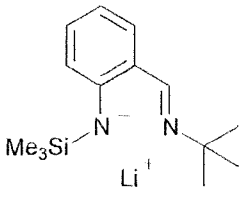

To a solution of **7.2** (3 g, 12 mmol) in petroleum ether (40/60) (50 cm^3) at –78 °C was added slowly n-BuLi (5.4 cm^3 of 2.45 M solution in hexanes, 13.2 mmol). The mixture was held at –78 °C for 1 hr then allowed to warm to room temperature and stirred for 12 hr. This produced a light yellow suspension. The product precipitate was isolated by filtration as a light yellow, extremely air sensitive solid. Yield: 2.2 g, ca. 71%.

[o-(*tert*-butyl)iminomethyl]-*N*-(3,5-dimethylphenyl)aniline 7.5.

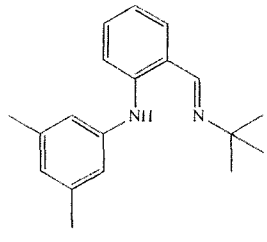

To a solution of *o*-(*tert*-butyl)iminoaniline (0.2 g, 1.1 mmol) in toluene (50 cm^3) was added sodium tert-butoxide (0.325 g, 3.4 mmol), 3,5-dimethylbromobenzene (0.209 g, 0.15 cm^3, 1.2 mmol), racemic BINAP (0.011g, 0.0018mmol) and $Pd_2(DBA)_3$ (0.005 g, 0.0006 mmol) and this was stirred for 4 days at room temperature. The solvent was removed *in vacuo*, the product extracted into petroleum ether and placed at –30°C, which

yielded crystalline product. The residual supernatant was decanted, solvent removed *in vacuo* to give a dark brown oil and further product was purified from this oil by column chromatography, 1:1 petroleum ether/toluene solvent mixture. Yield 37%, 0.114g. MS (ES+) *m/z* 281 $(M)^+$. NMR $\delta_H(CDCl_3)$ 1.3 [9H, s, $C(CH_3)_3$], 2.4 (6H, s, aromatic–CH_3), 6.7, 6.8 (2 x 1H, d and t, aromatic H), 7.2 – 7.5 (5H, m, aromatic H), 8.4 (1H, s, imino C-*H*), 9.8 (1H, s, NH). δ_C ($CDCl_3$) 21.6 [$C(CH_3)_3$], 30.1(aromatic-CH_3), 57.2 [$C(CH_3)_3$], 113.1, 116.8, 118.8, 124.3, 125.5, 128.4, 129.2, 130.6, 134.1, 138.0 (aromatic), 158.9 (imino methyl).

N,N'-Bis-(2-amino-benzylidene)-cyclohexane-1,2-diamine 7.6

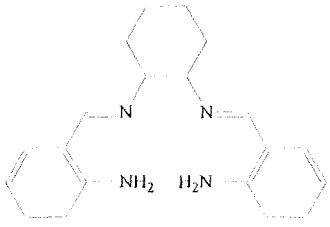

In a similar fashion to **7.1**, to a solution of *o*-aminobenzaldehyde (2.0 g, 16.0 mmol) in benzene (100 cm^3), 1,2-*trans*-diaminocyclohexane (0.942 g, 8.0 mmol) and conc. hydrochloric acid (5 drops) were added. The solution was refluxed overnight in Dean-Stark apparatus, the benzene removed *in vacuo* and the resulting solid was extracted with petroleum ether (3 x 20 cm^3). The petrol cooled to –30°C and crystalline product was collected. Yield 28%, 0.74 g, 2.3 mmol. MS (ES+) *m/z* 321 $(M)^+$, NMR δ_H ($CDCl_3$) 1.2-1.7 (8H, m, cyclohexyl ring *H*), 2.6 (2H, triplet of doublets, *H* adjacent imine N on cyclohexyl), 6.2 (4H, bs, NH_2), 6.5 - 6.7 (4H, m, aromatic *H*), 7.0-7.2 (4H, m, aromatic *H*), 8.4 (2H, s, imine *H*). δ_C ($CDCl_3$) 24.6, 33.4, 55.3 (Cyclohexyl *C*), 115.4, 116.2, 118.9, 130.5, 133.4, 148.5, (phenyl *C*) 163.2 (imino *C*).

7.4.2 Syntheses of Metal Complexes

Dimeric zirconium complex 7.7.

To a solution of **7.2** (0.20 g, 0.8 mmol) in toluene (5 cm^3) was added a solution of $Zr(NMe_2)_2Cl_2(THF)_2$ (0.33 g) in toluene (10 cm^3) and the reaction mixture stirred at 95 °C under partial vacuum for 3 days. The solution was then filtered, the solvent removed in vacuo and the resulting solid crystallised by dissolving in ether (3 cm^3) and standing overnight at room temperature. Two types of crystal were formed, one yellow and one orange which could not be separated by chemical means. The crystal structure obtained was that of the yellow crystal. δ_H (C_6D_6) 0.3 [9H, s, $Si(CH_3)_3$], 1.1 [9H, s, $C(CH_3)_3$], 1.5 [6H, s, $N(CH_3)_2$], 6.3 (1H, d, aromatic), 6.7 (1H, t, aromatic), 6.9 (1H, d, aromatic), 7.0 (1H, t, aromatic), 8.2 (1H, s, N–CH–N).

Crystal data for **7.7**: $C_{16}H_{29}N_3Cl_2Si_1Zr_1$, yellow block (0.01 x 0.005 x 0.005 mm), Mw 453.63, Monoclinic, $P2_1/n$ (No. 2), $a = 9.1721(18)$ Å, $b = 13.137(3)$ Å, $c = 17.476(4)$ Å, $\alpha = \gamma = 90°$, $\beta = 93.88(3)°$, $V = 2101.0(7)$ Å^3, $Z = 4$, $\mu = 0.404$ mm^{-1}, $T = 150$ K, Total reflections = 48258, unique reflections = 4293 ($R_{int} = 0.0778$), Final R indices [$I>2\sigma(I)$] R = 0.0305, R_w = 0.0743 (all data). CCDC reference no. 181542. Local Code 99skl007. Symmetry transformations used to generate equivalent atoms: –x + 1, -y + 1, -z.

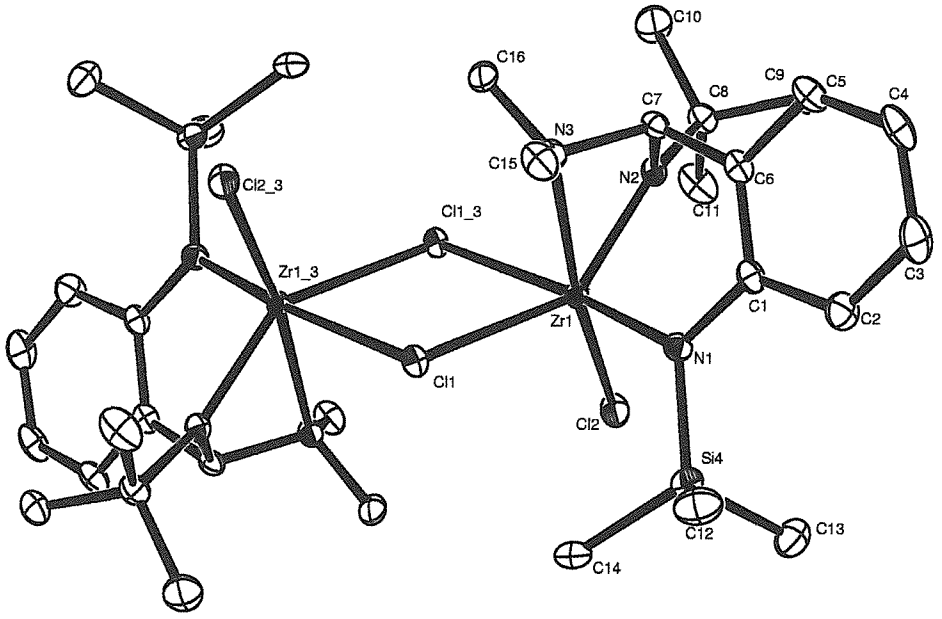

Fig 7.22 Crystal structure of dimeric **7.7**, hydrogen's removed for clarity.

Table 7.4 Bond lengths (Å) for **7.7**.

Zr1 – N2	2.0122(17)	Si4 – N1	1.7770(19)	C7 – C6	1.500(3)	C4 – C3	1.380(4)
Zr1 – N1	2.0882(18)	Si4 – C14	1.857(3)	C7 – N3	1.507(3)	C2 – C3	1.390(4)
Zr1 – N3	2.3582(17)	Si4 – C13	1.859(3)	N2 – C8	1.483(3)	C8 – C10	1.525(3)
Zr1 – Cl2	2.4395(7)	Si4 – C12	1.868(3)	C5 – C4	1.369(4)	C8 – C9	1.525(3)
Zr1 – Cl1	2.6142(7)	N1 – C1	1.424(3)	C5 – C6	1.396(3)	C8 – C11	1.527(3)
Zr1 – C7	2.653(2)	Cl1- Zr1_3	2.7067(8)	C6 – C1	1.413(3)	N3 – C15	1.477(3)
Zr1 – Cl1_3	2.7067(8)	C7 – N2	1.480(3)	C1 – C2	1.400(3)	N3 – C16	1.479(3)

Table 7.5 Selected bond angles for **7.7**.

N2 – Zr1 – N1	92.01(7)	N1 – Zr1 – Cl1_3	172.23(5)	C6 – C7 – N3	113.08(17)
N2 – Zr1 – N3	63.07(7)	N3 – Zr1 – Cl1_3	93.61(5)	C7 – N2 – C8	117.83(16)
N1 – Zr1 – N3	84.70(7)	Cl2 – Zr1 – Cl1_3	85.14(3)	C7 – N2 – Zr1	97.72(12)
N2 – Zr1 – Cl2	107.00(5)	Cl1 – Zr1 – Cl1_3	74.990(18)	C8 – N2 – Zr1	144.45(13)
N1 – Zr1 – Cl2	97.84(6)	C7 – Zr1 – Cl1_3	107.75(5)	C5 – C6 – C1	119.8(2)
N3 – Zr1 – Cl2	169.92(5)	C1 – N1 – Si4	117.43(14)	C5 – C6 – C7	119.0(2)
N2 – Zr1 – Cl1	142.23(5)	C1 – N1 – Zr1	120.66(14)	C1 – C6 – C7	121.17(19)
N1 – Zr1 – Cl1	97.25(5)	Si4 – N1 – Zr1	121.73(10)	C2 – C1 – C6	116.5(2)
N3 – Zr1 – Cl1	81.38(5)	Zr1 – Cl1 – Zr1_3	105.010(18)	C2 – C1 – N1	122.8(2)
Cl2 – Zr1 – Cl1	107.85(2)	N2 – C7 – C6	112.59(17)	C6 – C1 – N1	120.61(19)

N2 – Zr1 – Cl1_3	93.97(5)	N2 – C7 – N3	101.01(16)	C7 – N3 – Zr1	83.60(11)

Titanium macrocyclic complex 7.8.

To a solution of $TiCl_2(NMe_2)_2$ (0.07 g, 0.36 mmol) in toluene (10 cm^3) was added a solution of *o*-(*tert*-butyliminomethyl)aniline (0.13 g, 0.72 mmol) in toluene (5 cm^3). The mixture was heated at 95°C overnight before the resulting dark red solution was filtered and the toluene removed *in vacuo*. The resulting solid was recrystallised from diethylether at room temperature to give dark red, X-ray diffraction quality crystals. Yield: 0.082 g, 43%. $\delta_H(C_6D_6)$ 2.3 (9H, s, N–CH_3), 2.8 (9H, s, N–CH_3), 5.3 (3H, s, Ph–C*H*–N), 6.0 (3H, d, aromatic), 6.5 (3H, t, aromatic), 6.7 (3H, t, aromatic), 7.0 (3H, d, aromatic). δ_C C 41.5, 49.2 (N–CH_3), 87.2, 106.4, 118.1, 128.3, 129.4, 130.0 (aromatic C), 174.2 [Ph–*C*H-N].

Crystal data for **7.8**: $C_{31}H_{43}N_6Cl_1O_1Ti_1$, red prism (0.01 x 0.005 x 0.005 mm), Mw 599.06, Triclinic, *P*-1 (No. 2), a = 10.205(2) Å, b = 10.252(2) Å, c = 14.980(3) Å, α = 87.61(3) °, β = 84.12(3) °, γ = 76.98(3)°, V = 1518.7(5) $Å^3$, Z = 2, μ = 0.404 mm^{-1}, T = 150 K, Total reflections = 13977, unique reflections = 5918 (R_{int} = 0.0655), Final R indices [$I>2\sigma(I)$] R = 0.0518, R_w = 0.1352(all data). CCDC reference no.181544. Local Code 99skl003.

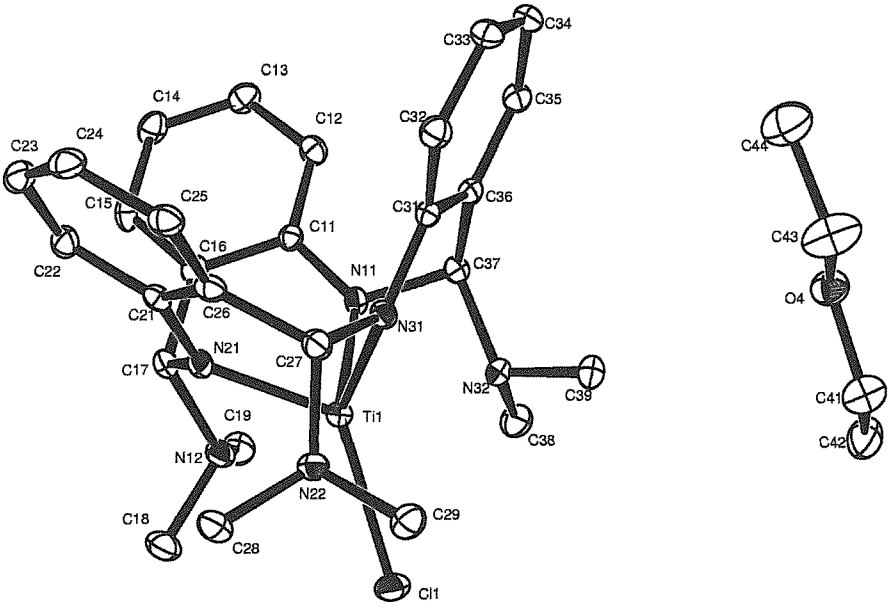

Fig 7.23 Crystal structure of **7.8**, hydrogen's removed for clarity.

Table 7.6 Selected Bond lengths (Å) for **7.8**.

Ti1 – N11	1.975(2)	Ti1 – N12	2.385(2)	C17 – N21	1.460(4)	C15 – C16	1.387(4)
Ti1 – N31	1.979(2)	N11 – C11	1.387(3)	C17 – C16	1.500(4)	C14 – C13	1.375(5)
Ti1 – N21	1.981(2)	N11 – C37	1.455(3)	C11 – C12	1.390(4)	O4 – C43	1.411(4)
Ti1 – N32	2.366(2)	N12 – C19	1.475(4)	C11 – C16	1.416(4)	O4 – C41	1.413(4)

Ti1 – Cl1	2.3722(10)	N12 – C18	1.479(4)	C12 – C13	1.387(4)	C41 – C42	1.482(5)
Ti1 – N22	2.380(2)	N12 – C17	1.498(3)	C15 – C14	1.384(4)	C43 – C44	1.469(5)

Table 7.7 Selected angles (°) for **7.8**.

N11 – Ti1 – Cl1	127.23(7)	C19 – N12 – C17	113.7(2)	C13 – C12 – C11	120.3(3)
N21 – Ti1 – Cl1	127.60(7)	C18 – N12 – C17	109.1(2)	C14 – C15 – C16	120.9(3)
N31 – Ti1 – Cl1	126.36(7)	N21 – C17 – N12	98.3(2)	C15 – C16 – C11	119.5(3)
N11 – Ti1 – N31	87.35(9)	N21 – C17 – C16	111.5(2)	C15 – C16 – C17	121.6(3)
N11 – Ti1 – N21	87.18(9)	N12 – C17 – C16	113.7(2)	C11 – C16 – C17	118.7(2)
N31 – Ti1 – N21	87.75(9)	N11 – C11 – C12	124.9(3)	C13 – C14 – C15	119.5(3)
C11 – N11 – C37	121.4(2)	N11 – C11 – C16	116.2(2)	C14 – C13 – C12	121.0(3)
C19 – N12 – C18	109.0(3)	C12 – C11 – C16	118.9(2)		

7.5 References

[1] P. M. Morse, *C & EN*, **1998**, 11

[2] H. H. Brintzinger, D. Fischer, R. Mulhaupt, B. Rieger, R. M. Waymouth, *Angew. Chem. Int. Ed. Engl.*, **1995**, *34*, 1143.

[3] R. F. Jordan, *Adv. Organomet. Chem.*, **1991**, *32*, 325.

[4] A. Togni, R. L. Halterman, *Metallocenes*, Wiley-VCH, **1998**.

[5] G. J. P. Britovsek, V. C. Gibson, D. F. Wass, *Angew. Chem. Int. Ed. Engl.*, **1999**, *38*, 428

[6] M. Bochmann, *J. Chem. Soc. Dalton. Trans.*, **1996**, 255.

[7] P. C. Mohring, N. J. Conville, *J. Organomet. Chem.*, **1994**, *479*, 1.

[8] S. D. Ittel, L. K. Johnson, M. Brookhart, *Chem. Rev.*, **2000**, *100*, 1169.

[9] D. D. Devore, F. J. Timmers, D. L. Hasha, R. K. Rosen, T. J. Marks, P. A. Deck, C. L. Stern, *Organometallics*, **1995**, *14*, 3132.

[10] V. C. Gibson, S. K. Spitzmesser, *Chem. Rev.*, **2003**, *103*, 283.

[11] L. Gade, *Chem. Commun.*, **2000**, 173

[12] J. D. Scollard, D. H. McConville, J. J. Vital, *Organometallics*, **1997**, *16*, 4415.

[13] H. Fuhrmann, S. Brenner, P. Arndt, R. Kempe, *Inorg. Chem.*, **1996**, *35*, 6742.

[14] R. Grubbs, T. Younkin, E. Connor, J. Henderson, S. Freidrich, D. Bansleben, *Science*, **2000**, *287*, 460.

[15] P. Cosse, *J. Catal*, **1964**, 80.

[16] E. J. Arlman, *J. Catal*, **1964**, *3*, 89.

[17] E. J. Arlman, P. Cosse, *J. Catal*, **1964**, *3*, 99.

[18] K. J. Ivin, J. J. Rooney, C. D. Stewart, M. L. H. Green, R. Mahtab, *Chem. Commun.*, **1978**, 604.

[19] E. R. Evitt, R. G. Bergman, *J. Am. Chem. Soc.*, **1979**, *101*, 3973.

[20] H. W. Turner, R. R. Schrock, *J. Am. Chem. Soc.*, **1982**, *104*, 2331.

[21] N. M. Doherty, J. E. Bercaw, *J. Am. Chem. Soc.*, **1985**, *107*, 2670.

[22] M. Brookhart, B. Grant, A. F. Volpe, *Organometallics*, **1992**, *11*, 3920.

[23] W. Kaminsky, *Macromol. Chem. Phys.*, **1996**, *197*, 3907.

[24] R. Kempe, *Angew. Chem., Int. Ed.*, **2000**, *39*, 468.

[25] P. G. Cozzi, E. Gallo, C. Floriani, A. Chiesivilla, C. Rizzoli, *Organometallics*, **1995**, *14*, 4994.

[26] C. Wang, S. K. Friedrich, T. R. Yunkin, R. T. Li, R. H. Grubbs, D. A. Bansleben, M. W. Day, *Organometallics*, **1998**, *17*, 3149.

[27] P. R. Woodman, N. W. Alcock, I. J. Munslow, C. J. Sanders, P. Scott, *J. Chem. Soc. Dalton. Trans.*, **2000**, 3340.

[28] J. Saito, M. Mitani, J. Mohri, Y. Yoshida, S. Matsui, S. Ishii, S. Kojoh, N. Kashiwa, T. Fujita, *Angew. Chem. Int. Ed. Engl.*, **2001**, *40*, 2918.

[29] C. Wang, S. K. Friedrich, T. R. Yunkin, R. T. Li, R. H. Grubbs, D. A. Bansleben, M. W. Day, *Organometallics*, **1998**, *17*, 3149.

[30] A. A. Danopoulos, G. Wilkinson, T. K. N. Sweet, M. B. Hursthouse, *J. Chem. Soc. Dalton. Trans.*, **1995**, 205.

[31] C. Weymann, A. A. Danopoulos, G. Wilkinson, T. K. N. Sweet, M. B. Hursthouse, *Polyhedron*, **1996**, *15*, 3605.

[32] J. Strauch, T. H. Warren, G. Erker, R. Frohlich, P.Saarenketo, *Inorg. Chim. Acta.*, **2000**, *300*, 810.

[33] A. G. Kolchinski, *Coord. Chem. Rev.*, **1998**, *174*, 207

[34] P. Pfeiffer, T. Hesse, R. Pfitzner, W. Scholl, H. Thielert, *J. Prakt. Chem. /Chem-Ztg*, **1937**, *149*, 217.

[35] G. L. Eichhorn, R. A. Latif, *J. Am. Chem. Soc.*, **1954**, *76*, 5180.
[36] M. C. Thompson, D. H. Busch, *J. Am. Chem. Soc.*, **1964**, *86*, 213.
[37] E. B. Fleischer, E. Klem, *Inorg. Chem.*, **1965**, *4*, 637.
[38] S. W. Hawkinson, E. B. Fleischer, *Inorg. Chem.*, **1969**, *8*, 2402.
[39] K. B. Yatsimirski, A. G. Kolchinski, V.V. Pavlishchuk, G. G. Talanova, *Synthesis of Macrocyclic Compounds*, Naukova Dumka, Kiev, **1987**.
[40] R. I. Sheldon, A. J. Jircitano, M. A. Beno, J. M. Williams, K. B. Metres, *J. Am. Chem. Soc.*, **1983**, *105*, 3028.
[41] V. Katovic, S. C. Vergez, D. H. Busch, *Inorg. Chem.*, **1977**, *16*, 1716.
[42] J. C. Dabrowiak, P. H. Merrel, J.A.Stone, D. H. Busch, *J. Am. Chem. Soc.*, **1973**, *95*, 6613.
[43] I. W. Pang, D.V.Stynes, *Inorg. Chem.*, **1977**, *16*, 2192.
[44] A. Reuveni, V. Malatesta, B. R. McGarvey, *Can. J. Chem.*, **1977**, *55*, 70.
[45] G. A. Melson, D. H. Busch, *Proc. Chem. Soc*, **1963**, 233.
[46] G. A. Melson, D. H. Busch, *J. Am. Chem. Soc.*, **1964**, *86*, 4834.
[47] G. A. Melson, D. H. Busch, *J. Am. Chem. Soc.*, **1965**, *87*, 1706.
[48] A. M. Tait, D. H. Busch, *Inorg. Synth.*, **1978**, *18*, 30.
[49] P. R. Shukla, B. B. Awasthi, R. Rastogi, G. Narain, *Indian J. Chem. A.*, **1984**, *23*, 241.
[50] F. Seidel, *Ber. Dtsch. Chem. Ges*, **1926**, *59*, 1894.
[51] S. Brawner, K. B. Mertes, *J. Inorg. Nucl. Chem.*, **1979**, *41*, 764.
[52] L. Smith, J. Opie, *Organic Synthesis Collective*, **1981**, *3*, 56.
[53] P. Ruggil, O. Scmid, *Helv. Chim. Acta*, **1945**, *28*, 1229.
[54] J. P. Wolfe, S. L. Buchwald, *J. Org. Chem.*, **2000**, *65*, 1144.
[55] J. P. Wolfe, S. Wagaw, S. L. Buchwald, *J. Am. Chem. Soc.*, **1996**, *118*, 7215.
[56] M. F. Lappert, P. P. Power, A. R. Sanger, R. C. Srivastava, *Metal and Metalloid Amides*, Ellis Horwood Publishers, Chichester, **1980**.
[57] D. Doyle, Y. K. Gun'ko, P. B. Hitchcock, M. F. Lappert, *J. Chem. Soc. Dalton. Trans.*, **2000**, *22*, 4093.
[58] J. R. Hagadorn, J. Arnold, *Inorg. Chem.*, **1997**, *36*, 132.
[59] K. Kicaid, C. P. Gerlach, G. R. Giesbrecht, J. R. Hagadorn, G. D. Whitener, J. Arnold, *Organometallics*, **1999**, *18*, 5360.
[60] J. S. Bradshaw, K. E. Krakowiak, R. M. Izatt, *Aza-Macrocycles*, Wiley, **1993**.
[61] R. M. Porter, S. Winston, A. A. Danopoulos, M. B. Hursthouse, *J. Chem. Soc. Dalton. Trans.*, **2002**, 3290.
[62] R. Kempe, P. Arndt, S. Brenner, *Z. Anorg. Allg. Chem*, **1995**, 2021.
[63] O. Beachley, C. Tessier-Youngs, *Inorg. Synth.*, **1986**, *24*, 95.
[64] R. R. Schrock, *J. Organomet Chem.*, **1976**, *122*, 209.
[65] R. Schrock, J. Wengrovious, *J. Organomet. Chem.*, **1981**, *205*, 319.

Chapter 8

Conclusions

Chapter 8

Conclusions

8.1 Conclusions

Synthetic routes to a range of pyridyl, picolyl and diethylacetamide functionalised mono-imidazolium salts and 2,6-lutidyl, pyridyl and various xylyl linked bis-imidazolium salts are reported in this thesis. Many of these salts have been used as precursors in a novel selective synthesis of functionalised 'free' mono- and bis-imidazol-2-ylidenes, allowing for the production of 'carbenes-in-a-bottle'. From the use of 'free' imidazol-2-ylidenes the synthesis of the corresponding imidazol-2-thiones has been reported. Use of the imidazolium salts and imidazol-2-ylidenes has led to the isolation of novel mono- and bis-imidazol-2-ylidene complexes of silver, palladium and nickel. Transamination reactions of amido/imino mixed donor ligands with zirconium and titanium amido complexes showed rare insertions of imines into metal amido bonds with unexpected isolation of a zirconium amidinato complex and a titanium 'template directed', cyclotrimerised, macrocyclic complex. The above results include:

i) A novel selective synthetic route to 'free' imidazol-2-ylidenes using $KN(SiMe_3)_2$ in THF.[1]

ii) The first fully characterised examples of pyridine functionalised mono-imidazol-2-ylidenes (Fig 8.1).[1, 2]

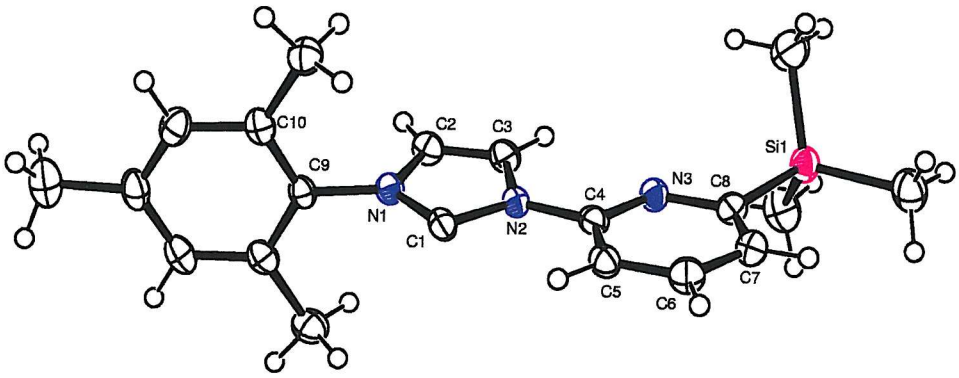

Fig 8.1 Novel pyridine functionalised mono-imidazol-2-ylidenes.

iv) Full characterisation of silver(I) mono- and bis-imidazol-2-ylidene complexes that contain ligands with a second 'dangling' functional group.[4]

v) Novel palladium(II) mono- and bis-imidazol-2-ylidene complexes exhibiting a variety of coordination motifs (Fig 8.2).

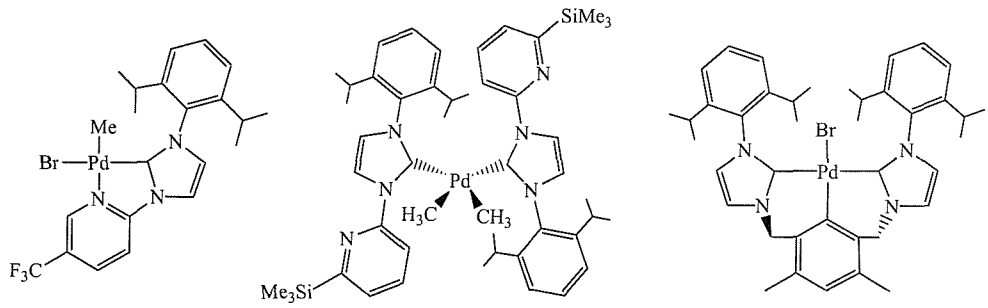

Fig 8.2 Variety of ligand coordination motifs observed for Pd(II) complexes.

vi) Structurally characterised examples of rigid Pd(II) imidazol-2-ylidene complexes that contain a C_2-symmetrical axis that was not pre-formed in the ligand.

vii) The first fully characterised examples of a nickel(II) pyridine functionalised mono-and bis-imidazol-2-ylidene complexes, and further examples of picolyl functionalised complexes.

viii) Observation of a rare insertion of imino groups into metal amido bonds.

The variety of novel imidazolium salts described in chapter 2 were prepared using different quaternisations of the precursor 3-(aryl)imidazole. From these salts it was possible to selectively deprotonate the 2-imidazolium proton using $KN(SiMe_3)_2$ under controlled conditions to isolate the corresponding stable 'free' imidazol-2-ylidene. These had previously had only been observed as a transient species in the NMR spectra as attempted isolations were not successful.[5] These isolated species showed no signs of decomposition on storage at room temperature under an inert environment, or in solutions of toluene over increased time periods, all showed good thermal stability up to at least 100°C before decomposition occurred. Exposure of the 'free' imidazol-2-ylidenes to air gave unidentifiable products by NMR spectroscopy. Reactions of selected imidazol-2-ylidenes with flowers of sulfur gave the corresponding mono- or bis-imidazol-2-thiones, which is behaviour typical of these species.[6] The isolation of imidazolium salts, imidazol-2-ylidenes and imidazol-2-thiones gives three routes of introducing imidazol-2-ylidenes to transition metal centres.

Chapter 3 describes the reactions of the imidazolium salts with silver(I) oxide to give the corresponding silver(I) imidazol-2-ylidene halide complexes. The use of metal fragments with ligands of sufficient basicity to deprotonate the 2-imidazolium proton has been previously reported[7] and successfully used by us to isolate a range of silver(I) functionalised imidazol-2-ylidene complexes.[4, 5]

The palladium(II) complexes described in chapter 4 are synthesised using the compounds described in the two preceding chapters; The imidazolium salts were *in situ* deprotonated by $Pd(OAc)_2$ to give bis-imidazol-2-ylidene complexes; The 'free' mono-imidazol-2-ylidenes were added to Pd(COD)MeX (X = halide) yielding the corresponding Pd(ligand)MeX or to $Pd(TMEDA)Me_2$ to give $Pd(Ligand)_2Me_2$; The silver (I) imidazol-2-ylidene complexes were used as transmetallation reagents with Pd(COD)MeX giving the same Pd(II) complexes [Pd(ligand)MeX] as were isolated from the 'free' imidazol-2-ylidenes.

Several of the novel Pd(II) imidazol-2-ylidene complexes isolated in chapter 4 are analogous to previously prepared Pd(II) imidazol-2-ylidene complexes which were shown to be highly active in Heck C-C coupling. Investigation into the coupling of activated aryl bromides showed that at low catalysts loadings, for bidentate, pyridyl functionalised imidazol-2-ylidenes the presence of an electron-withdrawing group increases coupling activity whereas the increase of steric bulk with minimal electronic variance on the pyridyl group causes no change in activity. For the larger tridentate ligands the exchange of a coordinated pyridine linkage between the imidazol-2-ylidenes to a cyclometallated aryl group bears no effect on coupling activity, even though the ligand system was observed to be more rigid. Variation of steric bulk on these tridentate ligands did not significantly effect coupling activity.

Investigations into nickel(II) imidazol-2-ylidene complexes are described in chapter 6. Using the silver(I) precursor complexes as transmetallation reagents yielded a family of picolyl functionalised mono-imidazol-2-ylidene nickel dihalide complexes containing different steric bulk. Whilst changing reaction conditions to increase yields by the use of a higher boiling chlorinated solvent caused halide exchange processes to occur and mixed halide content was observed in the bulk products. Synthesis of the pyridyl analogues using the silver(I) precursors gave a rare mixed geometry bi-nickel complex where one centre was octahedral and the second tetrahedral. An alternative synthetic route using the 'free' imidazol-2-ylidenes gave a related dimeric nickel bis-imidazol-2-ylidene complex as part of a three member co-

crystallised product in which the target nickel(II) mono-imidazol-2-ylidene complex was observed.

Chapter 7 describes mixed amido/imino six-electron donor ligands designed as amido analogues of the well-known salicyladimine ligands. As a continuation of previous work into the group 4 complexes of these ligands a change of methodology from introducing ligands *via* salt metathesis to transamination led to interesting examples of insertions of imines into metal amido bonds.

The large number of ligand precursors and complexes that have been reported here have already generated interest in the scientific community from colleagues and others.[1, 2, 4, 8-11] A range of investigative studies are already underway aiming to answer some of the questions that have been brought up by the synthesis of these new compounds, and to explore the chemistry of similar complexes.

8.2 References

[1] A. A. Danopoulos, S. Winston, T. Gelbrich, M. B. Hursthouse, R. P. Tooze, *Chem. Commun.*, **2002**, 482.

[2] A. A. Danopoulos, S. Winston, W. B. Motherwell, *Chem. Commun.*, **2002**, 1376.

[3] A. n. Caballero, E.Dy´ez-Barra, F. A. Jalo´n, S. Merino, J. Tejeda, *J. Organomet. Chem.*, **2001**, *617*, 395.

[4] A. A. D. Tulloch, A. A. Danopoulos, S. Winston, S. Kleinhenz, G. Eastham, *J. Chem. Soc. Dalton. Trans.*, **2000**, 4499.

[5] A. A. D. Tulloch, PhD thesis, University of Southampton (Southampton), **2001**.

[6] A. J. Arduengo, *Acc. Chem. Res.*, **1999**, *32*, 913.

[7] H. M. Wang, I. J. B. Lin, *Organometallics*, **1998**, *17*, 972.

[8] R. M. Porter, S. Winston, A. A. Danopoulos, M. B. Hursthouse, *J. Chem. Soc. Dalton. Trans.*, **2002**, 3290.

[9] A. A. D. Tulloch, S. Winston, A. A. Danopoulos, G. Eastham, M. B. Hursthouse, *J. Chem. Soc. Dalton. Trans.*, **2003**, 1009.

[10] S. Winston, A. A. Danopoulos, A. A. D. Tulloch, G. Eastham, M. B. Hursthouse, *J. Chem. Soc. Dalton. Trans.*, **2003**, 699.

[11] W. A. Herrmann, *Angew. Chem. Int. Ed. Engl.*, **2002**, *41*, 1290